DISS. ETH NO. 23720

MOLECULAR CHARACTERIZATION OF IRON AND ZINC DEFICIENCY RESPONSE IN CEREALS

A thesis submitted to attain the degree of
DOCTOR OF SCIENCES of ETH ZURICH
(Dr. sc. ETH Zurich)

Presented by
Meng Wang

M.Sc. in Cell Biology, Northeast Normal University, China

Born on 17th March 1984
Citizen of China

Accepted on the recommendation of

Prof. Dr. Wilhelm Gruissem, examiner
Dr. Navreet Bhullar, co-examiner
Prof. Dr. Rainer Schulin, co-examiner
Prof. Dr. Samuel Zeeman, co-examiner

2016

ACKNOWLEDGEMENTS

I am very grateful to ETH Zurich research grants and State Secretariat for Education, Research and Innovation (SERI) within the COST FA0905 program for supporting my Ph.D. studies and related research.

I would like to express my sincere gratitude to my supervisor, Dr. Navreet K. Bhullar, for her tireless guidance, patience, and encouragement in both my studies and daily life. I also sincerely acknowledge Prof. Dr. Wilhelm Gruissem for providing me with valuable comments and serving as a resource of immense knowledge. In addition to my supervisors, I would like to thank the rest of my thesis committee members, Prof. Dr. Rainer Schulin and Prof. Dr. Samuel Zeemen, for their insightful suggestions and stimulating discussions during my Ph.D. committee meetings.

I would also like to thank Prof. Dr. Olivier Voinnet for generous access to the qRT-PCR machine.

I also greatly appreciate the invaluable bioinformatics and IT support provided by Dr. Hubert Rehrauer (FGCZ), Dr. Katja Bärenfaller, Dr. Johannes Fütterer, Mr. Matthias Hirsch-Hoffmann, and Mr. Rolf Joho.

I gratefully thank Irene Zurkirchen, Doris Russenberger, and Kim Schlegel for their useful technical support. Thanks to Phillip Ihmor for German translation of my thesis summary. I also deeply appreciate Daniela Rothe for all of her kind help.

Many sincere thanks are also expressed to Ravi Bodampalli Anjanappa, Huan Shu, Huahong Wang, Qiyan Wang-Mueller, and Kuan-Te Li for their kind and much needed assistance when I just started my new life in Switzerland.

I also thank my fellow labmates, Kulaporn Boonyaves, Kumar Vasudevan, Simrat Pal Singh, Ting-Ying Wu, Devang Metha, and Wuyan Wang from Prof. Samuel Zeemen's lab for their generous help and discussions about our work, and the many fun times that we spent together.

I would like to thank my family, my parents and my partner, for their supportive spirit and attention throughout my Ph.D. study, especially during the period in which I was writing my thesis.

SUMMARY

Iron and zinc are essential micronutrients in the living world. They function as cofactors to many key enzymes, and participate in various metabolic and biosynthetic pathways. Iron and zinc deficiency in crops lead to yield losses, as well as poor nutritional quality. In order to develop iron and zinc deficiency stress tolerant crops as well as to improve the iron and zinc concentration of cereal grains, more information is needed on the molecular mechanisms controlling iron and zinc homeostasis in staple food crops, such as rice and wheat.

In order to understand the molecular mechanisms underlying iron and zinc translocation and regulation in bread wheat, I used RNA sequencing and qRT-PCR approaches. Under iron deficiency, wheat genes involved in phytosiderophore (PS) biosynthesis, TCA cycle, and genes encoding transcription factors, as well as several iron transporter families, such as MAJOR FACILITATOR SUPERFAMILY (MFS), ATP-BINDING CASSETTE (ABC) transporter superfamily, NATURAL RESISTANCE ASSOCIATED MACROPHAGE PROTEIN (NRAMP) family and OLIGOPEPTIDE TRANSPORTER (OPT) family were significantly up-regulated, suggesting their important functions in iron homeostasis. Under zinc deficiency, genes encoding zinc transporters ZINC-REGULATED TRANSPORTER (ZRT), IRON-REGULATED TRANSPORTER (IRT)-LIKE PROTEIN (ZIP) were up-regulated in roots and flag leaves, suggesting their important roles in zinc uptake and mobilization. The expression of deoxymugineic acid (DMA) synthesis- and transport-related genes such as *DEOXYMUGINEIC ACID SYNTHASE* (*DMAS*), *ZINC-INDUCED FACILITATOR-LIKE* (*ZIFL*), and *YELLOW STRIPE-LIKE* (*YSL*) was down-regulated in zinc-deficient roots but up-regulated in flag leaves, indicating a stronger role of DMA in zinc mobilization than zinc acquisition.

Further, in line with development of biofortified transgenic cereal crops with increased iron content or iron deficiency tolerance, it is necessary to study the impact of transgenes on endogenous iron homeostasis related genes. In my PhD study, the expression of 28 endogenous rice genes was studied in high grain iron containing NFP rice (transgenic rice expressing *NICOTIANAMINE SYNTHASE*, *FERRITIN*, and *PHYTASE* genes) and its non-transgenic siblings, which were subjected to iron-deficient and iron-sufficient hydroponic systems (Wirth *et al.*, 2009). The overall iron homeostasis was not significantly affected in the NFP rice, but the expression of genes related to PS biosynthesis was positively modulated in NFP rice.

Together, this PhD work provides integrated information on the molecular response of bread wheat to iron- and zinc-deficiency stress. Additionally, it provides insight into expression modulation of endogenous genes in high iron transgenic rice. The characterization of gene expression changes could also provide useful information for future biofortification programs.

ZUSAMMENFASSUNG

Eisen und Zink sind essenzielle Spurenelemente in allen Organismen der belebten Welt. Sie agieren als Kofaktoren für viele Schlüsselenzyme und sind involviert in verschiedensten metabolischen und biosynthetischen Stoffwechselwegen. In Nutzpflanzen führt Eisen- und Zink-Mangel zu substantiellen Ertragsverlusten und vermindert dem Nährwert. Um biotechnologisch verbesserte (biofortifizierte) Nutzpflanzen erstellen zu können, die entweder Eisen- und Zink-Mangel besser tolerieren können oder erhöhten Eisen- und Zink-Konzentrationen liefern, fehlt es jedoch an Informationen, insbesondere bezüglich der molekularen Mechanismen der Eisen- und Zink-Homöostase in Nutzpflanzen, wie Weizen und Reis.

In der vorliegenden Doktorarbeit habe ich RNA-Sequenzierungen und qRT-PCRs verwendet um die molekularen Mechanismen aufzudecken, die für die Regulation und den Transport von Eisen und Zink in Brotweizen (*Triticum aestivum*) verantwortlich sind. Weizen exprimiert unter Eisen-Mangel verstärkt Gene, die involviert sind in der Biosynthese von Phytosiderophore, dem Citratzyklus, und verschiedenen Transkriptionsfaktoren. Des Weiteren sind Gene aus mehreren Eisen-Transporter Familien signifikant hochreguliert, unter anderem aus der Genfamilie der MAJOR FACILITATOR SUPERFAMILY (MFS), der ATP-BINDING CASSETTE (ABC) Transporter Superfamilie, der NATURAL RESISTANCE ASSOCIATED MACROPHAGE PROTEIN (NRAMP) Familie und der OLIGOPEPTIDE TRANSPORTER (OPT) Familie. Dies deutet auf eine wichtige Rolle dieser Gene für die Eisen-Homöostase hin.

Unter Zink-Mangel waren in den Wurzeln und Fahnenblättern des Brotweizen verschiedene Zink-Transporter Gene signifikant hochreguliert, insbesondere ZINC-REGULATED TRANSPORTER (ZRT), IRON-REGULATED TRANSPORTER (IRT)-LIKE PROTEIN (ZIP) Gene. Diese Gene sind daher wahrscheinlich involviert in der Aufnahme und Mobilisation von Zink.

Des Weiteren sind unter Zink-Mangel Synthese- und Transporter-Gene von Deoxymugineic acid (DMA), wie *DEOXYMUGINEIC ACID SYNTHASE* (*DMAS*), *ZINC-INDUCED FACILITATOR-LIKE* (*ZIFL*), und *YELLOW STRIPE-LIKE* (*YSL*), in Fahnenblättern stark exprimiert, während sie in Wurzeln schwächer exprimiert sind. Dies deutet darauf hin, dass DMA stärker involviert ist in der Mobilisation von Zink als in dessen Aufnahme.

Darüber hinaus ist es für die Entwicklung von transgenem Getreidepflanzen mit erhöhter Toleranz von Eisen-Mangel oder mit erhöhtem Nährstoffgehalt an Eisen wichtig die Auswirkungen von überexprimierten Transgenen auf die Expression endogener Eisen-Homöostase-Gene zu untersuchen. Daher habe ich die Expression von 28 endogenen Reisgenen der NFP Linie und ihrer nicht-transgenen Schwesterlinie bestimmt. NFP ist eine transgene Reislinie, die biotechnologisch mit *NICOTIANAMINE SYNTHASE*, *FERRITIN*, und *PHYTASE* Genen transformiert wurde. Ich habe die endogene und transgene Genexpression unter Eisen-Mangel und Kontrollbedingungen in hydroponischem Kultur verglichen (Wirth *et al.*, 2009). Im Allgemeinen waren die endogenen Eisen-Homöostasegene in der NFP-Linie nicht beeinflusst, jedoch waren die Phytosiderophor-Synthesegene im NFP Reis verstärkt exprimiert im Vergleich zur nicht-veränderten Schwesterlinie.

Zusammengefasst liefert die vorliegende Doktorarbeit ganzheitlichen Einblick in die molekulare Stressantwort vom Brotweizen auf Eisen- und Zink-Mangel. Des Weiteren liefert die Arbeit Erkenntnisse bezüglich der Regulation von Eisen-Homöostasegenen in biofortifiziertem Reislinien. Somit stellen diese Beschreibungen wertvolle Informationen für zukünftige Biofortifikation Initiativen dar.

LIST OF ABBREVIATIONS

ABC	ATP-BINING CASSETTE
ABI/VP	ABA-INSENSITIVE/VIVIPAROUS
AGO	ARGONAUTE
AHA	Arabidopsis H^+-ATPase
AP	APETALA
ARF	AUXIN RESPONSIVE FACTOR
bHLH	BASIC HELIX-LOOP-HELIX
bZIP	BASIC LEUCINE-ZIPPER
Cd	cadmium
GCN	GENERAL CONTROL NON-REPRESSED PROTEIN
Cit	citrate
Co	cobalt
cv.	cultivar
DCL	DICER-LIKE
DEGs	differentially expressed genes
DMA	DEOXYMUGINEIC ACID
DMAS	DEOXYMUGINEIC ACID SYNTHASE
DMT	DRUG/METABOLITE TRANSPORTER
DPA	days post anthesis
Fe	iron
FER	IRON DEFICIENCY RESPONSE
FIT	IRON DEFICIENCY RESPONSE-LIKE IRON DEFICIENCY INDUCED TRANSCRIPTION FACTOR
FRD	FERRIC REDUCTASE DEFECTIVE
FRDL	FERRIC REDUCTASE DEFECTIVE-LIKE
FRO	FERRIC REDUCTASE OXIDASE
GC-MS	gas chromatography-mass spectrometry
HMA	HEAVY METAL ATPases
3-HMA	3- hydroxymugineic acid
epiHDMA	3-epihydroxy-2-deoxymugineic acid

epiDMA	3-epihydroxymugineic acid
IAA	indoleacetic acid
IDA	iron deficiency anemia
IDE	IRON DEFICIENCY-RESPONSE CIS-ACTING ELEMENT
IDEF	IDE BINDING FACTOR
IDF	IRT1 DEGRADATION FACTOR1
IDS	IRON DEFICIENCY-SPECIFIC CLONE
IRE/IRP	iron responsive element (IRE)/iron regulatory protein (IRP)
IREG/FPN	IRON REGULATED PROTEIN/FERROPORTIN
IRT	IRON REGULATED METAL TRANSPORTER
IRO	IRON DEFICIENCY-INDUCIBLE bHLH TRANSCRIPTION FACTOR
MA	mugineic acid
MAL	malate
MATE	MULTIDRUG AND TOXIC EFFLUX
MFS	MAJOR FACILITATOR SUPERFAMILY
MIR	MITOCHONDRIAL IRON REGULATED
MIT	MITOCHONDRIAL IRON TRANSPORTER
Mn	manganese
MRP	MULTIDRUG RESISTANCE-ASSOCIATED PROTEIN
MTP	METAL TOLERANCE PROTEIN
MYB	MYELOBLASTOSIS
NA	nicotianamine
NAC	NO APICAL MERISTEM (NAM)/ARABIDOPSIS TRANSCRIPTION ACTIVATION FACTOR (ATAF)/CUP-SHAPED COTYLEDON (CUC)
NAS	NICOTIANAMINE SYNTHASE
NAAT	NICOTIANAMINE AMINOTRANSFERASE
NO	nitric oxide
NRAMP	NATURAL RESISTANCE ASSOCIATED MACROPHAGE PROTEIN
NTS	non-transgenic siblings
OPT	OLIGOPEPTIDE TRANSPORTER
Pb	plumbum

PCR	polymerase chain reaction
PCR	PLANT CADMIUM RESISTANCE
PDR	PLEIOTROPIC DRUG RESISTANCE
PIC	PERMEASE IN CHLOROPLAST
PS	phytosiderophore
qRT-PCR	quantitative real time-PCR
SAMS	S-ADENOSYLMETHIONINE SYNTHETASE
SKB/PRMT	NEUROTOXIN (ShK1) BINDING PROTEIN/PROTEIN ARGININE METHYLTRANSFERASE
SNX	SORTING NEXIN
TCA	glycolysis and tricarboxylic acid
TOM	TRANSPORTER OF MUGINEIC ACID
VIT	VACUOLAR IRON TRANSPORTER
WHO	World Health Organization
YS	YELLOW STRIPE
YSL	YELLOW STRIPE-LIKE
ZDRE	zinc deficiency response element
ZIF	ZINC-INDUCED FACILITATOR
ZIP	ZINC-REGULATED TRANSPORTER (ZRT), IRON-REGULATED TRANSPORTER (IRT)-LIKE PROTEIN
ZIFL	ZINC INDUCED FACILITATOR-LIKE
Zn	zinc

TABLE OF CONTENTS

1 GENERAL INTRODUCTION

1.1 Importance of iron and zinc

1.1.1 Importance of iron for plants

Iron is an essential micronutrient required in many biological processes as it functions as a cofactor to some key enzymes, including cytochrome, hydrogenase, nitrogenase, and peroxidase. Iron is involved in the electron transport chain in respiration and photosynthesis, and regulates the biosynthesis of chlorophyll, vitamins, and cytochromes (Balk and Schaedler, 2014). Although iron is the second most abundant metal in the Earth's crust, plants often suffer from iron deficiency due to the insolubility of iron in aerobic, calcareous and/or high pH soils (Morrissey and Guerinot, 2009). In most cereals, iron deficiency leads to interveinal chlorosis resulting in pattern of green and yellow stripes, particularly in the young leaves, thereby affecting crop yield and quality (Barker and Stratton, 2015).

1.1.2 Importance of zinc for plants

Zinc is an essential element for all organisms. In plants, zinc binds to more than 500 proteins (Graham, 2008) and is an integral component of many enzymes, such as alcohol dehydrogenase, carbonic anhydrase, RNA polymerase, alkaline phosphatase, and copper/zinc superoxide dismutase (Guerinot and Eide, 1999). Consequently, zinc is crucial for many biological processes, such as carbohydrate metabolism, tryptophan and indoleacetic acid (IAA) synthesis, cellular membrane integrity maintenance, and protein synthesis (Broadley *et al.*, 2012). Nearly half of the soil worldwide is estimated to be zinc-deficient (Das and Green, 2016). The deficiency of zinc in plants often causes chlorosis in older leaves and small emerging leaves, leading to photosynthesis retardation. Zinc deficiency also cause short internodal distance, growth retardation and slows down the flowering and development of fruit (Das and Green, 2016), leading to crop-yield losses and decreased quality (Alloway, 2008).

1.1.3 Importance of iron and zinc for humans, and crop biofortification

Iron-deficiency anemia affects the health of over one-third of the world’s population, especially women and children in developing countries (WHO, 2016). The symptoms of iron deficiency include shortness of breath, headache, cold hands and feet, extreme fatigue, and

even mental retardation (Boccio and Iyengar, 2003; WHO, 2016). Zinc deficiency affects the health of nearly 2 billion people globally, causing syndromes such as rough skin, neuro-sensory disorders, growth and immune impairment (Cakmak, 2008; Prasad, 2012).

Rice and wheat constitute two most widely consumed staple food crops that offer nutrition and caloric intake to humans. The United States Department of Agriculture (USDA) estimates that the worldwide production of rice and wheat in the year 2016/2017 will be 480.72 and 730.83 million tons, respectively (World-Rice-Production, 2016; World-Wheat-Production, 2016). Nearly 3 billion people worldwide rely on rice as a staple food, and over 90% of the world's rice is consumed in Asia (IRRI, 2016). Likewise, wheat is the most widely grown commercial crop around the world, and feeds almost half of the world's population (Gupta *et al.*, 2005). However, rice and wheat are poor source of iron and zinc, and cannot fulfill the nutritional requirements of humans, especially for the ones who live on a plant-based diet. Biofortification of cereal grains is an efficient and long-term solution to combat iron and zinc malnutrition. Transformation of cereals with iron and zinc storage, uptake and transport related genes, such as *FERRITIN*, *NICOTIANAMINE SYNTHASE* (*NAS*), *IRON-REGULATED TRANSPORTER* (*IRT*) and *YELLOW STRIPE-LIKE* (*YSL*), either independent or in combination, could increase the iron and zinc concentration in endosperms (Boonyaves *et al.*, 2016; Ishimaru *et al.*, 2010; Masuda *et al.*, 2012; Trijatmiko *et al.*, 2016; Wirth *et al.*, 2009). Therefore, there is an increasing demand for information on the molecular players that participate in iron and zinc homeostasis.

1.2 Molecular mechanisms of iron and zinc uptake, translocation, and regulation in plants

1.2.1 Iron and zinc uptake strategies in plants

1.2.1.1 Iron uptake in plants

Non-graminaceous and graminaceous plants utilize reduction (strategy I) or chelation (strategy II) strategies for iron acquisition, respectively. In the reduction strategy, protons are released into the soil via H^+-ATPases (AHA) to increase the solubility of Fe(III), as well as to establish an ion gradient, which then provides a driving force for Fe(II) transport across the root cell plasma membrane (Palmgren, 2001). In Arabidopsis, this acidification step is mediated by AHA2 (Santi and Schmidt, 2009). Subsequently, the Fe(III) is reduced to Fe(II) on the root surface by FERRIC CHELATE REDUCTASE (FRO). In Arabidopsis, the *FRO2*

gene, one of the eight members of the FRO family, encode this Fe(III) chelate reductase (Robinson *et al.*, 1999). The Fe(II) is then transported into root cells by the plasma membrane localized transporter IRT1, which is a member of the ZINC-REGULATED TRANSPORTER (ZRT), IRON-REGULATED TRANSPORTER (IRT)-LIKE PROTEIN (ZIP) divalent metal transporter family (Connolly *et al.*, 2002). The IRT1 is also known to transport Zn(II), Mn(II), Co(II), and Cd(II) (Korshunova *et al.*, 1999). The *AHA2*, *IRT1*, and *FRO2* are induced in the roots upon iron deficiency (Connolly *et al.*, 2002; Robinson *et al.*, 1999; Santi and Schmidt, 2009).

The strategy I plants generally take up Fe(II), whereas the strategy II plants solubilize soil Fe(III) by secreting Fe(III) chelators (Figure 1.1). The biosynthesis of mugineic acid (MA) family phytosiderophores (PSs) marks the first step. L-methionine is the predominant precursor, which is converted to deoxymugineic acid (DMA) via a conserved pathway of sequential enzymatic reactions mediated by S-ADENOSYLMETHIONINE SYNTHETASE (SAMS), NAS, NICOTIANAMINE AMINOTRANSFERASE (NAAT), and DEOXYMUGINEIC ACID SYNTHASE (DMAS) (Kobayashi *et al.*, 2010b). The DMA is further modified to form other MAs, such as 3-hydroxymugineic acid (3-HMA), 3-epi-hydroxymugineic acid (epi-HMA), and 3-epi-hydroxy-2'-deoxymugineic acid (epi-HDMA), depending on the plant species (Kim and Guerinot, 2007). Upon iron deficiency, the *OsSAMS1*, *OsSAMS2*, *OsNAS1*, *OsNAS2*, *OsNAS3*, *OsNAAT1* and *OsDMAS1* are up-regulated in rice roots, suggesting their important roles in iron acquisition (Bashir *et al.*, 2006; Inoue *et al.*, 2003; Inoue *et al.*, 2008; Kobayashi *et al.*, 2005; Zhou *et al.*, 2013).

The MAs are released to rhizosphere by the TRANSPORTER OF MUGINEIC ACID (TOM) (Nozoye *et al.*, 2011). The *TOM* genes are *ZINC INDUCED FACILITATOR-LIKE* (*ZIFL*) genes, which are members of the *MAJOR FACILITATOR SUPERFAMILY* (*MFS*). The expression of *TOM1* is induced in roots and shoots upon iron deficiency (Nozoye *et al.*, 2011). After secretion, the MAs bind Fe(III) to form Fe(III)-MA complexes, which are then transported into the root epidermis by YSL transporters. In rice, the plasma membrane-localized transporter OsYSL15 serves this function (Inoue *et al.*, 2009; Lee *et al.*, 2009a). In maize and barley, ZmYS1 and HvYS1 mediate this iron-uptake function, respectively. However, unlike ZmYS1, which transports MA and NA chelated metals, barley HvYS1 specifically transports Fe(III)-MA, but not Fe-NA (Curie *et al.*, 2001; Murata *et al.*, 2006; Schaaf *et al.*, 2004).

Additionally, rice plants take up Fe(III)-MA via the strategy II system as well as free Fe(II) through strategy I uptake system. The *OsIRT1* and *OsIRT2* genes are the rice homologs of Arabidopsis *AtIRT1* and their expression is induced under iron-deficiency stress (Ishimaru *et al.*, 2006). However, unlike the strategy I plants, the FRO activity is not iron deficiency-inducible on the surface of rice roots (Ishimaru *et al.*, 2006) (Figure 1.1).

1.2.1.2 Zinc uptake in plants

Zinc is acquired primarily as divalent cation Zn(II) by plant roots from the soil (Broadley *et al.*, 2012; Gupta *et al.*, 2016). The ZIP transporter family members are considered to facilitate the zinc-uptake function in plant roots (Figure 1.1). The ZIP proteins are predicted to have eight transmembrane domains, and localize on the plasma membrane and endomembrane system (Li *et al.*, 2013a; Ricachenevsky *et al.*, 2015). In Arabidopsis, *AtZIP1* and *AtZIP3* are expressed in roots in response to zinc deficiency, indicating their role in zinc acquisition from the soil (Grotz *et al.*, 1998). The rice ZIP transporters, including OsZIP1 and OsZIP8, function in zinc uptake from soil (Bashir *et al.*, 2012; Lee *et al.*, 2010b). In addition, organic ligands, such as organic acids and MAs, are suggested to be involved in zinc uptake (Gupta *et al.*, 2016). However, the release of MAs in response to zinc deficiency varies depending on the plant species. DMA is the predominant MA secreted by roots in response to zinc deficiency in wheat (Cakmak *et al.*, 1994). The expression of MAs biosynthesis genes, such as *HvNAS1*, *HvNAAT-A*, *HvNAAT-B*, barley *IRON DEFICIENCY-SPECIFIC CLONE* 2 (*HvIDS2)*, and *HvIDS3* are elevated in zinc-deficient barley roots, and MA synthesis increases as well (Suzuki *et al.*, 2006). Moreover, more Zn(II)-MAs than free Zn(II) were absorbed in zinc-deficient barley roots (Suzuki *et al.*, 2006).

1.2.2 Long-distance iron and zinc transport

1.2.2.1 Long-distance transport of iron

During translocation, iron binds with chelators to reduce the risk of toxic ROS production by free iron (Alvarez-Fernandez *et al.*, 2014). DMA is low-molecular-weight amino acid iron chelator that derives from nicotianamine (NA). Apart from facilitating iron uptake in graminaceous plants, DMA is also involved in long-distance transport of iron in xylem, as well as phloem (Aoyama *et al.*, 2009; Kakei *et al.*, 2009). NA is an intermediate in the production of DMA. It has a high affinity to Fe(II) and Fe(III), and also forms complexes with other divalent metals, such as Zn(II), Mn(II), Ni(II), and Cu(II) (Clemens *et al.*, 2013).

Additionally, organic acids, such as citrate (Cit) and malate (Mal) also bind Fe(III) and therefore form complexes with iron, such as $Fe(III)_3Cit_3$ (Rellan-Alvarez *et al.*, 2010), $Fe(III)Cit_2$, $Fe(III)_3Cit_2Mal_2$, and $Fe(III)_3Cit_3Mal_1$ (Grillet *et al.*, 2014).

When iron is loaded into roots, radial transport of iron occurs from the root epidermis to the xylem vessels either by the apoplastic or symplastic pathway (Kerkeb and Connolly, 2006). NA is suggested to chelate iron during symplastic translocation (Curie *et al.*, 2009). Iron is then loaded into xylem for translocation to shoot. Citrate is one of the major iron chelators in the xylem sap of graminaceous as well as non-graminaceous plants (Ariga *et al.*, 2014). Arabidopsis FERRIC REDUCTASE DEFECTIVE 3 (FRD3) is a plasma transmembrane protein, belonging to the MULTIDRUG AND TOXIN EFFLUX (MATE) family, and mediates citrate efflux into the root xylem in Arabidopsis (Durrett *et al.*, 2007). It also mediates citrate release for iron solubilization in the apoplastic space separating two tissues without symplastic connections (Roschzttardtz *et al.*, 2011) (Figure 1.1). The FERRIC REDUCTASE DEFECTIVE-LIKE transporter in rice, OsFRDL1, localizing at the pericycle cells, is also a citrate transporter that facilitates iron-citrate translocation from rice roots to shoots (Yokosho *et al.*, 2009). Working in parallel with the FDR3, the IRON REGULATED1/FERROPORTIN1 (IREG1/FPN1) also facilitates iron loading into the apoplastic space of the xylem (Morrissey *et al.*, 2009). In addition to citrate, DMA also serves iron translocation in the xylem (Ariga *et al.*, 2014). OsYSL16 transports Fe(III)-DMA via the vascular bundles, especially xylem (Kakei *et al.*, 2012).

Transpiration flow in the xylem is inefficient for iron translocation to developing organs such as apex, seeds and root tips, therefore plants also need to transport iron through the phloem. The mobilization of iron from older to younger leaves also occurs via the phloem. NA and DMA facilitate iron transport in the phloem as well (Jeong and Guerinot, 2009). Generally, the YSL family transports metal-DMA and/or metal-NA in plants. The proton-coupled symporter YS1 transports various PS-bound metals, including Fe(III)-DMA, Zn(II)-DMA, Cu(II)-DMA, Ni(II)-DMA, as well as Fe(II)-NA, Fe(III)-NA, and Ni(II)-NA complexes (Schaaf *et al.*, 2004). OsYSL2 mediates the phloem transport of Fe(II)-NA and Mn(II)-NA, but not Fe(III)-DMA, including iron loading to the leaves and grains (Ishimaru *et al.*, 2010; Koike *et al.*, 2004). OsYSL18 is an Fe(III)-DMA transporter involved in iron translocation in reproductive organs and phloem of lamina joints (Aoyama *et al.*, 2009). Other than the YSL family, peptide transport (PT) clade of OLIGOPEPTIDE TRANSPORTER (OPT), also transports Fe(II)-NA and Fe(III)-NA in rice (Vasconcelos *et al.*, 2008). The phloem-specific

iron transporter OPT3 in Arabidopsis facilitates the function of iron recirculation from the xylem to the phloem (Zhai *et al.*, 2014) (Figure 1.1).

1.2.2.2 Long-distance transport of zinc

Compared to iron, much less is currently known about the xylem and phloem transport of zinc. P_{1B}-type ATPase, also known as HEAVY METAL ATPases (HMAs), facilitate the function of metal transport and homeostasis in plants (Gupta *et al.*, 2016). In Arabidopsis, *HMA2* and *HMA4* mainly express in the vascular tissues of roots, stems, and leaves and are suggested to function in the root-to-shoot zinc translocation (Hussain *et al.*, 2004). Another root-to-shoot zinc transporter, Arabidopsis PLANT CADMIUM RESISTANCE2 (PCR2), works independently from HMA2 and HMA4. The PCR2 is involved in the radial transport of zinc from the epidermis to the cortex of roots (Song *et al.*, 2010) (Figure 1.1).

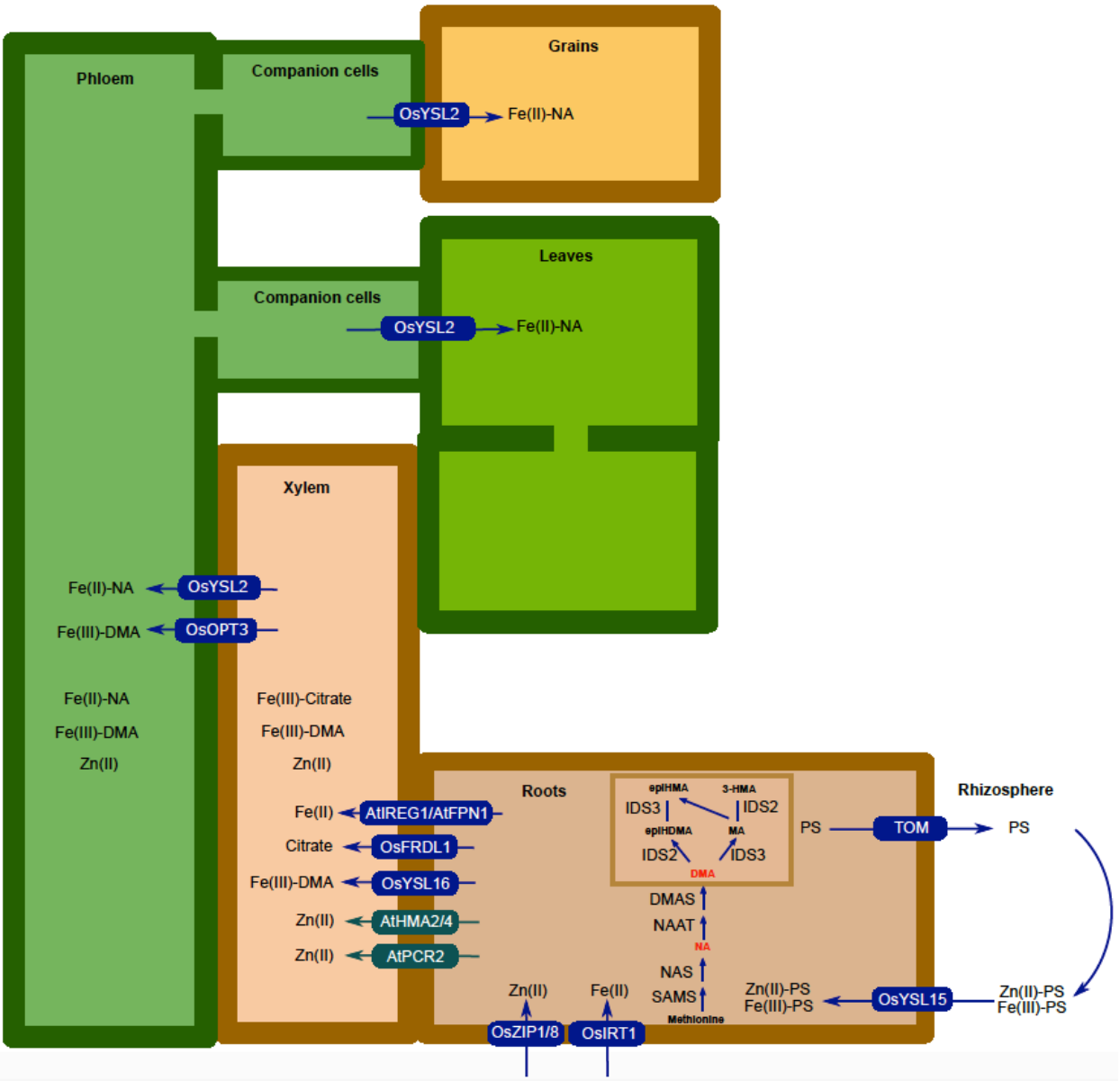

Figure 1.1. Mechanisms for iron and zinc uptake by cereal roots and long-distance translocation. Cereal plants utilize strategy II for iron acquisition from rhizosphere. Rice is unique among graminaceous plants, which utilizes part of the strategy I iron-uptake pathway in addition to strategy II pathway. Iron and zinc is loaded to xylem and phloem to transport to leaves and grains. Rice proteins are labeled with respect to their functions and where unknown, Arabidopsis proteins are mentioned. SAMS: S-ADENOSYL-L-METHIONINE SYNTHETASE; NAS: NICOTIANAMINE SYNTHASE; NAAT: NICOTIANAMINE AMINOTRANSFERASE; DMAS: DEOXYMUGINEIC ACID SYNTHASE; IDS: IRON DEFICIENCY SPECIFIC CLONE; PS: phytosiderophore; TOM: TRANSPORTER OF MUGINEIC ACID; YSL: YELLOW STRIPE-LIKE; IRT: IRON-REGULATED TRANSPORTER; ZIP: ZINC-REGULATED TRANSPORTER (ZRT), IRON-REGULATED TRANSPORTER (IRT)-LIKE PROTEIN; HMA: HEAVY METAL ATPases; FRDL: FERRIC REDUCTASE DEFECTIVE-LIKE; IREG/FPN: IRON REGULATED/FERROPORTIN; PCR: PLANT CADMIUM RESISTANCE; OPT: OLIGOPEPTIDE TRANSPORTER; NA: nicotianamine; DMA: deoxymugineic acid; MA: mugineic acid; 3-HMA: 3-hydroxymugineic acid; epi-HMA: 3-epi-hydroxymugineic acid; epi-HDMA:3-epi-hydroxy-2'-deoxymugineic acid.

1.2.3 Intracellular transport and storage of iron and zinc

1.2.3.1 Intracellular transport of iron

Most of the iron found in mesophyll cells is located in chloroplasts (Terry and Low, 1982). Iron needs to be reduced from Fe(III) to Fe(II) by chloroplast membrane-bound FRO before the uptake by chloroplasts. FRO7 is the only Arabidopsis FRO family member localizing in the chloroplast, and is essential for chloroplast iron acquisition (Jeong *et al.*, 2008). PERMEASE IN CHLOROPLAST (PIC) participates in iron transport into chloroplasts, thereby affecting plant growth and development in Arabidopsis and tobacco (Duy *et al.*, 2011; Duy *et al.*, 2007; Gong *et al.*, 2015). The Arabidopsis AtYSL4 and AtYSL6 perform the opposite function of PIC to export iron from the chloroplasts (Divol *et al.*, 2013). Iron transport and homeostasis in mitochondria is also controlled. MITOCHONDRIAL IRON TRANSPORTER (MIT) participates in transporting iron into mitochondria (Bashir *et al.*, 2011), and rice-specific *MITOCHONDRIAL IRON-REGULATED* gene (*OsMIR*) is suggested to regulate iron homeostasis in mitochondria (Ishimaru *et al.*, 2009). In the case of the storage organelle vacuole, iron influx and efflux are tightly controlled, according to the plant iron status. NATURAL RESISTANCE ASSOCIATED MACROPHAGE PROTEIN (NRAMP) is crucial for transporting iron out of vacuoles; while the VACUOLAR IRON TRANSPORTER (VIT) performs the opposite function (Lanquar *et al.*, 2005; Zhang *et al.*, 2012). In Arabidopsis, the MFS transporter IREG2/FPN2 localizes at the vacuolar membrane and facilitates transport of iron and cobalt into the vacuole. The gene encoding IREG2/FPN2 is induced by iron deficiency (Morrissey *et al.*, 2009) (Figure 1.2).

1.2.3.2 Intracellular transport of zinc

Plant cell vacuoles constitute the major cell organelle for zinc storage and detoxification of excess zinc (Sinclair and Kramer, 2012). The Arabidopsis METAL TOLERANCE PROTEIN 1 (AtMTP1) and AtMTP3 localize in the vacuolar membrane and transport zinc into the vacuole, however, they perform different physiological functions regarding zinc homeostasis (Arrivault *et al.*, 2006; Kobae *et al.*, 2004). AtMTP1 sequestrates excess zinc into vacuoles to function in zinc detoxification, and leads to zinc accumulation in leaves (Desbrosses-Fonrouge *et al.*, 2005; Kobae *et al.*, 2004). On the other hand, AtMTP3 contribute to basic zinc tolerance and zinc partitioning between the roots and shoots. The expression of AtMTP3 is induced to sequester zinc into root vacuoles by exposure to excess zinc in root epidermal and cortex cells, thereby protecting the plant by excluding zinc from the shoot (Arrivault *et*

al., 2006). In cereals, OsMTP1 in rice and HvMTP1 in barley also localize in the vacuolar membrane. However, unlike zinc-specific AtMTP1 in Arabidopsis, OsMTP1 and HvMTP1 transport more than one divalent metal, including Zn(II), Fe(II), Co(II) and Cd(II) (Menguer *et al.*, 2013; Podar *et al.*, 2012; Yuan *et al.*, 2012). Another vacuolar membrane localized transporter, HMA3, was reported to transport Zn(II) and Cd(II) into the vacuole, and therefore function in Zn(II), Cd(II), Co(II), and Pb(II) detoxification (Morel *et al.*, 2009). The vacuolar membrane localized MFS transporter in Arabidopsis, ZINC INDUCED FACILITATOR1 (ZIF1), transports NA into vacuoles, and over-expression of *ZIF1* leads to zinc accumulation in root vacuoles (Haydon and Cobbett, 2007; Haydon *et al.*, 2012). Localizing to the chloroplast envelope, AtHMA1 may export zinc out of plastids, and thereby functions in zinc detoxification (Kim *et al.*, 2009). IRT3 protein localizes in the plasma membrane and functions as a zinc- and iron-uptake transporter in Arabidopsis (Lin *et al.*, 2009). Unlike AtIRT1, Arabidopsis IRT2 does not participate in iron uptake in roots, but rather localizes to intracellular vesicles and may transport Fe(II) and Zn(II) (Vert *et al.*, 2009) (Figure 1.2).

1.2.3.3 Storage of iron and zinc

FERRITIN plays a role of iron-storage and exists ubiquitously in plants, animals, and bacteria (Briat *et al.*, 2010). One FERRITIN protein has the capacity to harbor up to 4,500 iron atoms (Harrison and Arosio, 1996). Unlike animal FERRITINs, which are mostly cytoplasmic, plant FERRITINs are largely found in plastids, such as chloroplasts, proplastids, etioplasts, chromoplasts, and amyloplasts (Seckback, 1982). FERRITINs may also localize in plant mitochondria, as shown in pea stem cells (Zancani *et al.*, 2004). Expression of *AtFERRITIN1* and *AtFERRITIN3* are elevated in response to iron excess (Petit *et al.*, 2001). Two genes encoding FERRITIN have been identified in rice (*OsFERRITIN1* and *OsFERRITIN2*), and the expression of *OsFERRITIN2* is induced upon exposure to excess iron (Stein *et al.*, 2009).

Metallothioneins (MTs) are cysteine-rich, low-molecular-weight proteins. They bind zinc, and participate in zinc storage (Hamer, 1986). AtMT4a and AtMT4b proteins exhibited high zinc-binding affinity in Arabidopsis (Guo *et al.*, 2008). They express in cytoplasm, nucleus and membrane, and contribute to zinc storage or buffering (Ren *et al.*, 2012). Overexpression of *AtMT4a* and *AtMT4b* increase zinc accumulation in siliques and seeds of Arabidopsis (Ren *et al.*, 2012). In barley, *MT4* predominantly expresses in embryo and aleurone layer, and therefore function in zinc storage in developing and mature grains (Hegelund *et al.*, 2012) (Figure 1.2).

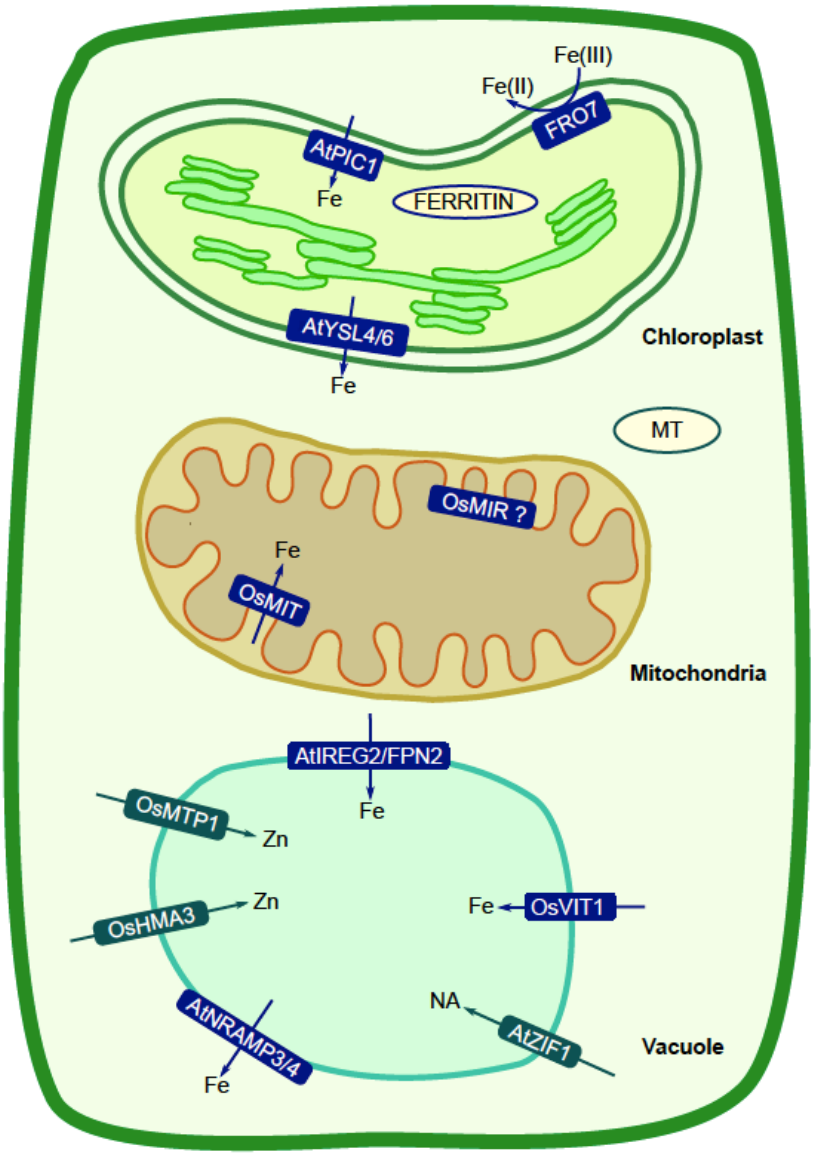

Figure 1.2. Intracellular iron and zinc transport and storage in plants. Cell organelles such as chloroplast, mitochondria and vacuole participate in iron and zinc transport and storage. Arabidopsis and/or rice proteins are labeled according to their proposed functions. Proteins and their functions are described in detail throughout the introduction text. FRO: FERRIC CHELATE REDUCTASES; PIC: PERMEASE IN CHLOROPLASTS; YSL: YELLOW STRIPE-LIKE; MIT: MITOCHONDRIAL IRON TRANSPORTER: MIR: MITOCHONDRIAL IRON REGULATED; NRAMP: NATURAL RESISTANCE ASSOCIATED MACROPHAGE PROTEIN; IREG/FPN: IRON REGULATED/FERROPORTIN; ZIF: ZINC INDUCED FACILITATOR; VIT: VACUOLAR IRON TRANSPORTER; HMA: HEAVY METAL ATPases; MTP: METAL TOLERANCE PROTEIN; MT: METALLOTHIONEIN.

1.2.4 Iron and zinc homeostasis regulation

The bHLH transcription factor family members, such as rice FER-LIKE IRON DEFICIENCY INDUCED TRANSCRIPTION FACTOR (FIT) (Colangelo and Guerinot, 2004) and IRON

DEFICIENCY-INDUCIBLE bHLH TRANSCRIPTION FACTOR 2 (OsIRO2) (Ogo *et al.*, 2006), are most widely reported to positively regulate iron homeostasis in plants. The iron deficiency-induced transcription factor FIT is an ortholog of tomato IRON DEFICIENCY RESPONSE (FER) (Ling *et al.*, 2002), which regulates *FRO2* gene expression and IRT1 protein accumulation in Arabidopsis (Colangelo and Guerinot, 2004). bHLH38 and bHLH39 form heterodimers with FIT, respectively, and thus perform a regulation function (Yuan *et al.*, 2008b). In rice, OsIRO2 regulates DMA biosynthesis genes and genes encoding iron transporters, including *OsNAS1*, *OsNAS2*, *OsNAAT1*, *OsDMAS1*, *OsYSL15*, and *TOM1* (Ogo *et al.*, 2006; Ogo *et al.*, 2011; Ogo *et al.*, 2007). Overexpression of *OsIRO2* results in elevated expression of its targeted genes and improved iron- deficiency tolerance in calcareous soil (Ogo *et al.*, 2011). However, another iron-deficiency induced rice transcription factor, OsbHLH133, suppresses root-to-shoot iron translocation (Wang *et al.*, 2013a). In addition, OsIRO3 suppresses iron-deficiency responsive genes, such as *OsNAS1*, *OsNAS2*, *OsIRO2*, *OsIRT1*, *OsYSL15*, and *OsNRAMP1*(Zheng *et al.*, 2010).

In addition to the bHLH family, some members from the NO APICAL MERISTEM (NAM)/ARABIDOPSIS TRANSCRIPTION ACTIVATION FACTOR (ATAF)/CUP-SHAPED COTYLEDON (CUC) (NAC) transcription factor family also participate in iron homeostasis regulation. IRON DEFICIENCY-RESPONSIVE CIS-ACTING ELEMENT 2 (IDE2) BINDING FACTOR (OsIDEF2) is a NAC family member bound to the promoter of *OsYSL2*, and therefore regulates the gene expression (Ogo *et al.*, 2008). Similar to OsIDEF2, OsIDEF1 from plant-specific transcription factor family ABA-INSENSITIVE3/VIVIPAROUS1 (ABI3/VP1) recognizes the CATGC sequence within cis-acting element, IDE1 (Kobayashi et al., 2007). IDEF1 directly binds to divalent metals, such as Fe(II) and Zn(II), and thereby senses cellular metal balance (Kobayashi *et al.*, 2007).

Zinc-deficiency stress response regulation is not as widely studied as iron. Other than OsIDEF1, which could sense zinc at the cellular level, NAC transcription factor NAM-B1 also could positively regulate zinc translocation from vegetative tissues to grains (Uauy *et al.*, 2006; Waters *et al.*, 2009). Moreover, transcription factors BASIC LEUCINE-ZIPPER19 (bZIP19) and bZIP23 regulate the expression of *AtZIP4* in Arabidopsis. These two transcription factors bind to the zinc deficiency response element (ZDRE) of the targeted genes, and thereby regulate the expression of *AtZIP1*, *AtZIP3*, *AtZIP9*, and *AtIRT3* (Assuncao *et al.*, 2010).

1.3 Transcriptomic studies to understand iron- and zinc-deficiency response

Utilizing the microarray hybridization and RNA sequencing approach, expression profiling of iron- and zinc-deficiency response on the transcriptomic level has been achieved in many plant species, such as Arabidopsis (Buckhout *et al.*, 2009; Rodriguez-Celma *et al.*, 2013; Thimm *et al.*, 2001; Yang *et al.*, 2010), soybean (Moran Lauter *et al.*, 2014; O'Rourke *et al.*, 2007; O'Rourke *et al.*, 2009), tomato (Zamboni *et al.*, 2012), rice (Kobayashi *et al.*, 2005), barley (Nagasaka *et al.*, 2009; Negishi *et al.*, 2002), and maize (Li *et al.*, 2014). These global transcription profiling studies provide an opportunity to elucidate the iron- and zinc-deficiency induced molecular responses. However, due to the complex genetic background and poor annotation of the bread wheat genome, there are no transcriptomic studies investigating wheat iron and zinc homeostasis so far.

1.4 Objectives of the thesis

Transcriptional response of bread wheat to iron and zinc deficiency was characterized through RNA sequencing and qRT-PCR based expression profiling approaches. The findings could provide a comprehensive perspective for micronutrient homeostasis studies in cereal plants, and an important reference for future breeding projects.

With regard to iron biofortification, a large number of transgenic plants have been produced by introducing one or multiple iron uptake and transport related genes. The metabolism of transgenic plants is modulated by expression of transgene(s), therefore the concentration of iron in grains is increased. However, the effect of transgenes on the endogenous genes is important to be analyzed. In my PhD study, transgenic NFP rice (transgenic rice expressing *AtNAS1*, *PvFERRITIN*, and *AfPHYTASE* genes) and its non-transgenic siblings, were examined to understand how the transgenes might be affecting other iron homeostasis related genes. Therefore, three objectives were considered in my PhD study:

Objective 1: transcriptome analysis of iron deficiency stress responses in bread wheat.

Objective 2: transcriptome analysis of zinc deficiency stress responses in bread wheat.

Objective 3: expression profiling of iron homeostasis-related genes in transgenic NFP rice plants.

2 EXPRESSION PROFILING OF IRON DEFICIENCY RESPONSIVE GENES IN HEXAPLOID WHEAT

Meng Wang[1], Wilhelm Gruissem[1], and Navreet K. Bhullar[1,*]

[1] Plant Biotechnology, Department of Biology, ETH Zurich (Swiss Federal Institute of Technology), Zurich, Switzerland

[*]Corresponding author

Prepared for submission to scientific publication

2.1 Abstract

Being the most widely cultivated staple food crop, wheat provides energy as well as micronutrients to people around the world. Wheat cultivation is often affected by various nutrient deficiencies, among which iron deficiency leads to severe chlorosis in the plants, thereby reducing total yield. Furthermore, grains of most bread wheat varieties are inherently poor in micronutrients, including iron, which are vital for human nutrition. Despite the significance, iron uptake and translocation mechanisms in bread wheat have not been studied in detail, particularly under iron limited growth conditions. We studied the expression of 19 endogenous bread wheat genes homologous to iron deficiency responsive genes of rice, barley, and Arabidopsis. The expression of the candidate genes were studied in the roots, flag leaves and grains collected at three distinct developmental time points during grain-filling. The wheat homologs of genes involved in phytosiderophores (PSs) synthesis and transport were significantly up-regulated in the iron-deficient roots through all development stages, confirming an important role of deoxymugineic acid (DMA) in iron acquisition. The up-regulation of *NICOTIANAMINE SYNTHASE* (*NAS*) and *DEOXYMUGINEIC ACID SYNTHASE* (*DMAS*) in flag leaves and grains suggests the involvement of nicotianamine (NA) and DMA in iron chelation and translocation in wheat, particularly at the commencement of grain-filling. In line with this, the homolog of gene encoding TRANSPORTER OF MUGINEIC ACID (Ta.5180) was also up-regulated in the wheat roots subjected to iron deficiency. Additionally, genes encoding long-distance iron transporter YELLOW STRIPE-LIKE (YSL), the vacuolar transporter NATURAL RESISTANCE ASSOCIATED MACROPHAGE PROTEIN (NRAMP), and the transcription factor BASIC HELIX-LOOP-HELIX (bHLH), were induced upon iron starvation. For the 19 genes studied here, tissue specific and growth stage specific gene expression differences in response to iron deficiency stress were observed, suggesting involvement of transcription factors and/or long distance metal transporters leading to these distinct changes. Together, the results provide an overview of expression of iron deficiency responsive genes in wheat and identify candidates for wheat improvement.

Keywords: iron deficiency, gene expression, wheat, phytosiderophore synthesis, transcription factors, iron transporters

2.2 Introduction

Iron is an essential micronutrient for all living organisms. In plants, iron functions as redox-active metal in many important metabolic processes such as photosynthesis, mitochondrial respiration, nitrogen assimilation, hormone biosynthesis, and the production and scavenging of reactive oxygen species (Hansch and Mendel, 2009). Although iron ranks as the fourth most abundant element in the earth's crust (Buckhout and Schmidt, 2013), plants often suffer from iron deficiency due to the low bioavailability of this element in aerobic, calcareous and/or high pH soils (Morrissey and Guerinot, 2009). Iron deficiency causes interveinal chlorosis due to failure of plants to produce sufficient chlorophyll and is often identified as alternate yellow and green stripes on younger leaves in most cereals (Barker and Stratton, 2015). As one of the key agricultural problems, iron deficiency restrains plant growth, ultimately leading to yield losses. Additionally, the grain iron content in the cereal crops affected by iron deficiency is further reduced, thereby impacting human nutrition. In this regard, a number of studies elaborated on plant response to iron deficiency stress, and provided an overview of processes involved in iron uptake, translocation and utilization (Buckhout *et al.*, 2009; Kobayashi *et al.*, 2005; Rodriguez-Celma *et al.*, 2013; Thimm *et al.*, 2001; Yang *et al.*, 2010). Such information assists breeding for nutrient-rich cereal grains as well as for iron deficiency tolerant crops.

Since the excess of iron can also be reactive and toxic via the Fenton reaction, plants tightly control and maintain iron homeostasis. Non-graminaceous and graminaceous plants utilize different strategies for iron acquisition from soil. Non-graminaceous plants acquire iron through the reduction strategy (strategy I), in which protons are first released into the rhizosphere by H^+-ATPases to increase the solubility of iron (Santi and Schmidt, 2009). Under the catalysis of FERRIC CHELATE REDUCTASES (FRO), ferric iron (Fe(III)) is reduced to ferrous iron (Fe (II)) (Robinson *et al.*, 1999; Waters *et al.*, 2002). IRON REGULATED TRANSPORTER 1 (IRT1), which is a divalent metal ion transporter localized on the plasma membrane, functions in the transport of Fe(II) into the plant roots (Vert *et al.*, 2002). The graminaceous plants avail the chelation strategy (strategy II) for iron uptake from the soil, where the production of the iron chelators, i.e., mugineic acid (MA) family phytosiderophores (PSs), marks the first key step. The PSs are synthesized from S-adenosyl-L-methionine, through a series of conserved reactions catalyzed by NICOTIANAMINE SYNTHASE (NAS), NICOTIANAMINE AMINOTRANSFERASE (NAAT) and DEOXYMUGINEIC ACID SYNTHASE (DMAS) (Kobayashi *et al.*, 2010b). In addition to

being a precursor for DMA production, NA also chelates iron forming Fe(II)-NA and Fe(III)-NA complexes, and translocates iron within the plants (Takahashi *et al.*, 2003; von Wiren *et al.*, 1999). The DMAs are either directly exported to soil as chelators for iron acquisition, example in rice; or are further converted into other MAs, example in barley (Kobayashi *et al.*, 2010b). The PSs are transported to the rhizosphere by the phytosiderophore efflux transporter TRANSPORTER OF MUGINEIC ACID 1 (TOM1) (Nozoye *et al.*, 2011). The released PSs chelate with Fe(III) and the resulting Fe(III)-PS complexes in the soil are transported back to roots cells by the YELLOW STRIPE-LIKE (YSL) transporter family (Kobayashi and Nishizawa, 2012). *OsYSL15* in rice encodes a Fe(III)-DMA and Fe(II)-NA transporter and is induced in the root epidermis under iron deficiency (Inoue *et al.*, 2008; Lee *et al.*, 2009a). Similar function in Fe(III)-PS transport has been suggested for maize ZmYS1 and barley HvYS1 (Curie *et al.*, 2001; Murata *et al.*, 2006). The YSL family of transporters is also suggested to facilitate long-distance iron transport through the phloem (Inoue *et al.*, 2009; Ishimaru *et al.*, 2010; Lee *et al.*, 2009a).

Specific transporters operate to control iron translocation between the subcellular compartments. The vacuole being a storage organelle, the iron import and export in the vacuoles is dynamically regulated by plant iron status. NATURAL RESISTANCE ASSOCIATED MACROPHAGE PROTEIN (NRAMP) functions in transporting iron out of vacuoles, whereas VACUOLAR IRON TRANSPORTER (VIT) has the opposite function (Lanquar *et al.*, 2005; Zhang *et al.*, 2012). Most of the iron is localized in the chloroplasts in plant leaves (Buckhout and Schmidt, 2013), and PERMEASE IN CHLOROPLASTS 1 (OsPIC1) is associated with iron transport across the inner envelope of chloroplasts in Arabidopsis and tobacco (Duy *et al.*, 2011; Duy *et al.*, 2007; Gong *et al.*, 2015) and Arabidopsis AtYSL4 and AtYSL6 have been shown to export iron out of the chloroplasts (Divol *et al.*, 2013). The MITOCHONDRIAL IRON TRANSPORTER (MIT) (Bashir *et al.*, 2011) is involved in iron transport to the mitochondria.

In addition to the storage in vacuoles, iron is also found in the plastids where it is bound to FERRITIN (Briat *et al.*, 2010). One FERRITIN protein has the capacity to harbor up to 4500 iron atoms (Harrison and Arosio, 1996) and therefore, functions as an iron storage protein in the plants. Due to the iron storage capacity of FERRITIN, endosperm specifically expressed *FERRITIN* genes are often utilized in iron biofortification strategies (Boonyaves *et al.*, 2016; Trijatmiko *et al.*, 2016; Wirth *et al.*, 2009). For example, the endosperm-specific expression of soybean *FERRITIN* in rice led to a 3-fold increase in the iron content of polished rice grains

(Goto *et al.*, 1999). Similarly, a 2-fold iron increase was observed in the milled seeds of aromatic *indica* rice expressing endogenous *OsFERRITIN 2* gene (Paul *et al.*, 2012).

Additionally, several transcription factor families, such as BASIC HELIX-LOOP-HELIX (bHLH), WRKY, and NO APICAL MERISTEM (NAM)/ARABIDOPSIS TRANSCRIPTION ACTIVATION FACTOR (ATAF)/CUP-SHAPED COTYLEDON (CUC) (NAC) are known to actively regulate the iron deficiency stress response (Ogo *et al.*, 2006; Sperotto *et al.*, 2008; Uauy *et al.*, 2006; Wang *et al.*, 2013a). Among these, bHLH transcription factors are the most widely studied with regard to regulation of iron deficiency responsive genes. Transcription factors from the bHLH family modulate iron homeostasis-related genes in many plants, such as IRON DEFICIENCY-INDUCIBLE bHLH TRANSCRIPTION FACTOR 2 (OsIRO2) and OsbHLH133 in rice (Ogo *et al.*, 2006; Wang *et al.*, 2013a), IRON DEFICIENCY RESPONSE (FER) in tomato (Du *et al.*, 2015; Ling *et al.*, 2002), and FER-LIKE IRON DEFICIENCY-INDUCED TRANSCRIPTION FACTOR (FIT) and the Ib subgroup of bHLH transcription factors in non-graminaceous plants such as Arabidopsis (Colangelo and Guerinot, 2004; Wang *et al.*, 2007). Studies have shown that bHLH proteins are also involved in the regulation of iron uptake in chrysanthemum (Zhao *et al.*, 2014) and *Populus* plants (Huang and Dai, 2015).

Being the most widely cultivated commercial crop in the world, wheat feeds nearly half (approximately 40%) of the population and provides 20% of the energy for human nutrition (Gupta *et al.*, 2005). However, unlike model plants such as Arabidopsis and rice, studies on molecular processes controlling iron homeostasis in bread wheat are limited (Uauy *et al.*, 2006; Waters *et al.*, 2009). In particular, molecular response of bread wheat to iron deficiency stress remains to be explored. In this study, we investigated the expression of 19 endogenous iron homeostasis-related genes in bread wheat subjected to iron deficiency stress. The results indicate tissue specific and growth stage specific roles of iron chelators, transporters and transcription factors during iron deficiency stress, providing new insights into iron translocation, storage and regulation in bread wheat.

2.3 Results

The expression of iron deficiency stress responsive endogenous genes was examined in bread wheat plants subjected to iron-deficient and iron-sufficient growth conditions, and at three distinct development stages during grain filling i.e., 8-10 DPA - days post anthesis (stage 1), 25-28 DPA (stage 2), and 33-35 DPA (stage 3). The 19 studied wheat genes included

phytosiderophore biosynthesis related genes as well as several genes encoding different iron transporters, transcription factors and storage protein such as *FERRITIN* (Table 2.1).

2.3.1 Iron deficiency induces expression of genes involved in the phytosiderophore synthesis and secretion

The relative expression levels of wheat homologous genes related to the PS biosynthesis i.e., *SAMS* (Ta.69768), *NAS* (Ta.37977, Ta.5549), *NAAT* (Ta.4977) and *DMAS* (Ta.5335) were significantly increased in response to iron-deficient conditions, particularly in the roots (Table 2.1; Figure 2.1). In the iron-sufficient growth condition, the expression of these five genes was relatively similar in all of the tissues and at all of the studied development stages. For most of the genes, highest elevation in expression was observed in growth stage 1 in roots, with a slight reduction in expression during the subsequent growth stages 2 and 3 (Figure 2.1). The expression of *SAMS* homolog (Ta.69768) increased in roots by 8.2-fold in stage 1, and around 3-fold in stage 2 and 3 (Table 2.1). The *NAS* homologs were up-regulated in roots at least 11-fold at all three stages, but in stage 2 increases as high as 231.3- and 852.6-fold were observed for Ta.37977 and Ta.5549, respectively (Table 2.1). Likewise, the expression of *NAAT* homolog (Ta.4977) increased in roots by 5-fold in stage 1 and 2, and by 3.6-fold in stage 3. The *DMAS* homolog (Ta.5335) exhibited highest increase in expression in the stage 1 (21.8-fold up-regulated in roots), followed by stage 2 (15.1-fold) and 3 (6.9-fold). In line with the increased expression of genes involved in phytosiderophore synthesis, the expression of phytosiderophore efflux transporter *TOM* homolog (Ta.5180) was also significantly up-regulated in the iron-deficient roots in all the development stages, with highest increase in expression in stage 2 (243.3-fold) (Table 2.1).

The expression of phytosiderophore biosynthesis related genes was also induced in the flag leaves, but not as high as in roots. Significant induction of *SAMS* (Ta.69768) in stage 1, *NAS* (Ta.37977, Ta.5549) in stage 2, and of *DMAS* (Ta.5335) in stage 3 could be observed. In addition to the roots and flag leaves, iron deficiency induced gene expression increases were also detected in developing wheat grains. Apart from few exceptions, most of the expression changes in grains were restricted to the growth stage 1 (Table 2.1). The induced expression of the phytosiderophore biosynthesis and acquisition related genes indicate that NA and DMA production was enhanced in response to iron deficiency stress, especially in the roots. A relatively higher induction of expression in the roots, as compared to leaves and grains, relates well to the required increase in phytosiderophore production by the roots and their release to

the rhizosphere for iron chelation. Furthermore, the up-regulation of *NAS* and *DMAS* in flag leaves and grains, suggest the involvement of NA and DMA in long-distance iron translocation within the plants, and also indicate an active transport of iron to the grains in growth stage 1.

2.3.2 Induced expression of genes encoding long-distance iron transporters

The transcript levels of the wheat homologs (Ta.48303, Ta.5463, Ta.29321) of genes encoding metal-nicotianamine transporter YSL increased significantly (Table 2.1). The expression of Ta.48303 was up-regulated over 9-fold in roots during all the stages, and by 2.4-fold in flag leaves in stage 2 (Table 2.1). The expression of Ta.5463 increased in roots by 48.3- and 49.3-fold in stages 2 and 3, respectively, and by 341.2-fold in the flag leaves in stage 1. A significant increase in the expression of the *YSL* homolog Ta.29321 was also observed in the roots, at all the growth stages. While a marginal increase in the expression of Ta.29321 was detected in the grains in stage 1, the gene was down-regulated in flag leaves collected in stage 2.

Nr.	Gene	Unigene ID	Roots			Flag Leaves			Grains		
			Stage1	Stage2	Stage3	Stage1	Stage2	Stage3	Stage1	Stage2	Stage3
1	*SAMS*	Ta.69768	8.2 ↑	3.1 ↑↑	3 ↑	2.8 ↑	1.2	1.4	2 ↑↑	1.5	2
2	*NAS*	Ta.37977	35.3 ↑↑	231.3 ↑↑	11.7 ↑↑	81.8	4.4 ↑	3.1	1.6 ↑↑	1.6 ↑	1.5
3	*NAS*	Ta.5549	70.7 ↑↑	852.6 ↑↑	18.2 ↑↑	612.1	5.6 ↑	36.9	1.5	9.8	2.8
4	*NAAT*	Ta.4977	5.3 ↑↑	5.6 ↑↑	3.6 ↑	1.9	14.1	1.5	1.7 ↑↑	1.3	1.1
5	*DMAS*	Ta.5335	21.8 ↑	15.1 ↑↑	6.9 ↑	2.9	1.2	1.6 ↑	1.4 ↑↑	1.7 ↑↑	1
6	*TOM*	Ta.5180	38.2 ↑↑	243.3 ↑↑	11.3 ↑↑	410.9	6.1	3.7	2.3	46.3	3.7
7	*YSL*	Ta.48303	14.8 ↑↑	22.8 ↑↑	9.8 ↑↑	3.4	2.4 ↑	1.4	1.6	1.6	3.4
8	*YSL*	Ta.5463	69.3	48.3 ↑↑	49.3 ↑↑	341.2 ↑	79.5	16.1	-	-	-
9	*YSL*	Ta.29321	9.8 ↑↑	12.9 ↑↑	6.2 ↑	2.6	1.6 ↓↓	1.2	1.2 ↑	2.1	1.5
10	*ZIP*	Ta.31727	3.2 ↑↑	2.8 ↑↑	2.5 ↑	1.8	1.3	1.1	1.4	1	1.2
11	*ZIP*	Ta.38190	2.9	10.4	1.1	8.1 ↓	43 ↓	21.8	1.2	1.4	1.3
12	*FRO*	Ta.10673	1.9 ↑↑	1.6 ↑	2.3	14.6 ↑	12.2 ↑	7.1 ↑	4.2 ↑↑	2.3	5.7
13	*NRAMP*	Ta.13247	2.2 ↑↑	2 ↑↑	2.3 ↑↑	12.3 ↑↑	2.5	2.1 ↑	1.9 ↑↑	1.1	1.2
14	*IREG/FPN*	Ta.72669	17.3 ↑↑	20.3 ↑↑	8.2 ↑	20.8	1.2	2.7 ↑	1.3 ↑↑	1.3 ↓	1.4
15	*VIT*	Ta.34653	11 ↑↑	7 ↑↑	14.2 ↑↑	-	-	-	1	14.4	2.6
16	*VIT*	Ta.22759	1.6	3.9 ↑	1	12.7	13.1	22.7 ↓	1.4	1.1	1.4
17	*FERRITIN*	Ta.5220	6.6 ↓↓	1.5	6	7.9 ↓	9.1 ↓↓	5.3	1.8 ↓	2 ↓↓	1.3
18	*bHLH*	Ta.34545	3112.1 ↑↑	8097.4 ↑↑	288.8 ↑↑	594.3 ↑↑	1185.2	1115.9 ↑	1.4	3.9	1.9
19	*IRO*	Ta.93472	8.8 ↑↑	20.1 ↑↑	4.8 ↑	194.8 ↑↑	3373.4	2599.2	10.3 ↑↑	1.7	2.6

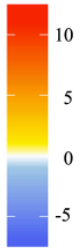

Table 2.1. Gene expression fold change between iron-deficient and sufficient-condition in bread wheat. The numbers indicate the fold change difference between iron deficient and iron sufficient growth conditions. Color indicates the log2 transformed fold change of differentially expressed genes. The upward arrow and yellow to red color indicates the up-regulation. The downward arrow and light blue to blue color indicates the down-regulation of the gene expression. Significant differences are marked with a single arrow when $p \leq 0.05$ or with double arrows when $p \leq 0.01$. "-" indicate no detection of expression. *SAMS: S-ADENOSYL-L-METHIONINE SYNTHETASE; NAS: NICOTIANAMINE SYNTHASE; NAAT: NICOTIANAMINE AMINOTRANSFERASE; DMAS: DEOXYMUGINEIC ACID SYNTHASE; TOM: TRANSPORTER OF MUGINEIC ACID; YSL: YELLOW STRIPE LIKE; ZIP: ZINC-REGULATED TRANSPORTER (ZRT)/ IRON-REGULATED TRANSPORTER (IRT)-LIKE; FRO: FERRIC CHELATE REDUCTASES; NRAMP: NATURAL RESISTANCE ASSOCIATED MACROPHAGE PROTEIN; IREG/FPN: IRON REGULATED/FERROPORTIN; VIT: VACUOLAR IRON TRANSPORTER; bHLH: BASIC HELIX-LOOP-HELIX; IRO: IRON DEFICIENCY-INDUCIBLE bHLH TRANSCRIPTION FACTOR.*

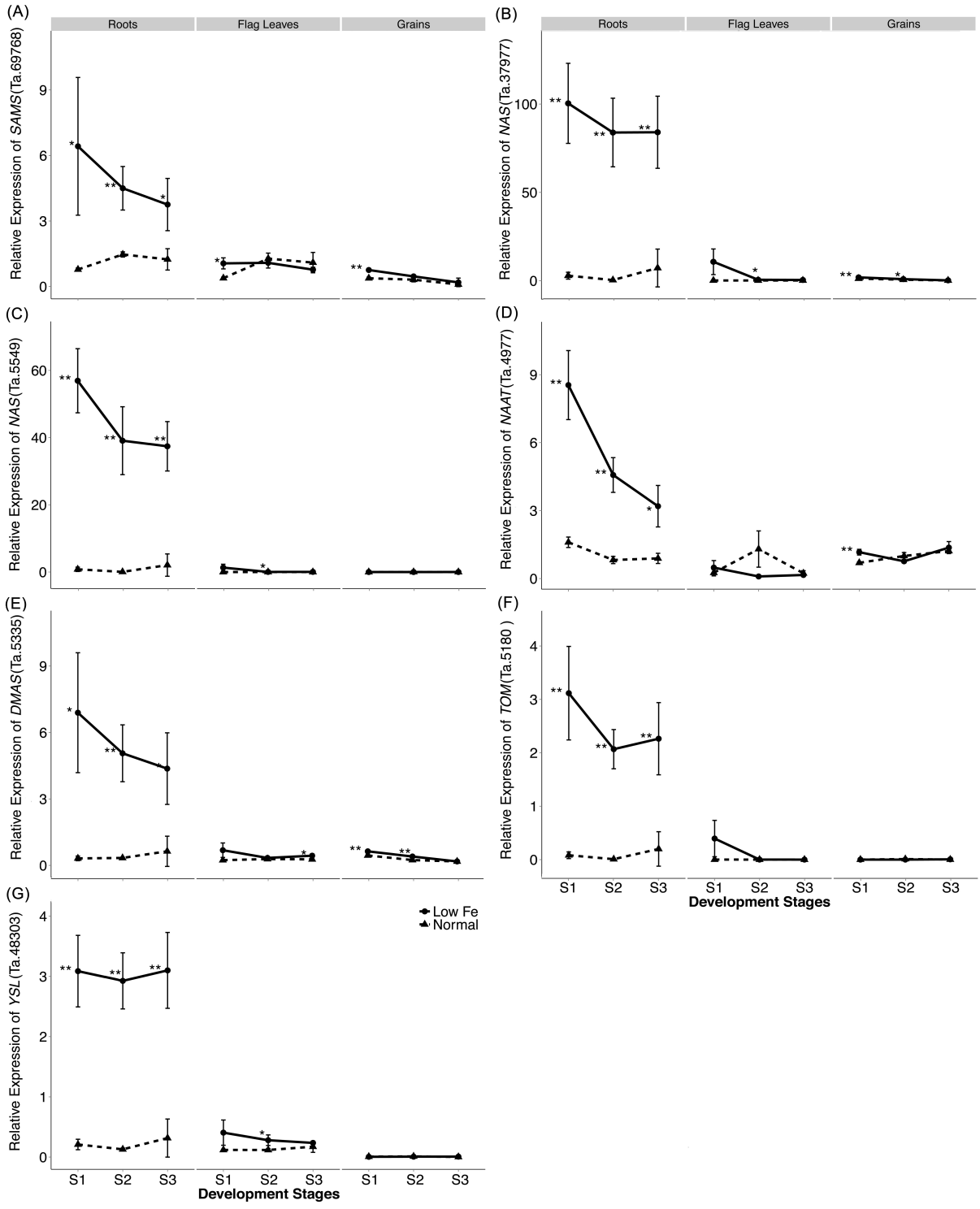

Figure 2.1. Iron deficiency induced differences in expression levels of wheat homologs of phytosiderophore synthesis related genes, the *TRANSPORTER OF MUGINEIC ACID* (*TOM*), and a *YELLOW STRIPE LIKE* (*YSL*) gene. Values are the mean ± standard deviation of the three biological replicates (*$p \leq 0.05$; **$p \leq 0.01$). Note the differences in scale at Y-axis for relative expression levels of tested genes. (A) *SAMS* (Ta.69768), (B) *NAS* (Ta.37977), (C) *NAS* (Ta.5549), (D) *NAAT* (Ta.4977), (E) *DMAS* (Ta.5335), (F) *TOM* (Ta.5180), (G) *YSL* (Ta. 48303).

The expression of two genes from the *ZIP* family (Ta.31727, Ta.38190) differed under the iron-deficient condition (Table 2.1). The expression of the *ZIP* homolog (Ta.31727) was significantly increased (more than 2.5-fold) in the roots during all the development stages but was not altered in flag leaves and grains. In contrast, a significant decrease in expression of Ta.38190 was observed in the flag leaves in stages 1 and 2.

Under iron limitation, the *FRO* homolog Ta.10673 was significantly up-regulated by 1.9- and 1.6-fold in the roots in stages 1 and 2, respectively (Table 2.1). Compared with the roots, the gene was relatively highly up-regulated in the flag leaves, i.e., by 14.6-, 12.2-, and 7.1-fold in the three respective developmental stages. The expression of Ta.10673 also increased by 4.2-fold in the grains during stage 1.

2.3.3 Differential expression of genes encoding intracellular iron transporters and storage proteins

The expression of *NRAMP* homolog (Ta.13247) increased in the flag leaves by 12- and 2-fold in stages 1 and 3, respectively. In the roots, the Ta.13247 expression increased approximately 2-fold in all of the development stages. In the grains, the gene was up-regulated in the stages 1 with 1.9-fold increase (Table 2.1). IRON REGULATED PROTEIN/FERROPORTIN (IREG/FPN) homolog (Ta.72669) showed increased expression in the roots during all stages. In addition, the expression of Ta.72669 also increased by 2.7- and 1.3-fold in stage 3 of flag leaves, and in stage 1 of the grains, respectively. However, a 1.3-fold decrease in expression of Ta.72669 was detected in the grains in stage 2 (Table 2.1). The expression of *VIT* homolog (Ta.34653) could not be detected in the flag leaves regardless of the growth conditions and stage of development. However, a significant increase in gene expression was observed in the roots, ranging from 7- to 14.2-fold changes (Table 2.1). The *VIT* homolog Ta.22759 was only up-regulated in the roots in stage 2, but a significant decrease (22.7-fold) in gene expression was observed in the flag leaves in stage 3 (Table 2.1). The dynamic modulation of vacuolar iron transporters suggest the plant cells need to keep the balance between iron storage and usage, therefore actively re-distributing iron to the cell organs based on the iron status and demand within the plants.

The expression of *FERRITIN* homolog (Ta.5220) was down-regulated in the roots, flag leaves and grains due to iron starvation. A more than 6-fold decrease in the expression of Ta.5220 was observed in the roots during stage 1. In the flag leaves and grains, the gene was down-

regulated in stages 1 and 2 by more than 7.9- and 1.8-fold, respectively (Table 2.1). The results indicate that the plants reduce iron storage under low iron availability.

2.3.4 bHLH transcription factors play a key role in regulating iron deficiency response

Upon iron deficiency stress, the expression of *bHLH* homolog Ta.34545 was significantly up-regulated by 3112.1-, 8097.4-, and 288.8-fold in the roots in stage 1, 2, and 3, respectively. Similar increases were observed for the flag leaves, particularly in stage 1 and 3, with at least a 594.3-fold increase in gene expression. However, no significant difference in gene expression was observed for the grains. Additionally, the expression of the *IRO2* homolog Ta.93472, which is also a bHLH member, was up-regulated by 4.8- to 20.1-fold in the roots when plants experienced iron-deficiency (Table 2.1). Increased expression of Ta.93472 was observed in flag leaves (195-fold) and grains (10-fold), particularly during stage 1 (Table 2.1, Figure 2.2). The observed increases in the bHLH gene transcripts indicate their role in iron deficiency-induced gene regulation.

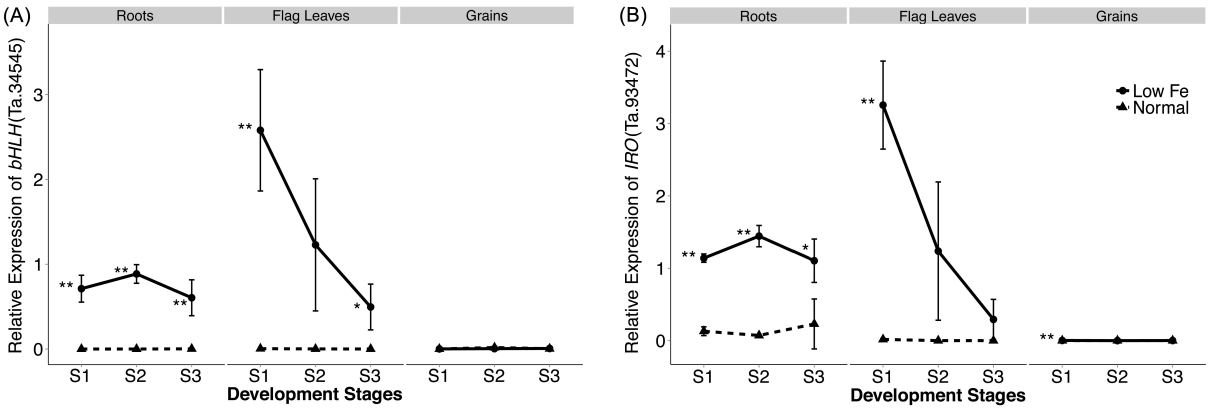

Figure 2.2. Iron deficiency induced differences in expression levels of wheat homologs of genes encoding transcription factors. Values are the mean ± standard deviation of the three biological replicates (*$p \leq 0.05$; **$p \leq 0.01$). Note the differences in scale at Y-axis for relative expression levels of tested genes. (A) *bHLH* (Ta.34545), (B) *IRO* (Ta.93472).

2.4 Discussion

During iron deficiency, an increase in production of PS has been suggested in strategy II plants, including barley, rice, maize, sorghum and red fescue (Ishimaru *et al.*, 2006; Kanazawa *et al.*, 1994; Ma *et al.*, 2003; Tsednee *et al.*, 2012). Similarly, increased secretion of MAs by wheat roots (Kanazawa *et al.*, 1994) and an increased expression of *DMAS* in both wheat roots as well as shoots have been reported, in response to iron-limited conditions

(Bashir *et al.*, 2006). In addition to these limited reports on wheat, a number of studies on rice, barley and maize reported iron deficiency triggered up-regulation of genes involved in NA and DMA synthesis (Bashir *et al.*, 2006; Inoue *et al.*, 2003; Inoue *et al.*, 2008; Kobayashi *et al.*, 2005; Negishi *et al.*, 2002; Zheng *et al.*, 2009; Zhou *et al.*, 2013). We observed increased expression of *SAMS*, *NAS*, *NAAT* and *DMAS* upon iron deficiency, particularly in the wheat roots, suggesting enhanced production of NA and DMA for iron acquisition and translocation. NA is known to chelate iron for long-distance and intracellular iron transport, in addition to serving as an intermediate in DMA production (Schuler *et al.*, 2012; Takahashi *et al.*, 2003). There are recent evidences suggesting the role of DMA in chelating with iron in the xylem and phloem for long-distance iron transport in rice, in addition to its well-known role in iron uptake (Kakei *et al.*, 2009; Nishiyama *et al.*, 2012). The increased expression of NAS and DMAS genes in the flag leaves and grains suggest similar roles of DMA and NA in long distance iron translocation in wheat.

In parallel with the increased production of phytosiderophores, the phytosiderophore transporters are also positively modulated by iron deficiency for efficient iron translocation. TOM1 and TOM2 transporters facilitate DMA secretion into the rhizosphere and vascular loading, respectively (Nozoye *et al.*, 2015; Nozoye *et al.*, 2011). The wheat *TOM* homolog Ta.5180 having high sequence identity with the barley and rice *TOM1* genes was significantly induced in wheat roots experiencing iron deficiency stress, suggesting its potential role in DMA efflux by wheat roots into rhizosphere. The YSL transporters have long been known to participate in iron translocation in many crop plants including, rice, maize and barley (Aoyama *et al.*, 2009; Curie *et al.*, 2001; Ishimaru *et al.*, 2010; Kakei *et al.*, 2012; Koike *et al.*, 2004; Murata *et al.*, 2006). The significantly increased *YSL* transcripts in wheat roots and flag leaves under the iron-deficient conditions suggest their important functions in iron uptake and transport in bread wheat as well. The YSL transporters in non-grass plants such as Arabidopsis have been studied in detail with regard to iron transport and homeostasis related functions: e.g., the *YSL2* is suggested to be involved in the lateral movement of metals in the vasculature (DiDonato *et al.*, 2004), and *YSL4* and *YSL6* coordinate iron release from chloroplasts (Divol *et al*., 2013). It is unclear how the wheat *YSL* homologs studied here must be contributing to iron deficiency response and/or in maintaining homeostasis, but increased expression in roots at all stages suggest their primary role in iron uptake. It is however noteworthy that not all wheat *YSL* homologs were analyzed and it is highly likely that there are several *YSLs* involved in distinct roles relating to iron homeostasis, as is the case for 18 characterized *YSLs* in rice.

The signal activating the iron deficiency response in plants is controlled by several factors. In rice, the transcription factor OsIRO2 is suggested to regulate the expression of genes involved in phytosiderophore synthesis (*OsNAS1*, *OsNAS2*, *OsNAAT1*, *OsDMAS1)*, and genes encoding PS transporter TOM1 as well as other iron transporters such as OsYSL15 (Ogo *et al.*, 2006; Ogo *et al.*, 2011; Ogo *et al.*, 2007). Under iron deficiency, *OsIRO2* was positively regulated by the transcription factor IDE BINDING FACTOR (OsIDEF1) (Kobayashi and Nishizawa, 2012), and also coordinates with the NAC family transcription factor IDEF2 to regulate some of the iron deficiency responsive genes in rice (Ogo *et al.*, 2008). In the case of Arabidopsis, the Ib subgroup bHLH transcription factors, including *bHLH38*, *bHLH39*, *bHLH100* and *bHLH101*, have a closer phylogenetic relationship with the rice *OsIRO2* (Hindt and Guerinot, 2012), function in maintaining iron homeostasis in Arabidopsis and were up-regulated under iron starvation (Wang *et al.*, 2007). bHLH38 and bHLH39 can form heterodimers with the FIT transcription factor (FIT/bHLH38; FIT/bHLH39); and can regulate the expression of *FRO2* and *IRT1* in Arabidopsis (Yuan *et al.*, 2008b). Although *bHLH100* and *bHLH101* are in a close subgroup similar to bHLH38 and bHLH39, they function in a FIT-independent manner (Sivitz *et al.*, 2012). The homologs of *bHLH100* and *IRO2* were significantly up-regulated in roots as well as leaves of wheat plants under iron deficiency stress, indicating their role in iron homeostasis and in regulating iron deficiency responsive genes in wheat. In line with reports on other plants, the increased expression of phytosiderophore synthesis related genes and of genes encoding iron transporters parallels the up-regulation of *bHLH100* and *IRO2* during iron deficiency.

The expression levels of several iron homeostasis related genes often depend on external and/or internal iron status of the plants. This is also relevant for the gene encoding important iron storage protein FERRITIN. Similar to the Arabidopsis *AtFERRITIN* genes (Buckhout *et al.*, 2009; Rodriguez-Celma *et al.*, 2013), the *FERRITIN* genes in bread wheat were down-regulated under the iron-deficient conditions. Excess iron induces the *FERRITIN* transcript levels (Briat *et al.*, 2010), supporting the storage function of FERRITIN in wheat. Further, we observed that the expression level of the *FERRITIN* gene in the grains was also growth stage dependent, since a gradual increase in the expression of *FERRITIN* was observed during the three development stages (Supplementary figure 2.1).

Localizing on the vacuolar membrane, AtNRAMP3 and AtNRAMP4 mediate iron efflux from the vacuoles in Arabidopsis (Lanquar *et al.*, 2005). The VIT and IRON REGULATED PROTEIN2/FERROPORTIN2 (IREG2/NPN2) performs the opposite function (Lanquar *et*

al., 2005; Morrissey *et al.*, 2009; Zhang *et al.*, 2012). The expression of their homologs in wheat roots was significantly induced upon iron deficiency, which is in agreement with the expression modulation of *AtNRAMP3*, *AtNRAMP4* and *IREG2/FPN2* in Arabidopsis but conflict with the *OsVIT2* expression in rice (Lanquar *et al.*, 2005; Morrissey *et al.*, 2009; Zhang *et al.*, 2012). The up-regulation of transporters facilitating opposite functions indicates that the influx and efflux of iron to/from the vacuoles is dynamically regulated in the roots. In contrast to the roots, the *VIT* expression was either unaltered or reduced in the flag leaves and grains.

Localized on the root epidermal cells, FROs have been reported to function in iron reduction in strategy I plants (Robinson *et al.*, 1999; Waters *et al.*, 2002). Furthermore, leaf mesophyll cells (Bruggemann *et al.*, 1993) and chloroplasts (Jeong *et al.*, 2008) also rely on FROs for iron uptake. The induction of *FRO* expression in bread wheat roots, flag leaves and grains under iron limited conditions suggested their role in cellular and organelle iron homeostasis in wheat. However, whether FROs in wheat are involved in iron uptake from the soil into root cells needs to be verified by further experimentation.

In summary, iron homeostasis in bread wheat is maintained via a comprehensive modulation of various genes and gene families. Under iron-limited conditions, overall iron uptake and transport appears to be regulated by iron deficiency-inducible transcription factors, such as those from the *bHLH* gene family. In order to cope with reduced iron supply during iron deficiency stress, the genes related to the synthesis of iron chelators (NA and DMA) as well as those encoding various iron translocation related transporters are induced. A comprehensive study comprising of transcriptome profiling of the iron deficiency wheat plants could provide better understanding of the coordinated roles of different transporters in combating iron deficiency stress.

2.5 Materials and methods

2.5.1 Plant material and growth conditions

Bread wheat (*Triticum aestivum* cv. Bobwhite S26) seeds were germinated on wet filter paper for one week. The seedlings were then transferred to hydroponic nutrient solutions (pH 6.0): 0.88 mM K_2SO_4, 2 mM $Ca(NO_3)_2$, 0.2 mM KH_2PO_4, 1.0 mM $MgSO_4$, 0.1 mM KCl, 1.0 µM H_3BO_3, 1.0 µM $MnSO_4$, 0.2 µM $CuSO_4$, 0.02 µM $(NH_4)_6Mo_7O_{24,}$ 1.0 µM $ZnSO_4$, and 100.0 µM Fe(III)-EDTA for maintenance of growth (control condition) (Durmaz *et al.*, 2011). After

one week, half of seedlings were transferred to hydroponic nutrient solutions with 10.0 µM Fe(III)-EDTA (for iron deficiency stress treatment) under greenhouse conditions (22˚C/18˚C with 16-hour light/8-hour dark cycle, 60% humidity). Air was continuously pumped into the hydroponic system for better circulation. The nutrient solutions were renewed weekly. Roots, flag leaves and grains were harvested at three different development stages, i.e., 8-10 DPA - days post anthesis (stage 1), 25-28 DPA (stage 2), and 33-35 DPA (stage 3). Three biological replicates were collected for each sample.

2.5.2 Total RNA extraction and cDNA synthesis

Isolation of total RNA from the roots and flag leaves was carried out using the Isol- RNA Lysis Reagent (5 PRIME, USA). RNA extraction from wheat grains was carried out following the protocol described by Singh *et al*., 2013 (Singh *et al.*, 2003). Total RNA used for real-time quantitative PCR was treated with DNase I (Thermo Fisher Scientific, USA). The RevertAid™ first strand cDNA synthesis kit (Thermo Fisher Scientific, USA) was used for cDNA synthesis. All steps were carried out following the manufacturers' instructions.

2.5.3 qRT-PCR and statistics

qRT-PCR was performed using the LightCycler® 480 Instrument II Real Time PCR system (Roche, Switzerland) with Taqman hydrolysis probes (Roche, Switzerland). The total reaction volume of each sample was set as 10 µl, comprising 5 µl of mastermix (Applied Biosystems, USA), 3 µl of 10× diluted cDNA, 0.9 µl of forward primer, 0.9 µl of reverse primer, 0.1 µl of the probe and 0.1 µl of H_2O.

The primers were designed based on the Roche universal probe library assay design center website (https://lifescience.roche.com/shop/CategoryDisplay?catalogId=10001&tab=&identifier=Universal±Probe±Library&langId=-1&storeId=15006). The corresponding probes were also selected using the same webportal. The primer sequences and probe numbers are provided in Supplementary table 2.1. Primer efficiency was determined using a standard curve calculated with the following formula: E = 10^(-1/slope)-1 (Supplementary table 2.1). However, due to the high sequence identity between the wheat homoeologous and paralogous genes, some of the expected amplicons match to more than one IWGSC cDNA entries (Supplementary table 2.2). The qRT-PCR reaction was carried out using the following steps: incubation at 50°C for 2 min, initialization at 95°C for 10 min, followed by denaturation at 95°C for 15 s, and

annealing and extension at 60°C for 1 min (these two steps were repeated for 40 cycles).

The reference genes for qRT-PCR normalization were chosen from 16 candidate genes that were demonstrated as stably expressed genes in the Genevestigator™ database and the literature (Zimmermann *et al*., 2005; Paolacci *et al*., 2009). Among these 16 tested genes, Ta.55681 (casein kinase II subunit beta-like), Ta.40026 (BTB/POZ and MATH domain-containing protein 4-like) and Ta.22845 (26S proteasome regulatory subunit) were found to be the most stable reference genes across all of the tested samples (unpublished data) and were further used for data normalization. Data normalization was performed as described by Schefe and colleagues (Schefe *et al.*, 2006). Statistical analysis (one-way ANOVA) was carried out using RStudio (Version 0.98.976) and Excel. Figure plotting was performed in RStudio using the R plotting packages (ggplot2, pheatmap).

2.6 Acknowledgements

This research was supported by ETH Zurich research grants to W.G. and to N.K.B., and from State Secretariat for Education, Research and Innovation (SERI) within the COST FA0905 program to N.K.B. We thank Irene Zurkirchen, Kulaporn Boonyaves, Ting-Ying Wu, Katja Bärenfaller, Kumar Vasudevan, and Simrat Pal Singh for the technical support in the greenhouse and the laboratory.

2.7 Author contributions

N.K.B. designed the experiments. M.W. carried out the experiments. M.W. and N.K.B. analyzed the data. M.W. and N.K.B. wrote the manuscript. W.G. and N.K.B. edited the manuscript. All authors have read the manuscript and agree with its content.

2.8 Supplementary materials

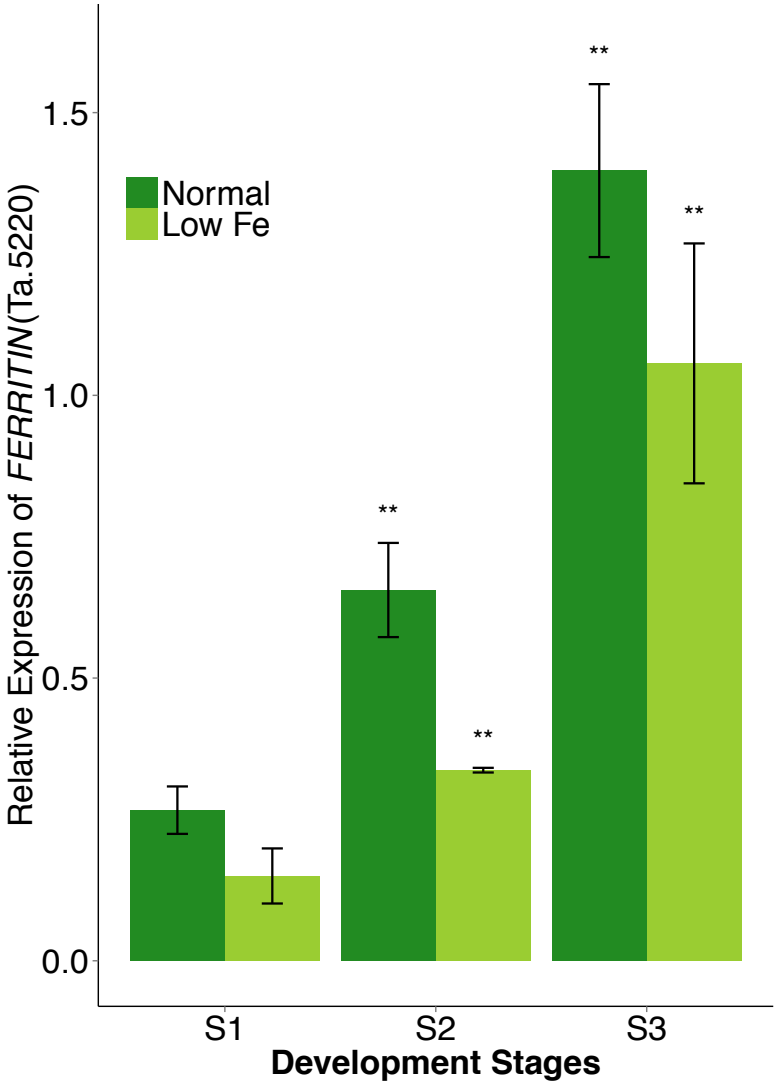

Supplementary figure 2.1. *FERRITIN* expression levels increase during grain development. Values are mean ± standard deviation of the three biological replicates. ** indicate significant differences in the gene expression at $p \leq 0.01$ in comparison to the previous development stage under the same treatment.

Nr.	Genes	Unigene ID	GenBank ID	Left primer	Right primer	Primer efficiency	probe No.	Amplicon
1	*SAMS*	Ta.69768	HP612105.1	gcgcacgatcttctcgtagt	gtcatggtctttggcgaga	2	119	gcgcacgatcttctcgtagtcgacggtggccttggtggtgatctcgccaaagaccatgac
2	*NAS*	Ta.37977	JP215700.1	aggcgcactactccgaca	gaagatgccgaggtggtc	1.83	149	aggcgcactactccgacatgctcgccgccttcgacaacccgctcgaccacctcggcatcttc
3	*NAS*	Ta.5549	GAEF01037484.1	ttcttggtgaccggaagaac	tctagcgttcagaggcacac	2	2	ttcttggtgaccggaagaactctggaagcaggagaaaaatgtgtgcctctgaacgctaga
4	*NAAT*	Ta.4977	BT009504.1	gaccatttagccaaggttgc	tacctcgtcagcaatcacca	1.85	137	gaccatttagccaaggttgcagaggtggcaagaaagctcggaatattggtgattgctgacgaggta
5	*DMAS*	Ta.5335	AB269908.1	caccgtcaatcaggtggag	cctctgcagaactccctca	1.88	6	caccgtcaatcaggtggaggtgaacccggtgtggcagcagaggaagctgagggagttctgcagagg
6	*TOM*	Ta.5180	JP874085.1	tggagaatgcaatgatagggtttt	agatgttttgcctcgctgtt	2	87	tggagaatgcaatgatagggttttctcccaatacgatctgccacacacacccaaaacagcgaggcaaaacatct
7	*YSL*	Ta.48303	HP631418	tgcatggaccaagataaacaag	acatatcaaagcggatgcaa	2	75	tgcatggaccaagataaacaagaaggaggctggcttcatggtgcccgcagttgcatccgctttgatatg
8	*YSL*	Ta.5463	BJ278653.1	gcagcgtgtggtgttatgat	aaggtacccagtcttgatgtcc	2	78	gcagcgtgtggtgttatgatgtccatagtatccacagctggagatctcatgcaggacatcaagactgggtaccttt
9	*YSL*	Ta.29321	HP639088.1	cgcgatgtttcggtatatca	tgacataggcaaccaggaca	2	97	cgcgatgtttcggtatatcagagcatacggcgccttccaggggctgtcctggttgcctatgtca
10	*ZIP*	Ta.31727	HP621024.1	ttgccacacatcaacctttc	gcaatcccatcgtgtttctt	1.99	155	ttgccacacatcaacctttcttgcgctctgaaggcaaggaccaagaaacacgatgggattgc
11	*ZIP*	Ta.38190	AY864924.1	tggccacaatggtgatagac	cgtgccttgctgaagtga	2	3	tggccacaatggtgatagactcgctggctgctgggtactaccgccggtctcacttcagcaaggcacg
12	*NRAMP*	Ta.13247	AK334756.1	tggaaaggagcttctgatcg	gcctgcttgatggtctttg	2	119	tggaaaggagcttctgatcggtttggtggttccaaagctgagctcaaagaccatcaagcaggc
13	*IREG*	Ta.72669	GAEF01080888.1	tgtacacagcccatgattcc	tggagggtcggtgttacg	1.84	58	tgtacacagcccatgattcccagcagggcaggatggagaggcgctccgtaacaccgaccctcca
14	*VIT*	Ta.34653	BE426855.1	agagtacgtgtccgtctgctc	gcttggcagtgccttctc	1.91	149	agagtacgtgtccgtctgctcccagcgggacatggagatcgcggagctggaccaggccggaaagcgtggcggcgaggaggagaaggcactgccaagc
15	*VIT*	Ta.22759	AK331977.1	tttcttcggctacgtcaagg	gatgatggcggtctggat	1.89	48	tttcttcggctacgtcaagggccgcttcactgggaaccgcccgttcctcagcgccatccagaccgccatcatc
16	*FERRITIN*	Ta.5220	HP635522.1	gagtgtggcacttcgatcag	cgtagtcgtcgtgtccttca	2	16	gagtgtggcacttcgatcagatgctgcttgaggaggcagcttgaaggacacgacgactacg
17	*FRO*	Ta.10673	GAEF01117259.1	cggtcaaccgggtagatgt	gtcgtatcctcgtcgttcg	2	15	cggtcaaccgggtagatgtagaaccgctgcagcacggcgacgagcaggaggaacgcggcgaacgacgaggatacgac
18	*bHLH*	Ta.34545	CD872522.1	ggctaggtagctacgttccatc	tgatccatcacaggcagttg	2	97	ggctaggtagctacgttccatctgcggccttccaaagatactgcccaactgcctgtgatggatca
19	*IRO*	Ta.93472	JP895423.1	ttggacatgggcagaactc	ctcgacgacagggaaatcat	2	85	ttggacatgggcagaactccggccatggtgctcactaggctgacctggaccatgatttccctgtcgtcgag

Supplementary table 2.1. List of primers used in the study. The table enlists the primer sequences, primer efficiency, probe number, and amplicon for the tested genes.

Nr.	Genes	Unigene ID	GenBank ID	Homologous GenBank ID in Other Species	Identity to Homologous Gene	Homologous Gene Description	Amplicon 100% match to IWGSC cDNA database
1	*SAMS*	Ta.69768	HP612105.1	AM039893.1	93%	Hordeum vulgare sam1 gene for putative AdoMet synthase 1	Traes_6AL_643CE8D7C; Traes_6BL_FBF9DA7CE
2	*NAS*	Ta.37977	JP215700.1	KU529957.1	99%	Triticum aestivum cultivar Gladius nicotianamine synthase (NAS6-D) gene, complete cds	Traes_4DL_AF0869DDB
3	*NAS*	Ta.5549	GAEF01037484.1	KU529963.1	96%	Triticum aestivum cultivar Gladius nicotianamine synthase (NAS2-D1) gene, complete cds	
4	*NAAT*	Ta.4977	BT009504.1	AB005788.1	91%	Hordeum vulgare mRNA for nicotianamine aminotransferase B, complete cds	Traes_1BL_D8276D3DB
5	*DMAS*	Ta.5335	AB269908.1	AB269908.1	100%	Triticum aestivum TaDMAS1 mRNA for deoxymugineic acid synthase1, complete cds	Traes_4BL_FAB8CACD6
6	*TOM*	Ta.5180	JP874085.1	AB683951.1	96%	Hordeum vulgare HvTOM1 mRNA for DMA efflux transporter, complete cds	Traes_4BS_B3CC8E408; Traes_2DL_95F9B36A7; Traes_5AL_9AA8A9036; Traes_4DL_380EE71BD; Traes_4BL_45838A7CB
7	*YSL*	Ta.48303	HP631418	AB214183.1	93%	Hordeum vulgare HvYS1 mRNA for iron-phytosiderophore transporter, complete cds	Traes_6BL_D65EC1432; Traes_6DL_5DBBFECCE; Traes_6AL_E36FCEF64
8	*YSL*	Ta.5463	BJ278653.1	XM_003579577.2	86%	PREDICTED: Brachypodium distachyon probable metal-nicotianamine transporter YSL6 (LOC100839874), mRNA	Traes_2AL_05E2128A0
9	*YSL*	Ta.29321	HP639088.1	XM_010241277.2	87%	PREDICTED: Brachypodium distachyon probable metal-nicotianamine transporter YSL9-like (YSL9), transcript variant X1, mRNA	Traes_2BL_6C5206B6D; Traes_2DL_8C4BFA3CB
10	*ZIP*	Ta.31727	HP621024.1	XM_003571208.3	89%	PREDICTED: Brachypodium distachyon zinc transporter ZTP29 (LOC100844783), transcript variant X2, mRNA	
11	*ZIP*	Ta.38190	AY864924.1	AY864924.1	100%	Triticum aestivum zinc transporter ZIP mRNA, complete cds	Traes_2AL_3983FD077
12	*NRAMP*	Ta.13247	AK334756.1	XM_003558487.3	89%	PREDICTED: Brachypodium distachyon metal transporter Nramp2 (LOC100845842), mRNA	Traes_4BL_C6A3F5C8A; Traes_4DL_CA00023AB
13	*IREG*	Ta.72669	GAEF01080888.1	XM_003563707.3	89%	PREDICTED: Brachypodium distachyon solute carrier family 40 member 1 (LOC100843334), mRNA	
14	*VIT*	Ta.34653	BE426855.1	XM_008665531.1	82%	PREDICTED: Zea mays vacuolar iron transporter homolog 5-like (LOC103642220), mRNA	Traes_2BL_A70AD4EC5
15	*VIT*	Ta.22759	AK331977.1	XM_003578034.3	93%	Brachypodium distachyon vacuolar iron transporter 1.2 (LOC100826494), mRNA	Traes_5DL_DA6449AC6
16	*FERRITIN*	Ta.5220	HP635522.1	FJ225144.1	100%	Triticum aestivum clone Fer1-1 ferritin 1C mRNA, complete cds	Traes_5DL_95DBDBAD1
17	*FRO*	Ta.10673	GAEF01117259.1	AB564558.1	93%	Hordeum vulgare HvFRO2 mRNA for putative ferric reductase oxidase, complete cds	
18	*bHLH*	Ta.34545	CD872522.1	XM_003572469.3	87%	PREDICTED: Brachypodium distachyon transcription factor bHLH100-like (LOC100840834), mRNA	
19	*IRO*	Ta.93472	JP895423.1	AB206536.1	88%	Hordeum vulgare HvIRO2 mRNA for basic helix-loop-helix protein, complete cds	Traes_3DL_C73683B71

Supplementary table 2.2. Description of the wheat homologs studied and the amplicon match to the IWGSC database. The table enlists the information regarding the tested wheat homologs and amplicon blast hit to gene IDs in IWGSC (International Wheat Genome Sequencing Consortium) chromosome-based wheat genome sequencing (version 2.2).

3 IDENTIFICATION OF MOLECULAR RESPONSES OF BREAD WHEAT TO IRON DEFICIENCY STRESS

Meng Wang[1], Hubert Rehrauer[2], Wilhelm Gruissem[1], and Navreet K. Bhullar[1,*]

[1] Plant Biotechnology, Department of Biology, ETH Zurich (Swiss Federal Institute of Technology), Zurich, Switzerland

[2] Functional Genomics Center, ETH Zurich (Swiss Federal Institute of Technology), Zurich, Switzerland

[*]Corresponding author

Prepared for submission to scientific publication

3.1 Abstract

A series of complex transport, storage and regulation mechanisms control the metabolism of iron and thereby maintain iron homeostasis in plants. Despite several studies on iron deficiency responses of different plant species, these mechanisms remain unclear in the allohexaploid wheat, which is the most widely cultivated commercial crop. We used RNA sequencing approach to reveal the transcriptomic changes in the wheat flag leaves and roots, when subjected to iron limited conditions. We identified 7954 and 4567 differentially expressed genes in the flag leaves and roots, respectively. Genes involved in the synthesis of different iron ligands i.e., citrate, malate, nicotianamine and deoxymugineic acid were significantly induced during iron deficiency. In total, 591 and 975 genes encoding transporters exhibited altered expression in roots and flag leaves, respectively. Several genes related to *MAJOR FACILITATOR SUPERFAMILY* (*MFS*), *ATP-BINDING CASSETTE* (*ABC*) transporter superfamily, *NATURAL RESISTANCE ASSOCIATED MACROPHAGE PROTEIN* (*NRAMP*) family and *OLIGOPEPTIDE TRANSPORTER* (*OPT*) family were regulated, indicating their important roles in combating iron deficiency stress. Among the regulatory factors, the transcription factors belonging to *BASIC HELIX-LOOP-HELIX* (*bHLH*) family were highly up-regulated (350-fold) in both roots and the flag leaves. Our findings provide an integrated overview on regulated molecular processes in response to iron deficiency stress in wheat. The information generated here could potentially serve as a guideline for breeding iron deficiency stress tolerant crops as well as for designing appropriate wheat iron biofortification strategies.

Key words: iron deficiency, RNA sequencing, transcriptomic profiles, wheat

3.2 Introduction

Iron plays a pivotal role in several metabolic and biosynthetic pathways essential for plant growth. It functions not only as a cofactor to some key enzymes such as cytochromes and hydrogenase, but is also involved in the electron transport chain of photosynthesis and respiration (Balk and Schaedler, 2014). Iron deficiency in plants severely affects the overall crop yield. At the same time, iron is a crucial micronutrient for human diet. Iron deficiency anemia is reported to cause severe health problems to nearly one-third of the world's population, especially to women and children in developing countries (WHO, 2016). However, our staple crops, including rice and wheat, are very limited in the grain iron content. For sustainable crop production and biofortification efforts for improved iron content to be successful, a thorough understanding of factors involved in iron acquisition and translocation within the plants is essential. Several transcriptomic studies, using either microarray hybridization or RNA sequencing, have been conducted to characterize the mechanisms underlying iron deficiency induced response in different plant species, for example, in Arabidopsis (Buckhout *et al.*, 2009; Rodriguez-Celma *et al.*, 2013; Thimm *et al.*, 2001; Yang *et al.*, 2010), soybean (Moran Lauter *et al.*, 2014; O'Rourke *et al.*, 2007; O'Rourke *et al.*, 2009), tomato (Zamboni *et al.*, 2012), rice (Kobayashi *et al.*, 2005), barley (Nagasaka *et al.*, 2009; Negishi *et al.*, 2002) and maize (Li *et al.*, 2014). It became evident with such studies that the uptake, transport and storage of iron in plants involve a systematic cooperation between tissues and cell organelles, as well as a fine coordination of iron chelators, transporters and several regulatory factors.

Citrate, nicotianamine (NA) and deoxymugineic acid (DMA) are among the well- known iron chelators responsible for iron acquisition and translocation. Citrate chelates with Fe(III) in xylem sap of graminaceous as well as non-graminaceous plants (Ariga *et al.*, 2014) and functions in root-to-shoot iron translocation (Durrett *et al.*, 2007). The transporter FERRIC REDUCTASE DEFECTIVE 3 (FRD3), a member of the MULTIDRUG AND TOXIN EFFLUX (MATE) family, facilitates efflux of citrate into the root vasculature in Arabidopsis for translocation of iron to the leaves (Durrett *et al*, 2007). NA functions in long-distance as well as cellular iron transport (Takahashi *et al.*, 2003). NA also serves as an intermediate for the production of DMA (also referred as phytosiderophores (PSs)), produced in graminaceous plants for iron uptake and transport. The PSs are synthesized from S-adenosyl-L-methionine via a conserved pathway of sequential enzymatic reactions mediated by NICOTIANAMINE SYNTHASE (NAS), NICOTIANAMINE AMINOTRANSFERASE (NAAT), and

DEOXYMUGINEIC ACID SYNTHASE (DMAS) (Kobayashi *et al.*, 2010b). Unlike NA, which is known to exist widely among higher plants, PSs are specific to graminaceous plants. DMA is either directly involved in iron transport and acquisition, or is further processed leading to production of other PSs such as mugineic acid (MA), 3-hydroxymugineic acid (HMA), 3-epihydroxy-2′-deoxymugineic acid (epiHDMA) and 3-epihydroxymugineic acid (epiDMA), depending on plant species (Kobayashi *et al.*, 2010b; Nakanishi *et al.*, 2000). DMA is released into the rhizosphere by the efflux transporter TRANSPORTER OF MUGINEIC ACID 1 (TOM1), a member of the MAJOR FACILITATOR SUPERFAMILY (MFS) (Nozoye *et al.*, 2011). The Fe(III)-MA complex is transported back to roots by the members of YELLOW STRIPE LIKE (YSL) transporter family. The YSL proteins belong to OLIGOPEPTIDE TRANSPORTER (OPT) family and have been widely studied in rice. The OsYSL15 is a plasma membrane-localized transporter which functions to transport Fe(III)-DMA from the rhizosphere (Inoue *et al.*, 2009; Lee *et al.*, 2009a). The other YSL proteins including OsYSL2, OsYSL16 and OsYSL18 also play a role in translocation of Fe(III)-DMA and/or Fe(II)-NA complexes (Aoyama *et al.*, 2009; Ishimaru *et al.*, 2010; Kakei *et al.*, 2012; Koike *et al.*, 2004; Zheng *et al.*, 2012). The peptide transport (PT) clade, second subfamily of the OPT family, also transports Fe(II)-NA as well as Fe(III)-NA in rice (Vasconcelos *et al.*, 2008).

Intracellular iron translocation is relatively less understood, however a few vacuolar and mitochondrial transporters have been identified. The NRAMP transporters export iron from the vacuoles (Lanquar *et al.*, 2005) and the VACUOLAR IRON TRANSPORTERs perform the opposite function (Zhang *et al.*, 2012). *FERRITIN*, mainly found in the plastids, encodes the main iron storage protein, and its expression level often correlates with iron level in the plant (Briat *et al.*, 2010). Among the regulatory factors, BASIC HELIX-LOOP-HELIX (bHLH) transcription factors such as rice OsIRO2 (Ogo *et al.*, 2006), rice OsbHLH133 (Wang *et al.*, 2013a) and FER-LIKE IRON DEFICIENCY-INDUCED TRANSCRIPTION FACTOR 1 (FIT) (Colangelo and Guerinot, 2004) are reported to regulate iron deficiency responsive genes and iron homeostasis in general. Additionally, the NO APICAL MERISTEM (NAM)/ARABIDOPSIS TRANSCRIPTION ACTIVATION FACTOR (ATAF)/CUP-SHAPED COTYLEDON (CUC) (NAC) and WRKY transcription factor families have also been identified as iron deficiency responsive (Ogo *et al.*, 2006; Ogo *et al.*, 2008; Sperotto *et al.*, 2008).

Although there is increasing knowledge available on iron homeostasis related mechanisms in

different plant species, the iron deficiency responses have not been systematically studied so far in bread wheat. The hexaploid bread wheat containing three subgenomes, namely A, B and D, is one of the world's most important staple food. In order to gain a comprehensive insight into molecular responses of bread wheat when exposed to iron deficiency, we studied transcriptomic changes in the roots and flag leaves of wheat plants subjected to iron-deficient and iron-sufficient conditions. A number of iron deficiency responsive genes and key regulatory factors are identified. Our results serve as an important genetic resource for future investigations aimed at deciphering the molecular mechanisms involved in iron homeostasis regulation in wheat and for designing optimal breeding strategies to protect yield losses to iron deficiency stress in the field.

3.3 Results

3.3.1 RNA sequencing analysis for identification of differentially expressed genes (DEGs) responding to iron deficiency stress

High quality reads were generated ranging from 17.7 to 30.1 million among different samples. Among these, 56 to 80% of the reads aligned to high confidence (HC) genes of chromosomal survey sequences (CSSs), which contain 111,982 annotated genes. Over 53% (around 60,000 genes) of identified IWGSC genomic features have more than 10 reads assigned in our dataset and were therefore detected as 'expressed genes' (Supplementary Table 3.1).

Differential expression analysis identified 7954 genes as differentially expressed (p value < 0.01, fold change ≥ 2) in flag leaves, among which 5653 genes were up-regulated and 2301 genes were down-regulated (Figure 3.1) under iron deficiency condition. The roots samples had less number of DEGs (4567 genes) as compared to the flag leaves, with 2259 up-regulated and 2308 down-regulated genes (Figure 3.1). The flag leaves and roots share 1103 common DEGs, with 715 genes exhibiting a similar expression pattern between the two tissues. Among these 715 genes, 526 genes were up-regulated and 189 genes were down-regulated in both the tissues. The remaining 388 genes have the opposite regulation patterns between flag leaves and roots (Figure 3.1).

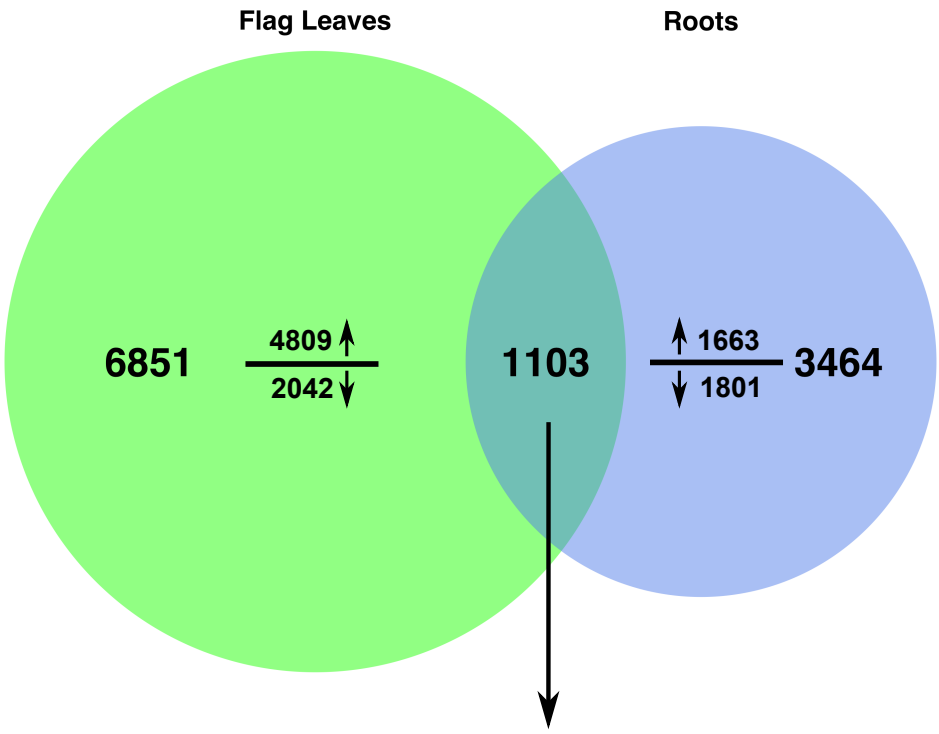

		Flag Leaves	
		Up-regulated	Down-regulated
Roots	Up-regulated	526	70
	Down-regulated	318	189

Figure 3.1. Summary of differentially expressed genes (DEGs) in the roots and flag leaves samples subjected to iron-deficient condition. Venn diagram shows total DEGs ($p < 0.01$, fold change ≥ 2) in roots and flag leaves. Green color represents total DEGs in flag leaves; blue color represents total DEGs in roots. Upward arrow indicates up-regulation of gene expression; downward arrow indicates down-regulation of gene expression.

3.3.2 Gene ontology (GO) analysis of the DEGs

To acquire functional information on the DEGs, GO enrichment analysis was carried out and DEGs were assigned into three categories i.e., biological process (BP), molecular function (MF) and cellular component (CC). The GO terms with p value < 0.01 were considered as significantly enriched. Most of the DEGs were comprised within MF (2855 in roots; 5192 in

flag leaves), followed by BP (2304 in roots; 4163 in flag leaves) and CC (855 in roots; 1272 in flag leaves), respectively (Figure 3.2). Gene ontology analysis of root DEGs revealed 20 biological process GO terms to be significantly enriched (Figure 3.2A; Supplementary table 3.2). Nearly half of these GO terms were related to plant metabolic and biosynthetic processes, e.g. 'single-organism metabolic process' (GO:0044710), 'metabolic process' (GO:0008152), 'organic substance metabolic process' (GO:0071704), 'secondary metabolic process' (GO:0019748), 'nitrogen compound metabolic process' (GO:0006807), 'organic substance biosynthetic process' (GO: GO:1901576) etc. Stress or stimulus related GO terms i.e., 'response to abiotic stimulus' (GO:0009628), 'response to stress' (GO:0006950), 'response to stimulus' (GO:0050896), etc. were also enriched. The enriched GO term 'transport' (GO:0006810) reflected an important role of transporters during iron deficiency. The overrepresented cellular component GO term 'membrane' (GO:0016020), 'extracellular region' (GO:0005576), 'cell wall' (GO:0005618) indicated that a cooperation of different cellular compartments was involved to maintain iron homeostasis. Among the molecular function GO terms, 'catalytic activity' (GO:0003824), 'transporter activity' (GO:0005215), 'organic cyclic compound binding' (GO:0097159), 'hydrolase activity' (GO:0016787), 'nucleic acid binding transcription factor activity' (GO:0001071), 'chromatin binding' (GO:0003682) were enriched in roots DEGs (Figure 3.2A). In general, the overrepresentation of flag leaves DEGs GO terms were similar as that in case of roots, with few GO terms as exception (Figure 3.2B; Supplementary table 3.2). For example, the biological process GO term 'photosynthesis' (GO:0015979) associated genes were significantly down-regulated in flag leaves. The cellular component 'thylakoid' (GO:0009579) in flag leaves was also regulated but not 'cell wall' (GO:0005618) as in roots. This correlates well with the reduced chlorophyll content in the flag leaves of wheat plants subjected to iron deficiency (Supplementary figure 3.1). Among the molecular function GO terms, the 'kinase activity' (GO:0016301) and 'oxygen binding' (GO:0019825) were enriched in flag leaves but not in roots. These results highlight the significance of membrane and/or membrane localized metal ion transporters as well as of regulatory and metabolic proteins during iron deficiency stress.

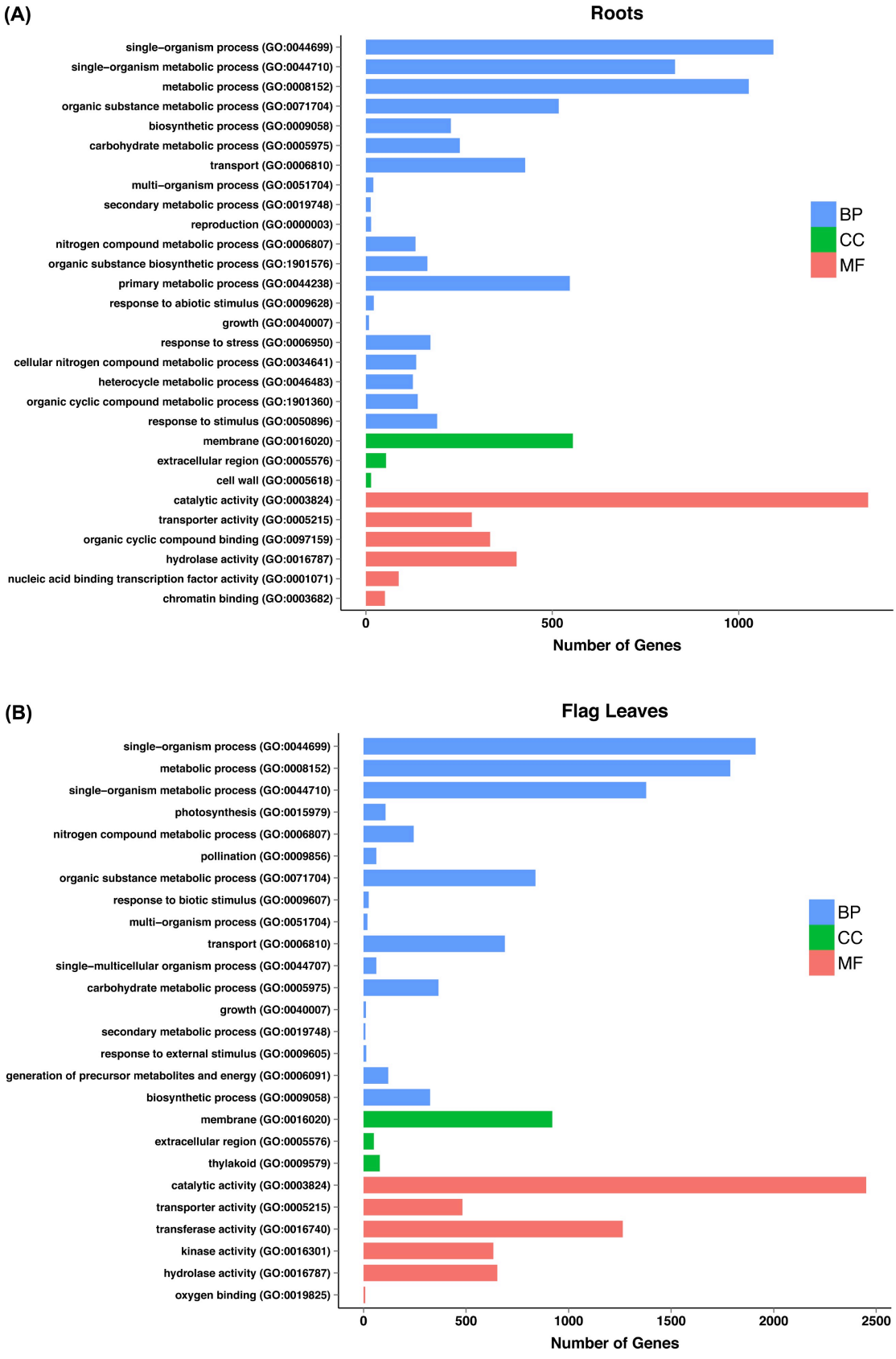

Figure 3.2. Gene Ontology (GO) analysis of the DEGs in iron-deficient wheat roots and flag leaves. DEGs are distributed to three major gene ontology categories: i.e., BP: Biological process; CC: Cellular component; MF: Molecular cunction. X-axis represents the number of DEGs in each GO term. (A) roots, (B) flag leaves.

3.3.3 Genes encoding iron chelators and iron storage proteins are modulated under iron limited conditions

Iron deficiency stress significantly affected the production of iron ligands. TCA cycle is an important pathway for organic acid production through carboxylation of iron ligands such as citrate and malate (Figure 3.3; Table 3.1). More than 2-fold increased expression of *SUCCINYL-COA SYNTHETASE*, *SUCCINATE DEHYDROGENASE*, and *CITRATE SYNTHASE* was observed in iron-deficient roots. Wheat roots also exhibited over 440-fold elevated expression for the homologs of *MALATE DEHYDROGENASE*. The induced expression levels of four *omega-AMIDASE* (Traes_4AS_CDEB9D532, Traes_4BL_14E0D4AEE, Traes_XX_921740A4F and Traes_4DL_1AD8A0318) have likely promoted an increased production of alpha- ketoglutarate, eventually leading to enhanced production of malate and citrate through series of reactions. These results indicate an important role of citrate and malate as iron chelators in bread wheat. In flag leaves, the TCA cycle was differently regulated than roots and a 4.4 to 7.9-fold reduction in expression of *ACONITASE/ISOPROPYLMALATE DEHYDRATASE* was observed. However, the expression of gene encoding MALATE DEHYDROGENASE (Traes_4DL_1184F6F68) was over 20-fold elevated (Table 3.1; Supplementary figure 3.2).

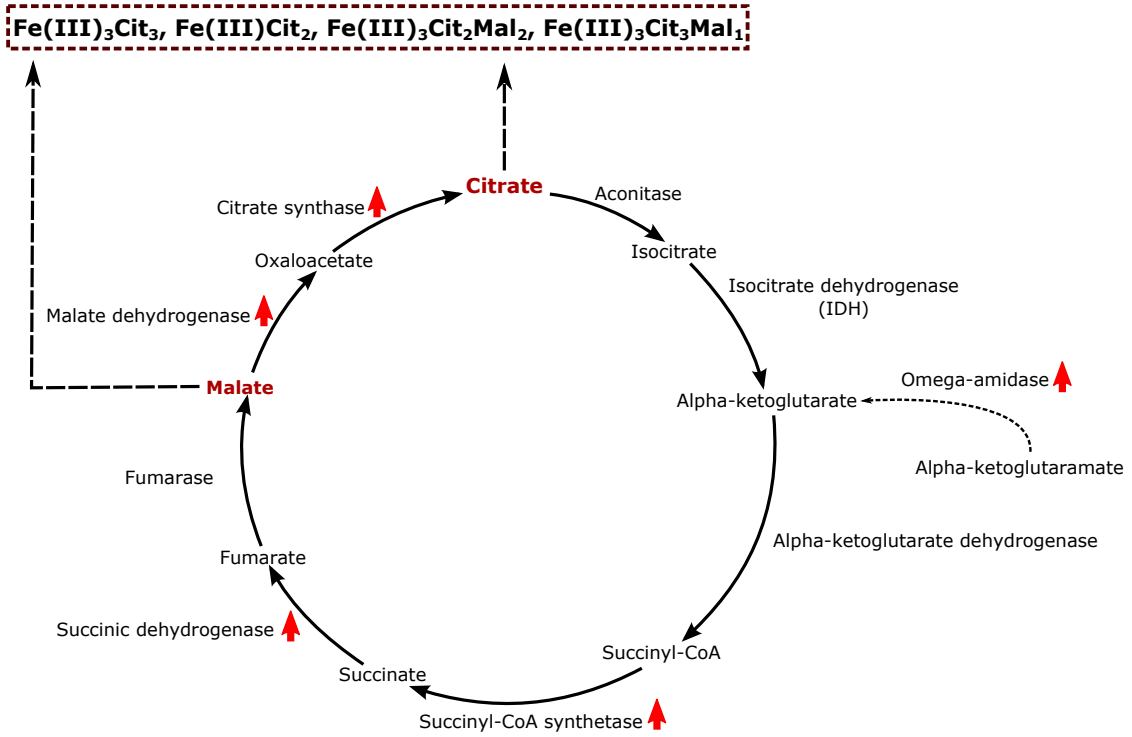

Figure 3.3. Gene expression regulation in the TCA cycle in iron deficient roots. Red arrows represent up-regulated expression. $Fe(III)_3Cit_3$, $Fe(III)Cit_2$, $Fe(III)_3Cit_2Mal_2$ and $Fe(III)_3Cit_3Mal_1$ represent the complexes that chelators citrate and malate form with Fe(III).

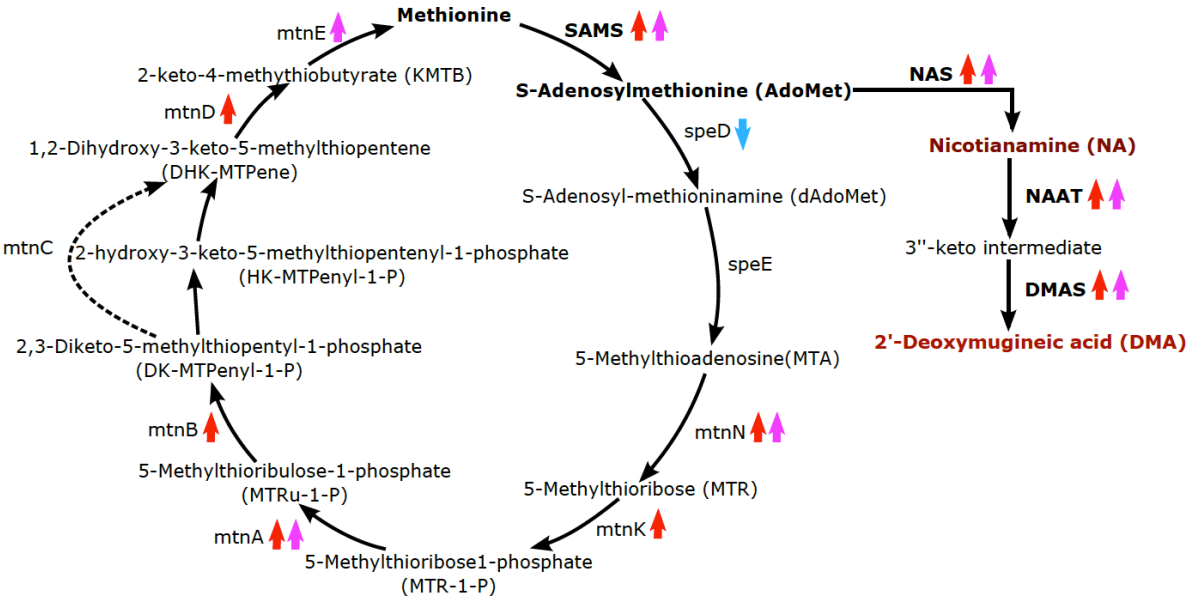

Figure 3.4. Gene expression regulation in the methionine salvage and phytosiderophore synthesis pathway in roots and flag leaves. Red and pink arrows represent up-regulated gene expression in roots and flag leaves, respectively. Light blue arrow represent down-regulated gene expression in flag leaves.

Identifier	Tissue	Description	Fold Change
ACONITASE/ISOPROPYLMALATE DEHYDRATASE			
Traes_6AS_5D4E461FD	Flag Leaves	3-isopropylmalate dehydratase large subunit 1	-4.8
Traes_2BS_27D0DFE12	Flag Leaves	3-isopropylmalate dehydratase large subunit 1	-4.9
Traes_6AS_8C76F6F50	Flag Leaves	3-isopropylmalate dehydratase large subunit	-4.8
Traes_6BS_87381C857	Flag Leaves	3-isopropylmalate dehydratase large subunit	-4.8
Traes_XX_23132EB0F	Flag Leaves	3-isopropylmalate dehydratase large subunit 1	-4.4
Traes_7AS_60F755E22	Flag Leaves	Aconitate hydratase 1	-7.7
Traes_7BS_B2B2B5D1A	Flag Leaves	3-isopropylmalate dehydratase large subunit 2	-7.9
Traes_7DS_8C23DD4C2	Flag Leaves	Aconitate hydratase 1	-7.4
Traes_4AL_643946F0C	Flag Leaves	3-isopropylmalate dehydratase large subunit 2	-5.7
ISOCITRATE DEHYDROGENASE			
Traes_XX_6D898FD80	Flag Leaves	Isocitrate dehydrogenase [NADP]	-62.6
ALPHA-KETOGLUTARATE DEHYDROGENASE			
Traes_2AS_4AB51ACE2	Flag Leaves	2-oxoglutarate dehydrogenase, E1 component	2.1
SUCCINYL-CoA SYNTHETASE			
Traes_XX_2020DA362	Roots	Succinyl-CoA ligase [ADP-forming] subunit alpha	8.4
Traes_XX_B99927138	Flag Leaves	Succinyl-CoA ligase [ADP-forming] subunit alpha	-16.1
SUCCINATE DEHYDROGENASE			
Traes_XX_DC97012D8	Roots	Succinate dehydrogenase flavoprotein subunit	2.5
Traes_XX_6B7A58C14	Flag Leaves	Succinate dehydrogenase flavoprotein subunit	-59.3
FUMARASE			
Traes_XX_8E1B70CAC	Flag Leaves	Fumarate hydratase class II	-54.2
MALATE DEHYDROGENASE			
Traes_5AL_3AB81DF9B	Roots	Malate dehydrogenase	442.9
Traes_4DL_8DBE42AE9	Roots	Malate dehydrogenase	310
Traes_7DS_309E71F44	Roots	Malate dehydrogenase	103.3
Traes_4DL_1184F6F68	Roots	Malate dehydrogenase [NADP], chloroplastic	299.4
Traes_7BL_0367BBFE6	Roots	Malate dehydrogenase	95.8
Traes_XX_95CC375AE	Roots	Malate dehydrogenase	54.9
Traes_2AL_C9A69DBA9	Roots	Malate dehydrogenase	2.9
Traes_7DL_B176F9FBC	Roots	Malate dehydrogenase (NADP) 1, chloroplastic n=1	2.6
Traes_4DL_1184F6F68	Flag Leaves	Malate dehydrogenase [NADP], chloroplastic	23.7
CITRATE SYNTHASE			
Traes_XX_D6A82A457	Roots	Citrate synthase family protein	8.4
omega-AMIDASE			
Traes_4AS_CDEB9D532	Roots	Omega-amidase NIT2-B	4.9
Traes_4BL_14E0D4AEE	Roots	Omega-amidase NIT2	4.8
Traes_XX_921740A4F	Roots	Omega-amidase NIT2	4.8
Traes_4DL_1AD8A0318	Roots	Omega-amidase NIT2	5.5

Table 3.1. Differentially expressed genes (DEGs) in the TCA cycle. The table enlists the DEGs ($p < 0.01$, fold change ≥ 2) in TCA cycle in roots and flag leaves when plants suffer from iron deficiency. Positive number of fold change indicates up-regulation of gene expression. Negative number of fold change indicates down-regulation of gene expression.

Identifier	Tissue	Description	Fold Change	Number of Genes
SAMS				
Traes_XX_BE5631000	Roots	S-adenosylmethionine synthase	10.3	
Traes_6BL_FBF9DA7CE	Roots	S-adenosylmethionine synthase 2	7	Total:18
Traes_6AL_643CE8D7C	Roots	S-adenosylmethionine synthase 1	6.4	Up:18
Traes_2DS_784A6C081	Roots	S-adenosylmethionine synthase 3	6.4	Down:0
Traes_6DL_1C00C93A5	Roots	S-adenosylmethionine synthase 3	6.4	
Traes_6BL_6EA64DF06	Flag Leaves	S-adenosylmethionine synthase 1	3.6	Total:3
Traes_6BL_FBF9DA7CE	Flag Leaves	S-adenosylmethionine synthase 2	2.1	Up:2
Traes_XX_06C640CC9	Flag Leaves	S-adenosylmethionine synthase	-37.8	Down:1
NAS				
Traes_6DL_202647A85	Roots	nicotianamine synthase 3	285.4	
Traes_XX_57C9BFE99	Roots	nicotianamine synthase 3	193.5	Total:44
Traes_6AL_2D6B1391C	Roots	Nicotianamine synthase 2	178.7	Up:44
Traes_XX_DE8AAABA6	Roots	nicotianamine synthase 4	160.5	Down:0
Traes_6DL_AEF33B4F2	Roots	nicotianamine synthase 1	151.8	
Traes_6AS_C1AD027FA	Flag Leaves	Nicotianamine synthase 1	2019.8	
Traes_6AS_89FA598FB	Flag Leaves	nicotianamine synthase 4	1478.6	Total:37
Traes_6DS_7ED5D8F48	Flag Leaves	nicotianamine synthase 4	1287.2	Up:33
Traes_6DS_0BF81EADB	Flag Leaves	nicotianamine synthase 4	961.4	Down:4
Traes_6DS_8CF4D4ED5	Flag Leaves	Nicotianamine synthase 1	855.7	
NAAT				
Traes_1BL_9567F31C9	Roots	tyrosine aminotransferase 3	37.5	
Traes_1DL_7B4106561	Roots	Histidinol-phosphate aminotransferase	35.3	Total:33
Traes_1DL_F7AE109E2	Roots	Histidinol-phosphate aminotransferase	33.7	Up:26
Traes_XX_27C41E4DF	Roots	aspartate aminotransferase	30.6	Down:7
Traes_1AL_9D6B86169	Roots	Histidinol-phosphate aminotransferase	27.1	
Traes_1AS_6D38B2DA2	Flag Leaves	aspartate aminotransferase	287.2	
Traes_1DS_79B6C3D87	Flag Leaves	Histidinol-phosphate aminotransferase	203	Total:20
Traes_1BS_D5E16C471	Flag Leaves	aspartate aminotransferase	197.7	Up:19
Traes_XX_634015130	Flag Leaves	LL-diaminopimelate aminotransferase	10.1	Down:1
Traes_XX_533BEDE84	Flag Leaves	histidinol phosphate aminotransferase 1	-35.1	
DMAS				
Traes_4BL_FAB8CACD6	Roots	NAD(P)-linked oxidoreductase superfamily protein	43.6	
Traes_4AS_887399584	Roots	Aldose reductase	30.8	Total:24
Traes_XX_175EF4A84	Roots	Aldose reductase	25.7	Up:17
Traes_7DS_8B7C02BBC	Roots	Aldose reductase	6.1	Down:7
Traes_7AS_C63441B1D	Roots	Aldose reductase	5.8	
Traes_2DL_787806003	Flag Leaves	Aldose reductase	14.8	
Traes_2DL_55FF553FD	Flag Leaves	Aldo/keto-reductase family protein n=9	12.3	Total:50
Traes_2AL_322164EB3	Flag Leaves	NAD(P)-linked oxidoreductase superfamily protein	12.1	Up:45
Traes_2DL_47E335BA6	Flag Leaves	Aldose reductase	12	Down:5
Traes_1DL_03EFA2FE5	Flag Leaves	Aldose reductase	11.8	

Table 3.2. DEGs in the phytosiderophore synthesis pathway. The table summarizes five most differentially expressed genes for each PSs synthesis related genes in roots and flag leaves, respectively. Positive number of fold change indicates up-regulation of gene expression. Negative number of fold change indicates down-regulation of gene expression. *SAMS: S-ADENOSYLMETHIONINE SYNTHETASE*; *NAS: NICOTIANAMINE SYNTHASE*; *NAAT: NICOTIANAMINE AMINOTRANSFERASE*; *DMAS: DEOXYMUGINEIC ACID SYNTHASE*.

The expression levels of genes involved in synthesis of NA and DMA were also highly up-regulated in both roots and flag leaves. Several of the *NAS* gene homologs were up-regulated, with fold changes as high as 285.4-fold (Traes_6DL_202647A85) in roots and over 2000-fold (Traes_6AS_C1AD027FA) in flag leaves (Table 3.2; Supplementary table 3.3). Likewise, *NAAT* homologs including *ASPARTATE AMINOTRANSFERASE*, *LL-DIAMINOPIMELATE AMINOTRANSFERASE*, *TYROSINE AMINOTRANSFERASE* and *HISTIDINOL-*

PHOSPHATE AMINOTRANSFERASE were highly induced in both roots and flag leaves (Table 3.2; Supplementary table 3.3). DMAS genes belong to *ALDO/KETO REDUCTASE* gene family and most of the differentially expressed *ALDO/KETO REDUCTASE* genes had elevated transcripts levels both in roots and flag leaves (Table 3.2; Supplementary table 3.3). PSs synthesis links to methionine salvage pathway because S-adenosyl-L-methionine, a key precursor for the synthesis of MAs, is produced from methionine. In roots and flag leaves both, the methionine salvage was also accelerated as indicated by the increased expression of genes mediating sequential reactions in this pathway (Figure 3.4; Supplementary table 3.4). The induced expression levels of above discussed genes suggest increased production of NA and DMA in response to iron deficiency stress in wheat.

The expression levels of the three *FERRITIN* homologs (Traes_5AL_D01E0C753, Traes_5BL_CEA21A155, Traes_5DL_95DBDBAD1) significantly declined by 5 to 7-fold during iron deficiency condition in both roots and flag leaves (Supplementary table 3.5). The expression levels of several genes annotated as *METALLOTHIONEIN* (*MT*), encoding for metal binding protein involved in ion storage and detoxification, were also altered in both roots and flag leaves. Two of the *MT* gene homologs exhibited increased expression with changes as high as 44-fold (Traes_1BL_F81F006CC) and 27-fold (Traes_5BL_0B0EFC87C) in the iron-deficient roots. On the contrary, two other *MT* gene homologs (Traes_3B_78F5B1B09 and Traes_3DS_C917FF785) were down-regulated in iron-deficient roots and flag leaves (Supplementary table 3.5). The reduced expression of *FERRITIN* indicates plants' preference to distribute the available iron to different plant parts in order to combat iron deficiency rather than storage. The regulated *MTs* appear to play a significant role in maintaining metal ion homeostasis.

3.3.4 Multiple transporters coordinate effective iron translocation during iron deficiency stress

Gene ontology enrichment and transcript abundance analysis demonstrated that transport related genes were significantly regulated under iron deficiency conditions in both roots and flag leaves (Table 3.3; Supplementary table 3.6). In case of roots, 591 genes encoding for transporters and transmembrane channels were identified as differentially expressed and were further assigned into different protein families according to the protein InterPro IDs (Supplementary table 3.6). The *MFS* comprised the largest set among the differentially expressed genes encoding for transporters in wheat roots with 143 genes belonging to this

category (Supplementary table 3.6). The different gene families belonging to the MFS exhibited variable expression patterns. The genes encoding *SOLUTE CARRIER FAMILY 40 MEMBER 1* (*SLC40A1*, *IRON REGULATED PROTEIN/FERROPORTIN, IREG/FPN*), *ZINC INDUCED FACILITATOR-LIKE* (*ZIFL*), *MULTIDRUG RESISTANCE PROTEIN MdtG* (*mdtG*), and a high proportion of the differentially expressed genes encoding *PROTON-DEPENDENT OLIGOPEPTIDE TRANSPORTER* (*POT*) were significantly up-regulated during the iron deficiency condition, whereas some genes encoding for *SOLUTE CARRIER FAMILY 2*, *SOLUTE CARRIER FAMILY 22*, and *NITRATE TRANSPORTERS* were down-regulated (Table 3.3; Supplementary table 3.6). The *AQUAPORIN-LIKE* (*AQP*) superfamily is the second most regulated group with 54 down-regulated and 4 up-regulated differentially expressed genes. With 51 members differentially expressed, *ATP-BINDING CASSETTE* (*ABC)* superfamily contains up-regulated genes from A, B, C, G, and *LIPID A EXPORT ATP-BINDING/PERMEASE PROTEIN MsbA* (*msbA*) family. Most of the down-regulated genes encoding *ABC* transporters were from G family (Table 3.3; Supplementary table 3.6). *ZINC-REGULATED TRANSPORTER (ZRT), IRON-REGULATED TRANSPORTER (IRT)-LIKE PROTEIN* (*ZIP*) family, *OPT* superfamily, *VACUOLAR IRON TRANSPORTER* (*VIT*), *MATE* family, *NRAMP* family were mostly up-regulated. The expression levels of *DRUG/METABOLITE TRANSPORTER* (*DMT*) and most of the *HEAVY METAL TRANSPORT/DETOXIFICATION* (*HMA*) superfamily genes were repressed. However, two of the genes belonging to the *HMA* family were up-regulated with a relatively higher expression in roots (Table 3.3; Supplementary table 3.6).

Flag leaves showed a higher number of differentially expressed transporter encoding genes (975 genes) as compared to the roots. Genes encoding *ABC* transporter and *MFS* families contributed more than 30% of the DEGs encoding for transporters in the flag leaves. Among 176 differentially expressed genes encoding *ABC* transporters 171 were significantly up-regulated. Among the 160 *MFS* genes, the *SLC40A1* family, *mdtG* family, *ZIFL* family and nearly 75% of the DEGs from *POT* family were significantly induced. The other gene families, such as the amino acid transporter, *MATE* family, *HMA* family, *ZIP* family, *OPT* superfamily and the *NRAMP* also constituted a large proportion of the DEGs encoding for transporters in the flag leaves. Genes from *MATE* and *OPT* family were significantly induced, with 75% and 91% of genes up-regulated respectively. In contrast, over 89% of the *ZI*P family genes were down-regulated in flag leaves (Table 3.3; Supplementary table 3.6).

Apart from the differences observed for roots and flag leaves, 168 transport related DEGs were shared among roots and flag leaves (Figure 3.5; Table 3.3; Supplementary table 3.6). *MFS*, *ABC* transporter superfamily, *OPT*, *ZIP*, *HMA*, *VOLTAGE-DEPENDENT ANION CHANNEL* (*VDAC*), *NRAMP* and *AQP* ranked as the top 8 regulated gene (super) families. Over one fourth of the genes (43 genes) were classified as *MFS*. Among the 43 *MFS* genes, 20 *MFS* genes could be classified into *POT* family and 17 of these were expressed at least 2.8-fold higher, both in roots and flag leaves. The remaining three genes (Traes_1BL_8DB775116, Traes_XX_810ADAFC5 and Traes_1AL_E5AFC5752) were down-regulated in both the tissues. Seven genes, encoding the *mdtG*, had higher expression levels in both roots and flag leaves. In case of Traes_4DS_BB4FCE298, the expression levels increased nearly 32-fold in roots and over 1000-fold in flag leaves. The Traes_4DL_380EE71BD exhibited 38-fold and 454-fold increased expression in roots and leaves, respectively. Five members of *ZIFL* gene family were up-regulated as well, with expression changes between 2 and 48-fold in roots and between 5 and 756-fold in flag leaves. Among the genes encoding solute carrier family transporters, the *SLC40A1* was significantly up-regulated in both roots and leaves. The *ABC* transporter A family and G family contributed the most overlapping *ABC* transporter DEGs between roots and flag leaves, where the genes encoding *ABCA* transporter were up-regulated in both the tissues and *ABCG* gene homologs showed variable expression patterns. Besides, the two *msbA* gene homologs (Traes_5DL_EF92177BC, Traes_5AL_32C87EDAF) and one *ABCC* gene homolog (Traes_7BS_AD3104D73) also showed induced expression under iron-deficient conditions. In total, twelve *YSL* gene homologs and four *OPT* gene homologs belonging to the OPT superfamily were regulated. An expression increase of at least 3.7-fold in roots and 2.7-fold in flag leaves were observed among the genes belonging to the *OPT* superfamily. Similarly, six of the *NRAMP* gene homologs showed induced expression in both the tissues, when subjected to iron-deficient conditions. These results further illustrate that iron uptake and translocation mechanisms are mediated by diverse range of transporters and ion channels. These transporters seem to coordinate iron distribution during iron deficiency condition and at the same time maintain iron homeostasis in wheat.

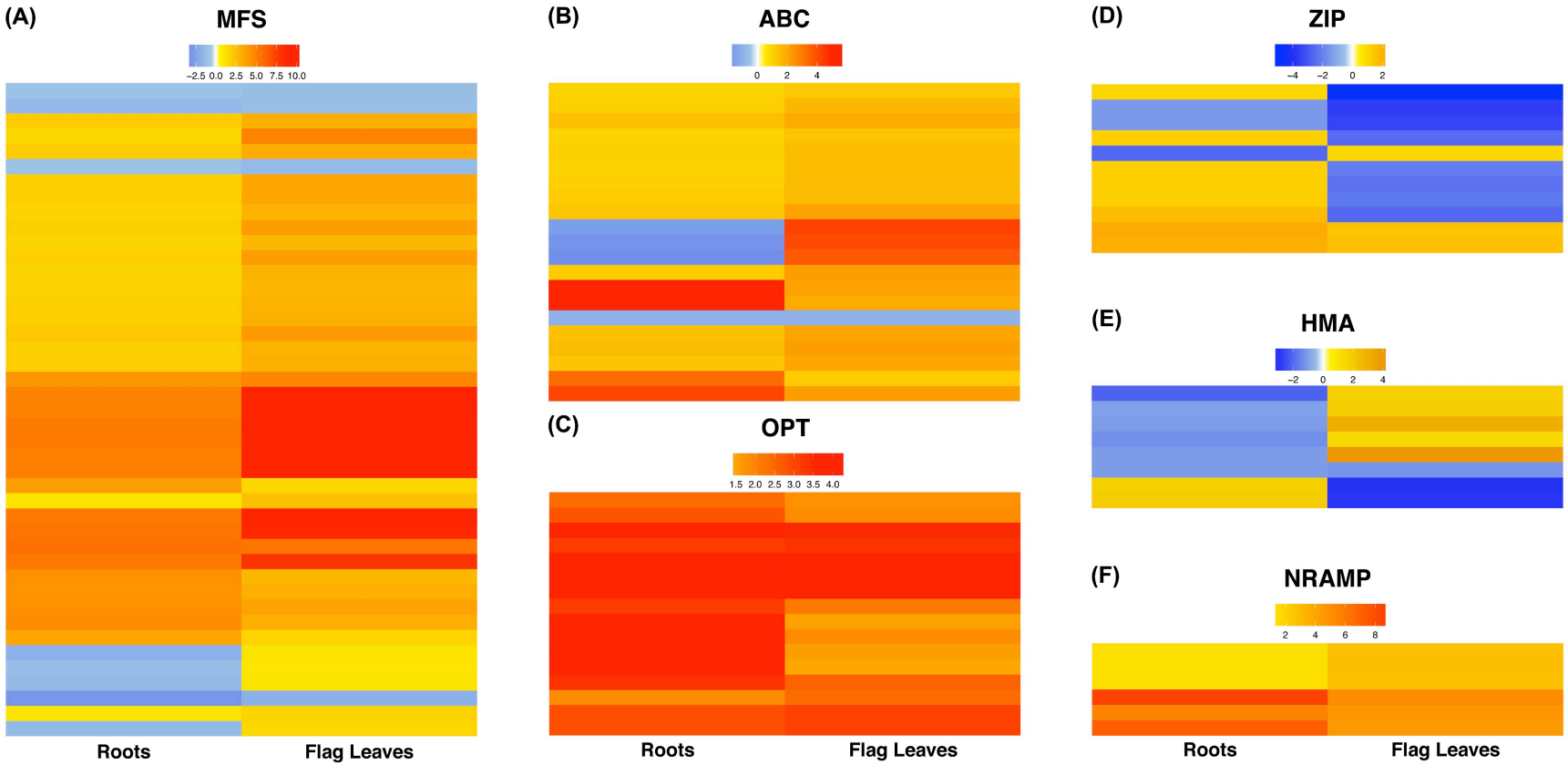

Figure 3.5. Six most differentially expressed transporter encoding gene families shared among roots and flag leaves. Heatmaps show six most differentially expressed transporter encoding gene families shared among roots and flag leaves, respectively. Yellow to red color indicates up-regulation of gene expression; light blue to blue color indicates down-regulation. Also refer to supplementary table 6 for gene IDs and for actual fold change information. (A) MFS, (B) ABC transporter, (C) OPT, (D) ZIP, (E) HMA, (F) NRAMP. MFS: MAJOR FACILITATOR SUPERFAMILY; ABC: ATP-BINING CASSETTE; ZIP: ZINC-REGULATED TRANSPORTER (ZRT), IRON-REGULATED TRANSPORTER (IRT)-LIKE PROTEIN; HMA: HEAVY METAL-ASSOCIATED; NRAMP: NATURAL RESISTANCE ASSOCIATED MACROPHAGE PROTEIN.

Identifier	Description	Fold Change Roots	Fold Change Flag Leaves
MFS			
Traes_2AL_8A3382BB2	Major facilitator superfamily protein LENGTH=584	-2.5	3
Traes_2BL_3C908C258	Solute carrier family 22 member 1	2	3.4
Traes_2BS_1CDFC2FF61	Solute carrier family 22 member 3	-8	-3.5
Traes_5BS_5B7315F37	Solute carrier family 2	-2.6	2.1
Traes_5DS_3032E79B5	Solute carrier family 2	-2.3	2.1
Traes_5AS_76C9E9E98	Major facilitator superfamily protein	-3.5	2.2
Traes_4DL_A266BC7CA	Solute carrier family 40 member 1	11.3	3.2
Traes_7BL_D5CC5C0C5	Solute carrier family 40 member 1	22.6	8.9
Traes_7DL_0A3BB7980	Solute carrier family 40 member 1	19.4	12.1
Traes_7BL_3FD446C53	Solute carrier family 40 member 1	18.8	9
Traes_7AL_A7020E7CC	Solute carrier family 40 member 1	20.7	6.8
Traes_2DL_95F9B36A7	zinc induced facilitator-like 1	39.6	261.2
Traes_7BL_94E5A40FC	zinc induced facilitator-like 1	48.3	41.8
Traes_4BS_4BC02509F	zinc induced facilitator-like 2	42.1	358.5
Traes_4DL_5FD207E12	zinc induced facilitator-like 1	40.6	756.4
Traes_4DS_D21EF1607	zinc induced facilitator-like 1	2	5.4
Traes_4BS_95007B0FF	Multidrug resistance protein MdtG	15.1	3.1
Traes_4BL_45838A7CB	Multidrug resistance protein MdtG	34.3	624.3
Traes_4BS_B3CC8E408	Multidrug resistance protein MdtG	34.2	628.2
Traes_4DL_380EE71BD	Multidrug resistance protein MdtG	37.8	454.1
Traes_5AL_9AA8A9036	Multidrug resistance protein MdtG	35.5	530.8
Traes_4AL_65E56F6F9	Multidrug resistance protein MdtG	32.2	958.7
Traes_4DS_BB4FCE298	Multidrug resistance protein MdtG	32	1144.1
Traes_3B_3AB690131	Proton-dependent oligopeptide transporter family	17.4	26.2
Traes_XX_E4204E4A7	Proton-dependent oligopeptide transporter family	3.8	8.3
Traes_XX_F1174997D	Proton-dependent oligopeptide transporter family	3.7	7.8
Traes_XX_9F048EEBA	Proton-dependent oligopeptide transporter family	4.5	16
Traes_XX_95154BE5D	Proton-dependent oligopeptide transporter family	3.7	8.3
Traes_XX_4879B2DF9	Proton-dependent oligopeptide transporter family	3.7	7.8
Traes_XX_776ACC81B	Proton-dependent oligopeptide transporter family	3.3	6.9
Traes_XX_C113C186A	Proton-dependent oligopeptide transporter family	3.3	7.3
Traes_4BS_3409CDE1E	Proton-dependent oligopeptide transporter family	3.6	14.1
Traes_XX_39586B0BE	Proton-dependent oligopeptide transporter family	3.3	6.9
Traes_2BS_7D0EA7319	Proton-dependent oligopeptide transporter family	3.7	14.7
Traes_XX_6E30390E2	Proton-dependent oligopeptide transporter family	3.3	7.3
Traes_XX_418AB6F6E	Proton-dependent oligopeptide transporter family	3.6	11.2
Traes_2BS_132B5028B	Proton-dependent oligopeptide transporter family	3.6	10.9
Traes_1BL_8DB775116	Proton-dependent oligopeptide transporter family	-2	-2.5
Traes_3B_207F350ED	Proton-dependent oligopeptide transporter family	4.1	9.8
Traes_3B_5E8A633D7	Proton-dependent oligopeptide transporter family	2.8	29.4
Traes_3B_6936ACE77	Proton-dependent oligopeptide transporter family	3.9	8.3
Traes_XX_810ADAFC5	Proton-dependent oligopeptide transporter family	-2.7	-2.2
Traes_1AL_E5AFC5752	Proton-dependent oligopeptide transporter family	-2	-2.3

Continued on next page

Continued from previous page

Identifier	Description	Fold Change Roots	Fold Change Flag Leaves
ABC			
Traes_5DL_EF92177BC	Lipid A export ATP-binding/permease protein MsbA	18.5	4.6
Traes_5AL_32C87EDAF	Lipid A export ATP-binding/permease protein MsbA	10.1	2.3
Traes_7BS_AD3104D73	ABC transporter C family member 10	2.5	4
Traes_7DL_D65B7D0F0	ABC transporter G family member 37	3	4.6
Traes_7BL_94589D01F	ABC transporter G family member 37	2.7	4.1
Traes_4AL_9B4EA417B	ABC transporter G family member 14	-2	-2.1
Traes_7DS_E47115636	ABC transporter G family member 31	59.8	3.9
Traes_4AL_6EB30F467	ABC transporter G family member 31	40.2	4.2
Traes_7BL_830B7A8CA	ABC transporter G family member 37	2.3	4.6
Traes_7AS_E1EA01D49	ABC transporter G family member 39	-3.9	13.7
Traes_7DS_D89F89766	ABC transporter G family member 39	-3.5	16.9
Traes_7BS_CF247665F	ABC transporter G family member 39	-2.9	19.7
Traes_1DL_A6FE85E09	ABC transporter A family member 7	2.2	3
Traes_1AL_3564C0828	ABC transporter A family member 8	2.1	2.8
Traes_5AL_9D148E259	ABC transporter A family member 7	2	3
Traes_4DL_4E68C58BB	ABC transporter A family member 8	2	3
Traes_1BL_9FCB31A4D	ABC transporter A family member 8	2	2.6
Traes_1BL_9828D7165	ABC transporter A family member 7	2.7	3.7
Traes_3DL_9F10B03B5	ABC transporter A family member 7	2.2	3.1
Traes_7BL_B5574EA06	ATP binding cassette subfamily A4	2	2.4
Traes_7AL_043F7AE3F	ABC transporter G family member 37	2.4	4.3
OPT			
Traes_5DL_253FD0F94	oligopeptide transporter	7.2	8.6
Traes_5BL_1FB170E61	oligopeptide transporter	7.1	8.6
Traes_6AL_E36FCEF64	YELLOW STRIPE like 3	16.1	2.7
Traes_6DL_5DBBFECCE	YELLOW STRIPE like 3	18.6	3
Traes_6DL_3D278E90B	YELLOW STRIPE like 3	15.5	3.6
Traes_6BL_D65EC1432	YELLOW STRIPE like 3	16.6	2.9
Traes_2DS_8412888CC	YELLOW STRIPE like 6	9.1	4.6
Traes_XX_C4B4AC930	oligopeptide transporter	3.8	5.3
Traes_2BS_22338066D	YELLOW STRIPE like 6	15.6	16.3
Traes_5AL_56B342438	oligopeptide transporter	10.3	6
Traes_2AL_05E2128A0	YELLOW STRIPE like 6	17.2	13.8
Traes_2BL_70A2B7D4D	YELLOW STRIPE like 6	16.8	11.7
Traes_2DS_44E756DF1	YELLOW STRIPE like 6	9.4	10.1
Traes_2DL_08D815674	YELLOW STRIPE like 6	12.7	11.2
Traes_2BS_F118753CB	YELLOW STRIPE like 6	6.8	3.8
Traes_2AS_8E650B00A	YELLOW STRIPE like 6	5.4	3.6

Continued on next page

Continued from previous page

Identifier	Description	Fold Change Roots	Fold Change Flag Leaves
ZIP			
Traes_7AL_DFE86911E	Zinc transporter ZupT	4.5	3.2
Traes_7DL_9CB5956DB	Zinc transporter ZupT	4.8	3.1
Traes_7AS_457E5890B	Zinc transporter 10	3.5	-5.9
Traes_7AL_A13A246B4	Zinc transporter 10	2.5	-4.9
Traes_7DL_24CBFF460	Zinc transporter 10	2.5	-5.1
Traes_7BL_E5CFC3DCE	Zinc transporter 10	2.3	-4.2
Traes_2DL_D0582A4B1	Zinc transporter 8	-6.1	2.1
Traes_7BL_5C965DB64	Zinc transporter 10	2.4	-5.9
Traes_2DL_96E58C1AB	Zinc transporter 3	-2.8	-11
Traes_XX_4C6DD3A91	Zinc transporter 3	-2.7	-12.4
Traes_4BL_68691F1FC	Zinc transporter 5	2.1	-34.8
HMA			
Traes_7DL_2F413CF0E	Heavy metal transport/detoxification superfamily protein	3.9	-7.8
Traes_7AL_7D691F809	Copper transport protein CCH	3.6	-8.3
Traes_2AS_95611CAD2	Heavy metal transport/detoxification superfamily protein	-2.1	-2.4
Traes_4DL_15C4B32F2	Heavy metal transport/detoxification superfamily protein	-2.1	16.2
Traes_4BS_B43F7236C	Heavy metal transport/detoxification superfamily protein	-2.6	2.8
Traes_4BL_42FE687F8	Heavy metal transport/detoxification superfamily protein	-2.1	8.7
Traes_4BL_31CA6CB0E	Heavy metal transport/detoxification superfamily protein	-2	3.9
Traes_4AL_8ECAE34E1	Heavy metal transport/detoxification superfamily protein	-4.4	3.5
VDAC			
Traes_1BL_EFFEA6E06	S-type anion channel SLAH2	-5.5	8.4
Traes_1AL_FACE446EE	S-type anion channel SLAH2	-3.3	36.5
Traes_1DL_DBAB8928C	C4-dicarboxylate transporter/malic acid transport protein	-4.2	29.3
Traes_1DL_912E742DC	C4-dicarboxylate transporter/malic acid transport protein	-3.6	13.7
Traes_1AL_07B3AC9EA	C4-dicarboxylate transporter/malic acid transport protein	-2.7	12.4
Traes_1AL_A7FBB0439	C4-dicarboxylate transporter/malic acid transport protein	-2.9	13.5
NRAMP			
Traes_7BL_03741F576	Divalent metal cation transporter MntH	153.1	25.2
Traes_7DL_365ECF19A	Divalent metal cation transporter MntH	45.9	26.1
Traes_7AL_76159C6DA	Divalent metal cation transporter MntH	365.6	38.5
Traes_4AS_BBF51CA2E	Divalent metal cation transporter MntH	2.7	7.1
Traes_4DL_CA00023AB	Divalent metal cation transporter MntH	2.7	8.3
Traes_4BL_C6A3F5C8A	Divalent metal cation transporter MntH	2.7	7.4
AQP			
Traes_XX_8F8470843	Aquaporin-like superfamily protein	-4	-2.9
Traes_7DL_AD746EA0B	Aquaporin-like superfamily protein	-3.7	-2.6
Traes_3B_4780C974B	Aquaporin-like superfamily protein	-2.2	2.9
Traes_1AL_4F0745006	Aquaporin-like superfamily protein	-6	11.1
Traes_XX_F880AD2BF1	Aquaporin-like superfamily protein	-4.3	10.4
Traes_XX_CED1B08C91	Aquaporin-like superfamily protein	-4.7	10.1

Table 3.3. DEGs encoding for transporters shared among roots and flag leaves. The table enlists eight most differentially expressed gene families encoding for transporters ($p < 0.01$, fold change ≥ 2) that are shared

among roots and flag leaves under iron-deficient condition. Positive number of fold change indicates up-regulation of gene expression. Negative number of fold change indicates down-regulation of gene expression.

3.3.5 Regulatory factors controlling iron deficiency responses in wheat

Genes encoding regulatory factors from *bHLH*, *NAC*, *WRKY* and *GAI, RGA, SCR* (*GRAS*) transcription factor families responded to iron deficiency stress in wheat. Over 57% of the differentially expressed genes encoding *bHLH* transcription factors were up-regulated in roots, ranging from 2-fold to over 620-fold changes (Supplementary table 3.7). The *bHLH* transcription factor gene family was also highly regulated in the flag leaves, with 68% of the DEGs up-regulated (Supplementary table 3.7). In total, 41 *bHLH* DEGs were shared between roots and flag leaves (Table 3.4). The expression of *bHLH29* homolog Traes_2DL_BDB1CAB26 increased by 11-fold and 17-fold in roots and flag leaves, respectively. Three *bHLH35* homolog genes i.e., Traes_2AL_088338613, Traes_2BL_F442E87DD and Traes_2DL_47E8C44C6 were induced over 7-fold in both tissues, while another five *bHLH35* homolog genes have opposite expression pattern in roots and flag leaves. The *ORG2* (*bHLH38* homolog) genes (Traes_2AL_ACBAA6A31, Traes_2BL_00608F8D6 and Traes_2DL_865346DA2) showed up-regulated expression levels in the range of 210 to 620-fold for both roots and flag leaves. The remaining *ORG2* (*bHLH38* homolog) genes were also at least 11-fold up-regulated. Among the *bHLH47* homolog genes, most exhibited at least 2.3-fold elevated expression under iron deficiency. The expression pattern of *ILR3* (*bHLH105* homolog) was similar in roots and flag leaves, with four genes (Traes_2AS_C4568AE60, Traes_XX_DB86ECE75, Traes_XX_EF7022C38 and Traes_2DS_1FE8E9DE9) up-regulated and three genes (Traes_XX_92E251AC6, Traes_1DL_A2C6C77E8 and Traes_1AL_81A6723C9) down-regulated.

Over 60% of the genes encoding transcription factors belonging to *NAC* and *WRKY* transcription factor families and over 80% of the *GRAS* transcription factor genes were up-regulated in roots (Supplementary table 3.7). In flag leaves, 92% and 100% of the genes encoding *NAC* and *WRKY* transcription factors, respectively, were up-regulated. Besides, six of the ten *GRAS* family genes were also up-regulated in flag leaves (Supplementary table 3.7). In total, 15 and 84 *NAC* genes were differentially expressed in roots and flag leaves, respectively (Table 3.4). However, only two of these *NAC* genes are shared among the roots and flag leaves. The Traes_3B_8BB0A0443 was induced by 3-fold in both the tissues, whereas Traes_4AS_DBDA5E9C6 had a reduced expression in roots but was up-regulated in the flag leaves. Similar to the *NAC* genes, only three *WRKY* transcription factor genes were

shared between both the tissues. All three of these shared *WRKY* DEGs (Traes_2DL_B8483F711, Traes_7DL_A9EF00572 and Traes_4AS_0DA136E0E) were up-regulated with 2.4 to 11.5-fold increase in roots and flag leaves. All the *GRAS* DEGs exhibited over 3-fold increase under iron-deficient conditions, in both roots and flag leaves. Most of the transcription factors that are shared among roots and flag leaves were highly induced (Table 3.4; Supplementary table 3.7). Given the high expression changes observed during iron deficiency stress, *bHLH* appeared to be the most regulated gene family as compared to the *NAC*, *WRKY* or *GRAS* (Table 3.4; Supplementary table 3.7). The observed differential and high expression changes in above transcription factors signify their regulatory role in controlling iron deficiency responses in bread wheat and indicate a complex regulatory network. Particularly, the transcription factors that are shared between the roots and flag leaves indicate a more systemic response to iron deficiency stress.

Identifier	Blast Hit	Description	Fold Change	Fold Change
bHLH				
Traes_2DL_BDB1CAB26	*bHLH29*	Transcription factor FER-LIKE IRON DEFICIENCY-INDUCED TRANSCRIPTION FACTOR	11.6	17.4
Traes_2AL_088338613	*bHLH35*	basic helix-loop-helix (bHLH) DNA-binding superfamily protein	10.9	13.9
Traes_2BL_F442E87DD	*bHLH35*	basic helix-loop-helix (bHLH) DNA-binding superfamily protein	10.8	15
Traes_2DL_47E8C44C6	*bHLH35*	basic helix-loop-helix (bHLH) DNA-binding superfamily protein	11.4	7.8
Traes_2DL_DE3909A32	*bHLH35*	basic helix-loop-helix (bHLH) DNA-binding superfamily protein	-7.5	14.7
Traes_2AL_411B944D6	*bHLH35*	basic helix-loop-helix (bHLH) DNA-binding superfamily protein	-7.3	13.2
Traes_2BL_8FED05903	*bHLH35*	basic helix-loop-helix (bHLH) DNA-binding superfamily protein	-6.9	15.4
Traes_XX_D84E3D996	*bHLH35*	basic helix-loop-helix (bHLH) DNA-binding superfamily protein	-2.3	2.2
Traes_5AL_EDF2DD187	*bHLH35*	Transcription factor bHLH35	-9.2	5.8
Traes_3B_2A12B8F93	*bHLH38*	basic helix-loop-helix (bHLH) DNA-binding superfamily protein	20.2	33.6
Traes_3DL_886A895A4	*bHLH38*	basic helix-loop-helix (bHLH) DNA-binding superfamily protein	15.3	117.9
Traes_2AL_ACBAA6A31	*bHLH38*	Transcription factor ORG2	619.1	257.4
Traes_2BL_00608F8D6	*bHLH38*	Transcription factor ORG2	624.7	353.4
Traes_2DL_865346DA2	*bHLH38*	Transcription factor ORG2	514.8	210.3
Traes_3AL_F577372C1	*bHLH38*	Transcription factor ORG2	18.9	97.1
Traes_3AL_95403ABBA	*bHLH38*	Transcription factor ORG2	13.1	30.2
Traes_3B_089C0C2EB	*bHLH38*	Transcription factor ORG2	25.6	185.5
Traes_XX_D5A7188DF	*bHLH38*	Transcription factor ORG2	11.8	115.2
Traes_3AL_B0A5AA3FD	*bHLH38*	Transcription factor ORG2 n=1 Tax=Triticum urartu RepID=M7Z1G9_TRIUA	15.5	96.7
Traes_3DL_C73683B71	*bHLH38*	Transcription factor ORG2 n=1 Tax=Triticum urartu RepID=M7Z1G9_TRIUA	13.7	71.6
Traes_3B_FAAFF83D5	*bHLH38*	Transcription factor ORG2 n=1 Tax=Triticum urartu RepID=M7Z1G9_TRIUA	14.5	123
Traes_XX_8E85AF8D3	*bHLH47*	Transcription factor bHLH47	12.9	15.6
Traes_XX_118CA7B60	*bHLH47*	Transcription factor bHLH47	10.7	13.4
Traes_2DS_FE62DB7F5	*bHLH47*	Transcription factor bHLH47	10.7	10.5
Traes_XX_98626A3B7	*bHLH47*	Transcription factor bHLH47	10.8	10.9
Traes_2AS_9AEA9BDEA	*bHLH47*	basic helix-loop-helix (bHLH) DNA-binding superfamily protein	8.8	13.6
Traes_2BS_8A40B568C	*bHLH47*	basic helix-loop-helix (bHLH) DNA-binding superfamily protein	12.2	16.1
Traes_XX_FD1358688	*bHLH47*	basic helix-loop-helix (bHLH) DNA-binding superfamily protein	2.3	3.9
Traes_XX_92E251AC6	*bHLH 105*	Transcription factor ILR3	-2.8	-11.3
Traes_1DL_A2C6C77E8	*bHLH 105*	Transcription factor ILR3	-2.8	-9.3

Continued on next page

Continued from previous page

Identifier	Blast Hit	Description	Fold Change	Fold Change
bHLH				
Traes_1AL_81A6723C9	*bHLH 105*	Transcription factor ILR3	-2.5	-11.2
Traes_2AS_C4568AE60	*bHLH 105*	Transcription factor ILR3	2.3	4.2
Traes_XX_DB86ECE75	*bHLH 105*	Transcription factor ILR3	2.1	3.8
Traes_XX_EF7022C38	*bHLH 105*	Transcription factor ILR3	2.1	3.8
Traes_2DS_1FE8E9DE9	*bHLH 105*	Transcription factor ILR3	2.2	3.7
Traes_3B_5D2D7A5A6		basic helix-loop-helix (bHLH) DNA-binding superfamily protein	-2.1	6
Traes_3AS_037375C84	*bHLH 41*	basic helix-loop-helix (bHLH) DNA-binding family protein	-2.4	7.4
Traes_XX_659B0ACB7		basic helix-loop-helix (bHLH) DNA-binding superfamily protein	-2.8	10.8
Traes_XX_23413A338		basic helix-loop-helix (bHLH) DNA-binding superfamily protein	-2.7	10
Traes_XX_209BC5D01	*bHLH 92*	basic helix-loop-helix (bHLH) DNA-binding superfamily protein	-2.1	2.7
Traes_5DL_7F04E547A	*bHLH 65*	Transcription factor PIF5	-2.2	-2.8
NAC				
Traes_3B_8BB0A0443		NAC domain protein,	3.2	2.7
Traes_4AS_DBDA5E9C6		NAC domain protein,	-2.2	3.2
WRKY				
Traes_2DL_B8483F711		WRKY45-like transcription factor n=3 Tax=Triticeae RepID=F8WPI8_WHEAT	5.8	2.4
Traes_7DL_A9EF00572		WRKY DNA-binding protein 46	3.1	2.8
Traes_4AS_0DA136E0E		WRKY DNA-binding protein 70	4.2	11.5
GRAS				
Traes_3AL_60B6CD0A5		GRAS family transcription factor	3.3	3.8
Traes_3B_A25F058E5		GRAS family transcription factor	3.1	3.6
Traes_XX_DFACD194B1		GRAS family transcription factor	3.1	3.7
Traes_XX_DFACD194B		GRAS family transcription factor	3.1	3.8
Traes_XX_5BC8C939F		GRAS family transcription factor	3.2	3.7
Traes_3DL_A3AC10E58		GRAS family transcription factor	3.3	3.6

Table 3.4. DEGs encoding transcription factors shared among roots and flag leaves. The table enlists the differentially expressed genes encoding for transcription factors ($p < 0.01$, fold change ≥ 2) and shared among roots and flag leaves under iron deficient condition. Positive number of fold change indicates up-regulation of gene expression. Negative number of fold change indicates down-regulation of gene expression

3.3.6 Expression analysis of the homeologous gene triplets

DEGs were assigned to the three wheat subgenomes A, B and D to get an overview if specific subgenomes contribute differentially to iron deficiency stress. The three subgenomes share a similar number of DEGs with an order of B genome (flag leaves: 2389; roots: 1380) > D genome (flag leaves: 2211; roots: 1192) > A genome (flag leaves: 2045; roots: 1163) > unknown (flag leaves: 1309; roots: 832), which is consistent with the number of annotated high confidence genes in each of these subgenomes (Supplementary figure 3.3). Among these DEGs, between 20 to 26% exist as triplets on bread wheat genome (Supplementary figure 3.4), which is consistent with the total number of triplets assigned to wheat subgenomes (25.1% to 26.8%) in the MIPS database (Supplementary figure 3.3). The differentially expressed homeolog triplets were compared across subgenomes. About 75 to 78% of the triplets were detected as significantly differentially expressed in all the subgenomes while around 14% of the triplets could be assigned to 2 subgenomes in flag leaves. Only 8 to 12% triplets showed differential expression specific to one subgenome in case of flag leaves. In case of roots, a slightly lower percentage (67-69%) of differentially expressed triplets overlapping the three subgenomes was observed, with 21% and 10% of the differentially expressed triplets assigned to 2 subgenomes and 1 subgenome, respectively (Supplementary figure 3.5). Except for some genes, the differentially expressed triplets appeared to be regulated in a very similar manner between the three subgenomes (Figure 3.6A and 3.6B).

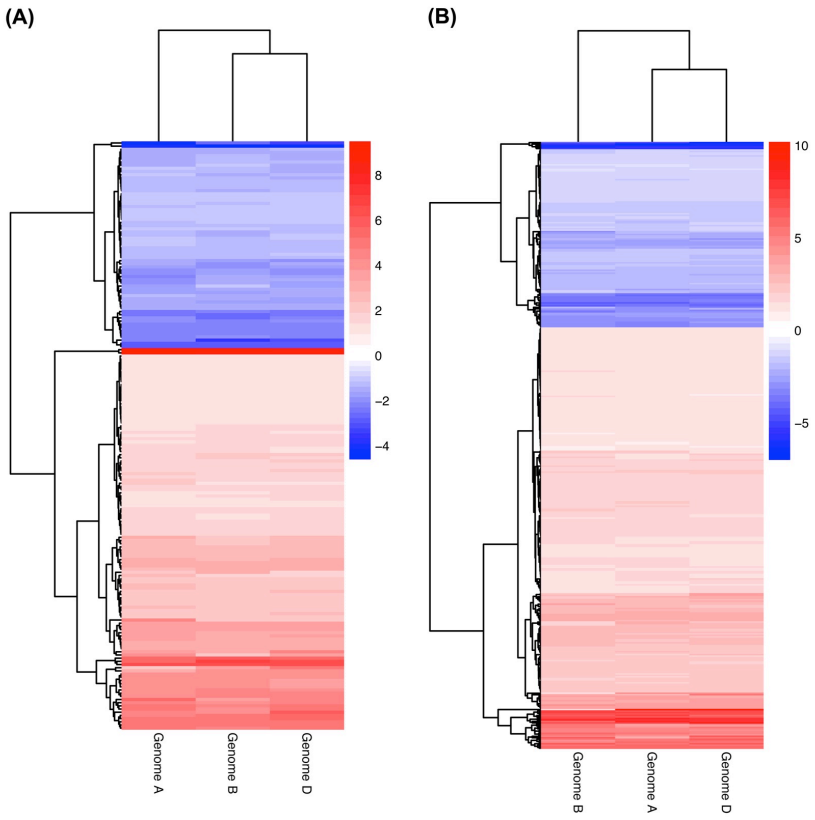

Figure 3.6. Profiling of differentially expressed genes in homeolog triplets in roots and flag leaves. Red color represents up-regulation of expression and blue color represents down-regulation of expression during iron deficiency stress condition. (A) roots, (B) flag leaves.

3.4 Discussion

Hexaploid bread wheat possesses a complex genomic and evolutionary background (Marcussen *et al.*, 2014). The large genome size, three sub-genomes and poor gene annotations all bring difficulties to effectively carry out molecular analyses in wheat. Therefore, many of the bread wheat RNA sequencing experiments still choose transcriptome database, such as NCBI UniGene database, Dana Farber Cancer Institute (DFCI) wheat gene index, or genome sequences of well annotated grass species like rice and *Brachypodium distachyon* for mapping of the wheat RNA sequencing reads (Gillies *et al.*, 2012; Pellny *et al.*, 2012). Besides, *de novo* assembly based approach was also used for analyzing results from RNA sequencing-based transcriptome studies in wheat (Li *et al.*, 2013a; Oono *et al.*, 2013; Xiao *et al.*, 2013). The recently released hexaploid bread wheat genome chromosome-based draft annotates 124,201 gene loci on individual chromosome arm sequences (IWGSC, 2014). With the IWGSC wheat genome sequence becoming available, it is expected that the omics studies could be widely and effectively conducted in wheat. In our study, we used RNA

sequencing to gain an insight into the global gene expression profiles in wheat when exposed to iron deficient condition, particularly at the commencement of grain filling. We analyzed our results by using IWGSC wheat genome sequence as a reference.

Although the soils are abundant in iron, conditions like high pH and presence of sodium carbonate in the soil adversely affect iron uptake and absorption by plants, thereby negatively affecting the agricultural produce. From human nutrition point of view as well, it is equally necessary to study the mechanisms controlling iron uptake and translocation, so as to design effective biofortification strategies to tackle iron deficiency anemia. Plant responses to iron deficiency have been extensively studied in non-graminaceous plant species like Arabidopsis (Brumbarova *et al.*, 2015) and graminaceous plants including rice (Lee *et al.*, 2012a). To date, there is very limited information available relating to iron deficiency responses of wheat (Bashir *et al.*, 2006; Neal *et al.*, 2013; Uauy *et al.*, 2006; Waters *et al.*, 2009).

3.4.1 Enhanced production of iron chelators during iron deficiency

Iron homeostasis in plants is tightly controlled by a concerted involvement of various iron ligands, transporters and regulatory factors. Generally, iron combines with ligands for transportation or storage to reduce the risk of toxic ROS production by the free iron (Alvarez-Fernandez *et al.*, 2014). Therefore, the production of iron ligands often depends on the amount of iron available for uptake and/or translocation. Citrate and malate are among the known iron chelators that form complexes with Fe (III), such as $Fe(III)_3Cit_3$ (Rellan-Alvarez *et al.*, 2010), $Fe(III)Cit_2$, $Fe(III)_3Cit_2Mal_2$ and $Fe(III)_3Cit_3Mal_1$ (Grillet *et al.*, 2014). Our results suggested increased expression of citrate and malate synthesis related genes, thereby identifying the roles of citrate and malate as iron ligands in bread wheat as well. Similar results with increased production of α-ketoglutarate, succinate, fumarate, malate and citrate were reported in case of iron-deficient sugar beet (Lopez-Millan *et al.*, 2000a). Additionally, the data also suggests increased production of NA and DMA, the two important and well described iron chelators. During iron deficiency stress, the key genes involved in PSs synthesis i.e., *S-ADENOSYLMETHIONINE SYNTHETASE* (*SAMS*), *NAS*, *NAAT*, *DMAS* were up-regulated in wheat roots and flag leaves, which is consistent with the findings from other monocots (Bashir *et al.*, 2006; Inoue *et al.*, 2003; Inoue *et al.*, 2008). We observed induced expression of *SAMS* in wheat roots during iron deficiency, which is unlike barley where no change in *SAMS* expression was reported when comparing iron deficient and control growth

conditions (Takizawa *et al.*, 1996). A proteomic study in cucumber roots even showed a reduction of SAMS protein (Donnini *et al.*, 2010).

Different graminaceous plants secrete their preferred MAs for iron acquisition. For example, rice releases DMA into the soil for iron chelation (Bashir and Nishizawa, 2006) while barley secretes MA, epiHMA and HMA in addition to the DMA which serves as precursor for the synthesis of these additional phytosiderophores (Nakanishi *et al.*, 2000). Two MA synthesis related genes, *IDS2* and *IDS3* (*IRON DEFICIENCY-SPECIFIC CLONE2* and *-3*), were identified in barley. In our study, the *IDS3* homolog gene expression could not be detected in either roots or flag leaves. Based on HPLC analysis of root washings collected from iron-deficient modern and ancestral wheat cultivars, it has been suggested that wheat only secrete DMA but not MA or HMA (Singh *et al.*, 2000). Our results also indicate that DMAs might be the only phytosiderophore released by bread wheat (cv. Bobwhite studied here).

3.4.2 Concerted action of a range of transporters is required for iron translocation in bread wheat

A variety of transporters play an important role in intercellular and intracellular plant iron translocation and the cooperation of these proteins is vital to plant growth and development. Under iron-deficient conditions, many transporter gene families were significantly differentially regulated in bread wheat flag leaves and roots, such as *MFS*, *ABC* transporter family, *MATE*, *OPT* superfamily and *NRAMP* family. The MFS together with ABC transporters, are the two universal transporter superfamilies across the living kingdom (Pao *et al.*, 1998). As the largest secondary transport carriers superfamily, MFS facilitates the transport of various substances such as amino acids, peptides, drugs, nucleotides, as well as iron chelates, etc. (Reddy *et al.*, 2012). An MFS family member, TOM1, exports DMA to the soil and is involved in internal iron transportation of DMA to the phloem and xylem in rice plants (Nozoye *et al.*, 2011). The zinc-induced facilitators *OsZIFL4*, *OsZIFL5*, *OsZIFL7* and *OsZIFL12* were up-regulated in rice roots under iron deficiency which suggested their role in iron transport (Ricachenevsky *et al.*, 2011). The expression of *ZIFLs* was not altered in rice leaves though (Ricachenevsky *et al.*, 2011). In case of wheat, we observed induced expression for most of the *ZIFL* genes in both the flag leaves and roots, and the *TOM1* homolog was highly up-regulated in the wheat roots. We also detected an increased expression of the *FPN* genes under iron-deficient conditions, which is similar to the response observed in Arabidopsis (Morrissey *et al.*, 2009). These results demonstrate that *MFS* genes play an

important role for iron transport in bread wheat and various subfamily members are involved in a coordinated manner, likely serving different functions to maintain overall iron homeostasis.

The ABC superfamily is one of the largest primary active transporter family, which transports mineral ions, lipids, and peptides, and hence is very crucial for import and export of metabolites (Rea, 2007). Several of the genes belonging to ABC transporter family were significantly regulated in wheat roots and flag leaves during iron deficiency. The expression of one ABC transporter G family (PLEIOTROPIC DRUG RESISTANCE, PDR) member - *NtPDR3* has been reported to be induced in *Nicotiana tabacum* suspension cells under iron-deficient conditions (Ducos *et al.*, 2005). Likewise, the *OsABCB14* gene belonging to B family of ABC transporters has been reported as an auxin transporter influencing iron homeostasis in rice plants (Xu *et al.*, 2014). In plants, the *MRP* genes (ABC transporter C family, *MULTIDRUG RESISTANCE-ASSOCIATED PROTEIN*) were reported to transport phytic acid into vacuoles (Nagy *et al.*, 2009). In mammalian cells, MRP1 was identified as GLUTATHIONE (GSH) conjugate transporter and was associated to NO-mediated iron efflux from cells (Lok *et al.*, 2012; Watts *et al.*, 2006). Similarly, our data identified several wheat homologs of genes encoding ABC transporters that were differentially regulated in wheat roots and flag leaves under iron-deficient conditions and suggests their direct and/or indirect involvement in iron transport.

The plant MATE family, localized in vacuoles and the plasma membrane, is known to mainly facilitate transportation of secondary metabolites and xenobiotics (Omote *et al.*, 2006). MATE transporters have been reported to mediate the efflux of citrate into the root vasculature in rice, soybean and Arabidopsis and therefore could improve plant iron transport efficiency (Durrett *et al.*, 2007; Rogers *et al.*, 2009; Tovkach *et al.*, 2013; Yokosho *et al.*, 2009). We also observed increased expression of several *MATE* genes, both in roots and flag leaves, which correlates with the increased production of citrate during iron deficiency (Supplementary table 3.6). These differentially expressing MATE transporters appear to be important for Fe(III)-citrate transport in wheat (Figure 3.3).

Transporter families such as OPTs, NRAMP and ZIP families have been studied in Arabidopsis, rice and maize. As one of the well characterized metal transporter family, YSLs have been shown to be involved in iron acquisition from the soil and its long-distance transport through phloem (Inoue *et al.*, 2009; Ishimaru *et al.*, 2010; Lee *et al.*, 2009a). The

NRAMP family is also considered as an important metal transporter family with several of these genes participating in iron transport through vacuoles and plasma membrane (Lanquar *et al.*, 2005). Similarly, the ZIP family is involved in transport of divalent metals such as iron, zinc and manganese (Guerinot, 2000). The expression of genes from *OPT*, *NRAMP* and *ZIP* families were significantly regulated in bread wheat during the iron deficiency conditions, suggesting a similar role in long-distance and/or intracellular iron translocation in wheat.

3.4.3 Complex regulatory network controls iron homeostasis

Among the regulatory factors, the bHLH transcription factor family is one of the most widely reported to be involved in regulation of plant iron homeostasis related genes. In our study, several *bHLH* members including homologs of *bHLH29*, *bHLH38*, *bHLH47*, and *bHLH105* were found to be highly up-regulated under iron deficiency. In case of rice, the IRO2 regulates expression of genes responsible for DMA synthesis and iron transport such as *OsNAS1*, *OsNAS2*, *OsNAAT1*, *OsDMAS1*, *OsYSL15* and *TOM1* (Ogo *et al.*, 2006; Ogo *et al.*, 2011; Ogo *et al.*, 2007). In Arabidopsis, *bHLH38*, together with the other three Ib subgroup bHLH transcription factors *bHLH39*, *bHLH100* and *bHLH101* were up-regulated in leaves as well as roots, under iron-deficient conditions (Wang *et al.*, 2007). The bHLH38 and bHLH39 have been reported to form heterodimers with FER-Like iron deficiency-induced transcription factor (FIT/bHLH29), in order to regulate the gene encoding *FERRIC CHELATE REDUCTASE* (*FRO2*) and *IRON-REGULATED TRANSPORTER* (*IRT1*) in Arabidopsis (Yuan *et al.*, 2008b).

Both NAC and WRKY transcription factor families have been widely reported to be involved in regulating abiotic stress such as cold, drought, salinity stress etc. (Chen *et al.*, 2012; Nakanishi *et al.*, 2000). Some of the factors in the NAC family have also been reported to regulate iron transport in both wheat and rice (Rushton *et al.*, 2010; Uauy *et al.*, 2006). The NAC family member, IRON DEFICIENCY-RESPONSIVE CIS-ACTING ELEMENT 2 (IDE2) BINDING FACTOR (OsIDEF2) binds to *OsYSL2* promoter region and regulates the expression of *OsYSL2* (Ogo *et al.*, 2008). Among the WRKY family, *OsWRKY80* was associated with gene regulation during iron excess (Ricachenevsky *et al.*, 2011). Increased gene expression of *OsWRKY17* and *OsWRKY45* were also observed in iron deficient rice roots and shoots, respectively (Ogo *et al.*, 2006; Sperotto *et al.*, 2008). We also detected elevated expression levels for many of the NAC and WRKY family members especially in leaves, suggesting their regulatory role in maintaining wheat iron homeostasis.

Together, our RNA sequencing data revealed the genes modulated during iron deficiency stress in wheat and reflected on the role of several iron ligands, transporters as well as regulatory mechanisms involved in iron homeostasis. TCA cycle, methionine salvage and phytosiderophore synthesis were observed as accelerated, perhaps due to a large demand of iron chelators such as citrate, NA and DMA during iron deficiency conditions. Several other gene families including the *MFS*, *ABC* transporters, *OPT*, *NRAMP* families were significantly regulated, thereby facilitating effective transport of iron. These observations lay an important foundation for further research on iron deficiency stress responses in wheat and as well for biofortification programs.

3.5 Experimental procedures

3.5.1 Plant material and iron deficiency stress treatment

Triticum aestivum cv. Bobwhite S26 seeds were germinated on wet filter paper for 7 days and then transferred to the hydroponic system in the greenhouse conditions (22˚C/18˚C with 16-hour-light/8-hour-dark cycle, 60% humidity). All the seedlings were first maintained in iron-sufficient hydroponic solution for 7 days and then half of the plants were transferred to iron-deficient hydroponic solutions. Hydroponic solutions (pH 6.0) were prepared according to protocol modified from Durmaz *et al*. (2011), using 0.88 mM K_2SO_4, 2 mM $Ca(NO_3)_2$, 0.2 mM KH_2PO_4, 1.0 mM $MgSO_4$, 0.1 mM KCl, 1.0 µM H_3BO_3, 1.0 µM $MnSO_4$, 0.2 µM $CuSO_4$, 0.02 µM $(NH_4)_6Mo_7O_{24}$, and 1.0 µM $ZnSO_4$ with different Fe(III)-EDTA concentrations (iron-sufficient condition: 100.0 µM Fe; iron-deficient condition: 10.0 µM Fe). The hydroponic solutions were refreshed every week. Air was continuously pumped into the hydroponics for efficient circulation. Roots and flag leaves were collected at 8-10 days post anthesis (DPA), i.e., around the commencement of grain filling. Three biological replicates were collected for each sample.

In order to verify that iron deficiency is induced in the experimental plants, the chlorophyll content was measured. Around 25mg of flag leaves samples were incubated in 15mL of 95% ethanol solution for 24 hours in dark at room temperature. Two technical replicates were measured from each of the three biological replicates. The ethanol extract was subjected to Ultrospec 3000 UV/ Visble spectrometer measurements (Pharmacia Biotech, Sweden) at A_{649}, A_{470} and A_{664}. The quantification of chlorophyll a, chlorophyll b and carotenoids were calculated according to the Lichtenthaler and Buschmann's protocol (Lichtenthaler and Buschmann, 2001). The chlorophyll a, chlorophyll b decreased nearly 70% and carotenoids

decreased over 50% (Supplementrary figure 3.1) in the wheat plants subjected to iron deficiency, confirming that the iron stress treatment was successfully implemented.

3.5.2 Total RNA extraction, library preparation and Illumina sequencing

Isolation of total RNA from the roots and flag leaves was carried out using the Isol- RNA Lysis Reagent (5 PRIME, USA). The total RNA was digested with RNase-Free DNase (Qiagen, Germany) to remove the genomic DNA followed by RNA cleaning with RNeasy Plant Mini Kit (Qiagen, Germany). The quality of the isolated RNA was determined with a Qubit® (1.0) Fluorometer (Life Technologies, USA) and a Bioanalyzer 2100 (Agilent, Germany).

Strand-specific cDNA libraries (dUTP method) were prepared using TruSeq Stranded mRNA Sample Prep Kit (Illumina, USA). Total RNA samples (1 μg) were poly-A enriched and then reverse-transcribed into double-stranded cDNA with Actinomycin added during first-strand synthesis. The cDNA samples were fragmented, and end-repaired before ligation of TruSeq adapters containing the index for multiplexing fragments. After ligation, these TruSeq adapters were selectively enriched by PCR amplification on both ends. The quality and quantity of the enriched libraries were validated using Qubit® (1.0) Fluorometer and the Caliper GX LabChip® GX (Caliper Life Sciences, USA). The product is a smear with an average fragment size of approximately 250bp. The libraries were normalized to 10nM in Tris-Cl 10 mM, pH8.5 with 0.1% Tween 20. TruSeq PE Cluster Kit v3-cBot-HS (Illumina, USA) was used for cluster generation using 8 pM of pooled normalized libraries on the cBOT. Sequencing was performed on the Illumina HiSeq 2000 paired end at 2 × 101 bp (Illumina, USA).

3.5.3 RNA sequencing data analysis

RNA sequencing reads were quality-checked with fastqc. The reads were trimmed by clipping 5 bases from the read start and end before mapping to the IWGSC (International Wheat Genome Sequencing Consortium) chromosome-based bread wheat genome. The IWGSC wheat chromosome-based genome information and gene annotations were provided by Dr. Klaus Mayer from Munich Information Center for Protein Sequences (MIPS, v2.2).

Reads were aligned to high confidence (HC) genes of IWGSC wheat chromosome-based genome with bowtie2 with no minimum fragment size but a maximum insert size of 1000bp.

To date, 111,982 genes have been identified as high confidence genes in the bread wheat genome, of which 32081, 34226 and 33079 are assigned to subgenomes A, B and D respectively. For 12,596 HC genes, the subgenome information is not available (Supplementrary figure 3.3).

Differential expression analysis was performed using edgeR. The genes which pass the threshold of p-value<0.01 and a fold change of ≥2 were considered as differentially expressed genes. Gene ontology enrichment analysis was performed with 'goseq' package in Bioconductor. GoSlim was performed to remove the redundant GO categories. Data statistics and figure plotting was performed in RStudio (Version 0.98.976) with R and various R plotting packages (ggplot2, VennDiagram and Pheatmap) and Excel.

3.6 Acknowledgements

This research was supported by ETH Zurich research grants to W.G. and to N.K.B., and from State Secretariat for Education, Research and Innovation (SERI) within the COST FA0905 program to N.K.B. We thank Irene Zurkirchen, Kulaporn Boonyaves, Ting-Ying Wu, Kumar Vasudevan, and Simrat Pal Singh for the technical support in the greenhouse and the laboratory.

3.7 Author contributions

N.K.B. conceived and designed the experiments. M.W. carried out the experiments. M.W. and N.K.B. analyzed the data. M.W. and N.K.B. wrote the manuscript. W.G. and N.K.B. edited the manuscript. All authors have read the manuscript and agree with its content.

3.8 Supplementary material

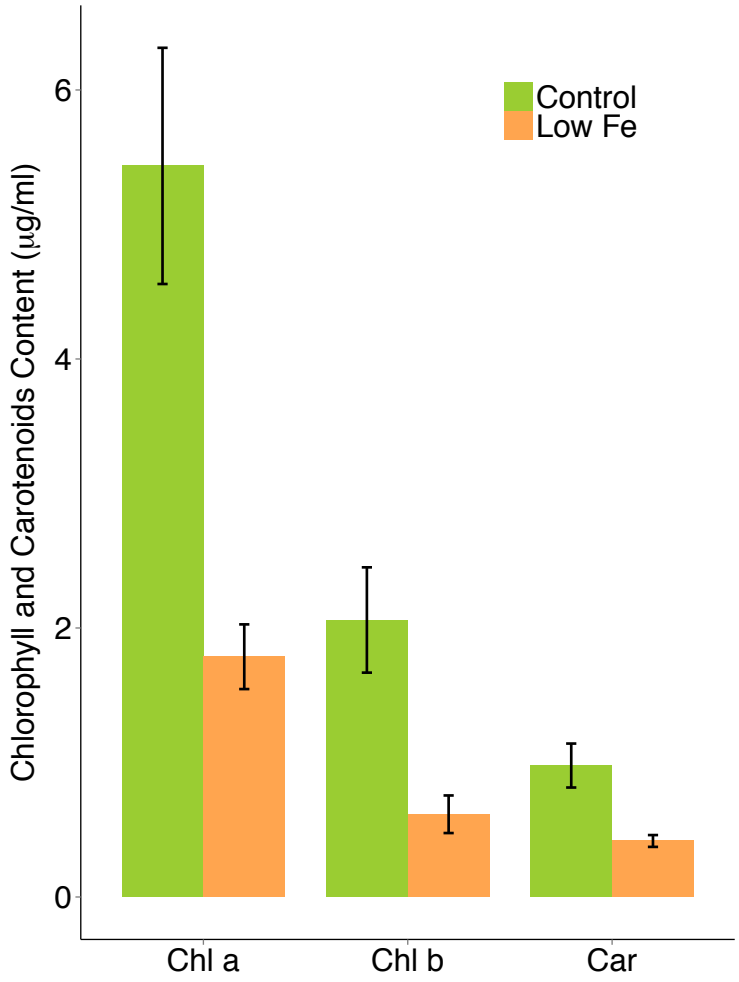

Supplementary figure 3.1. Chlorophyll and carotenoids content of flag leaves. Chlorophyll a, chlorophyll b and carotenoids content of flag leaves was measured by a spectrometer. Chl a stands for Chlorophyll a, Chl b stands for Chlorophyll b, Car stands for carotenoids. Green and orange color represents plants grown under iron sufficient and deficient condition, respectively.

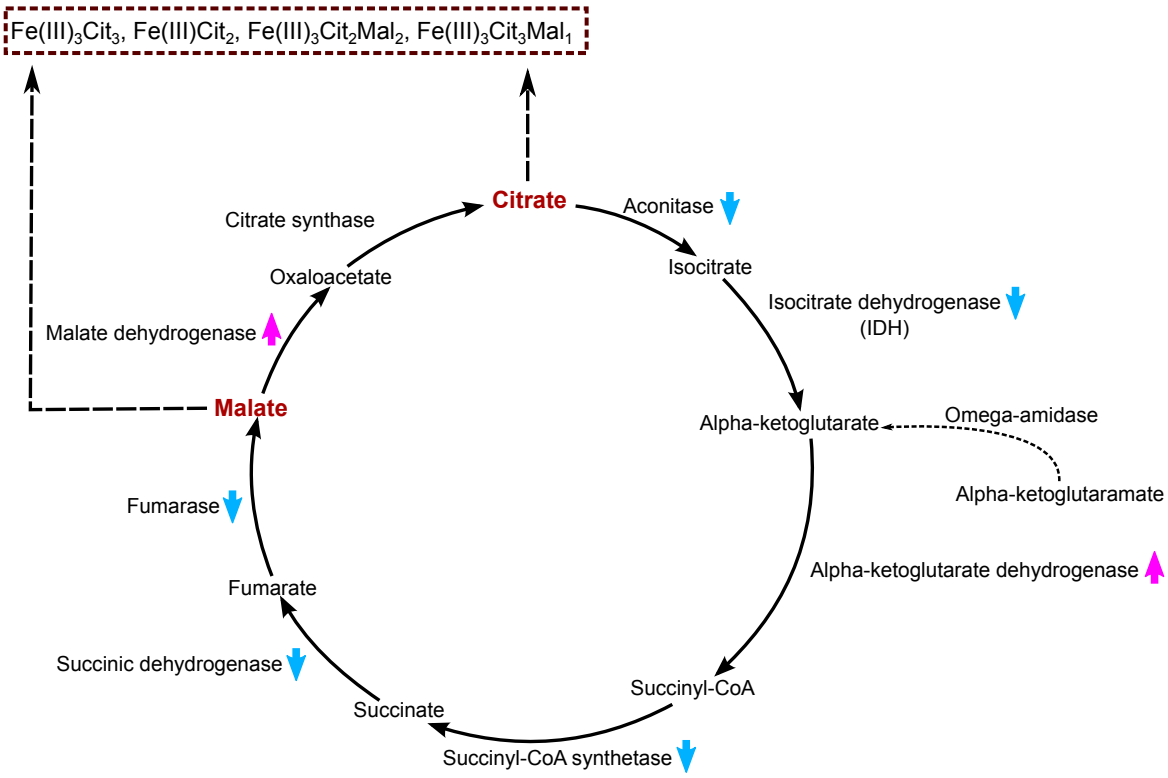

Supplementary figure 3.2. Gene expression regulation in the TCA cycle in flag leaves. Pink and light blue arrows represent up-regulated and down-regulated gene expression, respectively, in flag leaves. $Fe(III)_3Cit_3$, $Fe(III)Cit_2$, $Fe(III)_3Cit_2Mal_2$ and $Fe(III)_3Cit_3Mal_1$ represent the complexes that chelators citrate and malate form with Fe(III).

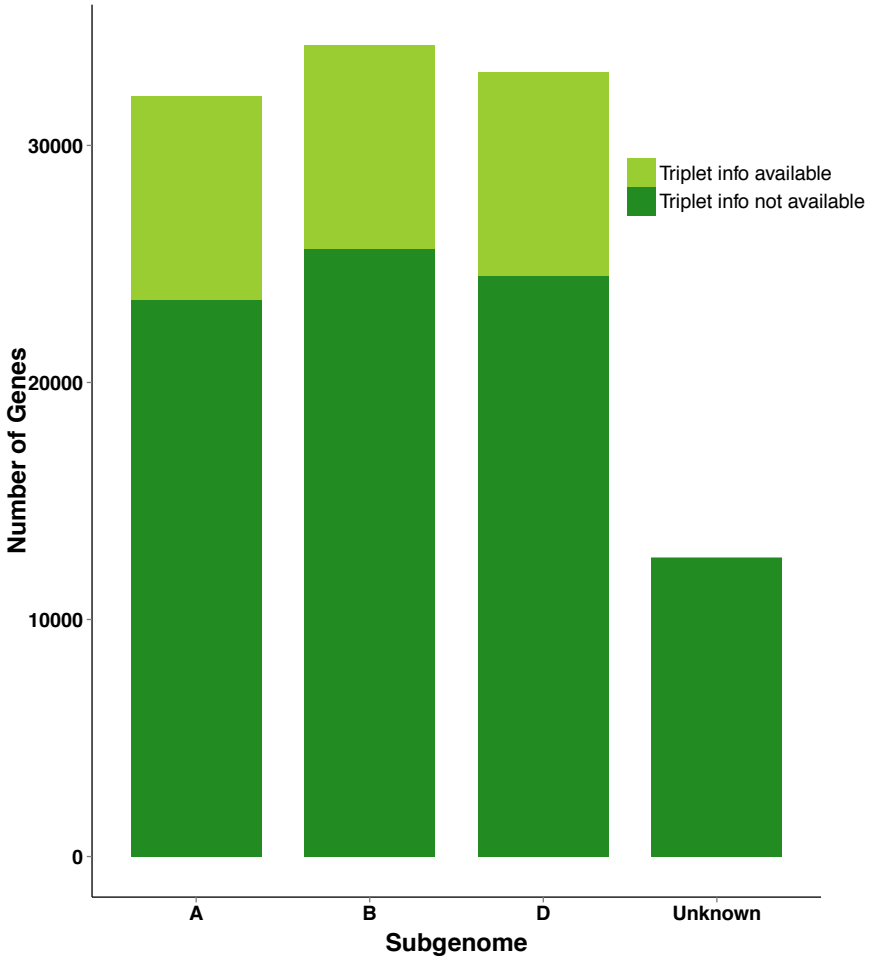

Supplementary figure 3.3. Summary of high confidence (HC) genes of IWGSC wheat chromosome-based genome. In total, 111,982 genes have been identified as high confidence genes in the MIPS 2.2 version wheat genome annotations. Barchart illustrates that 32081, 34226 and 33079 of the HC genes were assigned to bread wheat subgenomes A, B and D respectively. Additionally, 12596 HC genes do not contain the subgenome information and are labeled as 'Unknown' in the figure. Light green color indicates the genes with homeolog triplets annotation information. Dark green color indicates the genes without homeolog triplets annotation information.

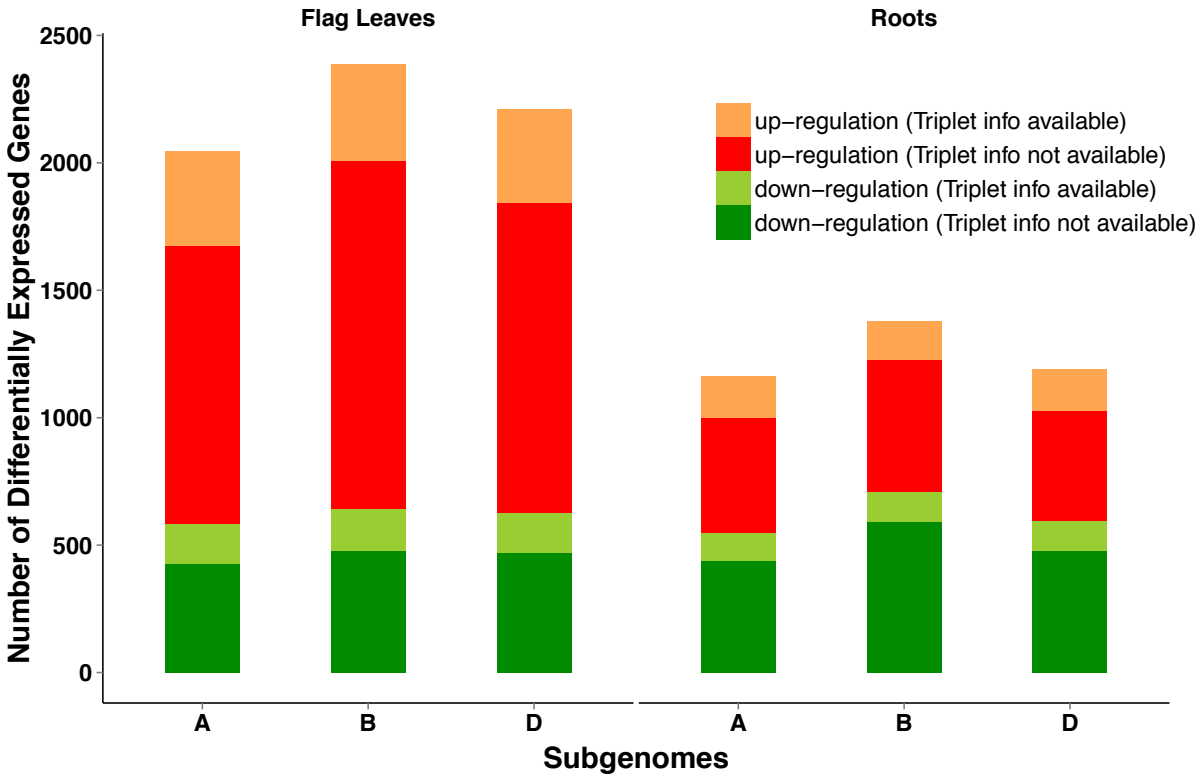

Supplementary figure 3.4. Homeolog triplets annotation information for differentially expressed genes. DEGs were assigned to three hexaploid wheat subgenomes. A, B and D stand for A, B and D subgenomes of bread wheat genome, respectively. Orange color represents up-regulated genes with homeolog triplets annotation information; red color represents up-regulated genes without homeolog triplets annotation information; light green color represents down-regulated genes with homeolog triplets annotation information; dark green color represents down-regulated genes without homeolog triplets annotation information during iron deficiency stress condition.

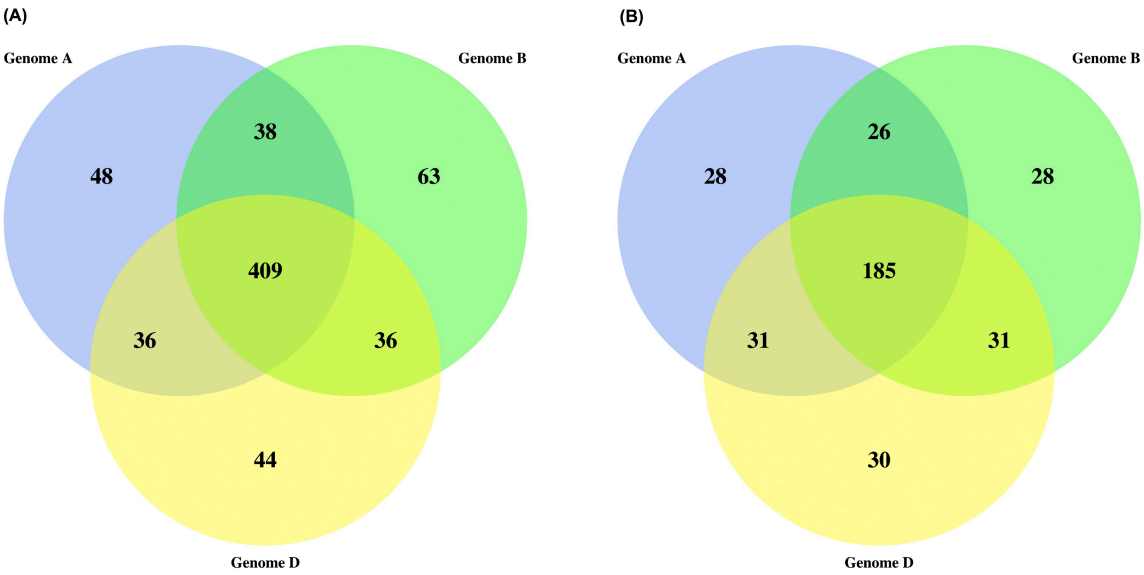

Supplementary figure 3.5. DEGs with homeolog triplets annotation information. Venn diagram shows the overlapping DEGs ($p < 0.01$ and fold change ≥ 2) with homeolog triplets gene information in flag leaves and roots. Blue color represents homeolog triplets DEGs in subgenome A; green represents homeolog triplets DEGs in subgenome B; yellow represents homeolog triplets DEGs in subgenome D. (A) Flag leaves, (B) Roots.

Biological replicates	Total number of reads (million)	Read counts mapped to wheat genome (million)	Pecentage of reads mapped to wheat genome (%)	Genomic features with reads above threshold	Genomic features with reads above threshold (%)
Leaf Control 1	20.6	16.3	79	59711	53.2
Leaf Control 2	17.7	13.8	78	59455	53
Leaf Control 3	21.8	17.1	78	59429	53
Leaf Low Fe 1	28.8	23	80	60560	54
Leaf Low Fe 2	24.9	20	80	60546	54
Leaf Low Fe 3	18.8	14.9	79	60368	53.8
Root Control 1	30.1	21.9	73	63957	57
Root Control 2	26.7	18.8	70	64181	57.2
Root Control 3	17.9	12.5	70	63927	57
Root Low Fe 1	29.8	20.4	68	63860	56.9
Root Low Fe 2	29.9	19.1	64	63977	57
Root Low Fe 3	22	12.4	56	63775	56.9

Supplementary table 3.1. RNA reads mapped to IWGSC wheat chromosome-based genome sequence. The table enlists the total number of reads and the mapping ratio of each biological replicate separately.

Supplementary tables 3.2 – 3.7 contain large dataset from RNA sequencing results and could not be integrated to the word document. They are provided in an independent folder. Their titles and legends are listed here.

Supplementary table 3.2. Gene ontology (GO) enrichment summary. The table enlists the enriched GO terms ($p < 0.01$) for the DEGs in roots and flag leaves under iron deficient condition. FDR stands for false discovery rate.

Supplementary table 3.3. DEGs in the phytosiderophore (PSs) synthesis pathway. The table enlists the DEGs ($p < 0.01$, fold change ≥ 2) related to PSs synthesis in roots and flag leaves under iron-deficient condition. FDR stands for false discovery rate. Positive number of fold change indicates up-regulation of gene expression. Negative number of fold change indicates down-regulation of gene expression.

Supplementary table 3.4. DEGs in the methionine salvage pathway. The table enlists the DEGs ($p < 0.01$, fold change ≥ 2) in methionine salvage pathway in roots and flag leaves under iron deficient-condition. FDR stands for false discovery rate. mtnK: methylthioribose kinase; mtnA:methylthioribose-1-phosphate isomerase; mtnB: 5-methylthioribulose-1-phosphate dehydratase; mtnD: 1,2-dihydroxy-3-keto-5-methylthiopentene dioxygenase 2; mtnE:2-keto-4-methylthiobutyrate aminotransferase;mtnN: methylthioadenosine nucleosidase. Positive number of fold change indicates up-regulation of gene expression. Negative number of fold change indicates down-regulation of gene expression.

Supplementary table 3.5. Differentially expressed *FERRITIN* and *METALLOTHIONEIN* genes. The table enlists the differentially expressed ($p < 0.01$, fold change ≥ 2) *FERRITIN* and *METALLOTHIONEIN* genes in roots and flag leaves under iron-deficient condition. FDR stands for false discovery rate. Positive number of fold change indicates up-regulation of gene expression. Negative number of fold change indicates down-regulation of gene expression.

Supplementary table 3.6. DEGs encoding for transporters, that are shared among roots and flag leaves. The table enlists the differentially expressed genes encoding for transporters ($p < 0.01$, fold change ≥ 2) in roots, flag leaves, and these genes are shared among roots and flag leaves under iron-deficient condition. FDR stands for false discovery rate. Positive number of fold change indicates up-regulation of gene expression. Negative number of fold change indicates down-regulation of gene expression.

Supplementary table 3.7. Differentially expressed *bHLH*, *NAC*, *WRKY* and *GRAS* genes in roots and flag leaves. The table summarizes the DEGs encoding for transcription factors belonging to *bHLH*, *NAC*, *WRKY* and *GRAS* gene families ($p < 0.01$, fold change ≥ 2) in roots and flag leaves under iron-deficient condition. Positive number of fold change indicates up-regulation of gene expression. Negative number of fold change indicates down-regulation of gene expression.

4 TRANSCRIPTOME ANALYSIS OF ZINC DEFICIENCY STRESS RESPONSES IN BREAD WHEAT

Meng Wang[1], Hubert Rehrauer[2], Wilhelm Gruissem[1], and Navreet K. Bhullar[1,*]

[1] Plant Biotechnology, Department of Biology, ETH Zurich (Swiss Federal Institute of Technology), Zurich, Switzerland

[2] Functional Genomics Center, ETH Zurich (Swiss Federal Institute of Technology), Zurich, Switzerland

[*]Corresponding author

Prepared for submission to scientific publication

4.1 Abstract

Zinc is an essential element for all living organisms. Zinc deficiency leads to serious health problems for humans and also affects plant development and nutritional quality. Zinc acquisition, distribution within plants, storage and regulation are complex molecular mechanisms for which several transporters, chelators and regulatory factors play a role. Despite several studies revealing certain mechanisms of zinc homeostasis, it remains unclear how zinc is transported and regulated in staple food crops such as bread wheat. RNA sequencing analysis together with real-time quantitative PCR (qRT-PCR) was carried out to reveal molecular changes in zinc-deficient roots and flag leaves of wheat during grain filling. We identified 4188 and 4089 differentially expressed genes in the roots and flag leaves at the commencement of the grain-filling period. Phytosiderophores (PSs) biosynthesis and transport related genes were mostly down-regulated in the roots but up-regulated in the flag leaves, suggesting a stronger role of PSs in long-distance translocation of zinc than in zinc acquisition in wheat. The expression of genes encoding transporters involved in free Zn(II) transport such as *ZINC-REGULATED TRANSPORTER (ZRT), IRON-REGULATED TRANSPORTER* (*IRT*)*-LIKE* (*ZIP*) genes were significantly induced in roots as well as flag leaves, suggesting their role in both zinc translocation and acquisition. The expression of genes encoding transcription factor families such as *WRKY*, *NO APICAL MERISTEM* (*NAM*)/*ARABIDOPSIS TRANSCRIPTION ACTIVATION FACTOR* (*ATAF*)/*CUP-SHAPED COTYLEDON* (*CUC*) (*NAC*), *ETHYLENE-RESPONSIVE ELEMENT BINDING FACTORS* (*ERFs*) and *BASIC LEUCINE-ZIPPER* (*bZIP*) was significantly induced, indicating their function in regulating zinc deficiency response. Our results provide insights into the molecular response of bread wheat to zinc deficiency stress, and also provide useful information for biofortification approaches.

Key words: zinc deficiency, RNA sequencing, transcriptomic profiles, wheat

4.2 Introduction

Zinc plays a vital role in the metabolism of plants, animals and microorganisms. As an integral component, zinc affects the catalytic activity or structure of many enzymes such as alcohol dehydrogenase, carbonic anhydrase, RNA polymerase, alkaline phosphatase and copper/zinc superoxide dismutase (Guerinot and Eide, 1999). Therefore, zinc is involved in various biological processes such as carbohydrate metabolism, tryptophan and indoleacetic acid (IAA) synthesis, cellular membrane integrity maintenance, and protein synthesis (Broadley *et al.*, 2012). It is known that zinc binds to 925 proteins in humans and over 500 proteins in plants (Graham, 2008). Zinc deficiency reduces plant growth, thereby affecting crop yield and nutritional quality of the harvest (Sadeghzadeh, 2013). Zinc is also an important micronutrient for humans and its deficiency can cause retarded growth, impaired immunity, rough skin, and neuro-sensory disorders (Cakmak, 2008; Prasad, 2012). Zinc deficiency affects nearly 2 billion people, especially widespread in communities relying on low zinc cereal-based diets as a calorie resource (Prasad, 2012).

Wheat is the most widely cultivated staple food crop and major source of energy for the world's population. However, most wheat varieties cannot provide the required daily intake of micronutrients such as iron and zinc for humans (Borrill *et al.*, 2014). Therefore, it is important to understand the molecular mechanisms controlling zinc transport and regulation for further improving zinc availability in wheat grains as well as for better overall yields. Zinc is predominantly absorbed by plants as a divalent cation Zn(II) (Broadley *et al.*, 2012). Localized in the plasma membrane and the endomembrane, the ZINC-REGULATED TRANSPORTER (ZRT), IRON-REGULATED TRANSPORTER (IRT)-LIKE PROTEIN (ZIP) family is required for acquisition of free Zn(II) from the soil (Li *et al.*, 2013b; Ricachenevsky *et al.*, 2015). The best-characterized *ZIP* members are the *IRON REGULATED METAL TRANSPORTER* (*IRT*) genes. Arabidopsis AtIRT1 mainly serves the function of Fe(II) uptake by roots but can also transport a broad range of other divalent metals such as Zn(II), Mn(II) and Cd(II) (Guerinot, 2000). In addition, the expression of *AtZIP1* to *AtZIP5*, *AtZIP9* to *AtZIP12*, and *AtIRT3* are induced upon zinc deficiency in roots, suggesting their likely role in zinc uptake in Arabidopsis (Lin *et al.*, 2009; van de Mortel *et al.*, 2006). Furthermore, many of the *ZIP* genes, such as *OsZIP1*, *-3*, *-4*, *-5* and *-8* in rice, *HvZIP3*, *-5*, *-7*, *-8*, *-10*, *-13* in barley, *ZmIRT1*, *ZmZIP3*, *-5*, and *-8* in maize, *MtZIP1*, *-5*, *-6* in *Medicago truncatula*, and *GmZIP1* in soybean, are suggested to function in zinc uptake and/or distribution (Ishimaru *et al.*, 2005; Lee *et al.*, 2010a; Lee *et al.*, 2010b; Li *et al.*, 2013b;

Lopez-Millan *et al.*, 2004; Moreau *et al.*, 2002; Pedas *et al.*, 2009; Ramesh *et al.*, 2003; Tiong *et al.*, 2015).

Two BASIC LEUCINE-ZIPPER (bZIP) transcription factors, AtbZIP19 and AtbZIP23, were shown to induce the expression of ZIP transporters and therefore regulate zinc-deficiency responses in Arabidopsis (Assuncao *et al.*, 2010). They bind to the zinc deficiency response element (ZDRE), which is present in the promoters of targeted genes such as *AtZIP4*, *AtZIP9*, and *AtIRT3* and thereby regulate the expression of *ZIP* genes (Assuncao *et al.*, 2010; Inaba *et al.*, 2015). However, there is a debate if AtbZIP19 and AtbZIP23 have redundant functions (Assuncao *et al.*, 2010; Inaba *et al.*, 2015).

Additionally, organic ligand-zinc complexes also contribute to zinc uptake by plants. To enhance the solubility of zinc in the rhizosphere, plant roots secrete hydrogen ions and organic acids such as citric acid and malic acid (Gupta *et al.*, 2016). Graminaceous plants also produce mugineic acid (MA) family phytosiderophores (PSs), such as deoxymugineic acid (DMA), MA, 3- hydroxymugineic acid (HMA), and 3-epi-hydroxymugineic acid (epi-HMA), which are divalent chelators for Fe(III) and Zn(II), and contribute to their uptake from rhizosphere and long-distance translocation in plants (Kim and Guerinot, 2007; Murakami *et al.*, 1989). In wheat, deoxymugineic acid (DMA) is the dominant PS released under zinc deficiency (Cakmak *et al.*, 1994). The synthesis of DMA is initiated from S-adenosyl-L-methionine (SAM), and occurs via a conserved pathway involving sequential enzymatic reactions mediated by NICOTIANAMINE SYNTHASE (NAS), NICOTIANAMINE AMINOTRANSFERASE (NAAT), and DEOXYMUGINEIC ACID SYNTHASE (DMAS) (Kobayashi *et al.*, 2010b). Nicotianamine (NA) is an intermediate in the production of DMA. It also forms complexes with divalent metals such as Fe(II), Fe(III), Zn(II), Mn(II), Ni(II), and Cu(II) and facilitate the function of intercellular and long-distance transport of zinc (Clemens *et al.*, 2013).

Transporters from the MAJOR FACILITATOR SUPERFAMILY (MFS) and OLIGOPEPTIDE TRANSPORTER (OPT) families are required for NA, DMA, metal-NA complexes, and metal-DMA complexes translocation. The MFS is a universal transporter superfamily in all organisms that transports a diverse range of small organic molecules (Pao *et al.*, 1998; Reddy *et al.*, 2012). The ZINC-INDUCED FACILITATOR (ZIF) protein family is a clan of the MFS, which also functions in zinc homeostasis (Haydon and Cobbett, 2007). The TRANSPORTER OF MUGINEIC ACID 1 (TOM1), which is a ZINC INDUCED

FACILITATOR-LIKE (ZIFL) family member, exports DMA to the soil and is also involved in transportation of Fe(III)-DMA to the phloem and xylem in graminaceous plants (Nozoye *et al.*, 2011). OsTOM2, the homolog of OsTOM1transporter in rice, transports DMA to the cell exterior, and is involved in internal metal transport (Nozoye *et al.*, 2015). The YELLOW STRIPE-LIKE (YSL) transporter family is a clade of OPT. Members from the YSL family facilite the uptake of Fe(III)-PS complexes from soil (Inoue *et al.*, 2008; Lee *et al.*, 2009a) as well as distribution of Fe(III)-DMA and/or Fe(II)-NA complex in plants (Aoyama *et al.*, 2009; Ishimaru *et al.*, 2010; Kakei *et al.*, 2012; Koike *et al.*, 2004; Zheng *et al.*, 2012). In addition to function as iron transporters, ZmYS1 is also responsible for the transport of Zn(II)-DMA, as shown in maize roots (Schaaf *et al.*, 2004; Von Wiren *et al.*, 1996).

Although the understanding of zinc homeostasis in different plant species is increasing, the information regarding zinc deficiency stress responses in wheat is scarce. We studied zinc deficiency stress responses of bread wheat using RNA sequencing approach and further studied the expression of selected set of genes in roots, leaves, and grains collected at different developmental stages during grain filling period. Differentially regulated genes (DEGs) that are responsive to zinc-deficiency stress were analyzed from the aspects of metal translocation, storage, and regulation. Our study provides comprehensive overview of zinc deficiency response in bread wheat, and may serve candidate genes for future biofortification approaches.

4.3 Results

To obtain an overview of the zinc deficiency-triggered response in roots and flag leaves, bread wheat (*Triticum aestivum* cv. Bobwhite S26) was subjected to Illumina high-throughput RNA sequencing. A total of 60.1 (control flag leaves), 63.8 (zinc-deficient flag leaves), 74.7 (control roots), and 86.8 (zinc-deficient roots) million high quality reads were generated. The reads that aligned to the high confidence (HC) genes of the chromosomal survey sequences (CSSs) ranged between 68% and 80% (Supplementary table 4.1).

4.3.1 Evaluation of DEGs and gene ontology (GO) analysis

DEGs ($p < 0.01$, fold change ≥ 2) were identified by comparing the gene expression changes in roots and flag leaves from plants grown in zinc-deficient condition as compared to the control condition. A similar number of DEGs were observed in the flag leaves (4089 DEGs) and roots (4188 DEGs) (Figure 4.1). The flag leaves showed a higher proportion of up-

regulated genes, with 3542 genes up-regulated and 547 genes down-regulated. In roots, the number of up-regulated (2192 DEGs) and down-regulated (1996 DEGs) genes was similar (Figure 4.1). Roots and flag leaves shared 543 DEGs, with 342 up-regulated and 25 down-regulated genes in both tissues. The remaining 176 genes showed opposite regulation in the zinc-deficient roots and flag leaves (Figure 4.1). DEGs were subjected to GO analysis and were categorized by biological process (BP), molecular function (MF), and cellular component (CC). The roots and flag leaves shared similar overrepresented GO terms. The GO terms such as metabolic process (GO:0008152), catalytic activity (GO:0003824), and membrane (GO: 0016020) were significantly regulated (Figure 4.2).

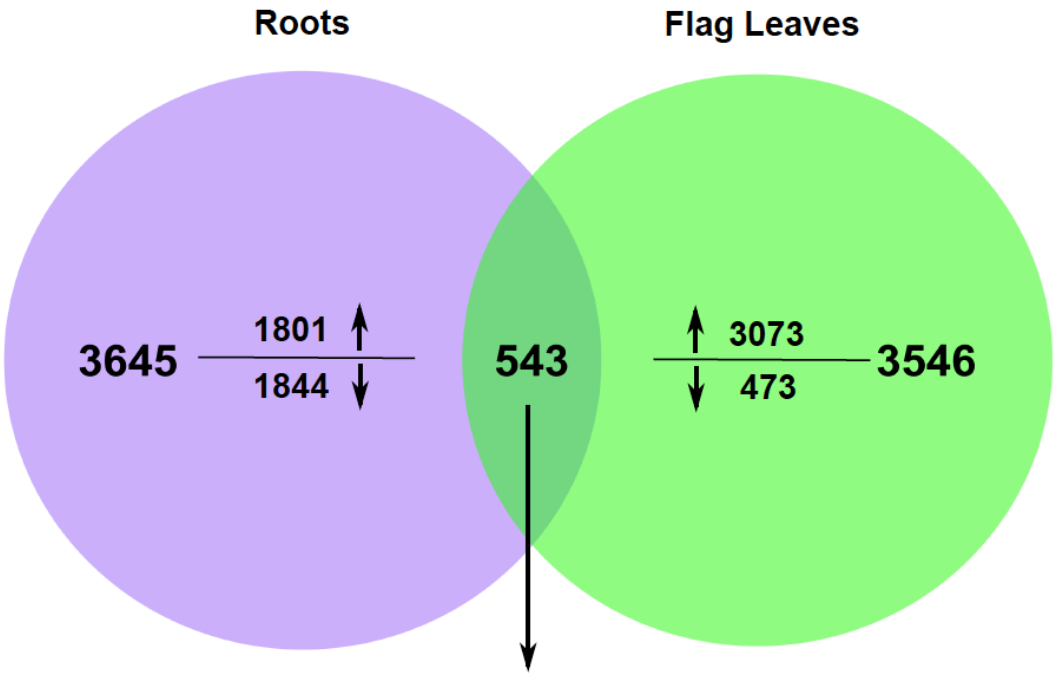

		Flag Leaves	
		Up-regulated	Down-regulated
Roots	Up-regulated	342	49
	Down-regulated	127	25

Figure 4.1. Summary of differentially expressed genes in the roots and flag leaves subjected to zinc-deficient conditions. Venn diagram shows total differentially expressed genes (DEGs) ($p < 0.01$, fold change ≥ 2) in roots and flag leaves. Green color represents total DEGs in flag leaves; purple color represents total DEGs in roots. Upward arrow indicates up-regulation of gene expression; downward arrow indicates down-regulation of gene expression.

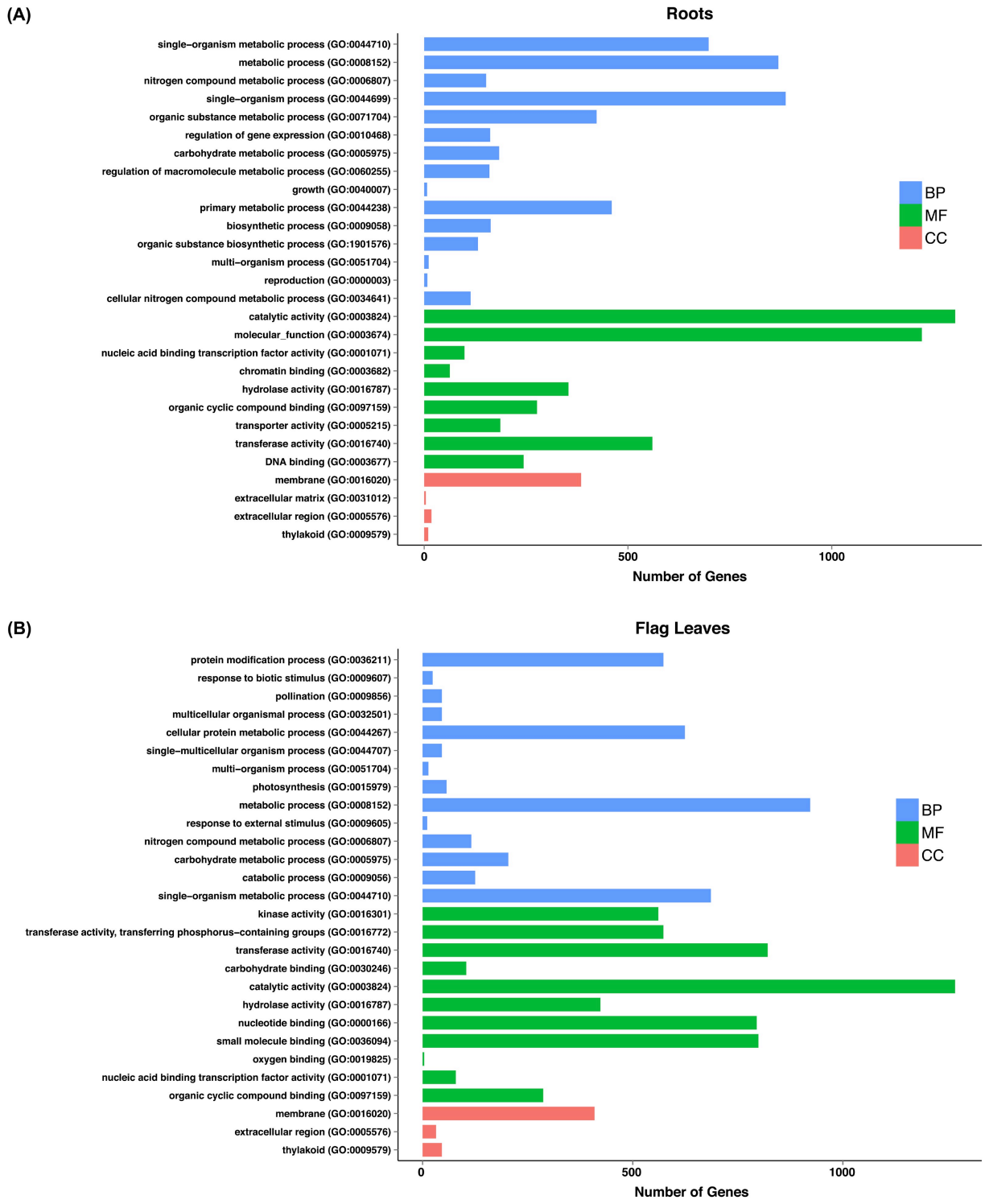

Figure 4.2. Gene ontology (GO) analysis of DEGs in zinc-deficient wheat roots and leaves. DEGs are distributed to three major gene ontology categories: i.e., BP: Biological process; CC: Cellular component; MF: Molecular function. X-axis represents the number of DEGs in each GO term. (A) Roots, (B) Flag leaves.

4.3.2 Regulation of genes encoding transporter families

We detected 448 differentially regulated transporter encoding genes in roots, of which 414 have InterPro IDs. Of these 414 genes, 122 genes were up-regulated and 292 genes were down-regulated (Figure 4.3; Supplementary table 4.2). The largest number of differentially regulated genes were among the MAJOR FACILITATOR SUPERFAMILY (MFS) (26/113 up-regulated/down-regulated genes), followed by the DRUG/METABOLITE TRANSPORTER (DMT) (1/47), ATP-BINDING CASSETTE (ABC) transporter (13/18), amino acid transporter (12/10), and ZIP (10/8) families. Unlike roots with nearly 70% of the differentially expressed transporter encoding genes down-regulated, most of the transporter encoding DEGs were up-regulated in flag leaves. Of the 383 differentially expressed transporters encoding genes in the flag leaves, 369 have InterPro IDs, with 303 up-regulated and 66 down-regulated genes. Most of the genes encoding ABC transporters were up-regulated (74/1 up-regulated/down-regulated). The other differentially expressed gene families in the flag leaves encode the MFS (46/9), ZIP (22/0), MULTI-ANTIMICROBIAL EXTRUSION PROTEIN (MATE) (19/1), and amino acid transporter (10/0). Highly induced expression of these transporter-encoding genes in the flag leaves suggests their role in zinc translocation during zinc deficiency stress. The roots and flag leaves had only 46 common differentially expressed transporter encoding genes, of which nine were up-regulated *ZIP* family members, indicating the significant contribution of ZIP transporters to zinc uptake and translocation (Figure 4.3D).

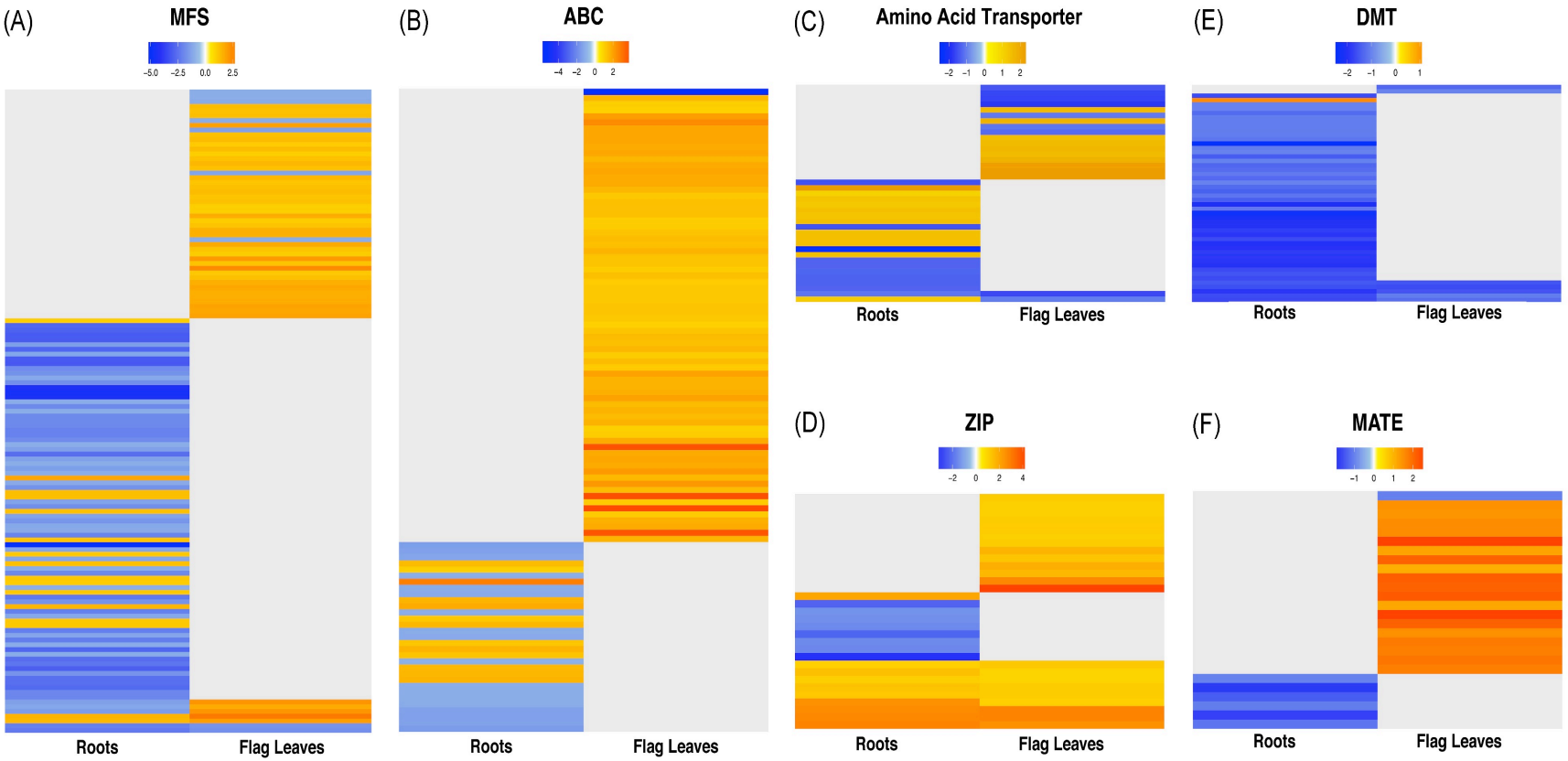

Figure 4.3. Five most differentially expressed transporter encoding gene families. Heatmaps show five most differentially expressed transporter encoding gene families in roots and flag leaves, respectively. Orange color indicates up-regulation of gene expression; blue color indicates down-regulation; gray color indicates no detection of differential gene expression. Also refer to supplementary table 4.2 for gene IDs and for actual fold change information. (A) MFS, (B) ABC transporter, (C) Amino acid transporter, (D) ZIP, (E) DMT, (F) MATE. MFS: MAJOR FACILITATOR SUPERFAMILY; ZIP: ZINC-REGULATED TRANSPORTER (ZRT)/IRON-REGULATED TRANSPORTER (IRT)-LIKE PROTEIN; DMT: DRUG/METABOLITE TRANSPORTER;

The expression of three genes encoding Zn(II) transporters i.e., *METAL TOLERANCE PROTEIN* (*MTP*) homolog Ta.27695, *HEAVY METAL ATPases* homolog (*HMA*) Ta.45138, and *ZIP* homolog Ta.38190, was further studied at three different developmental stages during grain filling (Table 4.1). The differential expression was observed only in the roots tissue for these three gene homologs, where the expression of *MTP* homolog (Ta.27695) was down-regulated by 1.6- and 1.9-fold in stage 1 and 2, respectively. Around 1.1-fold increase in the expression of *HMA* homolog (Ta.45138) was observed in stage 1 and 2. An over 4-fold increase in transcription was detected in stages 2 and 3 in the roots for the *ZIP* homolog (Ta.38190), demonstrating the genes encoding Zn(II) transporters are dynamically regulated during the grain-filling period in roots.

4.3.3 Expression patterns of genes facilitating metal uptake, transport and storage

Unlike iron deficiency response, the expression of PS biosynthesis related genes was not significantly induced upon zinc deficiency. RNA sequencing results showed that none of the NAS genes were significantly regulated in the flag leaves in stage 1. Unexpectedly, most of the differentially expressed *NAS* gene homologs in roots exhibited reduced transcript levels (Table 4.2; Supplementary table 4.3). The majority of the differentially expressed *NAAT* homologs such as *TYROSINE AMINOTRANSFERASE*, *HISTIDINOL PHOSPHATE AMINOTRANSFERASE*, *ASPARTATE AMINOTRANSFERASE* and LL-*DIAMINOPIMELATE AMINOTRANSFERASE* showed increased transcription in flag leaves. However, only a few of the *NAAT* homologous genes increased the expression in the zinc-deficient roots (Table 4.2; Supplementary table 4.3). The *DMAS* genes belong to the *ALDO/KETO REDUCTASE* (*AKR*) gene family. The roots and flag leaves exhibited opposite expression pattern of the *AKR* genes, with down-regulation in the roots but up-regulation in flag leaves (Table 4.2; Supplementary table 4.3). These findings indicated a stronger role of DMA in the zinc translocation than in uptake in the event of zinc deficiency.

Further, we studied the expression of *NAS* homologs (Ta.37977, Ta.95106, Ta.5549), *NAAT* homolog (Ta.4977) and *DMAS* homolog (Ta.5335) in the roots, flag leaves and grains at three different developmental stages during grain filling period (Table 4.1; Supplementary figure 4.1). Among these, only *NAAT* homolog (Ta.4977) was significantly regulated, with increased expression in roots during all three stages and in the flag leaves during stage 1. In addition, 1.35-fold increased expression was observed in the grains in stage 3. We also studied the expression of five potential NA and DMA transport related genes: *TOM* homolog (Ta.5180)

and *YSL* homologs (Ta.48303, Ta.5463, Ta.29321, Ta.29367) (Table 4.1). Similar to the *DMAS* and *NAS* genes, no significant differential gene expression was detected for most of these genes. Exceptionally, 2.77-fold increased expression was observed for *YSL* homolog (Ta.29367) in the stage 1 of grains, indicating its role in zinc transport into the developing grains (Table 4.1). To determine whether these observations were confined to the reproductive phase in wheat, we analyzed the expression of *NAS* homolog (Ta.37977), *NAAT* homolog (Ta.4977), *DMAS* homolog (Ta.5335), *TOM* homolog (Ta.5180), and *YSL* homolog (Ta.48303) in the roots and shoots of one-month-old seedlings subjected to zinc deficiency. Unlike in the grain-filling period, the expression of *NAS* (Ta.37977), *DMAS* (Ta.5335), *YSL* (Ta.48303), and *TOM* (Ta.5180) homologs was strongly induced in the wheat roots but not the shoots upon zinc deficiency (Supplementary figure 4.1F). This suggests that the PSs biosynthesis and transport-related genes are triggered when plants suffer from short-term zinc deficiency, or that a younger wheat plant reacts more strongly to the zinc deficiency stress.

In addition to the afore-mentioned genes, the expression of *METALLOTHIONEIN* (*MT*) and *FERRITIN* was also characterized. The expression of *MT* homolog Ta.13600 decreased 1.72-fold in the roots in stage 2 but increased approximately 1.3-fold in grains in stages 2 and 3 (Table 4.1), indicating its role in zinc chelation in wheat grains. In case of the *FERRITIN* gene homologs (Traes_5AL_D01E0C753, Traes_5BL_CEA21A155, Traes_5DL_95DBDBAD1), the expression increased in both the roots and flag leaves by 2.6- to 3-fold in stage 1 in response to zinc deficiency, as revealed by the RNA sequencing data (Supplementary table 4.4). The qRT-PCR analysis showed similar results. The expression of *FERRITIN* homolog (Ta.5220) also increased in the developing grains, by 1.55- and 1.24-fold in stages 1 and 2, respectively. Although it is unclear how zinc deficiency might affect iron translocation and storage, the increased expression of the *FERRITIN* genes in zinc-deficient roots and leaves reflects a crosstalk between iron and zinc homeostasis.

Nr.	Genes	Unigene ID	Roots			Flag Leaves			Grains		
			Stage 1	Stage 2	Stage 3	Stage 1	Stage 2	Stage 3	Stage 1	Stage 2	Stage 3
1	*NAS*	Ta.37977	-8.53	10.49	-8.21	2.28	-1.48	-1.28	1.34	1.05	1.74
2	*NAS*	Ta.95106	-12.64	21.63	-7.94	1.92	-9.59	-2.46	-1.01	1.97	1
3	*NAS*	Ta.5549	-6.2	38.09	-12.15	-1.86	2.03	1.77	-2.08	-2.71	3.69
4	*NAAT*	Ta.4977	1.32 *	4.87 **	1.61 *	6.38 **	1.35	1.55	1.02	-1.14	1.35 *
5	*DMAS*	Ta.5335	-1.82	1.33	-1.53	1.1	-1.02	-1.05	1.17	1.15	1.05
6	*TOM*	Ta.5180	-12.85	18.04	-8.92	-3.95	1.43	-1.3	-2.34	-3.49	4.06
7	*YSL*	Ta.48303	-2.32	2.43	-2.08	1	1.03	-1.3	-1.3	-1.91	2.4
8	*YSL*	Ta.5463	-1.1	2.84	-2.81	-1.18	1.68 *	-1.3	NA	NA	NA
9	*YSL*	Ta.29321	-1.75	1.84	-1.86	1.55	-1.34	-1.09	-1.14	1.82	1.16
10	*YSL*	Ta.29367	2.59	-1.25	-1.11	1.57	-3.54	-1.01	2.77 *	1.01	2.3
11	*MT*	Ta.13600	1.3	-1.72 **	1.05	1.23	1.01	1.31	1.08	1.32 *	1.33 *
12	*FERRITIN*	Ta.5220	3.13 *	3.24	-1.08	2.55	1.06	-1.5	1.55 **	-1.27	1.24 *
13	*MTP*	Ta.27695	-1.6 *	-1.98 *	1.67	-1.37	3.28	-1.78	-1.2	-1.43	1.12
14	*HMA*	Ta.45138	1.13 *	1.12 **	1.21	1.02	1.04	-1.17	1.1	-1.03	1.13
15	*ZIP*	Ta.38190	-1.45	4.06 *	4.79 *	1.6	-1.02	-1.24	1.59	1.27	1.42

Table 4.1. Summary of gene expression fold change between zinc-deficient and control condition. The numbers indicate the fold change difference between zinc-deficient and control growth conditions. The positive number represents the up-regulation and the negative number represents the down-regulation of the gene expression. Significant differences are marked with * when $p \leq 0.05$ or with ** when $p \leq 0.01$. Stage 1: 8-10 days post anthesis (DPA); stage 2: 25-28 DPA; stage 3: 33-35 DPA.

Identifier	Tissue	Description	Fold Change	Number of Genes
NAS				
Traes_6DL_202647A85	Roots	nicotianamine synthase 3	-51.2	
Traes_6AL_2D6B1391C	Roots	nicotianamine synthase 2	-48.6	Total:42
Traes_6DL_AEF33B4F2	Roots	nicotianamine synthase 1	-30.2	Up:2
Traes_XX_B63197846	Roots	nicotianamine synthase 2	-29.1	Down:40
Traes_4DL_1C0D18A5B	Roots	nicotianamine synthase 4	-21.6	
NAAT				
Traes_4DL_E9801DD6D	Roots	histidinol phosphate aminotransferase 1	2.7	
Traes_4BS_A7B66E010	Roots	histidinol phosphate aminotransferase 1	2.6	Total:10
Traes_1BL_9567F31C9	Roots	tyrosine aminotransferase 3	-2.5	Up:4
Traes_4AS_A78282154	Roots	histidinol phosphate aminotransferase 1	2.4	Down:6
Traes_1BL_A7ACBE825	Roots	histidinol phosphate aminotransferase 1	2.2	
Traes_XX_533BEDE84	Flag Leaves	histidinol phosphate aminotransferase 1	-33.4	
Traes_4AS_34CC18E64	Flag Leaves	LL-diaminopimelate aminotransferase	6.2	Total:12
Traes_1DL_F7AE109E2	Flag Leaves	histidinol-phosphate aminotransferase	6	Up:11
Traes_1BL_9567F31C9	Flag Leaves	tyrosine aminotransferase 3	5.8	Down:1
Traes_XX_27C41E4DF	Flag Leaves	aspartate aminotransferase	5.7	
DMAS				
Traes_1BL_4D2CB33FC	Roots	NAD(P)-linked oxidoreductase superfamily protein	-2.7	
Traes_2DL_0FADBEC03	Roots	aldo-keto reductase	-2.7	Total:9
Traes_XX_5339C975D	Roots	NAD(P)-linked oxidoreductase superfamily protein	-2.7	Up:0
Traes_1BL_3CB12266D	Roots	aldose reductase	-2.7	Down:9
Traes_2AL_3637458F8	Roots	aldo-keto reductase	-2.6	
Traes_1DL_03EFA2FE5	Flag Leaves	aldose reductase	21.4	
Traes_1BL_3CB12266D	Flag Leaves	aldose reductase	7.8	Total:25
Traes_1AL_7D7864504	Flag Leaves	NAD(P)-linked oxidoreductase superfamily protein	6.9	Up:23
Traes_XX_5339C975D	Flag Leaves	NAD(P)-linked oxidoreductase superfamily protein	6.1	Down:2
Traes_2DL_787806003	Flag Leaves	aldose reductase	5.4	

Table 4.2. Zinc deficiency induced DEGs in phytosiderophores synthesis pathway. The table summarizes five most differentially expressed wheat homologs of the phytosiderophore synthesis related genes, modulated in response to zinc deficiency in roots and flag leaves.

Identifier	Tissue	Gene Family	Fold Change	Number of Genes
Traes_4DS_CFC487CE5	Roots	*WRKY*	5.4	
Traes_5DL_C93641E43	Roots	*WRKY*	4.35	Total: 37
Traes_5BL_0A3D332A8	Roots	*WRKY*	4.13	Up: 36
Traes_5DL_5C93510D5	Roots	*WRKY*	4.03	Down: 1
Traes_XX_7E8739988	Roots	*WRKY*	3.77	
Traes_4AL_B44DF4ACC	Roots	*NAC*	3.92	
Traes_4DL_B29067862	Roots	*NAC*	3.87	Total: 34
Traes_XX_399CE240D	Roots	*NAC*	3.85	Up: 31
Traes_5BL_4497A137C	Roots	*NAC*	3.82	Down: 3
Traes_4DS_B98800798	Roots	*NAC*	3.79	
Traes_5BL_0C3609EF0	Roots	*ERF*	26.61	
Traes_5BL_027509D0D	Roots	*ERF*	15.26	Total: 29
Traes_5BL_F5D379AFC	Roots	*ERF*	14.7	Up: 27
Traes_5BL_6647931E2	Roots	*ERF*	13.52	Down: 2
Traes_5DL_91AE6CA271	Roots	*ERF*	12.64	
Traes_1AL_01E24503F	Roots	*HOMEODOMAIN-LIKE CONTAINING PROTEIN*	5.96	
Traes_1BL_1B12D7856	Roots	*HOMEODOMAIN-LIKE CONTAINING PROTEIN*	5.55	Total: 16
Traes_3DL_21E2888C9	Roots	*HOMEODOMAIN-LIKE CONTAINING PROTEIN*	3.87	Up: 8
Traes_6AS_52AE4A6E2	Roots	*HOMEODOMAIN-LIKE CONTAINING PROTEIN*	3.86	Down: 8
Traes_6BL_A3E9C02F0	Roots	*HOMEODOMAIN-LIKE CONTAINING PROTEIN*	-4.05	
Traes_5AS_EBCEA6601	Roots	*bHLH*	5.7	
Traes_XX_6E136BDD1	Roots	*bHLH*	4.46	Total: 12
Traes_XX_654C2B23A	Roots	*bHLH*	4.23	Up: 4
Traes_7DL_613E9123C	Roots	*bHLH*	-6.68	Down: 8
Traes_4BL_19F19CCC0	Roots	*bHLH*	-11.34	
Traes_5AL_04D3E97F0	Roots	*bZIP*	2.39	
Traes_5DL_743B870D9	Roots	*bZIP*	2.38	Total: 11
Traes_XX_874ABD957	Roots	*bZIP*	2.33	Up: 5
Traes_6AS_FDF16F4EA	Roots	*bZIP*	-2.58	Down: 6
Traes_4BL_80683C0B9	Roots	*bZIP*	-2.99	
Traes_3DL_A3AC10E58	Roots	*GRAS*	2.42	
Traes_XX_5BC8C939F	Roots	*GRAS*	2.3	Total: 10
Traes_3B_0949A7AA1	Roots	*GRAS*	-2.89	Up: 7
Traes_1AL_FB0C83DD9	Roots	*GRAS*	-3.45	Down: 3
Traes_1BL_DF66FC4FE	Roots	*GRAS*	-3.85	
Traes_1DL_46428511F	Flag Leaves	*WRKY*	35.43	
Traes_4AS_0DA136E0E	Flag Leaves	*WRKY*	18.83	Total: 50
Traes_5BL_90757F0CC	Flag Leaves	*WRKY*	9.32	Up: 50
Traes_7BL_53AA25AA1	Flag Leaves	*WRKY*	8.98	Down: 0
Traes_2DL_362A1F535	Flag Leaves	*WRKY*	8.33	
Traes_1AL_C76BCC7EC	Flag Leaves	*NAC*	33.01	
Traes_1DL_A556D8590	Flag Leaves	*NAC*	32.7	Total: 26
Traes_1AL_D6C49C3BC	Flag Leaves	*NAC*	21.77	Up: 25
Traes_1BL_8925B27BC	Flag Leaves	*NAC*	16.3	Down: 1
Traes_4DL_7CB8EC5A8	Flag Leaves	*NAC*	10.43	
Traes_1AS_CA75913B6	Flag Leaves	*HOMEODOMAIN-LIKE CONTAINING PROTEIN*	10.01	
Traes_1DS_AAEBFA9CC	Flag Leaves	*HOMEODOMAIN-LIKE CONTAINING PROTEIN*	9.34	Total: 11
Traes_3B_E82B2B6AC	Flag Leaves	*HOMEODOMAIN-LIKE CONTAINING PROTEIN*	3.41	Up: 6
Traes_1AL_BB4298457	Flag Leaves	*HOMEODOMAIN-LIKE CONTAINING PROTEIN*	-2.61	Down: 5
Traes_1DL_70CCAB0EF	Flag Leaves	*HOMEODOMAIN-LIKE CONTAINING PROTEIN*	-2.62	
Traes_5DS_1BDB9837E	Flag Leaves	*ERF*	38.32	
Traes_6AL_2CA7515B31	Flag Leaves	*ERF*	25.96	Total: 10
Traes_5BL_60510E4A7	Flag Leaves	*ERF*	7.05	Up: 6
Traes_2AL_43491B9E0	Flag Leaves	*ERF*	5.6	Down: 4
Traes_2AL_6B6086A7C	Flag Leaves	*ERF*	3.94	
Traes_5DL_431CCA490	Flag Leaves	*HSF*	3.29	
Traes_XX_625875413	Flag Leaves	*HSF*	3.1	Total: 10
Traes_5BL_65826E1A1	Flag Leaves	*HSF*	3	Up: 7
Traes_XX_BB9453292	Flag Leaves	*HSF*	2.98	Down: 3
Traes_4AS_491EF4D7F	Flag Leaves	*HSF*	-2.89	

Table 4.3. Zinc deficiency induced transcription factor encoding genes. The table summarizes five most differentially expressed wheat homologs for each transcription factor gene family in roots and flag leaves, respectively.

4.3.4 Zinc deficiency responsive transcription factors

We detected 205 and 144 differentially regulated transcription factor encoding genes in the roots and flag leaves, respectively. The *WRKY*, *NAC*, *ETHYLENE-RESPONSIVE TRANSCRIPTION FACTORS* (*ERFs*), *HOMEODOMAIN LIKE CONTAINING PROTEIN*, *bZIP*, *BASIC HELIX-LOOP-HELIX* (*bHLH*), and *GAI, RGA, SCR* (*GRAS*) transcription factor gene families were the most regulated in wheat roots in response to zinc deficiency stress, with 10 or more differentially expressed genes in each family. The WRKY family ranked as the most actively regulated family with 37 DEGs (36/1 up-regulated/down-regulated genes), followed by the NAC family with 34 DEGs (31/3), ERFs with 29 DEGs (27/2), *HOMEODOMAIN LIKE CONTAINING PROTEIN* with 16 DEGs (8/8), *bHLH* with 12 DEGs (4/8), *bZIP* with 11 DEGs (5/6), and GRAS with 10 DEGs (7/3) (Table 4.3). In case of leaves, *WRKY*, *NAC*, *HOMEODOMAIN LIKE CONTAINING PROTEIN*, *ERFs* and *HEAT STRESS TRANSCRIPTION FACTOR* (*HSF*) were the most regulated ones. *WRKY* and *NAC* were also the two most responsive gene families with 50 (50/0) and 26 (25/1) DEGs, respectively. The *HOMEODOMAIN LIKE CONTAINING PROTEIN*, *ERFs* and *HSF* families had less number of up-regulated genes (Table 4.3). Particularly, over 90% of the differentially expressed *WRKY* and *NAC* genes showed up-regulation in roots as well as flag leaves, suggesting their significant roles in regulating zinc deficiency responses in wheat.

4.4 Discussion

Most of the studies analyzing response of cereals to zinc deficiency have been carried out in the seedlings no more than one month old, i.e., in the vegetative phase, and/or under extreme zinc deficiency (i.e., no zinc supplied) (Cakmak *et al.*, 1994; Cakmak *et al.*, 1996; Suzuki *et al.*, 2006; Suzuki *et al.*, 2008). However, in nature, plants generally suffer from mild zinc deficiency throughout the growth period. Here, we focus on the grain-filling period during which the micronutrients are actively transported to developing grains and applied mild zinc deficiency stress.

MAs and NA are known to form complexes with zinc and function in zinc acquisition and transport (Von Wiren *et al.*, 1996). However, the secretion of MAs is reported to vary in different crop plants when exposed to zinc deficiency. For example, sorghum has been reported to release increased amount of MA under zinc deficiency, while in case of maize there is no change (Hopkins *et al.*, 1998). But in case of zinc-deficient wheat and barley, the reported secretion of MAs varies among different experiments with either increased or

unchanged MA production (Cakmak *et al.*, 1994; Cakmak *et al.*, 1996; Hopkins *et al.*, 1998; Pedler *et al.*, 2000; Suzuki *et al.*, 2006). Unlike MA, which is synthesized only in graminaceous plants, NA is present ubiquitously in all vascular plants (Takahashi *et al.*, 1999). Long-distance transport of zinc occurring in the rice phloem is facilitated by NA (Nishiyama *et al.*, 2012), along with the symplastic translocation towards the xylem in the zinc hyperaccumulator *A. halleri* (Deinlein *et al.*, 2012). The expression of NA and MA synthesis-related genes including *HvNAS1*, *HvNAAT-A*, *HvNAAT-B*, *HvIDS2* and *HvIDS3* was induced in barley roots under zinc deficiency (Suzuki *et al.*, 2006). Consistently, the expression of PSs biosynthesis and transport-related genes was induced in the roots of wheat seedlings experiencing zinc-deficient conditions in this study (Supplementary figure 4.1F). However, a reduction in the expression of genes involved in NA and DMA biosynthesis in the zinc-deficient wheat roots, including the *NAS* and *DMAS* homologs was observed during the grain filling period. However, an increase in *DMAS* expression was observed in the flag leaves (Table 4.2, Supplementary table 4.3). This result is in line with the observation in the zinc-deficient rice plants, which exhibited decreased DMA production in the roots but increased DMA in the shoots (Suzuki *et al*., 2008). In parallel, the expression of some genes encoding transporters in *YSL* and *ZIFL* family was also repressed in the roots but elevated in the flag leaves in this work (Supplementary figure 4.2, Supplementary table 4.2). Various transporters from YSL and ZIFL families have been shown to facilitate the translocation of NA, DMA, metal-NA, and metal-DMA. ZmYS1 functions in Zn(II)-DMA uptake by maize roots (Schaaf *et al.*, 2004; Von Wiren *et al.*, 1996). The *AtYSL2*, which shows close homology to *ZmYSL1*, was repressed in shoots and roots under zinc starvation, indicating its role in zinc storage or detoxification rather than acquisition (Schaaf *et al.*, 2005). In addition, some YSL members have also been shown to remobilize zinc from senescing leaves to reproductive tissues (Waters *et al.*, 2006). Previous studies also suggested the role of ZIF proteins in maintaining zinc homeostasis, particularly in response to zinc excess (Haydon and Cobbett, 2007; Haydon *et al.*, 2012; Ricachenevsky *et al.*, 2011; Tauris *et al.*, 2009). Together, our observations suggest that DMA plays an important role in zinc translocation within the plants rather than zinc acquisition under the zinc-deficient conditions, particularly during the grain filling period of development.

Unlike the expression of genes encoding Zn(II)-DMA or Zn(II)-NA transporters, the expression of certain genes encoding ZIP transporters which transport free Zn(II) was induced in the wheat roots as well as the flag leaves under zinc deficiency (Figure 4.3). The ZIP family has been reported to facilitate zinc translocation in plants (Ishimaru *et al.*, 2007; Li *et*

al., 2013b; Milner *et al.*, 2013; Tiong *et al.*, 2014). The up-regulated *ZIP* homologs in the zinc-deficient wheat roots had high sequence identity with rice *OsZIP5* and *OsZIP8* (Supplementary table 4.2). In case of flag leaves, all the differentially expressed *ZIP* genes were up-regulated (Figure 4.3; Supplementary table 4.2). Microarray analysis done in rice showed that *OsZIP4*, *OsZIP5*, and *OsZIP8* were up-regulated in zinc-deficient roots and shoots, while the expression of *OsZIP7* was only increased in the shoots (Suzuki *et al.*, 2012). Our findings are in agreement with the previous reports on expression patterns of *ZIP* family genes in response to zinc deficiency.

FERRITIN is the known iron storage protein, found in almost all living kingdoms (Harrison and Arosio, 1996). It has been shown previously that overexpression of *FERRITIN* also leads to increased accumulation of zinc in addition to the iron (Mhatre *et al.*, 2011; Vasconcelos *et al.*, 2003; Wirth *et al.*, 2009). In zinc-deficient barley, *FERRITIN* gene expression increased in the shoots and roots (Suzuki *et al.*, 2006). We also observed a similar increase in the expression of *FERRITIN* in the roots, flag leaves and grains of wheat experiencing zinc deficiency (Table 4.1; Supplementary table 4.4), suggesting a strong crosstalk between the regulation and homeostasis of iron and zinc. In addition to the FERRITINs, METALLOTHIONEINS (MTs), the cysteine-rich low molecular-weight proteins, have a remarkable affinity to bind to heavy metal ions (Hamer, 1986). The zinc-containing E_c protein purified from wheat embryos was the first MT identified in higher plants (Lane *et al.*, 1987). The AtMT4a and AtMT4b proteins showed stronger zinc binding preference than other MTs in Arabidopsis (Guo *et al.*, 2008). *AtMT4a* and *AtMT4b* are specifically expressed in late embryos in developing seeds, and overexpression of either of these genes led to increased accumulation of zinc in the siliques, and seeds of Arabidopsis (Ren *et al.*, 2012). The expression of *OsMT1a* is dominant in rice roots, and its overexpression positively modulated the zinc accumulation in grains and leaves (Yang *et al.*, 2009). In barley, *MT4* is specifically expressed in the embryo and aleurone layer, and has a higher affinity for zinc (Hegelund *et al.*, 2012). The *MT2a* was shown to be expressed throughout the grain but at a particularly high level in one of the endosperm samples, indicating its role in chelating zinc in the endosperm (Tauris *et al.*, 2009). Under zinc deficiency, expression of *MT* homolog Ta.13600 in wheat, having high sequence identity with the *MT2a* gene in barley, was significantly up-regulated in the developing grains, suggesting its involvement in zinc sequestration in wheat grains (Table 4.1). These results together suggest that the MTs could also be potential candidates for biofortification approaches aiming at increasing zinc concentration in wheat as well as in other cereal grains.

Unlike iron homeostasis, the regulation of response to zinc deficiency stress has not been widely studied. It has been shown that NAM-B1, which is an NAC transcription factor, regulates wheat grain nutrient concentrations by increasing protein, zinc and iron efflux from the vegetative tissues and transporting these to the grains (Uauy *et al.*, 2006; Waters *et al.*, 2009). However, the information pertaining to genes downstream of the NAM is missing. Moreover, two bZIP family transcription factors, bZIP19 and bZIP23, have been suggested to regulate the expression of the *AtZIP4* gene in *Arabidopsis*. Both factors were found to be related to ZDRE (zinc deficiency response element), which is in the upstream region of *AtZIP1*, *-3*, *-4*, *-9* and *AtIRT3* (Assuncao *et al.*, 2010). In our data, the NAC transcription factors were up-regulated in the zinc-deficient wheat roots and flag leaves (Table 4.3). In addition to the NAC factors, WRKY, ERFs and bZIP transcription factors were also modulated in both leaves and roots in our study. These results suggest a key role of these transcription factors in regulating response to zinc deficiency stress and indicate that a complicated molecular network functions to maintain overall zinc homeostasis.

4.5 Experimental procedures

4.5.1 Plant material and growth conditions

Seeds of bread wheat (*Triticum aestivum* cv. Bobwhite S26) were germinated on wet filter paper for one week. Seedlings were then transferred to zinc-sufficient hydroponic solutions (pH 6.0) (Durmaz *et al.*, 2011): 0.88 mM K_2SO_4, 2 mM $Ca(NO_3)_2$, 0.2 mM KH_2PO_4, 1.0 mM $MgSO_4$, 0.1 mM KCl, 0.1 mM Fe(III)-EDTA-NA, 1.0 μM H_3BO_3, 1.0 μM $MnSO_4$, 0.2 μM $CuSO_4$, 0.02 μM $(NH_4)_6Mo_7O_{24}$ and 1.0 μM $ZnSO_4$ for one week. After one week, the plants were treated with different $ZnSO_4$ concentrations according to the stress treatment (control condition: 1.0 μM zinc; zinc-deficient condition: 0.05 μM zinc). Air was continuously supplied to the nutrient solutions for better circulation. The nutrient solutions were renewed weekly. The greenhouse conditions were maintained at 22˚C and 18˚C under a respective 16-hour light/8-hour dark cycle, and 60% humidity. The roots, flag leaves and grains samples were collected at three developmental stages during the grain filling period: 8-10 days post anthesis (DPA) - stage 1; 25-28 DPA - stage 2; and 33-35 DPA - stage 3. In addition, roots and shoots were sampled at 19 days after zinc deficiency treatment from the one-month-old seedlings. Three biological replicates were collected for each sample.

4.5.2 Total RNA extraction and cDNA synthesis

Isolation of total RNA from the roots and flag leaves was carried out using the Isol- RNA Lysis Reagent (5 PRIME, USA). The total RNA from the roots and flag leaves from stage 1 was used for RNA sequencing. All of the RNA samples were converted to cDNA for qPCR analysis. The total RNA used for RNA sequencing was digested with RNase-Free DNase (Qiagen, Germany) to remove genomic DNA, followed by RNA cleaning using the RNeasy Plant Mini Kit (Qiagen, Germany). The quality of RNA for RNA sequencing was determined using a Qubit® (1.0) Fluorometer (Life Technologies, USA) and a Bioanalyzer 2100 (Agilent, Germany). The total RNA for qPCR was treated with DNase I (Thermo Fisher Scientific, USA). cDNA synthesis was carried out using the RevertAid™ First Strand cDNA Synthesis kit (Thermo Fisher Scientific, USA).

4.5.3 Library preparation and Illumina sequencing

Strand-specific cDNA libraries (dUTP method) were prepared using the TruSeq Stranded mRNA Sample Prep Kit (Illumina, USA). Total RNA samples (1 μg) were poly-A enriched and then reverse-transcribed into double-stranded cDNA with actinomycin added during first-strand synthesis. The cDNA samples were fragmented and end-repaired before ligation of TruSeq adapters, which contained the index for multiplexing fragments. After ligation, these TruSeq adapters were selectively enriched by PCR amplification at both ends. The quality and quantity of the enriched libraries were validated using the Qubit® (1.0) Fluorometer and the Caliper GX LabChip® GX (Caliper Life Sciences, USA). The product was a smear with an average fragment size of approximately 250 bp. The libraries were normalized to 10 nM in 10 mM Tris-Cl, pH 8.5, with 0.1% Tween 20. The TruSeq PE Cluster Kit v3-cBot-HS (Illumina, USA) was used for cluster generation using 8 pM of pooled normalized libraries on the cBOT. Sequencing was performed on the Illumina HiSeq 2000 paired end at 2 × 101 bp (Illumina, USA).

4.5.4 RNA sequencing data analysis

RNA sequencing reads were quality-checked using fastqc, which computes various quality metrics for the raw reads. The reads were trimmed by clipping 5 bases from the read start, and end before mapping to the IWGSC (International Wheat Genome Sequencing Consortium) chromosome-based bread wheat genome. The IWGSC wheat chromosome-based genome information and gene annotations were provided by Dr. Klaus Mayer from the Munich

Information Center for Protein Sequences (MIPS, v2.2).

Reads were aligned to high confidence (HC) genes of the IWGSC wheat chromosome-based genome with bowtie2 with no minimum fragment size, but a maximum insert size of 1000 bp. Differential expression analysis was performed using edgeR. A gene was considered as expressed ("present") under a particular condition (zinc-deficient or control condition) when more than two samples (biological replicates) contained more than 10 reads each. The genes that exceeded the threshold ($p < 0.01$, fold change ≥ 2) were considered as differentially expressed genes. Gene ontology enrichment analysis was performed using the goseq package in Bioconductor. GoSlim was performed to remove the redundant GO categories.

4.5.5 qRT-PCR and Statistics

The qRT-PCR analyses were performed using the LightCycler® 480 Instrument II Real Time PCR system (Roche, Switzerland) with Taqman hydrolysis probes (Roche, Switzerland). The total reaction volume for each sample was set as 10 µl: 5 µl of mastermix (Applied Biosystems Inc., USA), 3 µl of 10× diluted cDNA, 0.9 µl of forward primer, 0.9 µl of reverse primer, 0.1 of µl the probe (Roche, Switzerland) and 0.1 µl of H_2O.

Ta.55681 (casein kinase II subunit beta-like), Ta.40026 (BTB/POZ and MATH domain-containing protein 4-like) and Ta.22845 (26S proteasome regulatory subunit) were used as reference genes across all of the tested samples (unpublished data) and were further used for data normalization (Chapter 2). Primer design and the corresponding probe selection were carried out on the Roche Universal ProbeLibrary Assay Design Center website (https://lifescience.roche.com/shop/CategoryDisplay?catalogId=10001&tab=&identifier=Universal±Probe±Library&langId=-1&storeId=15006). The primer sequences and probe numbers are provided in the Supplementary table 4.5. Primer efficiency was determined by cDNA dilution and calculated using the following formula: E = 10^(-1/slope)-1. Data normalization of qRT-PCR results was performed as described in (Schefe *et al.*, 2006). The obtained data were further analyzed by one-way ANOVA for assessment of statistical significance.

Data statistics and figure plotting were performed in Excel and RStudio (Version 0.98.976) using R and various R plotting packages (ggplot2, and VennDiagram).

4.6 Acknowledgements

This research was supported by ETH Zurich research grants to W.G. and to N.K.B., and from State Secretariat for Education, Research and Innovation (SERI) within the COST FA0905 program to N.K.B. We thank Irene Zurkirchen, Kulaporn Boonyaves, Ting-Ying Wu, Kumar Vasudevan, and Simrat Pal Singh for the technical support in the greenhouse and the laboratory.

4.7 Author contributions

N.K.B. conceived and designed the experiments. M.W. carried out the experiments. M.W., H.R., and N.K.B. analyzed the data. M.W. and N.K.B. wrote the manuscript. W.G. and N.K.B. edited the manuscript. All authors have read the manuscript and agree with its content.

Biological replicates	Total number of reads (million)	Read counts mapped to wheat genome (million)	Pecentage of reads mapped to wheat genome (%)	Genomic features with reads above threshold	Genomic features with reads above threshold (%)
Leaf Control 1	20.6	16.3	79	59711	53.2
Leaf Control 2	17.7	13.8	78	59455	53
Leaf Control 3	21.8	17.1	78	59429	53
Leaf Low Zn 1	19.6	15.6	80	60358	53.8
Leaf Low Zn 2	22.2	17.9	81	60259	53.7
Leaf Low Zn 3	30.1	21.9	73	63957	57
Root Control 1	26.7	18.8	70	64181	57.2
Root Control 2	17.9	12.5	70	63927	57
Root Control 3	22	17.7	80	60361	53.8
Root Low Zn 1	24.7	17.2	70	63685	56.8
Root Low Zn 2	28.2	19.2	68	63902	57
Root Low Zn 3	33.9	22.8	67	63834	56.9

Supplementary table 4.1. RNA sequencing reads mapped to IWGSC wheat chromosome-based genome sequence. The table summarizes the number of total reads and the mapping percentage to the reference wheat genome for each biological replicate.

Supplementary tables 4.2 and 4.3 contain large dataset from RNA sequencing results and could not be integrated to the word document. They are provided in an independent folder. Their titles and legends are listed here.

Supplementary table 4.2. Differentially expressed genes encoding transporters. The table enlists the differentially expressed transporter encoding genes ($p < 0.01$, fold change ≥ 2) in roots and flag leaves under zinc-deficient condition. FDR stands for false discovery rate.

Supplementary table 4.3. Differentially expressed PS biosynthesis genes. The table enlists the DEGs ($p < 0.01$, fold change ≥ 2) in PSs synthesis pathway in roots and flag leaves under zinc-deficient condition. FDR stands for false discovery rate.

Identifier	Tissue	Description	Interpro-ID	Fold Change	*p* value	FDR
Traes_5DL_95DBDBAD1	Roots	ferritin 4 LENGTH=259	IPR001519 (Ferritin), IPR008331 (Ferritin/DPS protein domain), IPR009078 (Ferritin-like superfamily)	3	5.86E-09	3.82E-07
Traes_5AL_D01E0C753	Roots	ferritin 4 LENGTH=259	IPR001519 (Ferritin), IPR008331 (Ferritin/DPS protein domain), IPR009078 (Ferritin-like superfamily)	3.01	2.26E-08	1.25E-06
Traes_5BL_CEA21A155	Roots	ferritin 4 LENGTH=259	IPR001519 (Ferritin), IPR008331 (Ferritin/DPS protein domain), IPR009078 (Ferritin-like superfamily)	2.83	3.17E-07	1.25E-05
Traes_5DL_95DBDBAD1	Flag leaves	ferritin 4 LENGTH=259	IPR001519 (Ferritin), IPR008331 (Ferritin/DPS protein domain), IPR009078 (Ferritin-like superfamily)	2.66	0.000152	0.004951
Traes_5AL_D01E0C753	Flag leaves	ferritin 4 LENGTH=259	IPR001519 (Ferritin), IPR008331 (Ferritin/DPS protein domain), IPR009078 (Ferritin-like superfamily)	2.67	0.000196	0.005977
Traes_5BL_CEA21A155	Flag leaves	ferritin 4 LENGTH=259	IPR001519 (Ferritin), IPR008331 (Ferritin/DPS protein domain), IPR009078 (Ferritin-like superfamily)	2.66	0.000348	0.009076

Supplementary table 4.4. Differentially expressed *FERRITIN* genes. The table enlists the differentially expressed ($p < 0.01$, fold change ≥ 2) *FERRITIN* genes in roots and flag leaves under zinc deficient condition. FDR stands for false discovery rate.

Nr.	Gene	Unigene ID	GenBank ID	Left primer	Right primer	Primer efficiency	probe No.	Amplicon	Amplicon 100% match to IWGSC cDNA database
1	*NAS*	Ta.37977	JP215700.1	aggcgcactactccgaca	gaagatgccgaggtggtc	1.83	149	aggcgcactactccgacatgctcgccgccttcgacaacccgctcgaccacctcggcatcttc	Traes_4DL_AF0869DDB
2	*NAS*	Ta.95106	JP908123.1	atgaaaggcaggctagacca	tcaacacttacacctacaacgaca	1.86	142	atgaaaggcaggctagaccaggataatgtgccaagaaacaatatgtgtcgttgtaggtgtaagtgttga	
3	*NAS*	Ta.5549	GAEF01037484.1	ttcttggtgaccggaagaac	tctagcgttcagaggcacac	2	2	ttcttggtgaccggaagaactctggaagcaggagaaaaatgtgtgcctctgaacgctaga	
4	*NAAT*	Ta.4977	BT009504.1	gaccatttagccaaggttgc	tacctcgtcagcaatcacca	1.85	137	gaccatttagccaaggttgcagaggtggcaagaaagctcggaatattggtgattgctgacgaggta	Traes_1BL_D8276D3DB
5	*DMAS*	Ta.5335	AB269908.1	caccgtcaatcaggtggag	cctctgcagaactccctca	1.88	6	caccgtcaatcaggtggaggtgaacccggtgtggcagcagaggaagctgagggagttctgcagagg	Traes_4BL_FAB8CACD6
6	*TOM*	Ta.5180	JP874085.1	tggagaatgcaatgataggtttt	agatgttttgcctcgctgtt	2	87	tggagaatgcaatgataggttttctcccaatacgatctgccaccacaccccaaaacagcgaggcaaaacatct	Traes_4BS_B3CC8E408; Traes_2DL_95F9B36A7; Traes_5AL_9AA8A9036; Traes_4DL_380EE71BD; Traes_4BL_45838A7CB
7	*YSL*	Ta.48303	HP631418	tgcatggaccaagataaacaag	acatatcaaagcggatgcaa	2	75	tgcatggaccaagataaacaagaaggaggctggcttcatggtgcccgcagttgcatccgctttgatatg	Traes_6BL_D65EC1432; Traes_6DL_5DBBFECCE; Traes_6AL_E36FCEF64
8	*YSL*	Ta.5463	BJ278653.1	gcagcgtgtggtgttatgat	aaggtacccagtcttgatgtcc	2	78	gcagcgtgtggtgttatgatgtccatagtatccacagctggagatctcatgcaggacatcaagactgggtacctt	Traes_2AL_05E2128A0
9	*YSL*	Ta.29321	HP639088.1	cgcgatgtttcggtatatca	tgacataggcaaccaggaca	2	97	cgcgatgtttcggtatatcagagcatacggcgccttccaggggctgtcctggttgcctatgtca	Traes_2BL_6C5206B6D; Traes_2DL_8C4BFA3CB
10	*YSL*	Ta.29367	AK334828.1	cccaggctaacctcaggac	agcttggcgttgagcttc	2	10	cccaggctaacctcaggacgcagctggcgggcggcgcggtggaggtggaggtgaagctcaacgccaagct	
11	*MT*	Ta.13600	HP625403.1	agcagagcaagtgcagatca	gatgatctccctctgagtttatcc	1.99	126	agcagagcaagtgcagatcagatcagaccagaccagagacacagagcagagcggataaactcagagggagatcatc	Traes_3DS_C917FF785
12	*FERRITIN*	Ta.5220	HP635522.1	gagtgtggcacttcgatcag	cgtagtcgtcgtgtccttca	2	16	gagtgtggcacttcgatcagatgctgcttgaggaggcagcttgaaggacacgacgactacg	Traes_5DL_95DBDBAD1
13	*MTP*	Ta.27695	HP624384.1	gaagcttgctgaggatcgag	tcgttcaccttgatttcgagt	1.93	106	gaagcttgctgaggatcgagtgctctggcttgtggtcacactcgaaatcaaggtgaacga	Traes_4DL_84BDB65D9; Traes_4BL_7CCDE849C; Traes_4AS_B5D20D324
14	*HMA*	Ta.45138	HP631862.1	atgcacgagttgtcggatg	ctcaatacgggctctcaacc	2	113	atgcacgagttgtcggatgtcatctgcccaagaccatgtcggaggggttgagagcccgtattgag	Traes_7DL_271C7BED5
15	*ZIP*	Ta.38190	AY864924.1	tggccacaatggtgatagac	cgtgccttgctgaagtga	2	3	tggccacaatggtgatagactcgctggctgctgggtactaccgccggtctcacttcagcaaggcacg	Traes_2AL_3983FD077

Supplementary table 4.5. List of primers used in the study. The table enlists the primer sequences, primer efficiency, probe number, amplicon, and amplicon blast hit to gene IDs in IWGSC (International Wheat Genome Sequencing Consortium) chromosome-based wheat genome (version 2.2)

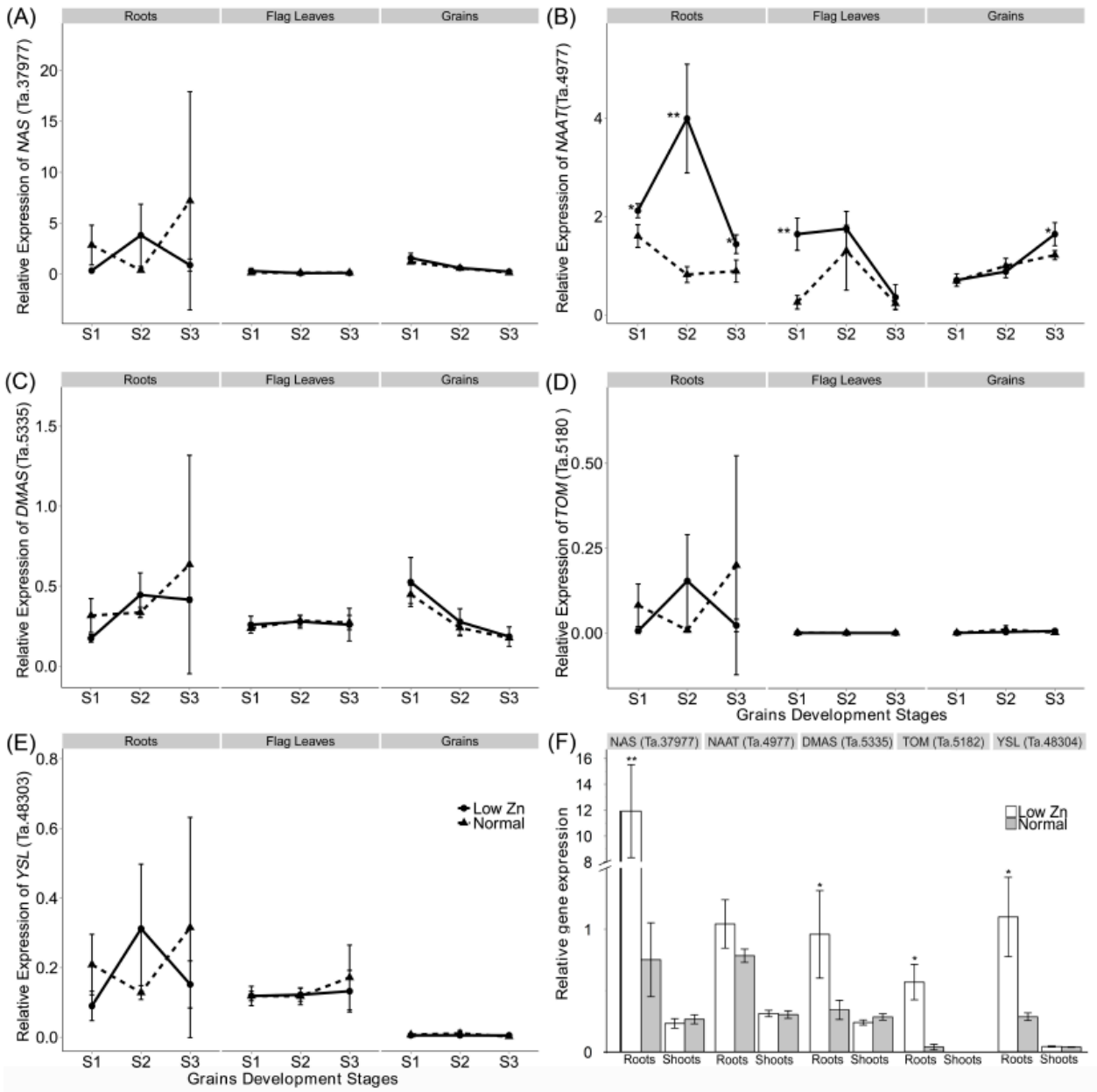

Supplementary figure 4.1. Differences in expression levels for genes involved in phytosiderophores biosynthesis and translocation between zinc deficiency and control condition. Values are the mean ± standard deviation of the three biological replicates (*p ≤ 0.05; **p ≤ 0.01). Note the differences in scale at Y-axis for relative expression levels of tested genes. (A) *NAS* homolog (Ta.37977), (B) *NAAT* homolog (Ta.4977), (C) *DMAS* homolog (Ta.5335), (D) *TOM* homolog (Ta.5180), (E) *YSL* homolog (Ta.48303). (A) to (E) demonstrate the expression profiles during three development stages during grain filling. (F) shows the expression profiles of the above genes in zinc-deficient seedlings.

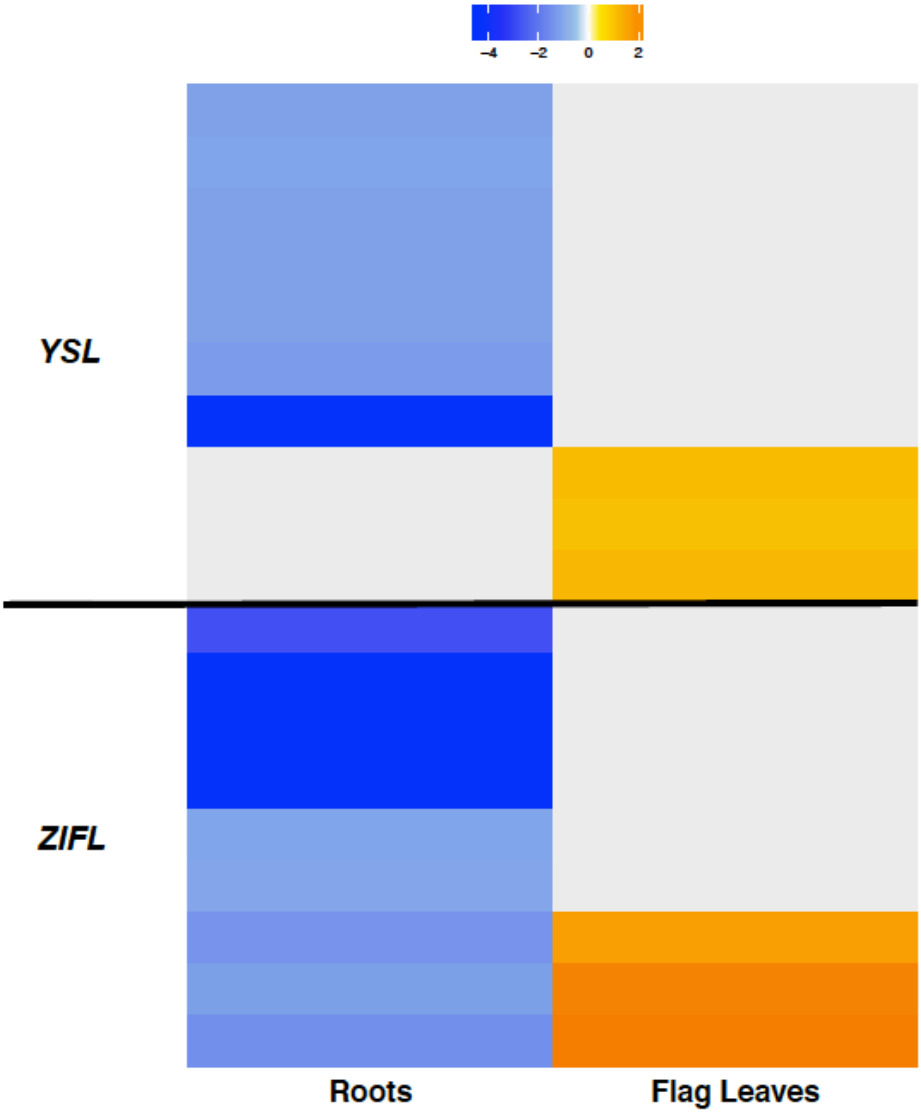

Supplementary figure 4.2. Differentially expressed YSL and ZIFL transporter encoding gene families. Orange color indicates up-regulation of gene expression; blue color indicates down-regulation; gray color indicates no detection of differential gene expression. YSL: YELLOW STRIPE LIKE; ZIFL: ZINC INDUCED FACILITATOR-LIKE.

5 NICOTIANAMINE SYNTHASE OVEREXPRESSION POSITIVELY MODULATES IRON HOMEOSTASIS-RELATED GENES IN HIGH IRON RICE

Meng Wang[1], Wilhelm Gruissem[1], and Navreet K. Bhullar[1,*]

[1] Plant Biotechnology, Department of Biology, ETH Zurich (Swiss Federal Institute of Technology), Zurich, Switzerland

[*]Corresponding author

Published on *Frontiers in Plant Science*

5.1 Abstract

Nearly one-third of the world population, mostly women and children, suffer from iron malnutrition and its consequences, such as anemia or impaired mental development. Biofortification of rice, which is a staple crop for nearly half of the world's population, can significantly contribute in alleviating iron deficiency. NFP rice (transgenic rice expressing *NICOTIANAMINE SYNTHASE*, *FERRITIN* and *PHYTASE* genes) has a more than six-fold increase in iron content in polished rice grains, resulting from the synergistic action of *NICOTIANAMINE SYNTHASE* (*NAS*) and *FERRITIN* transgenes. We investigated iron homeostasis in NFP plants by analyzing the expression of 28 endogenous rice genes known to be involved in the homeostasis of iron and other metals, in iron-deficient and iron-sufficient conditions. RNA was collected from different tissues (roots, flag leaves, grains) and at three developmental stages during grain filling. NFP plants showed increased sensitivity to iron-deficiency conditions and changes in the expression of endogenous genes involved in nicotianamine (NA) metabolism, in comparison to their non-transgenic siblings (NTS). Elevated transcript levels were detected in NFP plants for several genes encoding iron transporters. In contrast, expression of *YELLOW STRIPE-LIKE2* (*OsYSL2*), which encodes an Fe(II)-NA complex transporter, was reduced in NFP plants under low iron conditions, indicating that expression of *OsYSL2* is regulated by the endogenous iron status. Expression of the transgenes did not significantly affect overall iron homeostasis in NFP plants, which establishes the engineered push-pull mechanism as a suitable strategy to increase rice endosperm iron content.

Keywords: iron, homeostasis, NFP rice, biofortification, expression profiling

5.2 Introduction

Iron deficiency anemia (IDA) is the most severe degree of iron deficiency and a global problem that affects an estimated one-third of the world's population in both developing and developed countries. IDA has major consequences for human health as well as social and economic progress (WHO, 2016). Human IDA could be relieved by iron supplementation or food fortification. However, iron supplementation is difficult to achieve due to transportation and economic circumstances, especially in rural areas of developing countries. Iron fortification of food is also technically difficult and often results in unacceptable color and flavor of fortified products (Hurrell and Egli, 2010). In the recent years, bio-fortification has emerged as a possible solution to combat iron deficiency anemia through an economical and natural way.

Rice is the second largest produced cereal in the world and the most important grain with regard to human nutrition and caloric intake. It provides more than one fifth of the calories consumed worldwide. Around 3 billion people, mostly in Asia, depend on rice for 35–59% of their caloric intake. However, rice is a poor source of micronutrients, including iron. Most commercial rice varieties have only around 2 μg/g iron in the endosperm. Therefore, rice cannot provide daily iron needs of humans i.e., at least 8 mg/day for males and 18 mg/day for females, with pregnant women requirements rising up to 27 mg/day (Institute-of-Medicine, 2013). Considering these facts, enrichment of rice endosperm with bioavailable iron has the potential to decrease iron malnutrition worldwide. However, iron biofortification of rice strongly relies on information on the genes that control iron homeostasis in plants.

Iron translocation and homeostasis in rice has been well-studied. Several genes, most of which are transcriptionally regulated in response to iron availability, are known to coordinate iron uptake, translocation and storage in various tissues/compartments of the plant (Kobayashi and Nishizawa, 2012). However, the contribution of each type of transporter(s) and the precise iron flux still need to be clarified for each step involved in iron translocation. The transcription factors IDE BINDING FACTOR1 (OsIDEF1) and OsIDEF2 regulate iron homeostasis-related genes in rice during iron deficiency (Kobayashi *et al.*, 2009; Kobayashi *et al.*, 2010a; Ogo *et al.*, 2008). It has been suggested that OsIDEF1 senses the cellular iron status by binding directly to the metal ions (Kobayashi *et al.*, 2012). To cope with iron starvation, rice roots release phytosiderophores (PS), which are molecules of the mugineic acid (MAs) family that form strong hexadentate chelates with Fe(III) to solubilize and

transport it to the plant (Palmer and Guerinot, 2009; Walker and Connolly, 2008). The resulting Fe(III)-PS complexes are transported into root cells via transporters of the YELLOW STRIPE-LIKE (YSL) family of proteins (Inoue *et al.*, 2009; Lee *et al.*, 2009a). Nicotianamine (NA), which is synthesized by NICOTIANAMINE SYNTHASE (NAS) from S-adenosyl-L-methionine, is a ubiquitous metal chelator in plants and regulates iron translocation within and between cells and transports it to veins, flowers, and seeds (Takahashi *et al.*, 2003). NA also serves as a substrate for NICOTIANAMINE AMINOTRANSFERASE (NAAT) to produce a 3″-oxo intermediate and subsequently, DEOXYMUGINEIC ACID (DMA) is synthesized by DEOXYMUGINEIC ACID SYNTHASE (DMAS) (Haydon and Cobbett, 2007; Kim and Guerinot, 2007). Six members of *OsNAAT* family have been identified in rice plants, however, only *OsNAAT1* is regulated by plant iron status (Inoue *et al.*, 2008). *OsDMAS1* is also up-regulated in both roots and shoots under iron-deficient condition. In addition to the iron uptake using phytosiderophores/DMA, rice also possesses an Fe(II) uptake system. *IRON-REGULATED TRANSPORTER1* (*OsIRT1*) and *OsIRT2*, the homologs of *AtIRT1* in Arabidopsis, are specifically up-regulated in roots of iron-deficient rice plants (Ishimaru *et al.*, 2006).

Once iron is loaded into the xylem, the chelators such as citrate, NA, and DMA are required for further transport in the plant (Jeong and Guerinot, 2009). In rice, a FERRIC REDUCTASE DEFECTIVE-LIKE transporter, OsFRDL1, is involved in iron-citrate translocation from rice roots to shoots (Yokosho *et al.*, 2009). Transporters that are encoded by the *YSL* family of genes, *OsYSL2*, *OsYSL15*, *OsYSL16*, *OsYSL18*, are also involved in long-distance transport of Fe(III)-DMA and/or Fe(II)-NA complexes (Aoyama *et al.*, 2009; Inoue *et al.*, 2009; Ishimaru *et al.*, 2010; Kakei *et al.*, 2012; Zheng *et al.*, 2012). However, much still remains to be unraveled about intracellular metal transport involving vacuoles, chloroplasts, and mitochondria, although some transporters have been identified with specific iron translocation roles for these compartments. An iron deficiency-inducible *MITOCHONDRIAL IRON-REGULATED* (*MIR*) gene (Ishimaru *et al.*, 2009) and *MITOCHONDRIAL IRON TRANSPORTER* (*OsMIT*), whose expression increases under excessive iron condition, were identified in rice (Bashir *et al.*, 2011). PERMEASE IN CHLOROPLASTS1 (OsPIC1) is associated with chloroplast iron transport, while the vacuolar membrane localized OsVIT1 and OsVIT2 (VACUOLAR IRON TRANSPORTER1 and 2) mediate sequestration of Fe(II), Zn(II), and Mn(II) into vacuoles, with *OsVIT2* being very responsive to iron treatments (Zhang *et al.*, 2012). Conversely, transporters of the NATURAL RESISTANCE ASSOCIATED MACROPHAGE PROTEIN (NRAMP) family

appear to have important roles in mobilizing export of vacuolar iron stores (Lanquar *et al.*, 2005). Despite these advancements, the coordinated function of different transporters that have a role in iron homeostasis is not fully understood.

Strategies to improve iron content in rice grains were mostly targeted at effective iron uptake from the soil and translocation in the plant, in addition to directing iron into the rice endosperm. Most of the strategies used NAS and FERRITIN, a protein that stores iron in a bioavailable form (Jin *et al.*, 2009; Lonnerdal *et al.*, 2006). Endosperm-specific expression of *FERRITIN* or the constitutive expression of *NAS* mostly achieved around 2- to 3-fold increases of iron in the endosperm (Goto *et al.*, 1999; Lee *et al.*, 2009b; Lee *et al.*, 2012b; Lucca *et al.*, 2001; Qu *et al.*, 2005; Vasconcelos *et al.*, 2003). A 4.2-fold increase in iron content was reported in plants over-expressing *OsNAS2* under the control of the CaMV35S promoter (Johnson *et al.*, 2011). The possibility of using other transporters for improving endosperm iron content has also been explored recently. Specific expression of *OsYSL2* in the vascular tissue and around the endosperm lead to a 4.4-fold increase of iron concentration in the polished rice grains (Ishimaru *et al.*, 2010). Over-expression of *OsIRT1* under the control of the maize ubiquitin promoter also increased iron concentration to 113% compared to wild type grains (Lee and An, 2009). Alternatively, a few studies focused on the endosperm-specific expression of *PHYTASES* (Lucca *et al.*, 2001). These enzymes can degrade phytate, a chelating agent that binds iron as well as other metals and store them in a non-bioavailable form for human consumption within the grain (Brinch-Pedersen *et al.*, 2002).

The overexpression of multiple genes through a single construct, i.e., barley *NAS* expressed under rice actin promoter, soybean *FERRITIN* duplicated and expressed under two different endosperm specific promoters as well as rice *OsYSL2* duplicated and expressed under endosperm specific and sucrose transporter promoters, resulted in 4.4-fold increase of iron in polished grains of field grown T3 rice plants (Masuda *et al.*, 2012). In another approach, Wirth and collaborators reported a more than 6-fold increase in endosperm of rice plants constitutively expressing *A. thaliana NAS* (*AtNAS*), together with endosperm-specific expression of *Phaseolus vulgaris FERRITIN* (*PvFERRITIN*) and *Aspergillus fumigates PHYTASE* (*AfPHYTASE*) as a single construct (NFP rice) (Wirth *et al.*, 2009). The effect of *NAS* and *FERRITIN* genes was synergistic in these plants, indicating that none of the iron uptake, transport, or storage systems in the engineered rice plants were saturated.

Here, we investigated the molecular impact of the transgenes on the expression of endogenous

iron homeostasis-related genes in the engineered NFP rice plants. We performed targeted expression profiling of 28 genes involved in iron homeostasis. Our data suggests that the transgenes did not interfere with endogenous iron homeostasis at large, but modulated the expression of a few genes to facilitate iron uptake, translocation, and storage. The results provide new insights into coordinated role of different genes, particularly those involved in phytosiderophore synthesis and iron translocation, in maintaining iron homeostasis within the NFP plants while transporting more iron to the grains in these plants.

5.3 Results

The relative expression levels of 28 endogenous rice genes related to iron (or metal) homeostasis (Table 5.1) were analyzed in transgenic NFP plants and non-transgenic control plants (NTS). The genes studied included those involved in NA and DMA synthesis, and genes encoding the YSL transporters, ZINC-REGULATED TRANSPORTER (ZRT), IRON-REGULATED TRANSPORTER (IRT)-LIKE PROTEIN (ZIP) transporters, transcription factors, as well as the inter- and intra-cellular transporters. The plants were subjected to sufficient- and deficient- iron availability conditions and the expression levels of selected genes were studied in flag leaf, root, and grain samples collected at three grain development stages, i.e., milky, dough, and mature. In order to select for the reference genes which could be used for all the different sample types and growth stages, a preliminary test with at least 13 genes selected from the gene expression database, Genevestigator™ (Zimmermann *et al.*, 2005) as well as literature were tested. The genes with medium to high expression in all rice tissues were chosen from Genevestigator™ for the pilot qRT-PCR test. Among these tested genes, IWS1 C-terminus family protein (LOC_Os01g05420) and ATP binding protein (LOC_Os11g43970.1) ranked among the best five genes identified in our analysis and were therefore used in the experiment. The data from LOC_Os01g05420 expression was used for normalization of real-time quantitative expression of the test genes. The observed changes in the expression patterns of the tested genes in the NFP plants in comparison to their non-transgenic siblings (NTS plants) are summarized below.

Genes tested	Root	Leaf	Grain	Reference
PHYTOSIDEROPHORES SYNTHESIS RELATED GENES				
S-ADENOSYLETHIONINE SYNTHETASE2 (OsSAMS2)	X	X	X	Lee *et al*., 1997
NICOTIANAMINE SYNTHASE1 (OsNAS1)	X	X		Inoue *et al*., 2003; Kobayashi *et al*., 2005
NICOTIANAMINE SYNTHASE2 (OsNAS2)	X	X	X	Inoue *et al*., 2003; Kobayashi *et al*., 2005
NICOTIANAMINE SYNTHASE3 (OsNAS3)	X	X		Inoue *et al*., 2003
NICOTIANAMINE AMINOTRANSFERASE (OsNAAT1)	X	X	X	Inoue *et al*., 2008
DEOXYMUGINEIC ACID SYNTHASE (OsDMAS1)	X	X	X	Bashir *et al*., 2006
INTER-AND INTRA-CELLULAR METAL TRANSPORTERS AND OTHER IRON RESPONSIVE GENES				
IRON-REGULATED TRANSPORTER1 (*OsIRT1*)	X	X	X	Ishimaru *et al*., 2006
IRON-REGULATED TRANSPORTE2 (*OsIRT2*)	X	X		Ishimaru *et al*., 2006
YELLOW STRIPE-LIKE2 (*OsYSL2*)	X	X	X	Koike *et al*., 2004
YELLOW STRIPE-LIKE5 (*OsYSL5*)	X	X		Narayanan *et al*., 2007
YELLOW STRIPE-LIKE6 (*OsYSL6*)	X	X	X	Narayanan *et al*., 2007
YELLOW STRIPE-LIKE9 (*OsYSL9*)	X	X		Aoyama *et al*.,2009
YELLOW STRIPE-LIKE13 (*OsYSL13*)	X	X		Nozoye *et al*., 2011
YELLOW STRIPE-LIKE15 (*OsYSL15*)	X			Inoue *et al*., 2009
ZINC-REGULATED TRANSPORTER, IRON-REGULATED TRANSPORTER-LIKE PROTEIN1 (*OsZIP1*)	X	X		Ramesh *et al*., 2003
ZINC-REGULATED TRANSPORTER, IRON-REGULATED TRANSPORTER-LIKE PROTEIN3 (*OsZIP3*)	X	X		Ramesh *et al*., 2003
ZINC-REGULATED TRANSPORTER, IRON-REGULATED TRANSPORTER-LIKE PROTEIN4 (*OsZIP4*)	X	X	X	Ihsimaru *et al*., 2005
ZINC-REGULATED TRANSPORTER, IRON-REGULATED TRANSPORTER-LIKE PROTEIN8 (*OsZIP8*)	X			Narayanan *et al*., 2007
HEAVY METAL ATPASE2 (*OsHMA2*)	X	X		Takahashi *et al*., 2012
FERRIC REDUCTASE DEFECTIVE3 LIKE (OsFRDL1)	X			Yokosho *et al*., 2009
NATURAL RESISTANCE ASSOCIATED MACROPHAGE PROTEIN4 (*OsNRAMP4*)	X	X		Narayanan *et al*., 2007
MITOCHONDRIAL IRON-REGULATED GENE (*OsMI*R)	X	X	X	Ishimaru *et al*., 2009
METAL TOLERANCE PROTEIN1 (*OsMTP1*)	X	X		Yuan *et al*., 2012
VACUOLAR IRON TRANSPORTER2 (*OsVIT2*)	X	X	X	Zhang *et al*., 2012
PERMEASE IN CHLOROPLAST1 (*OsPIC1*)		X	X	Duy *et al*., 2007
GENES ENCODING IRON STORAGE PROTEINS AND TRANSCRIPTION FACTORS				
FERRITIN1 (*OsFER1*)	X	X	X	Stein *et al*, 2009
IDE-BINDING FACTOR1 (OsIDEF1)	X	X	X	Kobayashi *et al*., 2012; Kobayashi *et al*., 2009
IDE-BINDING FACTOR2 (OsIDEF2)	X	X	X	Ogo *et al*., 2008

Table 5.1. List of genes tested for their expression pattern in the NFP plants in comparison to their non-transgenic siblings. The symbol "X" marks the tissue (root, flag leaf, or grain) in which the corresponding gene was tested.

5.3.1 Expression profiles of genes involved in phytosiderophore synthesis and iron uptake in roots

Six rice genes encoding enzymes in phytosiderophore synthesis, and thus involved in iron uptake as well as in iron translocation, were studied. The genes included S-*ADENOSYL-L-METHIONINE SYNTHETASE 2* (*OsSAMS2*), the *NAS* family members *OsNAS1*, *OsNAS2* and *OsNAS3*, *OsNAAT1*, as well as *OsDMAS1*. The genes (except *OsNAS3*) are predominantly expressed in roots and induced by low iron availability as a part of the iron deficiency response that serves to increase iron acquisition (Figures 5.1–5.3, A5.1). As could be expected, over-expression of *AtNAS* in NFP plants resulted in higher expression of *OsSAMS2*, *OsNAS1*, *OsNAS3*, and *OsDMAS1* as compared to the NTS plants, primarily under iron-deficient conditions (Figure A5.1).

OsSAMS2 was expressed at higher levels during iron deficiency (mainly in the early development stages) in both NFP and NTS plants, but at the milky stage of grain filling the NFP roots showed further 1.7-fold higher expression of *OsSAMS2* (Figure A5.1, Table 5.2) than NTS roots. At other stages and in other tissues tested, the NFP and NTS plants did not differ significantly for *OsSAMS2* expression. Among the *NAS* genes, *OsNAS3* was overall expressed at low levels compared to *OsNAS1* and *OsNAS2*, but its expression in NFP roots was significantly increased at mature stage under high iron condition and at the milky stage in the plants grown in iron-deficient conditions (Figure A5.1). In the mature stage of grain filling, *OsNAS1* was up-regulated in NFP roots (2.3-fold) as compared to NTS roots. *OsDMAS1* was generally up-regulated in iron-deficient conditions in both the genotypes, but at the milky and mature stages of grain filling, its expression was 2-fold and 1.8-fold higher in the NFP roots than NTS roots, respectively (Figure A5.1, Table 5.2). A significant increase of *OsDMAS1* expression could also be detected in NFP grains at the milky stage in iron-deficient conditions. These results suggest that the genes involved in NA and DMA synthesis are coordinately regulated in NFP plants, which contributed to increased iron uptake and facilitated translocation within these plants.

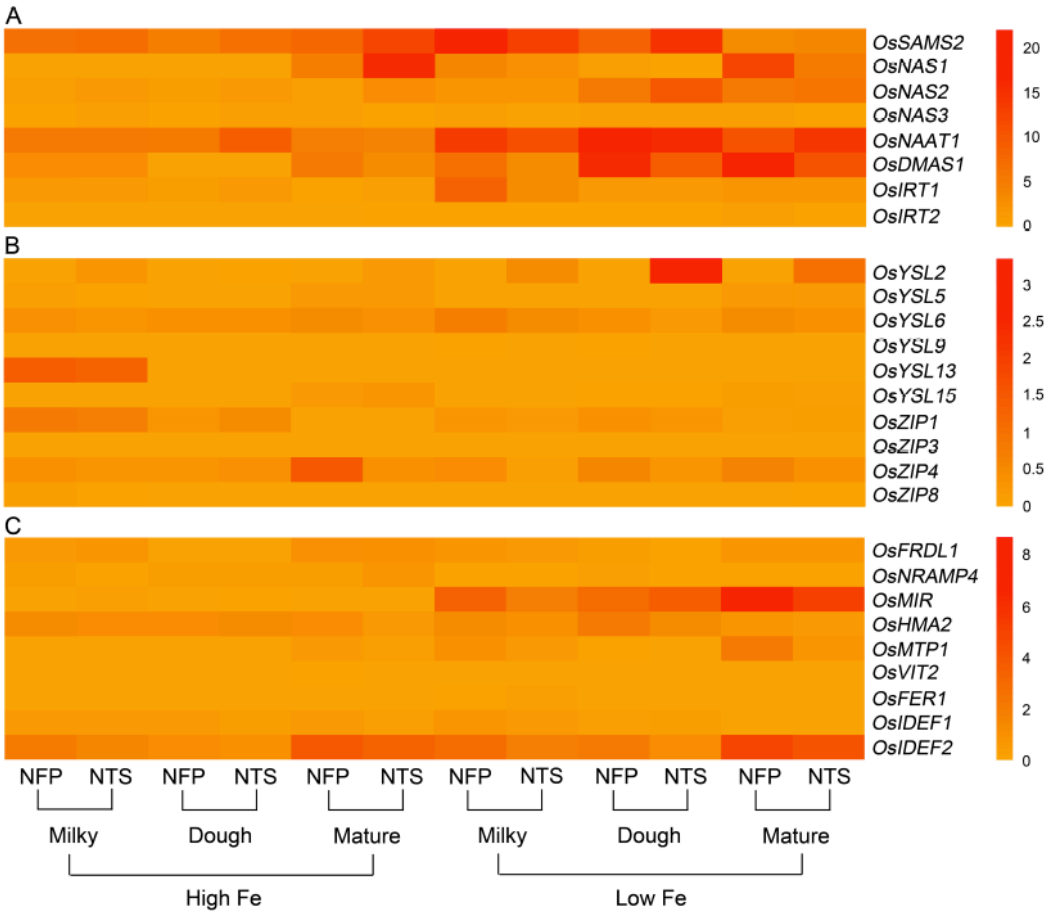

Figure 5.1. Overall view of genes that are differentially expressed in NFP roots as compared to NTS roots over different plant development stages (corresponding to grain filling stages—milky, dough, and mature) and upon different iron supplies (high and low Fe). (A) Expression levels of genes involved in nicotianamine and deoxymugeneic acid synthesis as well as the iron-regulated transporters. **(B)** Expression levels of genes belonging to *YSL* and *ZIP* families. **(C)** Expression levels of genes encoding transcription factors *OsIDEF1* and *OsIDEF2* regulating iron homeostasis as well as other inter- and intra-cellular metal transporters. Data represents the mean of three biological replicates. Note the differences in scale between panels **(A), (B),** and **(C)** for normalized expression levels of tested genes to reference gene (LOC_Os01g05420).

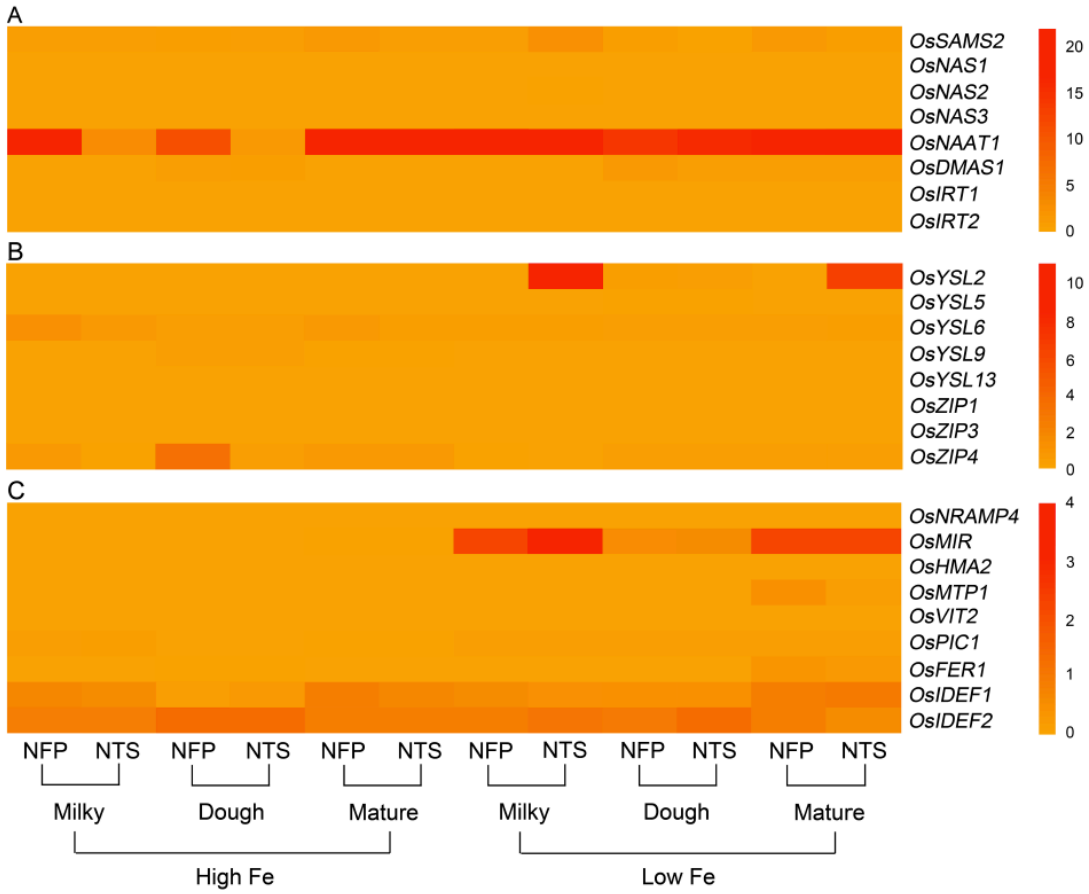

Figure 5.2. Overall view of genes that are differentially expressed in NFP flag leaves as compared to NTS flag leaves over different plant development stages (corresponding to grain filling stages—milky, dough, and mature) and upon different iron supplies (high and low Fe). (A) Expression levels of genes involved in nicotianamine and deoxymugeneic acid synthesis as well as the iron-regulated transporters. **(B)** Expression levels of genes belonging to *YSL* and *ZIP* families. **(C)** Expression levels of genes encoding transcription factors *OsIDEF1* and *OsIDEF2* regulating iron homeostasis as well as other inter- and intra-cellular metal transporters. Data represents the mean of three biological replicates. Note the differences in scale between panels **(A), (B),** and **(C)** for normalized expression levels of tested genes to reference gene (LOC_Os01g05420).

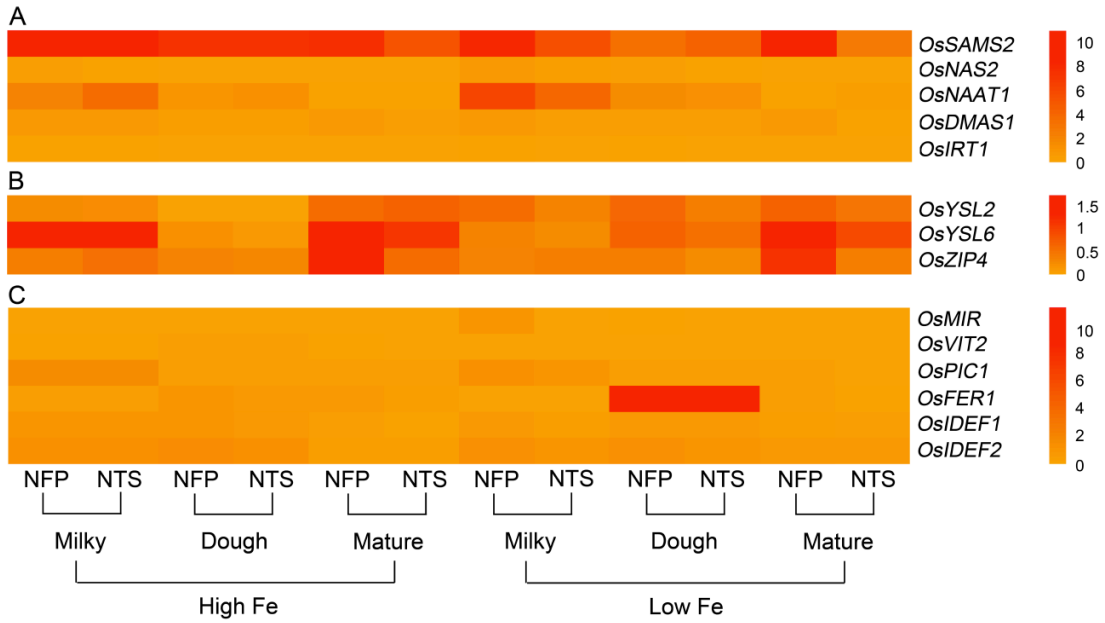

Figure 5.3. Overall view of genes that are differentially expressed in NFP grains as compared to NTS grains over different plant development stages (corresponding to grain filling stages—milky, dough, and mature) and upon different iron supplies (high and low Fe). (A) Expression levels of genes involved in nicotianamine and deoxymugeneic acid synthesis as well as the iron-regulated transporters. **(B)** Expression levels of genes belonging to *YSL* and *ZIP* families. **(C)** Expression levels of genes encoding transcription factors *OsIDEF1* and *OsIDEF2* regulating iron homeostasis as well as other inter- and intra-cellular metal transporters. Data represents the mean of three biological replicates. Note the differences in scale between panels **(A), (B),** and **(C)** for normalized expression levels of tested genes to reference gene (LOC_Os01g05420).

5.3.2 Other genes involved in iron uptake and iron translocation within the plant

The two iron-regulated transporters encoding genes, *OsIRT1* and *OsIRT2*, as well as several members of the *YSL* and *ZIP* family were studied, including *OsYSL2*, *OsYSL5*, *OsYSL6*, *OsYSL9*, *OsYSL13*, *OsYSL15* among *YSLs* and *ZIP1*, *ZIP3*, *ZIP4*, and *ZIP8* from the *ZIP* family (Figures 5.1–5.3).

Expression of *OsIRT1* and *OsIRT2* were mainly induced during iron deficiency and particularly in the roots, with *OsIRT1* expressed at higher levels than *OsIRT2* as was previously reported (Ishimaru *et al.*, 2006). Further, *OsIRT1* was expressed 2.6-fold higher in NFP roots than NTS roots at the milky stage of grain filling (Figure A5.2, Table 5.2), while *OsIRT2* expression was not significantly different in NFP and NTS plants. *OsIRT1* was also significantly up-regulated in the grains (1.5-fold) and leaves (3.5-fold) of NFP plants growing under sufficient iron conditions, both at milky and mature stages of grain filling, respectively, but expression levels were generally low in these tissues.

Among the *YSL* genes, significant transcript level differences were detected for *OsYSL2* and *OsYSL6*, while *OsYSL5*, *OsYSL9*, *OsYSL13*, and *OsYSL15* showed no or negligible expression differences between NFP and the NTS plants (Figures 5.1–5.3). *OsYSL2*, a transporter of the NA-Fe(II) complex, is induced during iron deficiency (Ishimaru *et al.*, 2010), which is also the case in NTS plants where *OsYSL2* is significantly up-regulated in leaves at the milky stage and in the roots at the dough stage of grain filling (Figure A5.3, Table 5.2). However, the *OsYSL2* expression remained unchanged in NFP plants grown in low iron conditions. In contrast, a significant overexpression of *OsYSL6* was observed in NFP grains at maturity and a slightly increased expression in the roots at the dough stage of grain filling in iron-deficient conditions, as compared to NTS plants. Also, *OsYSL6* was up-regulated in NFP flag leaves at the milky stage of grain filling as compared to NTS leaves in iron-sufficient conditions. *OsYSL6* has been suggested as a Mn(II)-NA transporter and also to play a role in detoxification of high manganese in roots and shoots (Sasaki *et al.*, 2011). NFP and NTS plants contain similar manganese concentrations, except for some increase in polished and brown grains in iron-deficient conditions (Wirth *et al.*, 2009). It is possible that the induced expression of *OsYSL6* in NFP plants contributes to the small increase of manganese in NFP grains when iron availability is low.

OsZIP4 was up-regulated in NFP leaves at dough stage of grain filling (6.3-fold) and in roots at grain maturity (4.2-fold) in iron-sufficient conditions. In iron-deficient conditions, NFP grains at maturity and NFP roots at the dough stage of grain filling had 3.3-fold and 2.1-fold higher expression of *OsZIP4* as compared to NTS plants, respectively (Figure A5.3, Table 5.2). *OsZIP1* was also up-regulated in low iron conditions in NFP roots at the dough stage (1.3-fold) and leaves at the milky stage of grain filling (2.5-fold). In addition, an approximate 6-fold higher expression was detected at the milky and mature stages of grain filling in the leaves of NFP plants grown with sufficient iron supply. However, it should be noted that *OsZIP1* is expressed only weakly in the leaves. *OsZIP3* and *OsZIP8* were expressed at even lower levels than *OsZIP1*, and their expression profiles were not significantly different between the genotypes, except for up-regulated *OsZIP3* expression in NFP roots at the dough stage of grain filling and down regulation in leaves at the milky stage of grain filling in low iron conditions, as compared to NTS plants (Table 5.2). The up-regulation of *OsZIP1* and *OsZIP4* under high iron conditions suggests that NFP plants signaled zinc deficiency when external iron concentration was high. Nevertheless, NFP plants perform better than the NTS plants in terms of zinc content in leaves and grains (Wirth *et al.*, 2009) both low and high iron conditions.

5.3.3 Transcription factors and other inter- and intra-cellular transporters

The transcription factors encoded by *OsIDEF1* and *OsIDEF2* are known to be constitutively expressed and not affected by iron deficiency (Kobayashi *et al.*, 2007; Ogo *et al.*, 2008). Similar expression patterns were obtained in our experiments, with an exception of *OsIDEF2*, which responded to iron deficiency in NFP plants. *OsIDEF2* expression was increased by 1.5- and 1.8-fold in NFP roots at milky and dough stages of grain filling as compared to NTS roots (Figure A5.2, Table 5.2). This up-regulation of *OsIDEF2* in NFP roots perhaps reinforced the Fe deficiency signal and thus led to up-regulation of genes involved in Fe translocation. *OsIDEF2* is known to be dominantly expressed in vascular bundles in the roots (Kobayashi *et al.*, 2010c).

The *OsMIR* gene was mainly expressed upon iron deficiency. In comparison to the NTS plants, NFP grains had elevated expression of *OsMIR* at milky and dough stages of grain filling in iron-deficient conditions and at the milky stage of grain filling with sufficient iron availability. However, *OsMIR* was less induced in NFP leaves than the NTS leaves at the milky stage of grain filling (Figure A5.2, Table 5.2), but no significant expression differences were found at other stages. *OsHMA2*, *OsPIC1*, *OsMTP1*, *OsNRAMP4*, *OsFRDL1*, *OsFERRITIN1 (OsFER1)*, and *OsVIT2* did not show any significant differences between NFP and NTS plants (Figures 5.1–5.3). Only in iron-deficient conditions, NFP mature grains showed a higher expression of *OsPIC1* and NFP roots had higher *OsHMA2* expression at the dough stage of grain filling when compared to NTS plants (Table 5.2). *OsVIT2* was mostly expressed under sufficient iron conditions, with low expression detected under iron deficiency in roots and leaves. *OsVIT1* does not respond to iron starvation while *OsVIT2* was found to be down-regulated in rice roots and shoots (Zhang *et al.*, 2012).

The summary of genes that are differentially regulated in the NFP plants as compared to NTS plants, under iron-deficient conditions is presented in Figure 5.4.

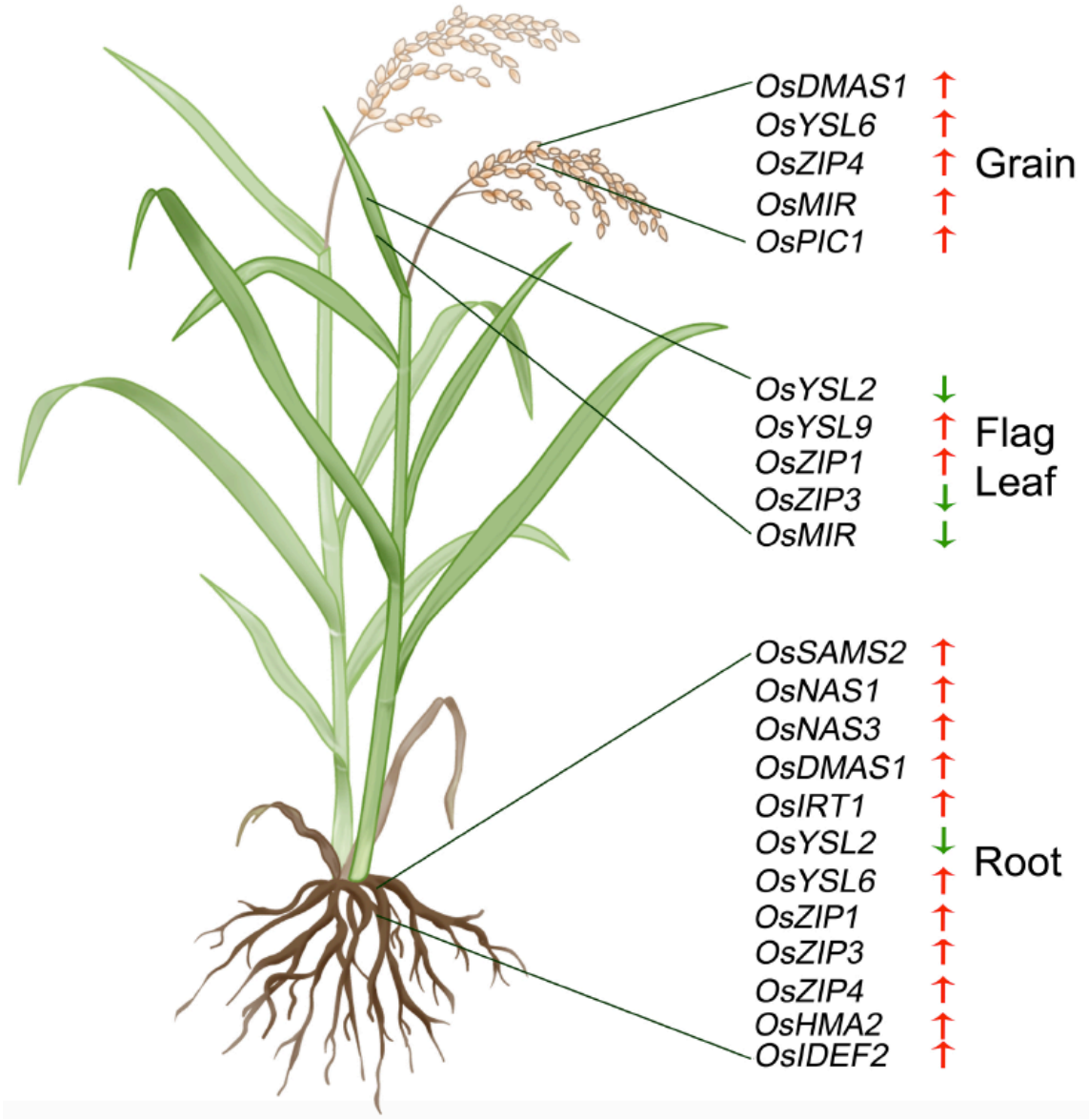

Figure 5.4. Summary of significant expression changes observed in case of NFP plants vs. NTS plants, when subjected to low iron conditions. Upward red arrows indicate up-regulated expression while downward green arrows indicate down-regulation of a particular gene, in the NFP plants as compared to the NTS plants. The genes are specifically marked according to the parts (roots, leaves, or grains) where the expression difference was observed.

	Root						Leaf						Grain					
	High Fe			Low Fe			High Fe			Low Fe			High Fe			Low Fe		
	Milky	Dough	Mature	Milky	Dough	Mature	Milky	Dough	Mature	Milky	Dough	Mature	Milky	Dough	Mature	Milky	Dough	Mature
OsSAMS2	-	-	-	1.7↑↑	-	-	-	-	-	-	-	-	-	-	-	-	-	-
OsNAS1	-	-	-	-	-	2.3↑	-	-	-	-	-	-	x	x	x	x	x	x
OsNAS2	-	-	-	-	-	-	-	-	-	-	-	-	-	-	-	-	-	-
OsNAS3	-	-	2.1↑	3.5↑	-	-	-	-	-	-	-	-	x	x	x	x	x	x
OsNAAT1	-	-	-	-	-	-	-	-	-	-	-	-	1.7↓↓	-	-	-	-	-
OsDMAS1	-	-	-	2.0↑↑	-	1.8↑	-	-	2.1↑	-	-	-	-	-	-	1.5↑	-	-
OsIRT1	-	-	-	2.6↑	-	-	-	-	3.5↑	-	-	-	1.5↑	-	-	-	-	-
OsYSL2	-	-	-	-	279↓	-	1.6↑	-	-	267↓↓	-	-	-	-	-	-	-	-
OsYSL5	-	-	-	-	-	-	-	-	1.9↑	-	-	-	x	x	x	x	x	x
OsYSL6	-	-	-	-	1.8↑↑	-	1.7↑↑	-	-	-	-	-	-	1.4↑	-	-	-	1.8↑↑
OsYSL9	-	-	-	-	-	-	-	-	-	2.1↑	-	-	x	x	x	x	x	x
OsZIP1	-	-	-	-	1.3↑	-	5.8↑↑	-	6.4↑	2.5↑↑	-	-	x	x	x	x	x	x
OsZIP3	-	-	-	-	2.1↑	-	-	-	-	4.3↓	-	-	x	x	x	x	x	x
OsZIP4	-	-	4.2↑↑	-	2.1↑	-	-	6.3↑↑	-	-	-	-	-	-	-	-	-	3.3↑
OsZIP8	-	-	-	-	-	-	x	x	x	x	x	x	x	x	x	x	x	x
OsFRDL1	-	-	-	-	-	-	x	x	x	x	x	x	x	x	x	x	x	x
OsMIR	-	-	-	-	-	-	-	-	-	1.7↓	-	-	3.2↑↑	-	-	38↑	17↑↑	-
OsHMA2	-	-	-	-	1.6↑	-	-	-	-	-	-	-	x	x	x	x	x	x
OsMTP1	-	-	-	-	-	-	-	-	-	-	-	-	x	x	x	x	x	x
OsPIC1	x	x	x	x	x	x	-	-	-	-	-	-	-	-	-	-	-	3.3↑
OsIDEF1	-	-	1.5↑	-	-	-	-	-	-	-	-	-	-	-	-	-	-	-
OsIDEF2	-	-	-	1.5↑	1.8↑↑	-	-	-	-	-	-	-	-	-	-	-	-	-

Table 5.2. Summary of expression differences obtained between NFP and NTS rice plants. For a particular gene studied, "-" represents no significant difference among the two genotypes. "x" represent no test made, and the values on the table represent fold changes observed in NFP plants as compared to NTS (statistically significant changes), where red upward arrows depict up-regulation while the downward green arrows depict down-regulation in the NFP plants, for a particular gene. Double arrows indicate significance at $p \leq 0.01$ and single arrows indicate significant at $p \leq 0.05$. The milky, dough, and mature represent respective grain filling stages at which the plant material was collected.

5.4 Discussion

The combined overexpression of *NAS* and endosperm-specific expression of *FERRITIN* have a synergistic effect in increasing the iron content in the endosperm of NFP grains (Wirth *et al.*, 2009) In the greenhouse, NFP plants show normal agronomic performance (e.g., plant height, tiller number, grain yield) and perform better under low iron conditions than NTS plants (Wirth *et al.*, 2009), suggesting that expression of *AtNAS1* and ferritin promoted iron increase in the endosperm without interfering with Fe homeostasis in NFP plants.

NA and DMA levels in plants are regulated by *NAS* and *NAAT* genes, and both NA and DMA are involved in iron distribution in plants (Aoyama *et al.*, 2009; Kakei *et al.*, 2009). DMA/phytosiderophore synthesis involves successive reactions that are catalyzed by SAMS, NAS, NAAT, and DMAS (Bashir *et al.*, 2010). *OsNAS1*, *OsNAS2*, and *OsNAS3* were proposed to perform different physiological functions in response to iron deficiency (Inoue *et al.*, 2003). Expression of *OsNAS1* and *OsNAS2*, both located on chromosome 3, is induced in rice roots exposed to iron deficiency. Thus, a main role of these enzymes in NA synthesis appears to be the increased production of phytosiderophores in iron-deficient roots (Inoue *et al.*, 2003). Expression of *OsNAS3*, which is located on chromosome 7, was found confined to pericycle cells close to protoxylem and companion cells, and was suggested to play rather limited role in phytosiderophore secretion from roots. Nevertheless, the OsNAS3 protein was shown to catalyze the trimerization of SAM to form NA (Inoue *et al.*, 2003).

During low iron availability, expression of *OsSAMS2* and *OsNAS3* was significantly up-regulated at the milky stage of grain filling while *OsNAS1* had elevated expression levels at maturity in NFP roots when compared to NTS roots. This suggests that under iron deficiency, *AtNAS1* overexpression together with the enhanced expression of *OsNAS3* and *OsNAS1* resulted in increased NA synthesis at milky and mature stages of grain filling. NFP plants produce more NA under iron deficiency (Wirth *et al.*, 2009). Since NA serves as the precursor for DMA, this increase in NA production most likely contributed to increased DMA content in NFP plants. Increased DMA production in NFP plants is further supported by the up-regulation of *OsDMAS1* in NFP roots, both at milky and mature stages of grain filling (Figure A5.1), as well as with increased DMA content in NFP leaves as compared to control plants (unpublished data). *OsNAS3* expression is also higher in NFP roots grown at high iron conditions, particularly at maturity. Together, these results suggest that the increased production of NA and DMA in NFP plants facilitated uptake of iron in roots and improved

iron translocation in the plants. In the roots of iron-deficient plants, *OsNAS1-3*, *OsNAAT1*, and *OsDMAS1* have similar expression patterns, with strong induction in pericycle cells adjacent to protoxylem (Bashir *et al.*, 2006; Inoue *et al.*, 2003; Inoue *et al.*, 2008). Rice plants have increased DMA concentration in the xylem in iron-deficient conditions (Kakei *et al.*, 2009). The specific contribution of *OsNAS3* to iron homeostasis has been previously reported (Lee *et al.*, 2009b), where *OsNAS3* activation resulted in increased iron and zinc concentration in the rice grains as well as increased tolerance to heavy metals. This increased iron concentration is also well-correlated with increased NA and DMA content in plants that have increased *OsNAS3* expression (Lee *et al.*, 2009b). Study also showed a positive correlation between increased NA content and increased grain iron content in rice plants overexpressing either of *OsNAS1*, *OsNAS2*, and *OsNAS3* (Johnson *et al.*, 2011).

Furthermore, the demand for methionine is increased in iron-deficient plants in order to support the increased production of NA and then subsequently DMA. In our experiment, *OsSAMS2* was significantly up-regulated in roots of iron-deficient NFP and NTS plants, with a further expression increase in NFP roots at the milky stage of grain filling as compared to NTS plants (Figure A5.1). This increase of *OsSAMS2* expression would be expected to meet the demand for SAM, which is an immediate precursor for NA synthesis. Increased expression of genes participating in the methionine cycle in the roots of iron-deficient wheat, rice, and barley has been reported earlier (Kobayashi *et al.*, 2005; Ma *et al.*, 1995; Negishi *et al.*, 2002).

In iron-deficient conditions, iron needs to be effectively transported from roots to the shoots via the xylem, and then between cells. Significant advances have been made in identifying transporters involved in iron translocation. However, our understanding of the exact contribution of each one of these transporters in metal flux is rather limited. To date, the principal chelators known to bind iron include citrate (Rellan-Alvarez *et al.*, 2010), NA and DMA (Aoyama *et al.*, 2009; Kakei *et al.*, 2009; Takahashi *et al.*, 2003). The major role of DMA was initially considered to be in iron uptake from the rhizosphere, but several lines of evidence support a chelating role of DMA in both xylem and phloem (Aoyama *et al.*, 2009; Kakei *et al.*, 2009). Based on the expression of *OsDMAS1* it has been proposed that DMA is synthesized in the phloem companion cells (Inoue *et al.*, 2008). High concentrations of DMA have been detected in phloem sap in independent studies advocating the involvement of DMA in long-distance iron transport (Nakashima *et al.*, 2012). Several transporters belonging to YSL family could be transporting these chelator-bound iron complexes to other parts of the

plant. OsYSL15 and OsYSL18 transport Fe(III)-DMA complexes and are involved in internal translocation of iron (Aoyama *et al.*, 2009; Inoue *et al.*, 2009), while OsYSL2 transports Fe(II)-NA and Mn(II)-NA complexes, but not Fe(III)-DMA (Ishimaru *et al.*, 2010; Koike *et al.*, 2004).

OsYSL2 is induced by iron-deficiency and may be actively involved in long-distance phloem transport of Fe(II)-NA complexes in the plant and into the grains (Ishimaru *et al.*, 2010; Koike *et al.*, 2004). Rice plants with reduced *OsYSL2* function (RNAi-OsYSL2) have reduced iron and manganese concentrations in the grains (Ishimaru *et al.*, 2010). Consistent with previous reports (Ishimaru *et al.*, 2010), NTS plants showed induced expression of *OsYSL2* upon iron deficiency, but the gene was not up-regulated in NFP roots and leaves under the same condition (Figure A5.3). In the grains, however, the expression of *OsYSL2* increased in NFP plants as well but was not significantly different than in NTS grains. A plausible explanation for this result could be that expression of *OsYSL2* is regulated by the endogenous iron status of the plants. It has also been suggested that OsIDEF2 directly regulates expression of *OsYSL2* (Ogo *et al.*, 2008). However, the up-regulation of *OsIDEF2* in iron-deficient NFP roots (Figure A5.2) did not lead to increased *OsYSL2* expression. It is possible that OsIDEF2 also senses cellular iron status in order to induce the iron-deficiency responsive genes, as was suggested for OsIDEF1 which binds directly to divalent metals for sensing cellular metal ion balance (Kobayashi *et al.*, 2012). Importantly, the NFP plants had higher iron content in the grains as compared to NTS plants. It is also possible that NFP plants deployed alternate modes of iron transport to grains than the transfer by OsYSL2 and that the function of OsYSL2 is complemented by another transporter. Our results also reflect effective crosstalk between molecular components involved in Fe homeostasis in different growth conditions and during development to meet the needs for Fe in the plant.

OsMIR, a recently evolved rice-specific mitochondrial gene, is strongly induced under iron deficiency (Ishimaru *et al.*, 2009). NFP leaves had lower expression levels of *OsMIR* as compared to NTS leaves under low iron conditions, but the gene was up-regulated in NFP grains (Figure A2). Since mitochondrial iron regulation is poorly understood, it is difficult to predict how and to what extent these expression differences contributed to higher grain iron content in the NFP plants. In addition, NFP leaves also had increased expression of *OsZIP1* and *OsZIP4* under high iron conditions, indicating that NFP plants might signal zinc deficiency when external iron concentration is high. Although *OsZIP4* is regulated by zinc (Ishimaru *et al.*, 2005), there exists a strong crosstalk between zinc and iron homeostasis in

plants. Iron concentrations doubled in zinc-deficient roots (Ishimaru *et al.*, 2005) and plants overexpressing *OsZIP4* had significantly increased iron in the shoots and roots, in addition to the zinc increases (Ishimaru *et al.*, 2007). This demonstrates the coordination of iron and zinc homeostasis in plants and also that the expression of *OsZIP1* and *OsZIP4* are affected by the external supply of iron to the plants (as in the case of both NFP and NTS plants) as well as by endogenous iron nutritional status of plants (further increases in NFP plants). Nevertheless, NFP plants had a similar zinc content in the leaves as compared to the controls over a range of tested external iron concentrations and outperformed NTS plants in terms of zinc content in the grains (Wirth *et al.*, 2009). Therefore, zinc homeostasis is also unaffected in NFP plants.

Together, the increased production of NA and DMA in NFP plants facilitated iron uptake from the rhizosphere as well as effective internal translocation. Expression of several genes encoding transporters appear to be adjusted in the NFP plants in order to utilize overproduced NA and DMA, and the expanded sink for iron storage in the grains via ferritin. However, these adjustments did not interfere with iron homeostasis in the NFP plants. Further investigations focused on iron speciation in the grain, i.e., Fe(II) or Fe(III), and the relative abundance of two forms together with the information on molecules chelated to these forms, will be required for elucidating the exact mechanisms of iron translocation to the grains in NFP plants.

5.5 Materials and methods

5.5.1 Plant material

The NFP plants and their non-transgenic siblings (NTS) were grown under greenhouse conditions, in the hydroponics system. The NFP plants are the *Oryza sativa* ssp. japonica cv. Taipei 309 transformed with *Arabidopsis NICOTIANAMINE SYNTHASE* gene, *Phaseolus vulgaris FERRITIN*, and *A. fumigatus PHYTASE* gene (NFP plants; Wirth et al., 2009). Solutions for the hydroponic system were prepared according to the protocol modified from Kobayashi et al. (2005), using 0.70 mM K_2SO_4, 0.10 mM KCl, 0.10 mM KH_2PO_4, 2.0 mM $Ca(NO_3)_2$, 0.50 mM $MgSO_4$, 10 μM H_3BO_3, 0.50 μM $MnSO_4$, 0.20 μM $CuSO_4$, 0.01 μM $(NH_4)_6Mo_7O_{24}$, and 0.5 μM $ZnSO_4$, with different iron concentrations added as Fe(III)-EDTA according to the treatment (high iron condition: 200 μM iron; iron-deficient condition: 10 μM iron). The nutrient solutions were renewed every seven days. Samples were collected at three different grain filling stages: milky stage, dough stage, and mature stage. At the milky stage grains are starting to fill with a white, milky liquid that can be squeezed by pressing the grain

between fingers, while in dough stage the milky portion of grain turns into a soft dough and at maturity, the grain is fully developed and hard (parameters as defined in the Rice Knowledge Bank, IRRI, Philippines). At each developmental stage, roots, flag leaves and grains were collected, with at least three biological replicates.

5.5.2 Total RNA extraction and cDNA synthesis

Total RNA was extracted from the root, flag leaf, and grain samples using Trizol® reagent (Invitrogen, USA) and was treated with DNase I (Thermo Fisher Scientific Inc., USA). RevertAid™ first strand cDNA synthesis kit (Thermo Fisher Scientific Inc., USA) was used for cDNA synthesis. All steps were carried out following the manufacturers' instructions.

5.5.3 Real-time quantitative PCR

Real-time quantitative PCRs (qRT-PCRs) were carried out using Taqman hydrolysis probes (Roche, Switzerland) on 7500 FAST Real Time PCR system (Applied Biosystems, Inc., USA). Total reaction volume of 25 µl was used, comprising of 12.5 µl mastermix (Applied Biosystems Inc., USA), 1 µl cDNA, 2.25 µl forward primer and 2.25 µl reverse primer, 0.25 µl probe (Roche Ltd., Switzerland) and 6.75 µl H2O.

Primers were designed using Roche primer design website (https://www.roche-applied-science.com/sis/rtpcr/upl/index.jsp?id=UP030000). Probe number and primer sequences are presented in the Appendix (Table A5.1). The Ct value was obtained from 7500 Fast System Software (Applied Biosystems, Inc., USA). The primer efficiency was calculated using LinReg PCR (Tuomi *et al.*, 2010). qRT-PCR data normalization was done as described by Schefe et al. (2006). The obtained data were further analyzed by ANOVA and significant differences between the tested plant materials are presented.

5.6 Conflict of interest statement

The authors declare that the research was conducted in the absence of any commercial or financial relationships that could be construed as a potential conflict of interest.

5.7 Acknowledgments

We thank ETH Zurich (ETH-06 10-3), the Swiss State Secretariat for Education and Research (through COST FA0905), and Ms. Jacqueline Imhof for support of our biofortification work.

We also acknowledge the help of our gardener Irene Zurkirchen and of Renato Guidon, Kumar Vasudevan, and Jonghwa Park for help with sample preparations. We acknowledge the contribution of Bernadette Rawyler for the rice plant drawing used in Figure 5.4 of the article.

5.8 Appendix

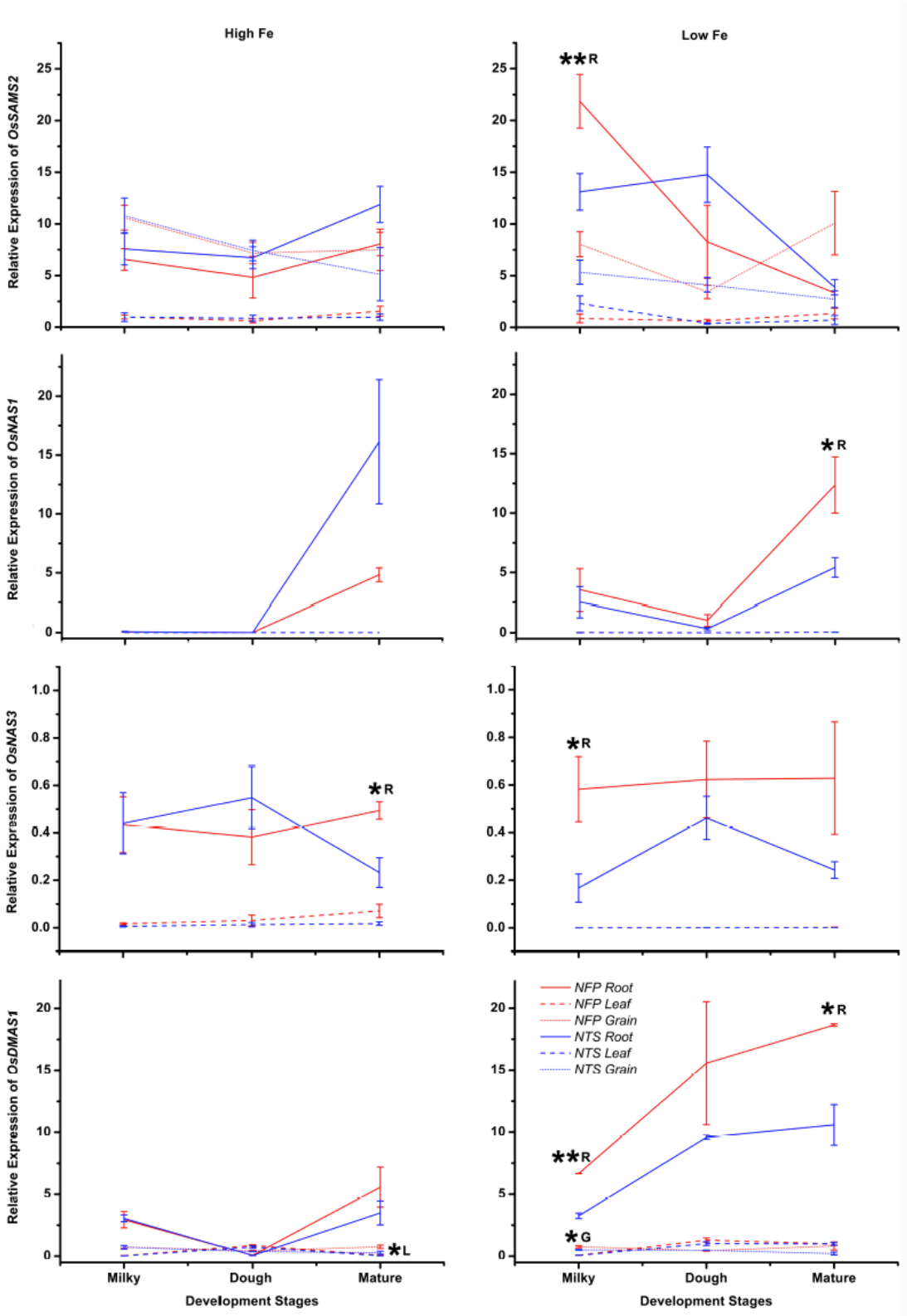

Figure A5.1. Differences in expression levels for genes involved in nicotianamine and deoxymugeneic acid synthesis (*OsSAMS2*, *OsNAS1*, *OsNAS3,* and *OsDMAS1*), in the roots, flag leaves, and grains of NFP vs. NTS plants are presented. Values are mean ± standard error of mean, of the three biological replicates. Significant differences between NFP and NTS tissues (roots, flag leaves, grains) under a particular treatment

(high Fe or low Fe) or at a particular development stage (milky, dough, or mature) are marked with single (*$p \leq 0.05$) or double asterisks (**$p \leq 0.01$), respectively. The letters R, L, and G represent root, leaf, and grain, respectively. Note the differences in scale at Y-axis for relative expression levels of tested genes.

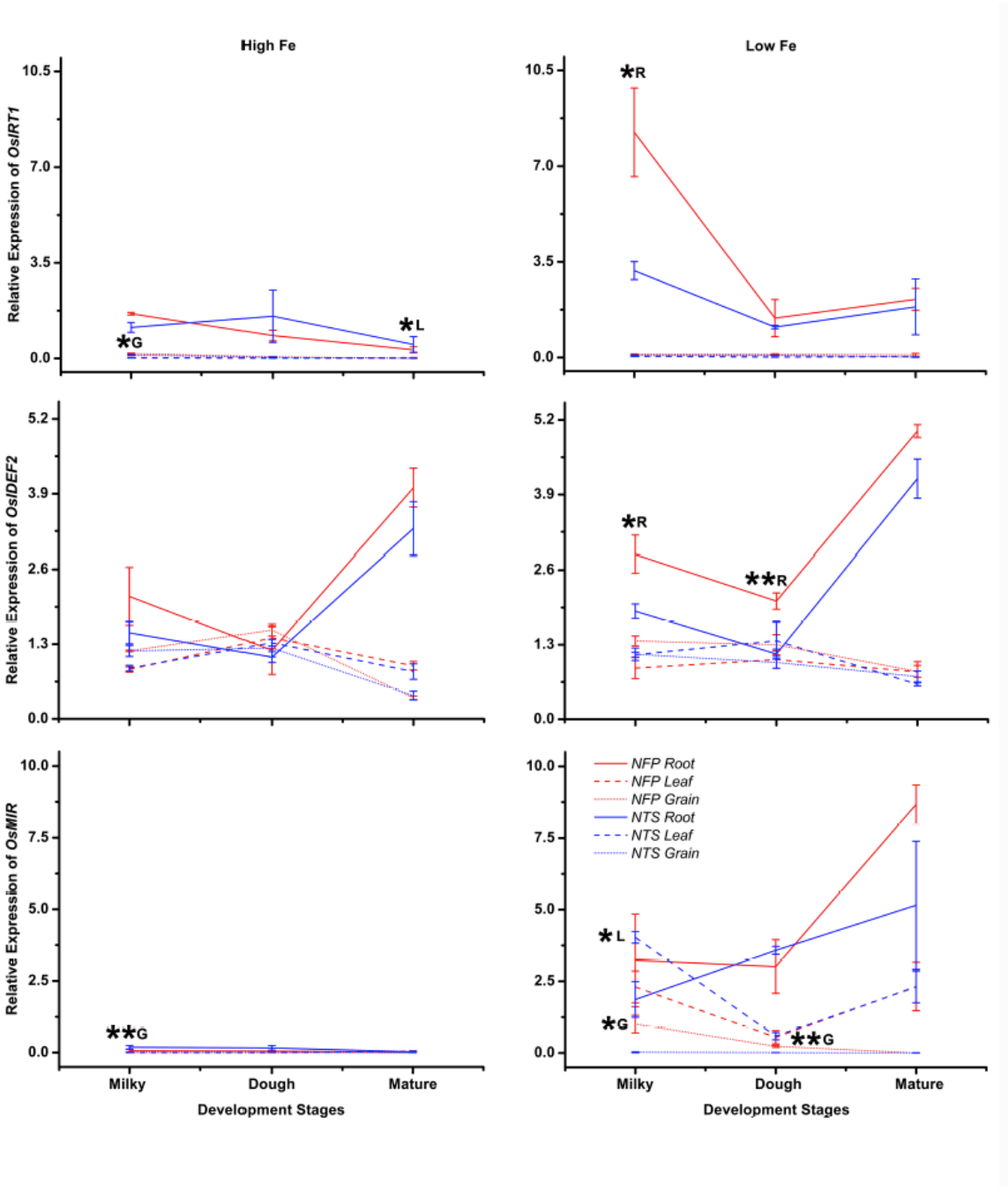

Figure A5.2. Differences in expression levels of genes encoding OsIRT1, OsIDEF2, and OsMIR, in the roots, flag leaves, and grains of NFP vs. NTS plants are presented. Values are mean ± standard error of mean, of the three biological replicates. Significant differences between NFP and NTS tissues (roots, flag leaves, grains) under a particular treatment (high Fe or low Fe) or at a particular development stage (milky, dough, or mature) are marked with single (*$p \leq 0.05$) or double asterisks (**$p \leq 0.01$), respectively. The letters R, L, and G represent root, leaf, and grain, respectively. Note the differences in scale at Y-axis for relative expression levels of tested genes.

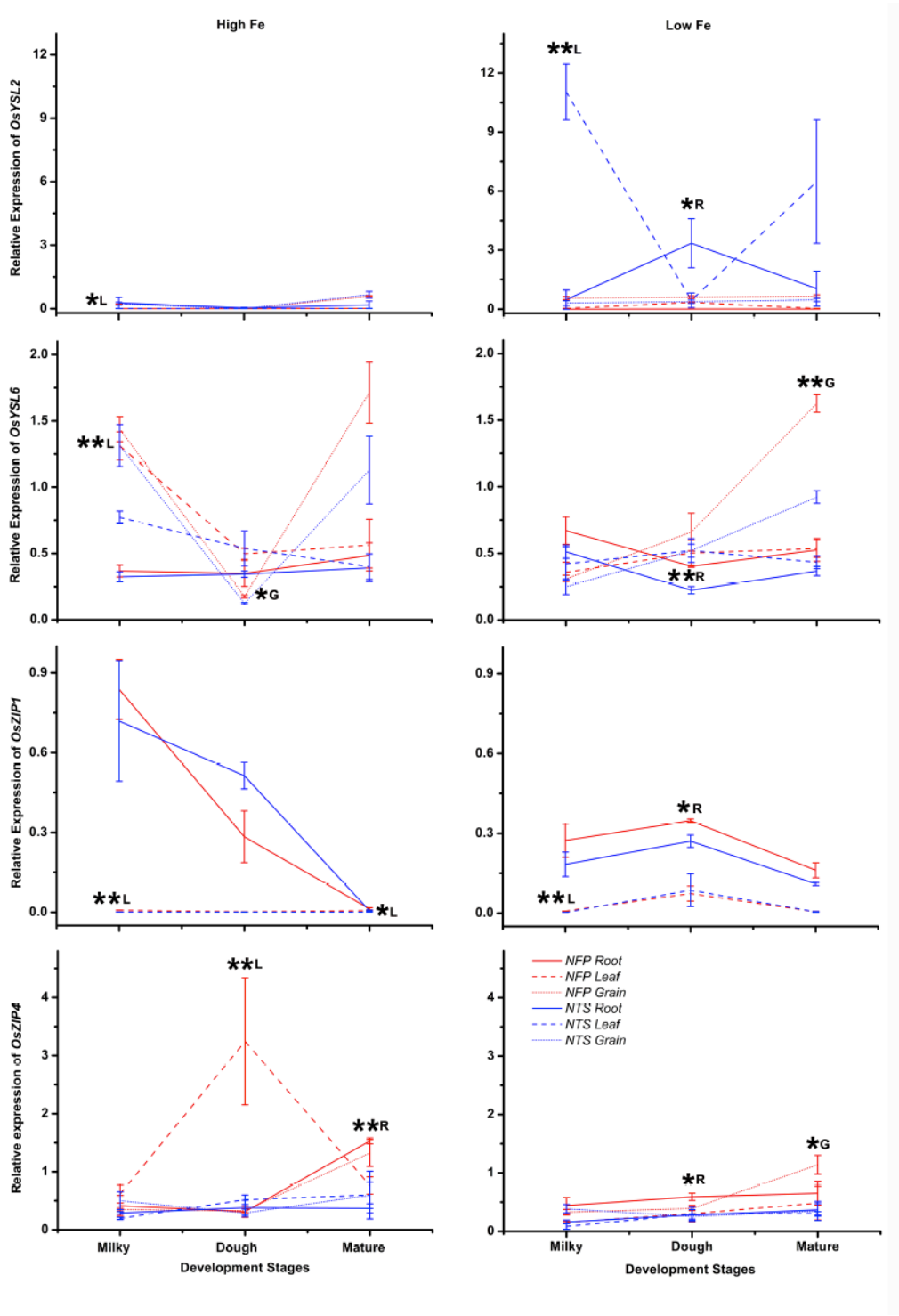

Figure A5.3. Differences in expression levels of genes encoding *OsYSL2* and *OsYSL6*, as well as *OsZIP1* and *OsZIP4*, in the roots, flag leaves, and grains of NFP vs. NTS plants are presented. Values are mean ± standard error of mean, of the three biological replicates. Significant differences between NFP and NTS tissues (roots, flag leaves, grains) under a particular treatment (high Fe or low Fe) or at a particular development stage (milky, dough, or mature) are marked with single (*$p \leq 0.05$) or double asterisks (**$p \leq 0.01$), respectively. The letters R, L, and G represent root, leaf, and grain, respectively. Note the differences in scale at Y-axis for relative expression levels of tested genes.

Nr.	Genes	Accession number	Forward Primer	Reverse Primer	TaqMan Probe
1	*OsSAMS2*	U82833	ccgaataaaggcgagaagc	gactcggaggtgaagaggaa	70
2	*OsNAS1*	AB021746	cggttgagaaggcagaagagt	cgatcgtccggctgttag	17
3	*OsNAS2*	AB023818	cacctcgaggcgcactac	tccagcttgctcaggttga	149
4	*OsNAS3*	AB023819	gaggaggaggtgatcgagaa	atcaccagctccgtgaaca	70
5	*OsNAAT1*	AB206814	ttgccaacttgcgaaagaa	aatgcgaacccaattcttca	61
6	*OsDMAS1*	AB269906	aaaagctcgacaccctgct	tccctcagcttcctctgct	39
7	*OsIRT1*	AB070226	gacactggtgcccattctg	gaggatggggatggagga	63
8	*OsIRT2*	AB126086	tcaggaatcgcgtcattgt	agcccgatcaccactgag	105
9	*OsYSL2*	AB164646	tggagcttcttccagtggtt	gaggctgaaatcaaaatagaacg	22
10	*OsYSL5*	AB190915	agcttgcatggaaaaacagaa	aaagaagctccagccaaaact	4
11	*OsYSL6*	AB190916	gaacaccgtcatccagacct	gttttctgatccattgcaagc	141
12	*OsYSL9*	AB190919	tgcgtggatgactggattc	tcccacttgggtaagttaatttgt	152
13	*OsYSL13*	AK067235	atccagacctgcgtcgtc	catggacaatatgtagttaccaaagc	161
14	*OsYSL15*	AB190923	tcgcctgctacaccatagc	cagctcgtacgtcctcttgtt	107
15	*OsZIP1*	AY302058	gtgatgagccgcaaggag	cctcgaacgacgatgtcc	159
16	*OsZIP3*	AY323915	tgcatctgtgaggccatcta	tgacggttgcccttacctta	31
17	*OsZIP4*	AB126089	gtcaatcaggccactcgtc	gctttcgccttaaaatttgc	31
18	*OsZIP8*	AK070864	atcagttcttcgagggcatc	gcgtcgtagacggaggag	143
19	*OsFRDL1*	NM_001055921	gactccacttcgatccacaaa	ctcgctccgcttatcacg	146
20	*OsNRAMP4*	AK102180	gccattggcttcctagatcc	aagatgacccacagaagctca	78
21	*OsMIR*	AK103636	acatttatcctactcgttgctcct	tgcctaagtgctgagtcacg	43
22	*OsHMA2*	HQ646362	gtcaacatactcatgctgattgc	cccagcctcagaatagtcctt	67
23	*OsMTP1*	AK100735	tcaatctccatcaccatcca	tcactcttgagcaatggttcc	157
24	*OsVIT2*	Os09g0396900	ggcctcggagggtatctg	acagtatgtccgcgatctcc	15
25	*OsPIC1*	XM_464386	accgagcaggacatcgag	ggaaacaactgtggacacca	93
26	*OsFER1*	AF519570	aggggatgccttgtatgct	cggtcagctgtggatcatt	148
27	*OsIDEF1*	AK107456	gtcttcaggctggggatgt	gggatttgttgtctgctgatg	91
28	*OsIDEF2*	AK099540	cagatgttgaactgtataaatttgctc	ttcaagatctctgctctggagac	15

Table A5.1. Primers and probes list for real-time quantitative PCR.

6 GENERAL DISCUSSION

Response to micronutrients starvation in plants is a complex and comprehensive but precisely modulated process, which balance plants' survival, growth, and development. Transcriptomic approaches have been used to reveal the regulation of gene expression in response to iron and zinc deficiency in strategy I as well as strategy II plants, including Arabidopsis (Buckhout *et al.*, 2009; Rodriguez-Celma *et al.*, 2013; Thimm *et al.*, 2001; Yang *et al.*, 2010), soybean (Moran Lauter *et al.*, 2014; O'Rourke *et al.*, 2007; O'Rourke *et al.*, 2009), tomato (Zamboni *et al.*, 2012), rice (Kobayashi *et al.*, 2005), barley (Nagasaka *et al.*, 2009; Negishi *et al.*, 2002), and maize (Li *et al.*, 2014). These studies suggest that gene transcripts accumulation is not only regulated by transcription factors during the transcription process, but is also mediated by epigenetics- and post-transcriptional regulation. In addition, iron- and zinc-deficiency also modulate protein accumulation and metabolites production in plants. Therefore, it is necessary to link the knowledge of epigenetic, post-transcriptional, translational, and post-translational regulations to transcriptional regulation response to gain a comprehensive insight into gene expression regulation in iron and zinc homeostasis.

6.1 Epigenetic regulation of iron homeostasis

Emerging evidence demonstrates that some genes encoding bHLH transcription factor family members are iron-deficiency-inducible and are responsible for regulation of the genes involved in iron homeostasis (Ogo *et al.*, 2011; Wang *et al.*, 2007; Wang *et al.*, 2013a) (Chapter 2; 3). Four Ib subgroup bHLH transcription factors that are AtbHLH38, AtbHLH39, AtbHLH100, and AtbHLH101, interact with FIT, and activate the transcription of *FRO* and *IRT1* in Arabidopsis (Wang *et al.*, 2013b; Yuan *et al.*, 2008a). The expression of the four genes is positively modulated by transcription factors bHLH34 and bHLH104 under iron deficiency (Li *et al.*, 2016; Wang *et al.*, 2007). At the same time, the expression of the four genes is repressed by *Stichodactyla helianthus* NEUROTOXIN (ShK1) BINDING PROTEIN1/PROTEIN ARGININE METHYLTRANSFERASE5 (SKB1/PRMT5), which catalyzes the symmetric dimethylation of histone 4 arginine 3 (H4R3sme2) (Fan *et al.*, 2014). When suffering from iron deficiency, SKB1 disassociates from the chromatin of the *bHLH* genes, leading to reduced H4R3sme2 level, and therefore positively regulates the transcription of *bHLH* genes (Fan *et al.*, 2014). In addition to histone methylation, histone acetylation mediated epigenetic modification also regulates iron homeostasis. In Arabidopsis, GENERAL CONTROL NON-REPRESSED PROTEIN5 (GCN5) mediates acetylation of histone 3 lysine

9 and histone 3 lysine 14 (H3K9/14ac) of FRD3, which effluxes citrate into the root vasculature (Durrett *et al.*, 2007; Xing *et al.*, 2015). The expression of GCN5 is induced by iron deficiency, and positively control the expression of FRD3 through H3K9/14ac modification (Xing *et al.*, 2015).

6.2 MicroRNAs (miRNAs) participate in iron- and zinc-homeostasis regulation

Many miRNAs are responsive to nutrient stresses and regulate the gene expression post-transcriptionally by targeting nutrient homeostasis or growth- and development-related genes (Zeng *et al.*, 2014). Under iron- and zinc-deficiency, the expression of miRNAs was found differentially expressed in Arabidopsis, rapeseed, rice, sorghum and *Brassica juncea* (Agarwal *et al.*, 2015; Buhtz *et al.*, 2010; Kong and Yang, 2010; Li *et al.*, 2013c; Shi *et al.*, 2013; Waters *et al.*, 2012). In Arabidopsis, 24 miRNA genes were identified harboring iron-deficiency responsive cis-acting elements 1 and 2 (IDE1/IDE2) motifs in their promoter regions, demonstrating possible regulation by iron deficiency. These miRNAs largely target genes related to DNA binding and processing, DNA conformation and recombination, and transcription activation, as well as genes related to subcellular components localization and development (Kong and Yang, 2010). In iron-deficient rice, differentially expressed miRNAs mainly target to transcription factors such as AUXIN RESPONSIVE FACTOR 12 (ARF12) and APETALA2 (AP2). The genes encoding DICER-LIKE1 (DCL1) and ARGONAUTE (AGO) are also the targets (Agarwal *et al.*, 2015). The differentially expressed miRNAs may target plant growth and development, abiotic stress response, and phytohormone response in zinc-deficient *Brassica juncea* roots (Shi *et al.*, 2013). In sorghum, differentially expressed miRNAs were predicted to target genes that encode transcription factors, metabolic processes, or responses proteins (Li *et al.*, 2013c).

6.3 Translational and post-translational studies relating to iron deficiency stress

Proteomic studies contribute new insight into the molecular mechanisms related to plant micronutrients on the translational, as well as the post-translational regulation. However, most of these studies were carried out in strategy I plants, such as Arabidopsis, sugar beet, cucumber, tomato, etc. Consistent with transcriptional regulation, the FRO2, IRT1, and AHA2 protein accumulation was also elevated in response to iron deficiency in Arabidopsis roots (Zargar *et al.*, 2015). In addition to iron uptake related proteins, carbohydrate metabolism, such as glycolysis and tricarboxylic acid (TCA) cycle, is actively regulated under iron deficiency. For example, enolases and fructose 1,6-bisphosphate aldolase protein levels

in glycolysis pathways increase in response to iron deficiency (Donnini *et al.*, 2010; Rellan-Alvarez *et al.*, 2010). The TCA cycle is a sequence of chemical reactions that produce ATP and reducing agent NADH and it also supports the production of organic acids such as citrate and malate, which could function as iron chelators (Mai and Bauer, 2016). Several enzymes in TCA cycle are elevated in the roots of sugar beet, tomato and cucumber in response to iron deficiency in roots (Donnini *et al.*, 2010; Li *et al.*, 2008; Lopez-Millan *et al.*, 2000b; Thimm *et al.*, 2001), which synchronizes with the increased transcription of genes encoding these enzymes as observed in this PhD study (Chapter 3).

Translational regulation of iron homeostasis in mammalian cells mainly rely on the iron responsive element (IRE)/iron regulatory protein (IRP) system, which control mRNA translation or stability of numerous iron metabolism related genes, such as *FERRITIN*, *FERROPORTIN* (*FPN*), *DIVALENT METAL TRANSPORTER 1* (*DMT1*), etc. However, plants modulate iron-deficiency response by post-translational regulation but not IRE/IRP mechanism (Wilkinson and Pantopoulos, 2014). As previously mentioned, transcription factor FIT targets iron acquisition-related genes, such as *FRO2* and *IRT1* genes. The accumulation of FIT is regulated by 26S proteasome mediated protein turnover (Sivitz *et al.*, 2011). Ethylene and NO are proposed to be iron-deficiency signaling molecules by reducing the proteosomal degradation of FIT (Lingam *et al.*, 2011; Meiser *et al.*, 2011). The accumulation of IRT1 protein is also post-translationally regulated. Constitutive degradation of IRT1 was suggested to be mediated by monoubiquitin-dependent endocytosis (Barberon *et al.*, 2011). The RING-type E3 ligases IRT1 DEGRADATION FACTOR1 (IDF1) interacts with IRT1 in the plasma membrane, and is one of the candidate functions in the ubiquitination process (Shin *et al.*, 2013). The recycling and prevention of the premature degradation of IRT1 might be regulated by the endosomal regulatory protein SORTING NEXIN1 (SNX1) (Ivanov *et al.*, 2014).

6.4 Metabolomic studies on plant iron-deficiency response

Metabolomic studies provide an opportunity for analyzing plants' metabolite production that is perturbed under iron deficiency. Previous studies demonstrated that the iron deficiency dynamically regulates the production of amino acids and TCA cycle metabolites. Gas chromatography–mass spectrometry (GC-MS) analysis of xylem sap metabolites in strategy I plants, such as tomato, lupine, and peach tree demonstrated reduced production of amino acids, N-related metabolites and carbohydrates, and increased production of TCA cycle

metabolites in response to iron deficiency. However, the iron-deficient leaf extracts of tomato, sugar beet, and peach showed increased production of amino acids, N-related metabolites, carbohydrates, and TCA cycle metabolites (Rellan-Alvarez *et al.*, 2011). Increase in amino acids, citrate, and phenolics have been reported in iron- deficient soybean root exudates (Zocchi *et al.*, 2007). However, enhanced accumulation of amino acids and phenolics, but decreased TCA cycle metabolites, such as citrate and malate, were observed in iron-deficient soybean leaf extracts (Lima *et al.*, 2014). Phenolic compounds coumarins, such as scopoletin, showed the strongest response to iron deficiency in Arabidopsis root exudates (Schmidt *et al.*, 2014). Specifically, the increased citrate production in iron deficient roots is in line with the accumulation of transcripts and proteins in the TCA cycle in the previous reports as well as in this PhD study (Donnini *et al.*, 2010; Li *et al.*, 2008; Lopez-Millan *et al.*, 2000b; Thimm *et al.*, 2001) (Chapter 3).

6.5 Thesis outlook

In my PhD study, expression pattern of iron homeostasis related endogenous genes was compared between iron biofortified transgenic rice (NFP) and its non-transgenic siblings, demonstrating that the overall gene expression was not altered. However, some phytosiderophore biosynthesis and transport-related genes were more sensitive in NFP plants when suffering from iron-deficiency stress. RNA sequencing and qRT-PCR approaches were utilized to obtain an overall, as well as targeted gene expression profiles, in response to iron and zinc deficiency in bread wheat roots, flag leaves, and grains. The results indicated that genes facilitating iron and zinc uptake, transport, storage and regulation were differentially expressed in response to iron- and zinc- deficiency stress.

RNA sequencing and qRT-PCR offers the opportunity to investigate gene expression perturbation on a transcriptional level. However, plant response to abiotic stress is not only regulated on the transcriptional level, but also controlled on the post-transcriptional and metabolite levels. Therefore, incorporating other 'Omics' studies such as proteomic and metabolomic studies together with the transcriptomic profiling could reveal systemic responses to iron and zinc deficiency. Such integrated studies could identify key factors that have stronger effects on the process of iron and zinc homeostasis. Based on the findings from this PhD work, further molecular experiments such as functional characterization and targeted validation of some key genes by full-length gene cloning, gene expression pattern and subcellular localization, protein–protein interaction and mutagenesis could be carried out.

Plant iron and zinc homeostasis involves a complex control of physiological, and developmental responses. It is necessary to link the knowledge of iron and zinc sensing and signaling to physiological and morphological changes. For example, the analysis of physiological responses to perturbations of phytohormones such as auxin, ethylene, cytokinin, jasmonate and nitric oxide (NO) could bridge the molecular responses and physiological reactions together. Further, developmental changes such as root architecture induced by micronutrient deficiency could also be studied.

Furthermore, the uptake and transport of iron and zinc is not independent from each other as well as from other divalent metals. Large numbers of transporters and chelators are unspecific to only one divalent metal. Iron or zinc deficiency stress may also affect the homeostasis of magnesium, manganese, copper, nickel and cadmium. Genetic engineering projects aimed at iron and zinc biofortification should take this factor into consideration. Therefore, studies aimed at revelation of the crosstalk between the divalent metals is necessary for better understanding of the regulation network of metal homeostasis, as well as for the future crop biofortification projects.

7 REFERENCES

Agarwal, S., Mangrauthia, S.K. and Sarla, N. (2015) Expression profiling of iron deficiency responsive microRNAs and gene targets in rice seedlings of Madhukar x Swarna recombinant inbred lines with contrasting levels of iron in seeds. *Plant Soil* **396**, 137-150.

Alloway, B.J. (2008) *Zinc in soils and crop nutrition (Second Edition)*:International Zinc Association (IZA), Brussels, and International Fertilizer Industry Association (IFA), Paris.

Alvarez-Fernandez, A., Diaz-Benito, P., Abadia, A., Lopez-Millan, A.F. and Abadia, J. (2014) Metal species involved in long distance metal transport in plants. *Front Plant Sci* **5**, 105.

Aoyama, T., Kobayashi, T., Takahashi, M., Nagasaka, S., Usuda, K., Kakei, Y., Ishimaru, Y., Nakanishi, H., Mori, S. and Nishizawa, N.K. (2009) OsYSL18 is a rice iron(III)-deoxymugineic acid transporter specifically expressed in reproductive organs and phloem of lamina joints. *Plant Mol Biol* **70**, 681-692.

Ariga, T., Hazama, K., Yanagisawa, S. and Yoneyama, T. (2014) Chemical forms of iron in xylem sap from graminaceous and non-graminaceous plants. *Soil Sci Plant Nutr* **60**, 460-469.

Arrivault, S., Senger, T. and Kramer, U. (2006) The Arabidopsis metal tolerance protein AtMTP3 maintains metal homeostasis by mediating Zn exclusion from the shoot under Fe deficiency and Zn oversupply. *Plant J* **46**, 861-879.

Assuncao, A.G., Herrero, E., Lin, Y.F., Huettel, B., Talukdar, S., Smaczniak, C., Immink, R.G., van Eldik, M., Fiers, M., Schat, H. and Aarts, M.G. (2010) Arabidopsis thaliana transcription factors bZIP19 and bZIP23 regulate the adaptation to zinc deficiency. *PNAS* **107**, 10296-10301.

Balk, J. and Schaedler, T.A. (2014) Iron cofactor assembly in plants. *Annu Rev Plant Biol* **65**, 125-153.

Barberon, M., Zelazny, E., Robert, S., Conejero, G., Curie, C., Friml, J. and Vert, G. (2011) Monoubiquitin-dependent endocytosis of the iron-regulated transporter 1 (IRT1) transporter controls iron uptake in plants. *PNAS* **108**, E450-458.

Barker, A.V. and Stratton, M.L. (2015) Iron. In: *Handbook of Plant Nutrition, Second Edition* pp. 399-426. CRC Press.

Bashir, K., Inoue, H., Nagasaka, S., Takahashi, M., Nakanishi, H., Mori, S. and Nishizawa, N.K. (2006) Cloning and characterization of deoxymugineic acid synthase genes from graminaceous plants. *J Biol Chem* **281**, 32395-32402.

Bashir, K., Ishimaru, Y. and Nishizawa, N.K. (2010) Iron uptake and loading into rice grains. *Rice* **3**, 122-130.

Bashir, K., Ishimaru, Y. and Nishizawa, N.K. (2012) Molecular mechanisms of zinc uptake and translocation in rice. *Plant Soil* **361**, 189-201.

Bashir, K., Ishimaru, Y., Shimo, H., Nagasaka, S., Fujimoto, M., Takanashi, H., Tsutsumi, N., An, G., Nakanishi, H. and Nishizawa, N.K. (2011) The rice mitochondrial iron transporter is essential for plant growth. *Nat Commun* **2**.

Bashir, K. and Nishizawa, N.K. (2006) Deoxymugineic acid synthase: a gene important for Fe-acquisition and homeostasis. *Plant Signal Behav* **1**, 290-292.

Boccio, J.R. and Iyengar, V. (2003) Iron deficiency: causes, consequences, and strategies to overcome this nutritional problem. *Biol Trace Elem Res* **94**, 1-32.

Boonyaves, K., Gruissem, W. and Bhullar, N.K. (2016) NOD promoter-controlled AtIRT1 expression functions synergistically with NAS and FERRITIN genes to increase iron in rice grains. *Plant Mol Biol* **90**, 207-215.

Borrill, P., Connorton, J.M., Balk, J., Miller, A.J., Sanders, D. and Uauy, C. (2014) Biofortification of wheat grain with iron and zinc: integrating novel genomic resources and knowledge from model crops. *Front Plant Sci* **5**.

Briat, J.F., Duc, C., Ravet, K. and Gaymard, F. (2010) Ferritins and iron storage in plants. *Biochim Biophys Acta* **1800**, 806-814.

Brinch-Pedersen, H., Sorensen, L.D. and Holm, P.B. (2002) Engineering crop plants: getting a handle on phosphate. *Trends Plant Sci* **7**, 118-125.

Broadley, M., Brown, P., Cakmak, I., Rengel, Z. and Zhao, F. (2012) Function of nutrients: micronutrients. In: *Marschner's Mineral Nutrition of Higher Plants (Third Edition)* pp. 191-248. San Diego: Academic Press.

Bruggemann, W., Maaskantel, K. and Moog, P.R. (1993) Iron uptake by leaf mesophyll-cells - the role of the plasma membrane-bound ferric-chelate reductase. *Planta* **190**, 151-155.

Brumbarova, T., Bauer, P. and Ivanov, R. (2015) Molecular mechanisms governing Arabidopsis iron uptake. *Trends Plant Sci* **20**, 124-133.

Buckhout, T.J. and Schmidt, W. (2013) Iron in Plants. In: *eLS*. John Wiley & Sons, Ltd.

Buckhout, T.J., Yang, T.J. and Schmidt, W. (2009) Early iron-deficiency-induced transcriptional changes in Arabidopsis roots as revealed by microarray analyses. *BMC Genomics* **10**, 147.

Buhtz, A., Pieritz, J., Springer, F. and Kehr, J. (2010) Phloem small RNAs, nutrient stress responses, and systemic mobility. *BMC Plant Biol* **10**, 64.

Cakmak, I. (2008) Enrichment of cereal grains with zinc: Agronomic or genetic biofortification? *Plant Soil* **302**, 1-17.

Cakmak, I., Gulut, K.Y., Marschner, H. and Graham, R.D. (1994) Effect of zinc and iron-deficiency on phytosiderophore release in wheat genotypes differing in zinc efficiency. *J Plant Nutr* **17**, 1-17.

Cakmak, I., Sari, N., Marschner, H., Ekiz, H., Kalayci, M., Yilmaz, A. and Braun, H.J. (1996) Phytosiderophore release in bread and durum wheat genotypes differing in zinc efficiency. *Plant Soil* **180**, 183-189.

Chen, L.G., Song, Y., Li, S.J., Zhang, L.P., Zou, C.S. and Yu, D.Q. (2012) The role of WRKY transcription factors in plant abiotic stresses. *Bba-Gene Regul Mech* **1819**, 120-128.

Clemens, S., Deinlein, U., Ahmadi, H., Horeth, S. and Uraguchi, S. (2013) Nicotianamine is a major player in plant Zn homeostasis. *BioMetals* **26**, 623-632.

Colangelo, E.P. and Guerinot, M.L. (2004) The essential basic helix-loop-helix protein FIT1 is required for the iron deficiency response. *Plant Cell* **16**, 3400-3412.

Connolly, E.L., Fett, J.P. and Guerinot, M.L. (2002) Expression of the IRT1 metal transporter is controlled by metals at the levels of transcript and protein accumulation. *Plant Cell* **14**, 1347-1357.

Curie, C., Cassin, G., Couch, D., Divol, F., Higuchi, K., Jean, M., Misson, J., Schikora, A., Czernic, P. and Mari, S. (2009) Metal movement within the plant: contribution of nicotianamine and yellow stripe 1-like transporters. *Ann Bot* **103**, 1-11.

Curie, C., Panaviene, Z., Loulergue, C., Dellaporta, S.L., Briat, J.F. and Walker, E.L. (2001) Maize yellow stripe1 encodes a membrane protein directly involved in Fe(III) uptake. *Nature* **409**, 346-349.

Das, S. and Green, A. (2016) Zinc in crops and human health. In: *Biofortification of Food Crops* (Singh, U., Praharaj, S.C., Singh, S.S. and Singh, P.N. eds), pp. 31-40. New Delhi: Springer India.

Deinlein, U., Weber, M., Schmidt, H., Rensch, S., Trampczynska, A., Hansen, T.H., Husted, S., Schjoerring, J.K., Talke, I.N., Kramer, U. and Clemens, S. (2012) Elevated

nicotianamine levels in Arabidopsis halleri roots play a key role in zinc hyperaccumulation. *Plant Cell* **24**, 708-723.

Desbrosses-Fonrouge, A.G., Voigt, K., Schroder, A., Arrivault, S., Thomine, S. and Kramer, U. (2005) Arabidopsis thaliana MTP1 is a Zn transporter in the vacuolar membrane which mediates Zn detoxification and drives leaf Zn accumulation. *FEBS Lett* **579**, 4165-4174.

DiDonato, R.J., Jr., Roberts, L.A., Sanderson, T., Eisley, R.B. and Walker, E.L. (2004) Arabidopsis Yellow Stripe-Like2 (YSL2): a metal-regulated gene encoding a plasma membrane transporter of nicotianamine-metal complexes. *Plant J* **39**, 403-414.

Divol, F., Couch, D., Conejero, G., Roschzttardtz, H., Mari, S. and Curie, C. (2013) The Arabidopsis YELLOW STRIPE LIKE4 and 6 transporters control iron release from the chloroplast. *Plant Cell* **25**, 1040-1055.

Donnini, S., Prinsi, B., Negri, A.S., Vigani, G., Espen, L. and Zocchi, G. (2010) Proteomic characterization of iron deficiency responses in Cucumis sativus L. roots. *BMC Plant Biol* **10**, 268.

Du, J., Huang, Z.A., Wang, B.A., Sun, H., Chen, C.L., Ling, H.Q. and Wu, H.L. (2015) SlbHLH068 interacts with FER to regulate the iron-deficiency response in tomato. *Ann Bot* **116**, 23-34.

Ducos, E., Fraysse, A.S. and Boutry, M. (2005) NtPDR3, an iron-deficiency inducible ABC transporter in Nicotiana tabacum. *FEBS Lett* **579**, 6791-6795.

Durmaz, E., Coruh, C., Dinler, G., Grusak, M.A., Peleg, Z., Saranga, Y., Fahima, T., Yazici, A., Ozturk, L., Cakmak, I. and Budak, H. (2011) Expression and cellular localization of ZIP1 transporter under zinc deficiency in wild emmer wheat. *Plant Mol Biol Report* **29**, 582-596.

Durrett, T.P., Gassmann, W. and Rogers, E.E. (2007) The FRD3-mediated efflux of citrate into the root vasculature is necessary for efficient iron translocation. *Plant Physiol* **144**, 197-205.

Duy, D., Stube, R., Wanner, G. and Philippar, K. (2011) The chloroplast permease PIC1 regulates plant growth and development by directing homeostasis and transport of iron. *Plant Physiol* **155**, 1709-1722.

Duy, D., Wanner, G., Meda, A.R., von Wiren, N., Soll, J. and Philippar, K. (2007) PIC1, an ancient permease in Arabidopsis chloroplasts, mediates iron transport. *Plant Cell* **19**, 986-1006.

Fan, H., Zhang, Z., Wang, N., Cui, Y., Sun, H., Liu, Y., Wu, H., Zheng, S., Bao, S. and Ling, H.Q. (2014) SKB1/PRMT5-mediated histone H4R3 dimethylation of Ib subgroup bHLH genes negatively regulates iron homeostasis in Arabidopsis thaliana. *Plant J* **77**, 209-221.

Gillies, S.A., Futardo, A. and Henry, R.J. (2012) Gene expression in the developing aleurone and starchy endosperm of wheat. *Plant Biotechnol J* **10**, 668-679.

Gong, X., Guo, C.H., Terachi, T., Cai, H.S. and Yu, D.S. (2015) Tobacco PIC1 mediates iron transport and regulates chloroplast development. *Plant Mol Biol Report* **33**, 401-413.

Goto, F., Yoshihara, T., Shigemoto, N., Toki, S. and Takaiwa, F. (1999) Iron fortification of rice seed by the soybean ferritin gene. *Nat Biotechnol* **17**, 282-286.

Graham, R.D. (2008) Micronutrient deficiencies in crops and their global significance. In: *Micronutrient Deficiencies in Global Crop Production* (Alloway, B.J. ed) pp. 41-61. Dordrecht: Springer Netherlands.

Grillet, L., Ouerdane, L., Flis, P., Hoang, M.T.T., Isaure, M.P., Lobinski, R., Curie, C. and Mari, S. (2014) Ascorbate efflux as a new strategy for iron reduction and transport in plants. *J Biol Chem* **289**, 2515-2525.

Grotz, N., Fox, T., Connolly, E., Park, W., Guerinot, M.L. and Eide, D. (1998) Identification of a family of zinc transporter genes from Arabidopsis that respond to zinc deficiency. *PNAS* **95**, 7220-7224.

Guerinot, M.L. (2000) The ZIP family of metal transporters. *BBA. Biomembranes* **1465**, 190-198.

Guerinot, M.L. and Eide, D. (1999) Zeroing in on zinc uptake in yeast and plants. *Curr Opin Plant Biol* **2**, 244-249.

Guo, W.J., Meetam, M. and Goldsbrough, P.B. (2008) Examining the specific contributions of individual Arabidopsis metallothioneins to copper distribution and metal tolerance. *Plant Physiol* **146**, 1697-1706.

Gupta, N., Ram, H. and Kumar, B. (2016) Mechanism of zinc absorption in plants: uptake, transport, translocation and accumulation. *Rev Environ Sci Bio* **15**, 89-109.

Gupta, P.K., Kulwal, P.L. and Rustgi, S. (2005) Wheat cytogenetics in the genomics era and its relevance to breeding. *Cytogenet Genome Res* **109**, 315-327.

Hamer, D.H. (1986) Metallothionein. *Annu Rev Biochem* **55**, 913-951.

Hansch, R. and Mendel, R.R. (2009) Physiological functions of mineral micronutrients (Cu, Zn, Mn, Fe, Ni, Mo, B, Cl). *Curr Opin Plant Biol* **12**, 259-266.

Harrison, P.M. and Arosio, P. (1996) Ferritins: Molecular properties, iron storage function and cellular regulation. *Bba-Bioenergetics* **1275**, 161-203.

Haydon, M.J. and Cobbett, C.S. (2007) A novel major facilitator superfamily protein at the tonoplast influences zinc tolerance and accumulation in Arabidopsis. *Plant Physiol* **143**, 1705-1719.

Haydon, M.J., Kawachi, M., Wirtz, M., Hillmer, S., Hell, R. and Kramer, U. (2012) Vacuolar nicotianamine has critical and distinct roles under iron deficiency and for zinc sequestration in Arabidopsis. *Plant Cell* **24**, 724-737.

Hegelund, J.N., Schiller, M., Kichey, T., Hansen, T.H., Pedas, P., Husted, S. and Schjoerring, J.K. (2012) Barley metallothioneins: MT3 and MT4 are localized in the grain aleurone layer and show differential zinc binding. *Plant Physiol* **159**, 1125-1137.

Hindt, M.N. and Guerinot, M.L. (2012) Getting a sense for signals: Regulation of the plant iron deficiency response. *Bba-Mol Cell Res* **1823**, 1521-1530.

Hopkins, B.G., Whitney, D.A., Lamond, R.E. and Jolley, V.D. (1998) Phytosiderophore release by Sorghum, wheat, and corn under zinc deficiency. *J Plant Nutr* **21**, 2623-2637.

Huang, D.Q. and Dai, W.H. (2015) Molecular characterization of the basic helix-loop-helix (bHLH) genes that are differentially expressed and induced by iron deficiency in Populus. *Plant Cell Rep* **34**, 1211-1224.

Hurrell, R. and Egli, I. (2010) Iron bioavailability and dietary reference values. *Am J Clin Nutr* **91**, 1461S-1467S.

Hussain, D., Haydon, M.J., Wang, Y., Wong, E., Sherson, S.M., Young, J., Camakaris, J., Harper, J.F. and Cobbett, C.S. (2004) P-type ATPase heavy metal transporters with roles in essential zinc homeostasis in Arabidopsis. *Plant Cell* **16**, 1327-1339.

Inaba, S., Kurata, R., Kobayashi, M., Yamagishi, Y., Mori, I., Ogata, Y. and Fukao, Y. (2015) Identification of putative target genes of bZIP19, a transcription factor essential for Arabidopsis adaptation to Zn deficiency in roots. *Plant J* **84**, 323-334.

Inoue, H., Higuchi, K., Takahashi, M., Nakanishi, H., Mori, S. and Nishizawa, N.K. (2003) Three rice nicotianamine synthase genes, OsNAS1, OsNAS2, and OsNAS3 are expressed in cells involved in long-distance transport of iron and differentially regulated by iron. *Plant J* **36**, 366-381.

Inoue, H., Kobayashi, T., Nozoye, T., Takahashi, M., Kakei, Y., Suzuki, K., Nakazono, M., Nakanishi, H., Mori, S. and Nishizawa, N.K. (2009) Rice OsYSL15 is an iron-regulated iron(III)-deoxymugineic acid transporter expressed in the roots and is

essential for iron uptake in early growth of the seedlings. *J Biol Chem* **284**, 3470-3479.

Inoue, H., Takahashi, M., Kobayashi, T., Suzuki, M., Nakanishi, H., Mori, S. and Nishizawa, N.K. (2008) Identification and localisation of the rice nicotianamine aminotransferase gene OsNAAT1 expression suggests the site of phytosiderophore synthesis in rice. *Plant Mol Biol* **66**, 193-203.

Institute-of-Medicine (2013) Food and nutrition board, dietary reference intakes (DRIs): estimated average requirements. Available online at: http://www.iom.edu/Activities/Nutrition/SummaryDRIs/~/media/Files/Activity Files/Nutrition/DRIs/New Material/5DRI Values SummaryTables 14.pdf (Accessed February 20, 2013).

IRRI (2016) Trends in global rice consumption. Available online at: http://irri.org/rice-today/trends-in-global-rice-consumption (Accessed June 20, 2016).

Ishimaru, Y., Bashir, K., Fujimoto, M., An, G., Itai, R.N., Tsutsumi, N., Nakanishi, H. and Nishizawa, N.K. (2009) Rice-specific mitochondrial iron-regulated gene (MIR) plays an important role in iron Homeostasis. *Mol Plant* **2**, 1059-1066.

Ishimaru, Y., Masuda, H., Bashir, K., Inoue, H., Tsukamoto, T., Takahashi, M., Nakanishi, H., Aoki, N., Hirose, T., Ohsugi, R. and Nishizawa, N.K. (2010) Rice metal-nicotianamine transporter, OsYSL2, is required for the long-distance transport of iron and manganese. *Plant J* **62**, 379-390.

Ishimaru, Y., Masuda, H., Suzuki, M., Bashir, K., Takahashi, M., Nakanishi, H., Mori, S. and Nishizawa, N.K. (2007) Overexpression of the OsZIP4 zinc transporter confers disarrangement of zinc distribution in rice plants. *J Exp Bot* **58**, 2909-2915.

Ishimaru, Y., Suzuki, M., Kobayashi, T., Takahashi, M., Nakanishi, H., Mori, S. and Nishizawa, N.K. (2005) OsZIP4, a novel zinc-regulated zinc transporter in rice. *J Exp Bot* **56**, 3207-3214.

Ishimaru, Y., Suzuki, M., Tsukamoto, T., Suzuki, K., Nakazono, M., Kobayashi, T., Wada, Y., Watanabe, S., Matsuhashi, S., Takahashi, M., Nakanishi, H., Mori, S. and Nishizawa, N.K. (2006) Rice plants take up iron as an Fe3+-phytosiderophore and as Fe2+. *Plant J* **45**, 335-346.

Ivanov, R., Brumbarova, T., Blum, A., Jantke, A.M., Fink-Straube, C. and Bauer, P. (2014) SORTING NEXIN1 is required for modulating the trafficking and stability of the Arabidopsis IRON-REGULATED TRANSPORTER1. *Plant Cell* **26**, 1294-1307.

IWGSC (2014) A chromosome-based draft sequence of the hexaploid bread wheat (Triticum aestivum) genome. *Science* **345**, 1251788.

Jeong, J., Cohu, C., Kerkeb, L., Pilon, M., Connolly, E.L. and Guerinot, M.L. (2008) Chloroplast Fe(III) chelate reductase activity is essential for seedling viability under iron limiting conditions. *PNAS* **105**, 10619-10624.

Jeong, J. and Guerinot, M.L. (2009) Homing in on iron homeostasis in plants. *Trends Plant Sci* **14**, 280-285.

Jin, F., Frohman, C., Thannhauser, T.W., Welch, R.M. and Glahn, R.P. (2009) Effects of ascorbic acid, phytic acid and tannic acid on iron bioavailability from reconstituted ferritin measured by an in vitro digestion-Caco-2 cell model. *Br J Nutr* **101**, 972-981.

Johnson, A.A., Kyriacou, B., Callahan, D.L., Carruthers, L., Stangoulis, J., Lombi, E. and Tester, M. (2011) Constitutive overexpression of the OsNAS gene family reveals single-gene strategies for effective iron- and zinc-biofortification of rice endosperm. *PLoS One* **6**, e24476.

Kakei, Y., Ishimaru, Y., Kobayashi, T., Yamakawa, T., Nakanishi, H. and Nishizawa, N.K. (2012) OsYSL16 plays a role in the allocation of iron. *Plant Mol Biol* **79**, 583-594.

Kakei, Y., Yamaguchi, I., Kobayashi, T., Takahashi, M., Nakanishi, H., Yamakawa, T. and Nishizawa, N.K. (2009) A highly sensitive, quick and simple quantification method

for nicotianamine and 2-deoxymugineic acid from minimum samples using LC/ESI-TOF-MS achieves functional analysis of these components in plants. *Plant Cell Physiol* **50**, 1988-1993.

Kanazawa, K., Higuchi, K., Nishizawa, N.K., Fushiya, S., Chino, M. and Mori, S. (1994) Nicotianamine aminotransferase activities are correlated to the phytosiderophore secretions under Fe-deficient conditions in gramineae. *J Exp Bot* **45**, 1903-1906.

Kerkeb, L. and Connolly, E.L. (2006) Iron transport and metabolism in plants. *Genet Eng (N Y)* **27**, 119-140.

Kim, S.A. and Guerinot, M.L. (2007) Mining iron: iron uptake and transport in plants. *FEBS Lett* **581**, 2273-2280.

Kim, Y.Y., Choi, H., Segami, S., Cho, H.T., Martinoia, E., Maeshima, M. and Lee, Y. (2009) AtHMA1 contributes to the detoxification of excess Zn(II) in Arabidopsis. *Plant J* **58**, 737-753.

Kobae, Y., Uemura, T., Sato, M.H., Ohnishi, M., Mimura, T., Nakagawa, T. and Maeshima, M. (2004) Zinc transporter of Arabidopsis thaliana AtMTP1 is localized to vacuolar membranes and implicated in zinc homeostasis. *Plant Cell Physiol* **45**, 1749-1758.

Kobayashi, T., Itai, R.N., Aung, M.S., Senoura, T., Nakanishi, H. and Nishizawa, N.K. (2012) The rice transcription factor IDEF1 directly binds to iron and other divalent metals for sensing cellular iron status. *Plant J* **69**, 81-91.

Kobayashi, T., Itai, R.N., Ogo, Y., Kakei, Y., Nakanishi, H., Takahashi, M. and Nishizawa, N.K. (2009) The rice transcription factor IDEF1 is essential for the early response to iron deficiency, and induces vegetative expression of late embryogenesis abundant genes. *Plant J* **60**, 948-961.

Kobayashi, T., Nakanishi, H. and Nishizawa, N.K. (2010a) Dual regulation of iron deficiency response mediated by the transcription factor IDEF1. *Plant Signal Behav* **5**, 157-159.

Kobayashi, T., Nakanishi, H. and Nishizawa, N.K. (2010b) Recent insights into iron homeostasis and their application in graminaceous crops. *P Jpn Acad B-Phys* **86**, 900-913.

Kobayashi, T. and Nishizawa, N.K. (2012) Iron uptake, translocation, and regulation in higher plants. *Annu Rev Plant Biol* **63**, 131-152.

Kobayashi, T., Ogo, Y., Aung, M.S., Nozoye, T., Itai, R.N., Nakanishi, H., Yamakawa, T. and Nishizawa, N.K. (2010c) The spatial expression and regulation of transcription factors IDEF1 and IDEF2. *Ann Bot* **105**, 1109-1117.

Kobayashi, T., Ogo, Y., Itai, R.N., Nakanishi, H., Takahashi, M., Mori, S. and Nishizawa, N.K. (2007) The transcription factor IDEF1 regulates the response to and tolerance of iron deficiency in plants. *PNAS* **104**, 19150-19155.

Kobayashi, T., Suzuki, M., Inoue, H., Itai, R.N., Takahashi, M., Nakanishi, H., Mori, S. and Nishizawa, N.K. (2005) Expression of iron-acquisition-related genes in iron-deficient rice is co-ordinately induced by partially conserved iron-deficiency-responsive elements. *J Exp Bot* **56**, 1305-1316.

Koike, S., Inoue, H., Mizuno, D., Takahashi, M., Nakanishi, H., Mori, S. and Nishizawa, N.K. (2004) OsYSL2 is a rice metal-nicotianamine transporter that is regulated by iron and expressed in the phloem. *Plant J* **39**, 415-424.

Kong, W.W. and Yang, Z.M. (2010) Identification of iron-deficiency responsive microRNA genes and cis-elements in Arabidopsis. *Plant Physiol Biochem* **48**, 153-159.

Korshunova, Y.O., Eide, D., Clark, W.G., Guerinot, M.L. and Pakrasi, H.B. (1999) The IRT1 protein from Arabidopsis thaliana is a metal transporter with a broad substrate range. *Plant Mol Biol* **40**, 37-44.

Lane, B., Kajioka, R. and Kennedy, T. (1987) The wheat-germ Ec protein is a zinc-containing metallothionein. *Biochem Cell Biol* **65**, 1001-1005.

Lanquar, V., Lelievre, F., Bolte, S., Hames, C., Alcon, C., Neumann, D., Vansuyt, G., Curie, C., Schroder, A., Kramer, U., Barbier-Brygoo, H. and Thomine, S. (2005) Mobilization of vacuolar iron by AtNRAMP3 and AtNRAMP4 is essential for seed germination on low iron. *EMBO J* **24**, 4041-4051.

Lee, S. and An, G. (2009) Over-expression of OsIRT1 leads to increased iron and zinc accumulations in rice. *Plant Cell Environ* **32**, 408-416.

Lee, S., Chiecko, J.C., Kim, S.A., Walker, E.L., Lee, Y., Guerinot, M.L. and An, G. (2009a) Disruption of OsYSL15 leads to iron inefficiency in rice plants. *Plant Physiol* **150**, 786-800.

Lee, S., Jeon, J.S. and An, G. (2012a) Iron homeostasis and fortification in rice. *Journal of Plant Biology* **55**, 261-267.

Lee, S., Jeon, U.S., Lee, S.J., Kim, Y.K., Persson, D.P., Husted, S., Schjorring, J.K., Kakei, Y., Masuda, H., Nishizawa, N.K. and An, G. (2009b) Iron fortification of rice seeds through activation of the nicotianamine synthase gene. *PNAS* **106**, 22014-22019.

Lee, S., Jeong, H.J., Kim, S.A., Lee, J., Guerinot, M.L. and An, G. (2010a) OsZIP5 is a plasma membrane zinc transporter in rice. *Plant Mol Biol* **73**, 507-517.

Lee, S., Kim, S.A., Lee, J., Guerinot, M.L. and An, G. (2010b) Zinc deficiency-inducible OsZIP8 encodes a plasma membrane-localized zinc transporter in rice. *Mol Cells* **29**, 551-558.

Lee, S., Kim, Y.S., Jeon, U.S., Kim, Y.K., Schjoerring, J.K. and An, G. (2012b) Activation of rice nicotianamine synthase 2 (OsNAS2) enhances iron availability for biofortification. *Mol Cells* **33**, 269-275.

Li, H.Z., Gao, X., Li, X.Y., Chen, Q.J., Dong, J. and Zhao, W.C. (2013a) Evaluation of assembly strategies using RNA-seq data associated with grain development of wheat (Triticum aestivum L.). *PLoS One* **8**, e83530.

Li, J., Wu, X.D., Hao, S.T., Wang, X.J. and Ling, H.Q. (2008) Proteomic response to iron deficiency in tomato root. *Proteomics* **8**, 2299-2311.

Li, S., Zhou, X., Huang, Y., Zhu, L., Zhang, S., Zhao, Y., Guo, J., Chen, J. and Chen, R. (2013b) Identification and characterization of the zinc-regulated transporters, iron-regulated transporter-like protein (ZIP) gene family in maize. *BMC Plant Biol* **13**, 114.

Li, X., Zhang, H., Ai, Q., Liang, G. and Yu, D. (2016) Two bHLH transcription factors, bHLH34 and bHLH104, regulate iron homeostasis in Arabidopsis thaliana. *Plant Physiol* **170**, 2478-2493.

Li, Y., Wang, N., Zhao, F.T., Song, X.J., Yin, Z.H., Huang, R. and Zhang, C.Q. (2014) Changes in the transcriptomic profiles of maize roots in response to iron-deficiency stress. *Plant Mol Biol* **85**, 349-363.

Li, Y., Zhang, Y., Shi, D., Liu, X., Qin, J., Ge, Q., Xu, L., Pan, X., Li, W., Zhu, Y. and Xu, J. (2013c) Spatial-temporal analysis of zinc homeostasis reveals the response mechanisms to acute zinc deficiency in Sorghum bicolor. *New Phytol* **200**, 1102-1115.

Lichtenthaler, H.K. and Buschmann, C. (2001) Chlorophylls and carotenoids: measurement and characterization by UV-VIS spectroscopy. In: *Current Protocols in Food Analytical Chemistry*. John Wiley & Sons, Inc.

Lima, M.R., Diaz, S.O., Lamego, I., Grusak, M.A., Vasconcelos, M.W. and Gil, A.M. (2014) Nuclear magnetic resonance metabolomics of iron deficiency in soybean leaves. *J Proteome Res* **13**, 3075-3087.

Lin, Y.F., Liang, H.M., Yang, S.Y., Boch, A., Clemens, S., Chen, C.C., Wu, J.F., Huang, J.L. and Yeh, K.C. (2009) Arabidopsis IRT3 is a zinc-regulated and plasma membrane localized zinc/iron transporter. *New Phytol* **182**, 392-404.

Ling, H.Q., Bauer, P., Bereczky, Z., Keller, B. and Ganal, M. (2002) The tomato fer gene encoding a bHLH protein controls iron-uptake responses in roots. *PNAS* **99**, 13938-13943.

Lingam, S., Mohrbacher, J., Brumbarova, T., Potuschak, T., Fink-Straube, C., Blondet, E., Genschik, P. and Bauer, P. (2011) Interaction between the bHLH transcription factor FIT and ETHYLENE INSENSITIVE3/ETHYLENE INSENSITIVE3-LIKE1 reveals molecular linkage between the regulation of iron acquisition and ethylene signaling in Arabidopsis. *Plant Cell* **23**, 1815-1829.

Lok, H.C., Rahmanto, Y.S., Hawkins, C.L., Kalinowski, D.S., Morrow, C.S., Townsend, A.J., Ponka, P. and Richardson, D.R. (2012) Nitric oxide storage and transport in cells are mediated by glutathione S-transferase P1-1 and multidrug resistance protein 1 via dinitrosyl iron complexes. *J Biol Chem* **287**, 607-618.

Lonnerdal, B., Bryant, A., Liu, X. and Theil, E.C. (2006) Iron absorption from soybean ferritin in nonanemic women. *Am J Clin Nutr* **83**, 103-107.

Lopez-Millan, A.F., Ellis, D.R. and Grusak, M.A. (2004) Identification and characterization of several new members of the ZIP family of metal ion transporters in Medicago truncatula. *Plant Mol Biol* **54**, 583-596.

Lopez-Millan, A.F., Morales, F., Abadia, A. and Abadia, J. (2000a) Effects of iron deficiency on the composition of the leaf apoplastic fluid and xylem sap in sugar beet. Implications for iron and carbon transport. *Plant Physiol* **124**, 873-884.

Lopez-Millan, A.F., Morales, F., Andaluz, S., Gogorcena, Y., Abadia, A., De Las Rivas, J. and Abadia, J. (2000b) Responses of sugar beet roots to iron deficiency. Changes in carbon assimilation and oxygen use. *Plant Physiol* **124**, 885-898.

Lucca, P., Hurrell, R. and Potrykus, I. (2001) Genetic engineering approaches to improve the bioavailability and the level of iron in rice grains. *Theor Appl Genet* **102**, 392-397.

Ma, J.F., Shinada, T., Matsuda, C. and Nomoto, K. (1995) Biosynthesis of phytosiderophores, mugineic acids, associated with methionine cycling. *J Biol Chem* **270**, 16549-16554.

Ma, J.F., Ueno, H., Ueno, D., Rombolà, A.D. and Iwashita, T. (2003) Characterization of phytosiderophore secretion under Fe deficiency stress in Festuca rubra. *Plant Soil* **256**, 131-137.

Mai, H.-J. and Bauer, P. (2016) From the proteomic point of view: Integration of adaptive changes to iron deficiency in plants. *Curr Plant Biol* **5**, 45-56.

Marcussen, T., Sandve, S.R., Heier, L., Spannagl, M., Pfeifer, M., Jakobsen, K.S., Wulff, B.B., Steuernagel, B., Mayer, K.F. and Olsen, O.A. (2014) Ancient hybridizations among the ancestral genomes of bread wheat. *Science* **345**, 1250092.

Masuda, H., Ishimaru, Y., Aung, M.S., Kobayashi, T., Kakei, Y., Takahashi, M., Higuchi, K., Nakanishi, H. and Nishizawa, N.K. (2012) Iron biofortification in rice by the introduction of multiple genes involved in iron nutrition. *Sci Rep* **2**, 543.

Meiser, J., Lingam, S. and Bauer, P. (2011) Posttranslational regulation of the iron deficiency basic helix-loop-helix transcription factor FIT is affected by iron and nitric oxide. *Plant Physiol* **157**, 2154-2166.

Menguer, P.K., Farthing, E., Peaston, K.A., Ricachenevsky, F.K., Fett, J.P. and Williams, L.E. (2013) Functional analysis of the rice vacuolar zinc transporter OsMTP1. *J Exp Bot* **64**, 2871-2883.

Mhatre, M., Srinivas, L. and Ganapathi, T.R. (2011) Enhanced iron and zinc accumulation in genetically engineered pineapple plants using soybean ferritin gene. *Biol Trace Elem Res* **144**, 1219-1228.

Milner, M.J., Seamon, J., Craft, E. and Kochian, L.V. (2013) Transport properties of members of the ZIP family in plants and their role in Zn and Mn homeostasis. *J Exp Bot* **64**, 369-381.

Moran Lauter, A.N., Peiffer, G.A., Yin, T., Whitham, S.A., Cook, D., Shoemaker, R.C. and Graham, M.A. (2014) Identification of candidate genes involved in early iron deficiency chlorosis signaling in soybean (Glycine max) roots and leaves. *BMC Genomics* **15**, 702.

Moreau, S., Thomson, R.M., Kaiser, B.N., Trevaskis, B., Guerinot, M.L., Udvardi, M.K., Puppo, A. and Day, D.A. (2002) GmZIP1 encodes a symbiosis-specific zinc transporter in soybean. *J Biol Chem* **277**, 4738-4746.

Morel, M., Crouzet, J., Gravot, A., Auroy, P., Leonhardt, N., Vavasseur, A. and Richaud, P. (2009) AtHMA3, a P1B-ATPase allowing Cd/Zn/Co/Pb vacuolar storage in Arabidopsis. *Plant Physiol* **149**, 894-904.

Morrissey, J., Baxter, I.R., Lee, J., Li, L.T., Lahner, B., Grotz, N., Kaplan, J., Salt, D.E. and Guerinot, M.L. (2009) The ferroportin metal efflux proteins function in iron and cobalt homeostasis in Arabidopsis. *Plant Cell* **21**, 3326-3338.

Morrissey, J. and Guerinot, M.L. (2009) Iron uptake and transport in plants: the good, the bad, and the ionome. *Chem Rev* **109**, 4553-4567.

Murakami, T., Ise, K., Hayakawa, M., Kamei, S. and Takagi, S.I. (1989) Stabilities of metal-complexes of mugineic acids and their specific affinities for iron(III). *Chem Lett*, 2137-2140.

Murata, Y., Ma, J.F., Yamaji, N., Ueno, D., Nomoto, K. and Iwashita, T. (2006) A specific transporter for iron(III)-phytosiderophore in barley roots. *Plant J* **46**, 563-572.

Nagasaka, S., Takahashi, M., Nakanishi-Itai, R., Bashir, K., Nakanishi, H., Mori, S. and Nishizawa, N.K. (2009) Time course analysis of gene expression over 24 hours in Fe-deficient barley roots. *Plant Mol Biol* **69**, 621-631.

Nagy, R., Grob, H., Weder, B., Green, P., Klein, M., Frelet-Barrand, A., Schjoerring, J.K., Brearley, C. and Martinoia, E. (2009) The Arabidopsis ATP-binding cassette protein AtMRP5/AtABCC5 is a high affinity inositol hexakisphosphate transporter involved in guard cell signaling and phytate storage. *J Biol Chem* **284**, 33614-33622.

Nakanishi, H., Yamaguchi, H., Sasakuma, T., Nishizawa, N.K. and Mori, S. (2000) Two dioxygenase genes, Ids3 and Ids2, from Hordeum vulgare are involved in the biosynthesis of mugineic acid family phytosiderophores. *Plant Mol Biol* **44**, 199-207.

Nakashima, K., Takasaki, H., Mizoi, J., Shinozaki, K. and Yamaguchi-Shinozaki, K. (2012) NAC transcription factors in plant abiotic stress responses. *Bba-Gene Regul Mech* **1819**, 97-103.

Neal, A.L., Geraki, K., Borg, S., Quinn, P., Mosselmans, J.F., Brinch-Pedersen, H. and Shewry, P.R. (2013) Iron and zinc complexation in wild-type and ferritin-expressing wheat grain: implications for mineral transport into developing grain. *J Biol Inorg Chem* **18**, 557-570.

Negishi, T., Nakanishi, H., Yazaki, J., Kishimoto, N., Fujii, F., Shimbo, K., Yamamoto, K., Sakata, K., Sasaki, T., Kikuchi, S., Mori, S. and Nishizawa, N.K. (2002) cDNA microarray analysis of gene expression during Fe-deficiency stress in barley suggests that polar transport of vesicles is implicated in phytosiderophore secretion in Fe-deficient barley roots. *Plant J* **30**, 83-94.

Nishiyama, R., Kato, M., Nagata, S., Yanagisawa, S. and Yoneyama, T. (2012) Identification of Zn-nicotianamine and Fe-2'-deoxymugineic acid in the phloem sap from rice plants (Oryza sativa L.). *Plant Cell Physiol* **53**, 381-390.

Nozoye, T., Nagasaka, S., Kobayashi, T., Sato, Y., Uozumi, N., Nakanishi, H. and Nishizawa, N.K. (2015) The phytosiderophore efflux transporter TOM2 is involved in metal transport in rice. *J Biol Chem* **290**, 27688-27699.

Nozoye, T., Nagasaka, S., Kobayashi, T., Takahashi, M., Sato, Y., Sato, Y., Uozumi, N., Nakanishi, H. and Nishizawa, N.K. (2011) Phytosiderophore efflux transporters are crucial for iron acquisition in graminaceous plants. *J Biol Chem* **286**, 5446-5454.

O'Rourke, J.A., Charlson, D.V., Gonzalez, D.O., Vodkin, L.O., Graham, M.A., Cianzio, S.R., Grusak, M.A. and Shoemaker, R.C. (2007) Microarray analysis of iron deficiency chlorosis in near-isogenic soybean lines. *BMC Genomics* **8**, 476.

O'Rourke, J.A., Nelson, R.T., Grant, D., Schmutz, J., Grimwood, J., Cannon, S., Vance, C.P., Graham, M.A. and Shoemaker, R.C. (2009) Integrating microarray analysis and the soybean genome to understand the soybeans iron deficiency response. *BMC Genomics* **10**, 376.

Ogo, Y., Itai, R.N., Inoue, H., Kobayashi, T., Suzuki, M., Takahashi, M., Mori, S., Nishizawa, N.K. and Nishizawa, N.K. (2006) Isolation and characterization of IRO2, a novel iron-regulated bHLH transcription factor in graminaceous plants. *J Exp Bot* **57**, 2867-2878.

Ogo, Y., Itai, R.N., Kobayashi, T., Aung, M.S., Nakanishi, H. and Nishizawa, N.K. (2011) OsIRO2 is responsible for iron utilization in rice and improves growth and yield in calcareous soil. *Plant Mol Biol* **75**, 593-605.

Ogo, Y., Itai, R.N., Nakanishi, H., Kobayashi, T., Takahashi, M., Mori, S. and Nishizawa, N.K. (2007) The rice bHLH protein OsIRO2 is an essential regulator of the genes involved in Fe uptake under Fe-deficient conditions. *Plant J* **51**, 366-377.

Ogo, Y., Kobayashi, T., Itai, R.N., Nakanishi, H., Kakei, Y., Takahashi, M., Toki, S., Mori, S. and Nishizawa, N.K. (2008) A novel NAC transcription factor, IDEF2, that recognizes the iron deficiency-responsive element 2 regulates the genes involved in iron homeostasis in plants. *J Biol Chem* **283**, 13407-13417.

Omote, H., Hiasa, M., Matsumoto, T., Otsuka, M. and Moriyama, Y. (2006) The MATE proteins as fundamental transporters of metabolic and xenobiotic organic cations. *Trends Pharmacol Sci* **27**, 587-593.

Oono, Y., Kobayashi, F., Kawahara, Y., Yazawa, T., Handa, H., Itoh, T. and Matsumoto, T. (2013) Characterisation of the wheat (Triticum aestivum L.) transcriptome by de novo assembly for the discovery of phosphate starvation-responsive genes: gene expression in Pi-stressed wheat. *BMC Genomics* **14**, 77.

Palmer, C.M. and Guerinot, M.L. (2009) Facing the challenges of Cu, Fe and Zn homeostasis in plants. *Nat Chem Biol* **5**, 333-340.

Palmgren, M.G. (2001) Plant plasma membrane H+-ATPases: powerhouses for nutrient uptake. *Annu Rev Plant Physiol Plant Mol Biol* **52**, 817-845.

Pao, S.S., Paulsen, I.T. and Saier, M.H., Jr. (1998) Major facilitator superfamily. *Microbiol Mol Biol Rev* **62**, 1-34.

Paul, S., Ali, N., Gayen, D., Datta, S.K. and Datta, K. (2012) Molecular breeding of Osfer 2 gene to increase iron nutrition in rice grain. *GM Crops Food* **3**, 310-316.

Pedas, P., Schjoerring, J.K. and Husted, S. (2009) Identification and characterization of zinc-starvation-induced ZIP transporters from barley roots. *Plant Physiol Biochem* **47**, 377-383.

Pedler, J.F., Parker, D.R. and Crowley, D.E. (2000) Zinc deficiency-induced phytosiderophore release by the Triticaceae is not consistently expressed in solution culture. *Planta* **211**, 120-126.

Pellny, T.K., Lovegrove, A., Freeman, J., Tosi, P., Love, C.G., Knox, J.P., Shewry, P.R. and Mitchell, R.A. (2012) Cell walls of developing wheat starchy endosperm: comparison of composition and RNA-Seq transcriptome. *Plant Physiol* **158**, 612-627.

Petit, J.M., Briat, J.F. and Lobreaux, S. (2001) Structure and differential expression of the four members of the Arabidopsis thaliana ferritin gene family. *Biochem J* **359**, 575-582.

Podar, D., Scherer, J., Noordally, Z., Herzyk, P., Nies, D. and Sanders, D. (2012) Metal selectivity determinants in a family of transition metal transporters. *J Biol Chem* **287**, 3185-3196.

Prasad, A.S. (2012) Discovery of human zinc deficiency: 50 years later. *J Trace Elem Med Biol* **26**, 66-69.

Qu, L.Q., Yoshihara, T., Ooyama, A., Goto, F. and Takaiwa, F. (2005) Iron accumulation does not parallel the high expression level of ferritin in transgenic rice seeds. *Planta* **222**, 225-233.

Ramesh, S.A., Shin, R., Eide, D.J. and Schachtman, D.P. (2003) Differential metal selectivity and gene expression of two zinc transporters from rice. *Plant Physiol* **133**, 126-134.

Rea, P.A. (2007) Plant ATP-binding cassette transporters. *Annu Rev Plant Biol* **58**, 347-375.

Reddy, V.S., Shlykov, M.A., Castillo, R., Sun, E.I. and Saier, M.H. (2012) The major facilitator superfamily (MFS) revisited. *FEBS J* **279**, 2022-2035.

Rellan-Alvarez, R., El-Jendoubi, H., Wohlgemuth, G., Abadia, A., Fiehn, O., Abadia, J. and Alvarez-Fernandez, A. (2011) Metabolite profile changes in xylem sap and leaf extracts of strategy I plants in response to iron deficiency and resupply. *Front Plant Sci* **2**, 66.

Rellan-Alvarez, R., Giner-Martinez-Sierra, J., Orduna, J., Orera, I., Rodriguez-Castrillon, J.A., Garcia-Alonso, J.I., Abadia, J. and Alvarez-Fernandez, A. (2010) Identification of a tri-iron(III), tri-citrate complex in the xylem sap of iron-deficient tomato resupplied with iron: new insights into plant iron long-distance transport. *Plant Cell Physiol* **51**, 91-102.

Ren, Y., Liu, Y., Chen, H., Li, G., Zhang, X. and Zhao, J. (2012) Type 4 metallothionein genes are involved in regulating Zn ion accumulation in late embryo and in controlling early seedling growth in Arabidopsis. *Plant Cell Environ* **35**, 770-789.

Ricachenevsky, F.K., Menguer, P.K., Sperotto, R.A. and Fett, J.P. (2015) Got to hide your Zn away: Molecular control of Zn accumulation and biotechnological applications. *Plant Sci* **236**, 1-17.

Ricachenevsky, F.K., Sperotto, R.A., Menguer, P.K., Sperb, E.R., Lopes, K.L. and Fett, J.P. (2011) ZINC-INDUCED FACILITATOR-LIKE family in plants: lineage-specific expansion in monocotyledons and conserved genomic and expression features among rice (Oryza sativa) paralogs. *BMC Plant Biol* **11**, 20.

Robinson, N.J., Procter, C.M., Connolly, E.L. and Guerinot, M.L. (1999) A ferric-chelate reductase for iron uptake from soils. *Nature* **397**, 694-697.

Rodriguez-Celma, J., Pan, I.C., Li, W., Lan, P., Buckhout, T.J. and Schmidt, W. (2013) The transcriptional response of Arabidopsis leaves to Fe deficiency. *Front Plant Sci* **4**, 276.

Rogers, E.E., Wu, X.L., Stacey, G. and Nguyen, H.T. (2009) Two MATE proteins play a role in iron efficiency in soybean. *J Plant Physiol* **166**, 1453-1459.

Roschzttardtz, H., Seguela-Arnaud, M., Briat, J.F., Vert, G. and Curie, C. (2011) The FRD3 citrate effluxer promotes iron nutrition between symplastically disconnected tissues throughout Arabidopsis development. *Plant Cell* **23**, 2725-2737.

Rushton, P.J., Somssich, I.E., Ringler, P. and Shen, Q.X.J. (2010) WRKY transcription factors. *Trends Plant Sci* **15**, 247-258.

Sadeghzadeh, B. (2013) A review of zinc nutrition and plant breeding. *J Soil Sci Plant Nut* **13**, 905-927.

Santi, S. and Schmidt, W. (2009) Dissecting iron deficiency-induced proton extrusion in Arabidopsis roots. *New Phytol* **183**, 1072-1084.

Sasaki, A., Yamaji, N., Xia, J.X. and Ma, J.F. (2011) OsYSL6 is involved in the detoxification of excess manganese in rice. *Plant Physiol* **157**, 1832-1840.

Schaaf, G., Ludewig, U., Erenoglu, B.E., Mori, S., Kitahara, T. and von Wiren, N. (2004) ZmYS1 functions as a proton-coupled symporter for phytosiderophore- and nicotianamine-chelated metals. *J Biol Chem* **279**, 9091-9096.

Schaaf, G., Schikora, A., Haberle, J., Vert, G., Ludewig, U., Briat, J.F., Curie, C. and von Wiren, N. (2005) A putative function for the arabidopsis Fe-phytosiderophore

transporter homolog AtYSL2 in Fe and Zn homeostasis. *Plant Cell Physiol* **46**, 762-774.

Schefe, J.H., Lehmann, K.E., Buschmann, I.R., Unger, T. and Funke-Kaiser, H. (2006) Quantitative real-time RT-PCR data analysis: current concepts and the novel "gene expression's CT difference" formula. *J Mol Med (Berl)* **84**, 901-910.

Schmidt, H., Gunther, C., Weber, M., Sporlein, C., Loscher, S., Bottcher, C., Schobert, R. and Clemens, S. (2014) Metabolome analysis of Arabidopsis thaliana roots identifies a key metabolic pathway for iron acquisition. *PLoS One* **9**, e102444.

Schuler, M., Rellan-Alvarez, R., Fink-Straube, C., Abadia, J. and Bauer, P. (2012) Nicotianamine functions in the phloem-based transport of iron to sink organs, in pollen development and pollen tube growth in Arabidopsis. *Plant Cell* **24**, 2380-2400.

Seckback, J. (1982) Ferreting out the secrets of plant ferritin - a review. *J Plant Nutr* **5**, 369-394.

Shi, D.-q., Zhang, Y., Ma, J.-h., Li, Y.-l. and Xu, J. (2013) Identification of zinc deficiency-responsive microRNAs in Brassica juncea roots by small RNA sequencing. *J Integr Agric* **12**, 2036-2044.

Shin, L.J., Lo, J.C., Chen, G.H., Callis, J., Fu, H. and Yeh, K.C. (2013) IRT1 degradation factor1, a ring E3 ubiquitin ligase, regulates the degradation of iron-regulated transporter1 in Arabidopsis. *Plant Cell* **25**, 3039-3051.

Sinclair, S.A. and Kramer, U. (2012) The zinc homeostasis network of land plants. *Biochim Biophys Acta* **1823**, 1553-1567.

Singh, G., Kumar, S. and Singh, P. (2003) A quick method to isolate RNA from wheat and other carbohydrate-rich seeds. *Plant Mol Biol Report* **21**, 93-93.

Singh, K., Sasakuma, T., Bughio, N., Takahashi, H., Nakanishi, H., Yoshimura, E., Nishizawa, N.K. and Mori, S. (2000) Ability of ancestral wheat species to secrete mugineic acid family phytosiderophores in response to iron deficiency. *Journal of Plant Nutrition* **23**, 1973-1981.

Sivitz, A., Grinvalds, C., Barberon, M., Curie, C. and Vert, G. (2011) Proteasome-mediated turnover of the transcriptional activator FIT is required for plant iron-deficiency responses. *Plant J* **66**, 1044-1052.

Sivitz, A.B., Hermand, V., Curie, C. and Vert, G. (2012) Arabidopsis bHLH100 and bHLH101 control iron homeostasis via a FIT-independent pathway. *PLoS One* **7**, e44843.

Song, W.Y., Choi, K.S., Kim, D.Y., Geisler, M., Park, J., Vincenzetti, V., Schellenberg, M., Kim, S.H., Lim, Y.P., Noh, E.W., Lee, Y. and Martinoia, E. (2010) Arabidopsis PCR2 is a zinc exporter involved in both zinc extrusion and long-distance zinc transport. *Plant Cell* **22**, 2237-2252.

Sperotto, R.A., Boff, T., Duarte, G.L. and Fett, J.P. (2008) Increased senescence-associated gene expression and lipid peroxidation induced by iron deficiency in rice roots. *Plant Cell Rep* **27**, 183-195.

Stein, R.J., Ricachenevsky, F.K. and Fett, J.P. (2009) Differential regulation of the two rice ferritin genes (OsFER1 and OsFER2). *Plant Sci* **177**, 563-569.

Suzuki, M., Bashir, K., Inoue, H., Takahashi, M., Nakanishi, H. and Nishizawa, N.K. (2012) Accumulation of starch in Zn-deficient rice. *Rice (N Y)* **5**, 9.

Suzuki, M., Takahashi, M., Tsukamoto, T., Watanabe, S., Matsuhashi, S., Yazaki, J., Kishimoto, N., Kikuchi, S., Nakanishi, H., Mori, S. and Nishizawa, N.K. (2006) Biosynthesis and secretion of mugineic acid family phytosiderophores in zinc-deficient barley. *Plant J* **48**, 85-97.

Suzuki, M., Tsukamoto, T., Inoue, H., Watanabe, S., Matsuhashi, S., Takahashi, M., Nakanishi, H., Mori, S. and Nishizawa, N.K. (2008) Deoxymugineic acid increases Zn translocation in Zn-deficient rice plants. *Plant Mol Biol* **66**, 609-617.

Takahashi, M., Terada, Y., Nakai, I., Nakanishi, H., Yoshimura, E., Mori, S. and Nishizawa, N.K. (2003) Role of nicotianamine in the intracellular delivery of metals and plant reproductive development. *Plant Cell* **15**, 1263-1280.

Takahashi, M., Yamaguchi, H., Nakanishi, H., Shioiri, T., Nishizawa, N.K. and Mori, S. (1999) Cloning two genes for nicotianamine aminotransferase, a critical enzyme in iron acquisition (Strategy II) in graminaceous plants. *Plant Physiol* **121**, 947-956.

Takizawa, R., Nishizawa, N.K., Nakanishi, H. and Mori, S. (1996) Effect of iron deficiency on S-adenosyl-methionine synthetase in barley roots. *J Plant Nutr* **19**, 1189-1200.

Tauris, B., Borg, S., Gregersen, P.L. and Holm, P.B. (2009) A roadmap for zinc trafficking in the developing barley grain based on laser capture microdissection and gene expression profiling. *J Exp Bot* **60**, 1333-1347.

Terry, N. and Low, G. (1982) Leaf chlorophyll content and its relation to the intracellular localization of iron. *J Plant Nutr* **5**, 301-310.

Thimm, O., Essigmann, B., Kloska, S., Altmann, T. and Buckhout, T.J. (2001) Response of arabidopsis to iron deficiency stress as revealed by microarray analysis. *Plant Physiol* **127**, 1030-1043.

Tiong, J., McDonald, G., Genc, Y., Shirley, N., Langridge, P. and Huang, C.Y. (2015) Increased expression of six ZIP family genes by zinc (Zn) deficiency is associated with enhanced uptake and root-to-shoot translocation of Zn in barley (Hordeum vulgare). *New Phytol* **207**, 1097-1109.

Tiong, J., McDonald, G.K., Genc, Y., Pedas, P., Hayes, J.E., Toubia, J., Langridge, P. and Huang, C.Y. (2014) HvZIP7 mediates zinc accumulation in barley (Hordeum vulgare) at moderately high zinc supply. *New Phytol* **201**, 131-143.

Tovkach, A., Ryan, P.R., Richardson, A.E., Lewis, D.C., Rathjen, T.M., Ramesh, S., Tyerman, S.D. and Delhaize, E. (2013) Transposon-Mediated Alteration of TaMATE1B Expression in Wheat Confers Constitutive Citrate Efflux from Root Apices. *Plant Physiol* **161**, 880-892.

Trijatmiko, K.R., Duenas, C., Tsakirpaloglou, N., Torrizo, L., Arines, F.M., Adeva, C., Balindong, J., Oliva, N., Sapasap, M.V., Borrero, J., Rey, J., Francisco, P., Nelson, A., Nakanishi, H., Lombi, E., Tako, E., Glahn, R.P., Stangoulis, J., Chadha-Mohanty, P., Johnson, A.A., Tohme, J., Barry, G. and Slamet-Loedin, I.H. (2016) Biofortified indica rice attains iron and zinc nutrition dietary targets in the field. *Sci Rep* **6**, 19792.

Tsednee, M., Mak, Y.W., Chen, Y.R. and Yeh, K.C. (2012) A sensitive LC-ESI-Q-TOF-MS method reveals novel phytosiderophores and phytosiderophore-iron complexes in barley. *New Phytol* **195**, 951-961.

Tuomi, J.M., Voorbraak, F., Jones, D.L. and Ruijter, J.M. (2010) Bias in the Cq value observed with hydrolysis probe based quantitative PCR can be corrected with the estimated PCR efficiency value. *Methods* **50**, 313-322.

Uauy, C., Distelfeld, A., Fahima, T., Blechl, A. and Dubcovsky, J. (2006) A NAC gene regulating senescence improves grain protein, zinc, and iron content in wheat. *Science* **314**, 1298-1301.

van de Mortel, J.E., Almar Villanueva, L., Schat, H., Kwekkeboom, J., Coughlan, S., Moerland, P.D., Ver Loren van Themaat, E., Koornneef, M. and Aarts, M.G. (2006) Large expression differences in genes for iron and zinc homeostasis, stress response, and lignin biosynthesis distinguish roots of Arabidopsis thaliana and the related metal hyperaccumulator Thlaspi caerulescens. *Plant Physiol* **142**, 1127-1147.

Vasconcelos, M., Datta, K., Oliva, N., Khalekuzzaman, M., Torrizo, L., Krishnan, S., Oliveira, M., Goto, F. and Datta, S.K. (2003) Enhanced iron and zinc accumulation in transgenic rice with the ferritin gene. *Plant Sci* **164**, 371-378.

Vasconcelos, M.W., Li, G.W., Lubkowitz, M.A. and Grusak, M.A. (2008) Characterization of the PT clade of oligopeptide transporters in rice. *The Plant Genome* **1**, 77-88.

Vert, G., Barberon, M., Zelazny, E., Seguela, M., Briat, J.F. and Curie, C. (2009) Arabidopsis IRT2 cooperates with the high-affinity iron uptake system to maintain iron homeostasis in root epidermal cells. *Planta* **229**, 1171-1179.

Vert, G., Grotz, N., Dedaldechamp, F., Gaymard, F., Guerinot, M.L., Briat, J.F. and Curie, C. (2002) IRT1, an Arabidopsis transporter essential for iron uptake from the soil and for plant growth. *Plant Cell* **14**, 1223-1233.

von Wiren, N., Klair, S., Bansal, S., Briat, J.F., Khodr, H., Shioiri, T., Leigh, R.A. and Hider, R.C. (1999) Nicotianamine chelates both FeIII and FeII. Implications for metal transport in plants. *Plant Physiol* **119**, 1107-1114.

Von Wiren, N., Marschner, H. and Romheld, V. (1996) Roots of iron-efficient maize also absorb phytosiderophore-chelated zinc. *Plant Physiol* **111**, 1119-1125.

Walker, E.L. and Connolly, E.L. (2008) Time to pump iron: iron-deficiency-signaling mechanisms of higher plants. *Curr Opin Plant Biol* **11**, 530-535.

Wang, H.Y., Klatte, M., Jakoby, M., Baumlein, H., Weisshaar, B. and Bauer, P. (2007) Iron deficiency-mediated stress regulation of four subgroup Ib BHLH genes in Arabidopsis thaliana. *Planta* **226**, 897-908.

Wang, L., Ying, Y., Narsai, R., Ye, L., Zheng, L., Tian, J., Whelan, J. and Shou, H. (2013a) Identification of OsbHLH133 as a regulator of iron distribution between roots and shoots in Oryza sativa. *Plant Cell Environ* **36**, 224-236.

Wang, N., Cui, Y., Liu, Y., Fan, H., Du, J., Huang, Z., Yuan, Y., Wu, H. and Ling, H.Q. (2013b) Requirement and functional redundancy of Ib subgroup bHLH proteins for iron deficiency responses and uptake in Arabidopsis thaliana. *Mol Plant* **6**, 503-513.

Waters, B.M., Blevins, D.G. and Eide, D.J. (2002) Characterization of FRO1, a pea ferric-chelate reductase involved in root iron acquisition. *Plant Physiol* **129**, 85-94.

Waters, B.M., Chu, H.H., Didonato, R.J., Roberts, L.A., Eisley, R.B., Lahner, B., Salt, D.E. and Walker, E.L. (2006) Mutations in Arabidopsis yellow stripe-like1 and yellow stripe-like3 reveal their roles in metal ion homeostasis and loading of metal ions in seeds. *Plant Physiol* **141**, 1446-1458.

Waters, B.M., McInturf, S.A. and Stein, R.J. (2012) Rosette iron deficiency transcript and microRNA profiling reveals links between copper and iron homeostasis in Arabidopsis thaliana. *J Exp Bot* **63**, 5903-5918.

Waters, B.M., Uauy, C., Dubcovsky, J. and Grusak, M.A. (2009) Wheat (Triticum aestivum) NAM proteins regulate the translocation of iron, zinc, and nitrogen compounds from vegetative tissues to grain. *J Exp Bot* **60**, 4263-4274.

Watts, R.N., Hawkins, C., Ponka, P. and Richardson, D.R. (2006) Nitrogen monoxide (NO)-mediated iron release from cells is linked to NO-induced glutathione efflux via multidrug resistance-associated protein 1 (vol 103, pg 7670, 2006). *PNAS* **103**, 9745-9745.

WHO (2016) Micronutrient deficiencies. Available online at: http://www.who.int/nutrition/topics/ida/en/ (Accessed June 20, 2016).

Wilkinson, N. and Pantopoulos, K. (2014) The IRP/IRE system in vivo: insights from mouse models. *Front Pharmacol* **5**, 176.

Wirth, J., Poletti, S., Aeschlimann, B., Yakandawala, N., Drosse, B., Osorio, S., Tohge, T., Fernie, A.R., Gunther, D., Gruissem, W. and Sautter, C. (2009) Rice endosperm iron biofortification by targeted and synergistic action of nicotianamine synthase and ferritin. *Plant Biotechnol J* **7**, 631-644.

World-Rice-Production (2016) World rice production 2016/2017. Available online at: https://www.worldriceproduction.com (Accessed June 20, 2016)

World-Wheat-Production (2016) World Wheat Production 2016/2017. Available online at: https://www.worldwheatproduction.com (Accessed June 20, 2016)

Xiao, J., Jin, X., Jia, X., Wang, H., Cao, A., Zhao, W., Pei, H., Xue, Z., He, L., Chen, Q. and Wang, X. (2013) Transcriptome-based discovery of pathways and genes related to resistance against Fusarium head blight in wheat landrace Wangshuibai. *BMC Genomics* **14**, 197.

Xing, J., Wang, T., Liu, Z., Xu, J., Yao, Y., Hu, Z., Peng, H., Xin, M., Yu, F., Zhou, D. and Ni, Z. (2015) General control nonrepressed protein5-mediated histone acetylation of ferric reductase defective3 contributes to iron homeostasis in Arabidopsis. *Plant Physiol* **168**, 1309-1320.

Xu, Y.X., Zhang, S.N., Guo, H.P., Wang, S.K., Xu, L.G., Li, C.Y., Qian, Q., Chen, F., Geisler, M., Qi, Y.H. and Jiang, D.A. (2014) OsABCB14 functions in auxin transport and iron homeostasis in rice (Oryza sativa L.). *Plant J* **79**, 106-117.

Yang, T.J.W., Lin, W.D. and Schmidt, W. (2010) Transcriptional profiling of the Arabidopsis iron deficiency response reveals conserved transition metal homeostasis networks. *Plant Physiol* **152**, 2130-2141.

Yang, Z., Wu, Y., Li, Y., Ling, H.Q. and Chu, C. (2009) OsMT1a, a type 1 metallothionein, plays the pivotal role in zinc homeostasis and drought tolerance in rice. *Plant Mol Biol* **70**, 219-229.

Yokosho, K., Yamaji, N., Ueno, D., Mitani, N. and Ma, J.F. (2009) OsFRDL1 Is a citrate transporter required for efficient translocation of iron in rice. *Plant Physiol* **149**, 297-305.

Yuan, L., Yang, S., Liu, B., Zhang, M. and Wu, K. (2012) Molecular characterization of a rice metal tolerance protein, OsMTP1. *Plant Cell Rep* **31**, 67-79.

Yuan, Y., Wu, H., Wang, N., Li, J., Zhao, W., Du, J., Wang, D. and Ling, H.Q. (2008a) FIT interacts with AtbHLH38 and AtbHLH39 in regulating iron uptake gene expression for iron homeostasis in Arabidopsis. *Cell Res* **18**, 385-397.

Yuan, Y.X., Wu, H.L., Wang, N., Li, J., Zhao, W.N., Du, J., Wang, D.W. and Ling, H.Q. (2008b) FIT interacts with AtbHLH38 and AtbHLH39 in regulating iron uptake gene expression for iron homeostasis in Arabidopsis. *Cell Res* **18**, 385-397.

Zamboni, A., Zanin, L., Tomasi, N., Pezzotti, M., Pinton, R., Varanini, Z. and Cesco, S. (2012) Genome-wide microarray analysis of tomato roots showed defined responses to iron deficiency. *BMC Genomics* **13**, 101.

Zancani, M., Peresson, C., Biroccio, A., Federici, G., Urbani, A., Murgia, I., Soave, C., Micali, F., Vianello, A. and Macri, F. (2004) Evidence for the presence of ferritin in plant mitochondria. *Eur J Biochem* **271**, 3657-3664.

Zargar, S.M., Fujiwara, M., Inaba, S., Kobayashi, M., Kurata, R., Ogata, Y. and Fukao, Y. (2015) Correlation analysis of proteins responsive to Zn, Mn, or Fe deficiency in Arabidopsis roots based on iTRAQ analysis. *Plant Cell Rep* **34**, 157-166.

Zeng, H., Wang, G., Hu, X., Wang, H., Du, L. and Zhu, Y. (2014) Role of microRNAs in plant responses to nutrient stress. *Plant Soil* **374**, 1005-1021.

Zhai, Z., Gayomba, S.R., Jung, H.I., Vimalakumari, N.K., Pineros, M., Craft, E., Rutzke, M.A., Danku, J., Lahner, B., Punshon, T., Guerinot, M.L., Salt, D.E., Kochian, L.V. and Vatamaniuk, O.K. (2014) OPT3 Is a phloem-specific iron transporter that is essential for systemic iron signaling and redistribution of iron and cadmium in Arabidopsis. *Plant Cell* **26**, 2249-2264.

Zhang, Y., Xu, Y.H., Yi, H.Y. and Gong, J.M. (2012) Vacuolar membrane transporters OsVIT1 and OsVIT2 modulate iron translocation between flag leaves and seeds in rice. *Plant J* **72**, 400-410.

Zhao, M., Song, A.P., Li, P.L., Chen, S.M., Jiang, J.F. and Chen, F.D. (2014) A bHLH transcription factor regulates iron intake under Fe deficiency in chrysanthemum. *Sci Rep* **4**.

Zheng, L., Ying, Y., Wang, L., Wang, F., Whelan, J. and Shou, H. (2010) Identification of a novel iron regulated basic helix-loop-helix protein involved in Fe homeostasis in Oryza sativa. *BMC Plant Biol* **10**, 166.

Zheng, L.Q., Huang, F.L., Narsai, R., Wu, J.J., Giraud, E., He, F., Cheng, L.J., Wang, F., Wu, P., Whelan, J. and Shou, H.X. (2009) Physiological and transcriptome analysis of iron and phosphorus interaction in rice seedlings. *Plant Physiol* **151**, 262-274.

Zheng, L.Q., Yamaji, N., Yokosho, K. and Ma, J.F. (2012) YSL16 is a phloem-localized transporter of the copper-nicotianamine complex that is responsible for copper distribution in rice. *Plant Cell* **24**, 3767-3782.

Zhou, X.J., Li, S.Z., Zhao, Q.Q., Liu, X.Q., Zhang, S.J., Sun, C., Fan, Y.L., Zhang, C.Y. and Chen, R.M. (2013) Genome-wide identification, classification and expression profiling of nicotianamine synthase (NAS) gene family in maize. *BMC Genomics* **14**.

Zimmermann, P., Hennig, L. and Gruissem, W. (2005) Gene-expression analysis and network discovery using Genevestigator. *Trends Plant Sci* **10**, 407-409.

Zocchi, G., De Nisi, P., Dell'Orto, M., Espen, L. and Gallina, P.M. (2007) Iron deficiency differently affects metabolic responses in soybean roots. *J Exp Bot* **58**, 993-1000.